AEA Energy & Environment
From the AEA group

Ozone June 2006

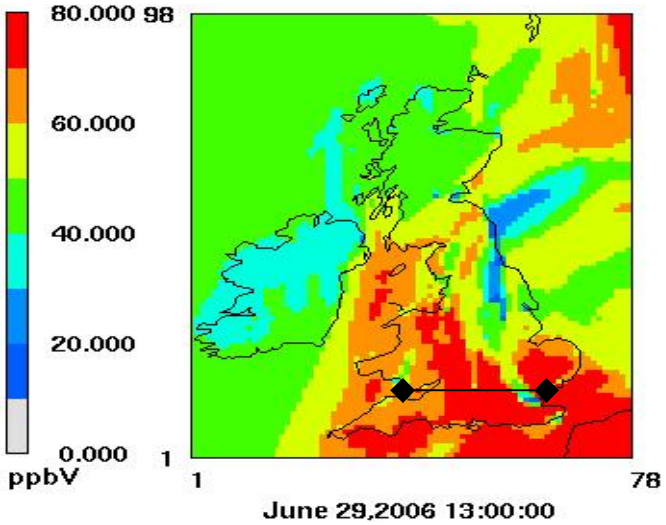

Ozone 2007
AOT40 (µg m^{-3}.hours)

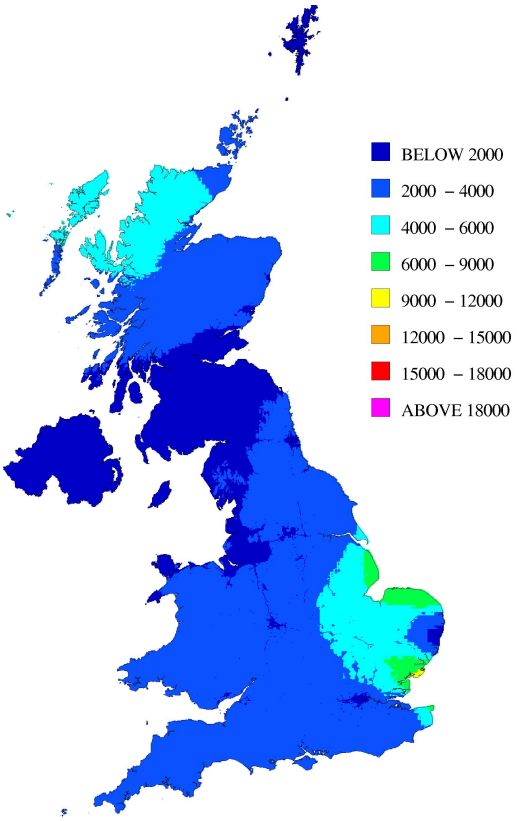

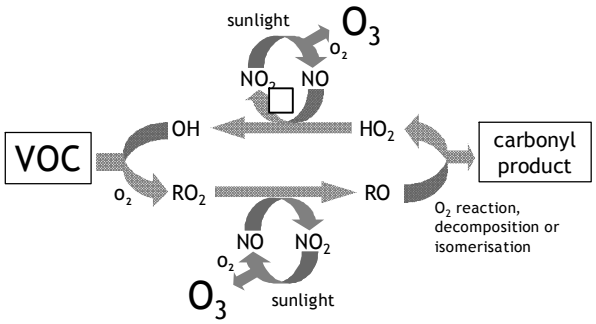

Modelling of Tropospheric Ozone
Annual Report: 2008

Report to The Department for Environment, Food and Rural Affairs, Welsh Assembly Government, the Scottish Executive and the Department of the Environment for Northern Ireland

ED48749001

February 2009

Title	Modelling of Tropospheric Ozone: Annual Report 2008
Customer	The Department for Environment, Food and Rural Affairs, Welsh Assembly Government, the Scottish Executive and the Department of the Environment for Northern Ireland
Customer reference	CSA 7267/AQ0704
Confidentiality, copyright and reproduction	
File reference	ED48749001
Reference number	AEAT/ENV/R/2748

AEA Energy & Environment
The Gemini Building
Fermi Avenue
Harwell International Business Centre
Didcot
OX11 0QR

t: 0870 190 6539
f: 0870 190 6318

AEA Energy & Environment is a business name of
AEA Technology plc

AEA Energy & Environment is certificated to ISO9001
and ISO14001

Authors	Name	Tim Murrells Sally Cooke Andrew Kent Susannah Grice Andrea Fraser Clare Allen Prof Dick Derwent (rdscientific) Mike Jenkin (Atmospheric Chemistry Services) Andrew Rickard (University of Leeds) Prof Mike Pilling (University of Leeds) Mike Holland (EMRC)
Approved by	Name	Tony Bush
	Signature	
	Date	16th February 2009

Executive summary

The concentrations of ground-level ozone, a pollutant that affects human health, ecosystems and materials, widely exceed environmental quality standards across the UK and Europe. Ozone is not emitted directly into the atmosphere, but is a secondary photochemical pollutant formed in the lower atmosphere from the sunlight-initiated oxidation of volatile organic compounds (VOCs) in the presence of nitrogen oxides (NO_x).

The non-linear nature of ground-level ozone production requires the use of sophisticated chemical transport models to understand the factors affecting its production and subsequent control. The Department for Environment, Food and Rural Affairs (Defra) and the Devolved Administrations (DAs, the Welsh Assembly Government, the Scottish Executive and the Department of the Environment for Northern Ireland) have funded the development of ozone modelling tools over the years. They seek to build on this work but now require a modelling capability to treat ozone formation (a) on all spatial scales from urban areas at high spatial resolution to the global scale so that ozone production on the regional and global scales is linked and (b) from timescales of hours to reproduce the diurnal behaviour of ozone to decades so that the influence of climate change and changes in emissions can be assessed.

The overall purpose of the project is to maintain, develop, and apply tools for modelling tropospheric ozone formation and distribution over a range of spatial scales (global, regional and national). The modelling will be used to support and guide Defra's policy on emission reductions and objectives for pollutants that influence ozone, and to verify compliance with UK policy and with European directives on ground-level ozone.

To meet these aims and to address the intended applications, the project currently has a programme of work comprised of five main objectives some of which have been been modified or extended since the project started:

Objective 1: Policy development and scenario analysis

Objective 2: Detailed assessment of relationship between ozone, nitrogen oxide and nitrogen dioxide levels, and factors controlling them

Objective 3: Improvements to photochemical reaction schemes

Objective 4: Maintenance and Improvements to the Ozone Source Receptor Model and Comparison With Eulerian Models

Objective 7: Costs, Benefits and Trade-offs: Volatile Organic Solvents

This is the second annual report on the project and reports progress over the period from 1st January 2008 to 31st December 2008. The work can be broadly categorised as **application** of existing models of tropospheric ozone formation for policy purposes and further **research and development** of the models and the underpinning science in relation to ozone and related air quality policy. The main conclusions from the work and the policy relevance are as follows:

Application of Tropospheric Ozone Models for Policy Support

UK Ozone Climate in 2007:

The UK ground-level ozone climate for 2007 has been characterised by the Pollution Climate Mapping (PCM) empirical modelling approach and the Ozone Source Receptor Model (OSRM). Both models indicated 2007 was a relatively low ozone year.

Results from the PCM, that are based on 2007 ozone monitoring data, are summarised for the EU Target Value for ozone concentration metrics for human health and vegetation in 2010 (an average over the past 3 years) and the Long-term Objectives for ozone in the following tables.

UK summary results of air quality assessment relative to the Target Values for ozone for 2010

Target Value	*Number of zones exceeding*
Max Daily 8-hour mean Target Value	none
AOT40 Target Value	none

UK summary results of air quality assessment relative to the Long-term Objectives for ozone

Long-term Objective	*Number of zones exceeding*
Max Daily 8-hour mean Long-term Objective	41 zones (24 measured + 17 modelled)
AOT40 Long-term Objective	3 zones (1 measured + 2 modelled)

The areas with the most number of days exceeding the objective concentration threshold for human health tended to be in the east of England.

The OSRM is a process model calculating the formation of ozone in the UK based on a chemical transport modelling approach using emissions inventory and real meteorological data for 2007. The OSRM shows broadly similar patterns to the empirical maps with higher concentrations in the east of the UK, however there are some specific spatial differences. The majority of the higher ozone concentration areas identified by the OSRM in 2007 are in coastal fringe areas. The OSRM in 2007 has generally overestimated Third Daughter Directive ozone metrics compared with measured data, continuing the trend found previously that indicates the OSRM overestimates these ozone metrics in low ozone years (2004, 2005 and 2007) and underestimates them in high ozone years (2003 and 2006) compared with measured data. The PCM empirical model continues to produce results that are closer to the measured concentrations than the OSRM and should continue to be used in its current capacity (contributing modelled data in fulfilment of UK reporting obligations to the European Commission.

Further Modelling and Assessments Relating to Ozone Policy:

The UK Photochemical Trajectory Model (UK PTM) has been used to study trends in both episodic peak and annual mean of the daily maximum ozone metrics from 1990-2010. The aim has been to determine the contribution to the observed trends in the ozone metrics from:

- NO_x and VOC precursor emission reductions
- intercontinental trans-Atlantic ozone transport
- non-linearities in ozone formation
- the ambition level achieved in international policy negotiations

The conclusion was that the balance between the contributions appear to be significantly different for the episodic peak and annual mean ozone metrics, but all four influences appear to be important to one or other of the ozone metrics.

The UK PTM model has been used to evaluate the contribution to ozone formation from solvents using the detailed emission speciation data from the NAEI and the explicit chemical mechanism described in the Master Chemical Mechanism (MCM). The contributions from usage of solvents and other products such as aerosol sprays are only slightly lower than that of VOC emissions from road transport. The contribution to episodic ozone from all 53 emission sub-sectors that make up the solvent and other product usage sector were examined. There is no one sector that dominates overall. The picture is one of detail and complexity, with many different solvent activities and applications and no dominant activity or process upon which to focus policy

The work on evaluating the potential impacts of solvent control policies has been extended by the development of a methodology for assessing the wider costs and benefits of solvent reduction and substitution policies covering a range of economic, health, social and environmental impacts. The methodology would enable full life cycle analysis of alternative approaches to inform and underpin future policy development to meet domestic and international commitments. It has also illustrated the role of air pollution models based on detailed chemical mechanisms like the MCM in providing inputs to wider policy analysis tools. This has been illustrated by a case study based on the substitution of trichloroethylene by other VOC solvents including a natural product, limonene, for metal degreasing. The OSRM, UK-PTM and PCM modelling approaches using reactivity information on these species based on the MCM were used to provide quantitative data on the impacts of replacing

trichloroethylene with limonene on ground-level ozone, secondary organic aerosols (SOAs, contributing to PM) and ambient concentrations of trichloroethylene in the UK.

Further work was undertaken with the UK-PTM to develop a particulate matter (PM) Closure Model. The PTM was used to estimate mass concentrations of $PM_{2.5}$ components at the Harwell site in each day in 2006 and to test the linearity of mechanisms forming secondary PM to reductions in precursor emissions. Emission sensitivity coefficients were developed for the different PM components for 30% across-the-board reductions in precursor emissions of SO_2, NO_x, NH_3, VOCs and CO. These revealed that the chemical environment is ammonia-limited such that policy strategies for secondary PM precursors should focus on the abatement of NH_3.

Research and Development of Models for Ozone and Secondary Organic Aerosols

Model Development and Validation:

As a scenario model for predicting UK ozone concentrations in response to changes in emissions, the OSRM has continued to be maintained and utilised. An initial assessment of specific recommendations of the independent review of existing ozone modelling tools commissioned by Defra in 2007 was carried out on the OSRM in terms of its performance and how far the OSRM goes in meeting these recommendations.

The assessment covered:

- The use of emission estimates in the OSRM;
- The evaluation of the performance of the OSRM and the PTM by comparison with ambient measurements of ozone concentrations;
- Quality control and outputs and how the OSRM follows the modelling guidelines of the Royal Meteorological Society

In the area of emissions information, it was concluded that the OSRM does treat emissions from UK and other European sources using the best available emissions inventory information, but there is room for improvement.

On model evaluation and comparison with monitoring data, further assessments were made for this study comparing the performance of the OSRM against 2005 and 2006 monitoring data at two rural and one urban AURN site and comparisons also made with the performance of the UK PTM. These showed reasonable model performance, but much more rigorous assessment is required against other models and this needs to be backed up by strong external peer-review.

On the modelling guidelines of the Royal Meteorological Society, these refer explicitly to atmospheric dispersion modelling and are not always directly appropriate for the applications of the OSRM to Defra policy support. Nevertheless, the general principles they invoke are applicable to the OSRM. All ten aspects of the modelling guidelines were considered and on balance the view was that the OSRM is fit-for-purpose and a better than satisfactory tool, but it is difficult to defend this position based on the current absence of peer-reviewed publications and widely accessible and transparent documentation and there are a number of areas where the OSRM falls short.

The Defra Review on ozone modelling made a strong case for Eulerian models. Progress has been made in this project on trialling certain Eulerian models for Defra's ozone policy. The USEPA's Eulerian model CMAQ has been set up to run with ECMWF meteorology data processed in WRF and a month's simulation of UK-scale ozone concentrations has been completed for June 2006. Initial results comparing ozone concentrations with AURN monitoring data look promising, but further work is required to optimise the meteorology and emissions inventory data before a year's simulation is carried out. Work will then be extended to the Chimere model. A protocol for carrying out a model comparison is required in order to give a fair and meaningful performance assessment. Defra is planning to extend the scope over the remaining 6 months of the project to enable such a protocol to be developed. The objectives of the model intercomprison protocol are more far-reaching covering a wider range of pollutants and air pollution issues than just tropospheric ozone, but the work to be carried out on CMAQ comparisons with the OSRM will be a good first demonstration of the protocol.

Chemical Mechanisms in Models for Ozone and Secondary Organic Aerosols:

Following the comprehensive review of the MCM in 2007, a work programme was agreed with the Department in 2008 aimed at improving and maintaining the status of the MCM and related mechanisms and assessing and guiding the improvement of the representation of organic chemistry in atmospheric models used in policy applications. The four main tasks to be carried out are:

- Development of a hierarchy of traceable reduced mechanisms from the MCM
- Development of new MCM schemes
- A major revision of the MCM protocol
- Development and application of a secondary organic aerosol (SOA) code

Considerable progress has been made in all these areas.

A reduced chemical mechanism describing the formation of ozone traceable to the MCM (Common Representative Intermediates mechanism, CRI v2) previously developed has been thoroughly tested and shown to perform well in comparison with the MCM over a range of conditions. The CRIv2 has been further reduced by progressive and systematic redistribution of emission species and lumping into groups. The most reduced version (CRIv2-R5) now comprises just 22 VOCs, 196 species and 555 reactions and still shows very good performance in comparison with the MCM.

Work is in progress on expanding the MCM with the development of new chemical degradation schemes for new biogenic VOCs covering a wider reactivity range. Four representative monoterpenes have been identified, mechanisms for two of which have already been developed (α- and β-pinene), and the construction of a detailed, MCM-compatible, gas phase mechanism for one of these, limonene, has been completed.

Work has commenced revising the protocol defining a set of rules for the development of the gas-phase degradation mechanisms in the MCM. The protocol ensures different people write consistent and compatible chemistry schemes and as new research information emerges this protocol needs to be periodically updated.

Codes for secondary organic aerosols (SOA) in the MCM have been developed and applied. A code for SOA has been developed, optimized and validated in the UK-PTM against measurements of organic aerosols from the TORCH campaign and shows good performance. A reduced SOA code for the CRIv2 and CRIv2-R5 has also been developed and tested. This represents a major advance in the treatment of secondary organic aerosol formation and hence modelling of PM in chemical transport models. As an application of this, the concept of the secondary organic aerosol potential, SOAP, has been developed to reflect the propensity of each organic compound to form SOA on an equal mass emitted basis relative to toluene. SOAPs for 18 different aromatic compounds plus α- and β-pinene were calculated by running the UK PTM model with the MCM for a range of conditions thus opening the door for efficient policy applications similar to the concept for POCPs.

NO_x-NO_2-O_3 Relationships:

A number of analyses of monitoring data has been undertaken to provide more information on local, regional and global contributions to oxidant at UK locations, and to improve the description of the partitioning of oxidant into its component species (i.e., O_3 and NO_2). The focus of the research this year has been on the analysis and interpretation of monitoring data to gain further insight into the geographical dependence of the hemispheric baseline contributions and regional modifications to the background oxidant concentrations in the UK. This has enabled the development of expressions describing the spatial variation in the hemispheric and regional oxidant components and year-specific parameters for use in empirical modelling of annual mean background oxidant concentrations in the UK. The outputs of these analyses are being used to improve and update the representation of the oxidant partitioning method in the Pollution Climate Model (PCM), in relation to assessments of annual mean NO_2 and O_3 levels. Further analysis of oxidant at roadside monitoring sites using the Netcen Primary NO_2 Model, extended to 2007, has yielded further information on regional variations in trends in primary NO_2 emissions to compare directly with trends predicted by the national emissions inventory.

Table of contents

Appendices

1 Introduction

The concentrations of ground-level ozone, a pollutant that affects human health, ecosystems and materials, widely exceed environmental quality standards across the UK and Europe. Ozone is not emitted directly into the atmosphere, but is a secondary photochemical pollutant formed in the lower atmosphere from the sunlight-initiated oxidation of volatile organic compounds (VOCs) in the presence of nitrogen oxides (NO_x). Elevated concentrations of ozone over the UK are especially generated when slow-moving or stagnant high pressure (anticyclonic) weather systems occurring in the spring or summer bring in photochemically reacting air masses from mainland Europe.

Under conditions characteristic of photochemical pollution episodes, the formation and transport of ozone can occur over hundreds of kilometres, with concentrations at a given location influenced by the history of the airmass over a period of up to several days. In addition to this, the increasing levels of ozone in the free troposphere on a global scale also influences regional scale photochemical processes by providing an increasing background ozone level upon which the regional and national scale formation is superimposed. This effect has to be considered when assessing whether proposed air quality standards for ozone are likely to be achieved.

The non-linear nature of ground-level ozone production requires the use of sophisticated chemical transport models to understand the factors affecting its production and subsequent control. The Department for Environment, Food and Rural Affairs (DEFRA) and the Devolved Administrations (DAs, the Welsh Assembly Government, the Scottish Executive and the Department of the Environment for Northern Ireland) have funded the development of ozone modelling tools over the years. They seek to build on this work but now require a modelling capability to treat ozone formation (a) on all spatial scales from urban areas at high spatial resolution to the global scale so that ozone production on the regional and global scales is linked and (b) from timescales of hours to reproduce the diurnal behaviour of ozone to decades so that the influence of climate change and changes in emissions can be assessed.

The previous contract funded by DEFRA and the DAs (Modelling of Tropospheric Ozone, EPG 1/3/200) had a strong emphasis on model application to evaluate planned and proposed policies, such as the Review of the Air Quality Strategy. Technical assistance was also provided to fulfill commitments arising from the implementation of the European Directives, in particular the 3rd Daughter Directive on Ozone. Model development work focused on the complex relationships between ozone and nitrogen oxides in order to improve the predictive capability of models in urban areas where local sources influence the balance between nitric oxide (NO), nitrogen dioxide (NO_2) and ozone. This current project aims to continue with the development and application of ozone modelling tools in these areas.

As part of their ozone research programme, DEFRA and the Devolved Administrations have over the years supported the development of near explicit chemical mechanisms, especially that of the Master Chemical Mechanism based on fundamental knowledge of the detailed photochemical reaction pathways involved in the formation of tropospheric ozone from the wide range of individual types of volatile organic compounds emitted into the atmosphere from anthropogenic and natural sources. This was in recognition that a more targeted approach on ozone precursor emissions would bring greater environmental benefits than a simple percentage mass reduction.

In the previous year of the current tropospheric ozone modelling project (2007), a comprehensive review of the MCM was undertaken. The initial assessment of the MCM was independently peer-reviewed and following this a series of recommendations were made on future development work. A work programme was agreed with the Department commencing in 2008 aimed at improving and maintaining the status of the MCM and related mechanisms and assessing and guiding the improvement of the representation of organic chemistry in atmospheric models used in policy applications. In parallel with this, the Department commissioned for this project the development of a methodology for assessing the wider costs and benefits of VOC abatement policies covering a range of economic, health, social and environmental impacts that would illustrate, through a case study based on solvent reduction substitution policies, the role of the MCM in providing inputs to wider policy analysis tools.

One of the model development objectives of the current project had been left undefined subject to the recommendations of an independent review of current ozone models commissioned by the Department in the first year of this project. This review made a strong case for Eulerian models and as a consequence, the scope of Objective 4 of the project, which was originally going to develop the treatment of meteorology and transport processes in the Ozone Source Receptor Model (OSRM), one of the main models used in this project for ozone policy analysis, was revised and now requires the testing and evaluation of selected Eulerian models for Defra ozone policy application, accompanied by more limited maintenance and performance evaluation of the OSRM. A model intercomparison of the CMAQ and Chimere models with the OSRM and Photochemical Trajectory Model (UK PTM) is now a major theme of this objective.

This is the second annual report on the current project covering the period from 1st January 2008 to 31st December 2008. The report is structured as follows:

Section	Contents
Section 2 - Overview and Progress	Description of the project, its aims and structure
Section 3 - Overview of the Ozone Source Receptor Model	A brief description of the OSRM model is given
Section 4 - Ozone in the UK: 2007 - Modelling Support for the Third Daughter Directive (Objective 1c)	Description of modelling and results from PCM and OSRM to characterise the UK ozone climate of 2007
Section 5 - Modelling for Policy Support (Objective 1)	Description of policy support using available tools and knowledge to guide policy implementation
Section 6 - Detailed Assessment of Relationship Between Ozone, Nitrogen Oxide and Nitrogen Dioxide Levels, and Factors Controlling Them (Objective 2)	Analysis of NO_x, NO_2 and O_3 monitoring data to understand the relationship between these pollutants to improve treatment in models
Section 7 - Improvements to Photochemical Reaction Schemes (Objective 3)	Further developments of the Master Chemical Mechanism and reduced schemes including expansion to include biogenic VOCs and code for secondary organic aerosols
Section 8 - Maintenance and Improvements to the OSRM and Comparison With Eulerian Models (Objective 4)	Assessment on the performance of the OSRM against recommendations of the Defra Review on tools for modelling tropospheric ozone and comparison with Eulerian models
Section 9 - Cost, Benefits and Trade-Offs: Volatile Organic Solvents (Objective 7)	Development of a methodology for assessing the costs and benefits of solvent reduction and substitution policies using results based on the MCM on impacts of solvents on ozone and PM
Section 10 - Other Project Activities	Description of other project activities, report, *ad-hoc* requests and publications
Section 11 - Conclusions and Policy Relevance	Summary of key conclusions of work and their policy relevance
Section 12 – Acknowledgements	

2 Overview of Project

2.1 Project Aims and Structure

The overall aim of this project is to maintain, develop, and apply tools for modelling tropospheric ozone formation and distribution over a range of spatial scales (global, regional and national). The modelling will be used to support and guide policy on emission reductions and objectives, and to verify policy compliance.

Since the start of the project, several of the main objectives have been modified or extended and one new objective was added. The programme of work now consists of 5 main objectives to meet the overall aims of the project (Objectives 5 and 6 were offered as options in the original proposal, but were not taken up).

Objective 1: **Policy development and scenario analysis**

Objective 2: **Detailed assessment of relationship between ozone, nitrogen oxide and nitrogen dioxide levels, and factors controlling them**

Objective 3: **Improvements to photochemical reaction schemes**

Objective 4: **Maintenance and Improvements to the OSRM and Comparison With Eulerian Models**

Objective 7: **Costs, Benefits and Trade-offs: Volatile Organic Solvents**

The linkages between these core objectives are shown in Figure 2.1.

Figure 2.1: Schematic showing linkages between different objectives

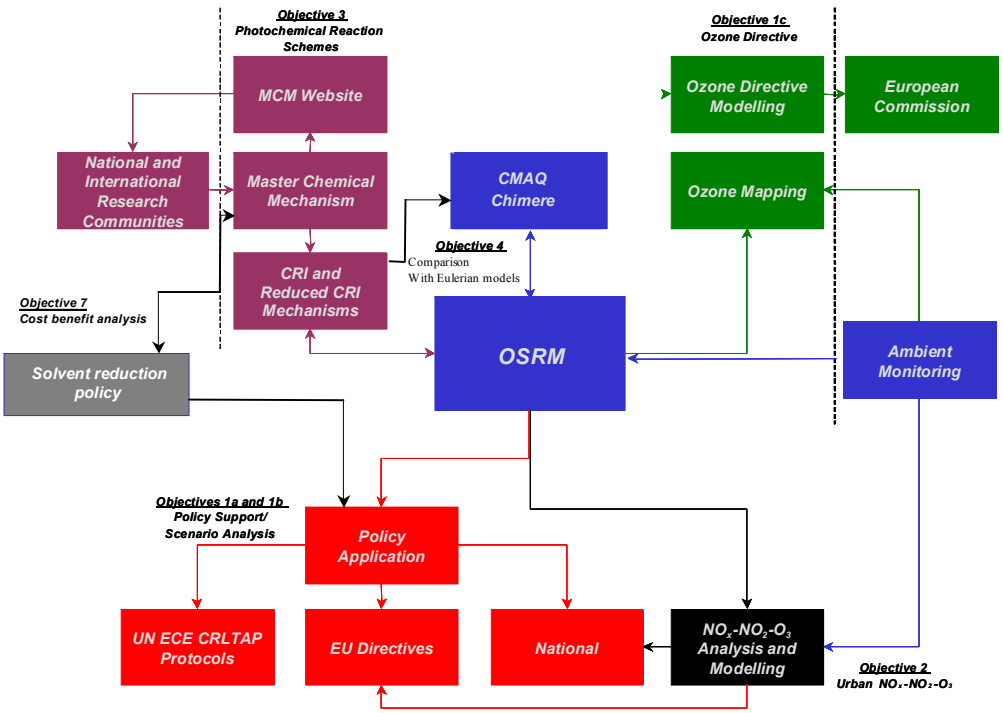

At the heart of this is the **Ozone Source Receptor Model (OSRM)**, developed in previous DEFRA tropospheric ozone modelling contracts and the now the main provider of health-and non-health-based

ozone concentration metrics on a national scale used for DEFRA ozone policy development. The OSRM simulates the chemical development of species in an air parcel moving along a trajectory to receptor points on a 10 x 10 km grid covering the UK. It uses real 6-hourly meteorological data for a calendar year to define 96-hour back trajectories to different receptor points, each trajectory picking up emissions within the EMEP domain and using a simplified chemistry scheme to simulate the photochemical production of ozone as the air parcel reaches each receptor point. The model provides national scale ozone concentration metrics and can demonstrate how these change in response to changes in emissions and meteorology. An overview of the OSRM is provided in Section 3 and more detail is given in Hayman et al. (2006a). Much of the model application work in this project is with the OSRM, but there are links between the OSRM and other models and tools used for ozone policy.

The **UK Photochemical Trajectory Model (UK PTM)** uses a linear trajectory under idealised anticyclonic, ozone episode conditions, to simulate photochemical ozone production as the air arrives at specific receptor sites over the UK. With its simplified description of meteorology, the UK PTM can accommodate large chemical schemes such as the Master Chemical Mechanism and therefore can examine policies aimed at targetting emissions of individual volatile organic compounds (VOCs). The UK PTM has been used to derive Photochemical Ozone Creation Potentials (POCPs) of over 100 different VOCs. More details of the UK PTM can be found in Derwent et al. (1998, 2004).

AEA's **empirical modeling approach** uses monitoring data from AURN network sites and empirical mapping techniques to develop maps of UK ozone concentration metrics reported under the 3rd Air Quality Daughter Directive. Bush and Targa (2005) have shown that the empirical modelling approach provides better agreement with monitoring data across the UK for the four concentration metrics reported annually to the Commission compared with output from the OSRM and thus it was decided in the last contract to use the empirical modelling approach to supplement measurement data reported to the Commission. This better agreement reflects the fact that monitoring data are used in both creating the rural field of the empirical maps and in calibrating the metrics in urban areas. However, while the empirical modelling approach does have some physical understanding of the processes occurring that influence ozone concentrations, the OSRM provides a better understanding of the fundamental photochemical processes occurring in ozone production in the UK. This means that in terms of ozone policy making, the OSRM is better suited than the empirical modelling approach at forecasting future ozone concentrations and how these might respond to changes in precursor emissions.

Thus the three modelling methods described are complementary:

- The **empirical modeling approach** provides the best means of quantifying and spatially representing the current UK ozone concentration climate;
- The **UK Photochemical Trajectory Model** provides the best means of quantifying how UK peak ozone concentrations at specific receptor sites will respond to changes in individual VOC emissions and demonstrating the relative reactivity of different VOC species;
- The **Ozone Source Receptor Model** provides the best means of forecasting ozone and associated health- and non-health-based metrics in a policy context on a UK-wide scale and the effect of changes in meteorology and changes in emissions caused by policy decisions.

While Objectives 2-4 are generally of a research nature and aimed at improving the understanding and treatment of chemical amd meteorological processes in ozone models, Objective 1 applies the existing models and knowledge to assisting with ozone policy. Thus Objective 1 is divided into three sub-tasks:

Objective 1a: **Modelling for national and international policy development –** using the OSRM and PTM to run scenarios relating to ozone policy

Objective 1b: **Support for policy implementation** – using available tools to guide policy implementation and provide general advice as required by DEFRA

Objective 1c: **Modelling support for the Third Daughter Directive –** using the empirical modelling approach and the OSRM to provide the modelling outputs (ozone metrics) to meet the

Supplementary Assessment Modelling requirements of the Third Air Quality Daughter Directive reporting each year.

The requirements of Objectives 1a and 1b are of an *ad-hoc* nature, as and when required by DEFRA and the DAs. Objective 1c represents an annual data delivery requirement.

The linkages between Objectives 1-4 shown in Figure 2.1 will bring the following benefits to the work:

- ✓ Linkage of scales. The work under Objective 2 on urban scale ozone production and ozone-NO_x-NO_2 relationships will have implications for ozone concentrations both in urban environments and downwind of urban centres. This could potentially have significant implications for policy modelling on the national scale using the OSRM and in improving the techniques for empirical mapping of ozone concentrations for reporting to the Commission (Objective 1).
- ✓ Improvements to the chemistry used in the OSRM ozone modelling tools will be made under Objectives 3 and 4 via development and application of reduced chemical schemes from the MCM. These improvements will be introduced into the version of the OSRM used for policy applications (Objective 1).
- ✓ Linking the Master Chemical Mechanism (MCM, Objective 3) to ozone modelling (Objective 1). The historic focus has been on increasing the number of VOCs in the MCM. One version of the MCM now treats the atmospheric oxidation of over 175 VOCs, representing 90% of the UK anthropogenic emissions. The insight gained from this work will be beneficial to the UK PTM applied in Objective 1.
- ✓ A comparison of the OSRM and UK PTM with UK-scale results from Eulerian models (Objective 4) will illustrate how Defra's main ozone policy tools compare against other state-of-the-art chemical transport models using different treatment of meteorology. The assessment of the Eulerian models will consider how flexible they are for introducing the robust chemical mechanisms developed from the MCM (Objective 3) and emissions data used in the OSRM.
- ✓ Linkages to other criteria used for developing policy controlling VOC emissions and ozone. Objective 7 shows how quantitative information from the MCM (Objective 3) can be part of the information used in wider Cost Benefit Analysis and Mulit-Criteria Analysis for assessing the costs, benefits and trade-offs of solvent reduction and substitution.

2.2 Project Partners

The project team for the main project encompassing Objectives 1-4 consists of a consortium of groups led by **AEA**. The other consortium partners are **Professor Dick Derwent (rdscientific), Dr Mike Jenkin (Atmospheric Chemistry Services) and Professor Mike Pilling (University of Leeds)**. Each of these partners will be undertaking specific tasks as shown in the schematic presented in Figure 2.2. **Dr Mike Holland (EMRC)** is the lead partner of Objective 7.

2.3 Project Schedule

The project schedule was revised in 2008 to take account of the expanded Objective 3, revised Objective 4 and new Objective 7. The current schedule for the project is shown in Figure 2.3.

The results of the work carried out in 2008 and progress made on each of the project objectives are described in the following Sections 4-10 with summary and conclusions presented in Section 11 of this report.

Figure 2.2 Schematic showing the involvement of consortium partners to the main project objectives

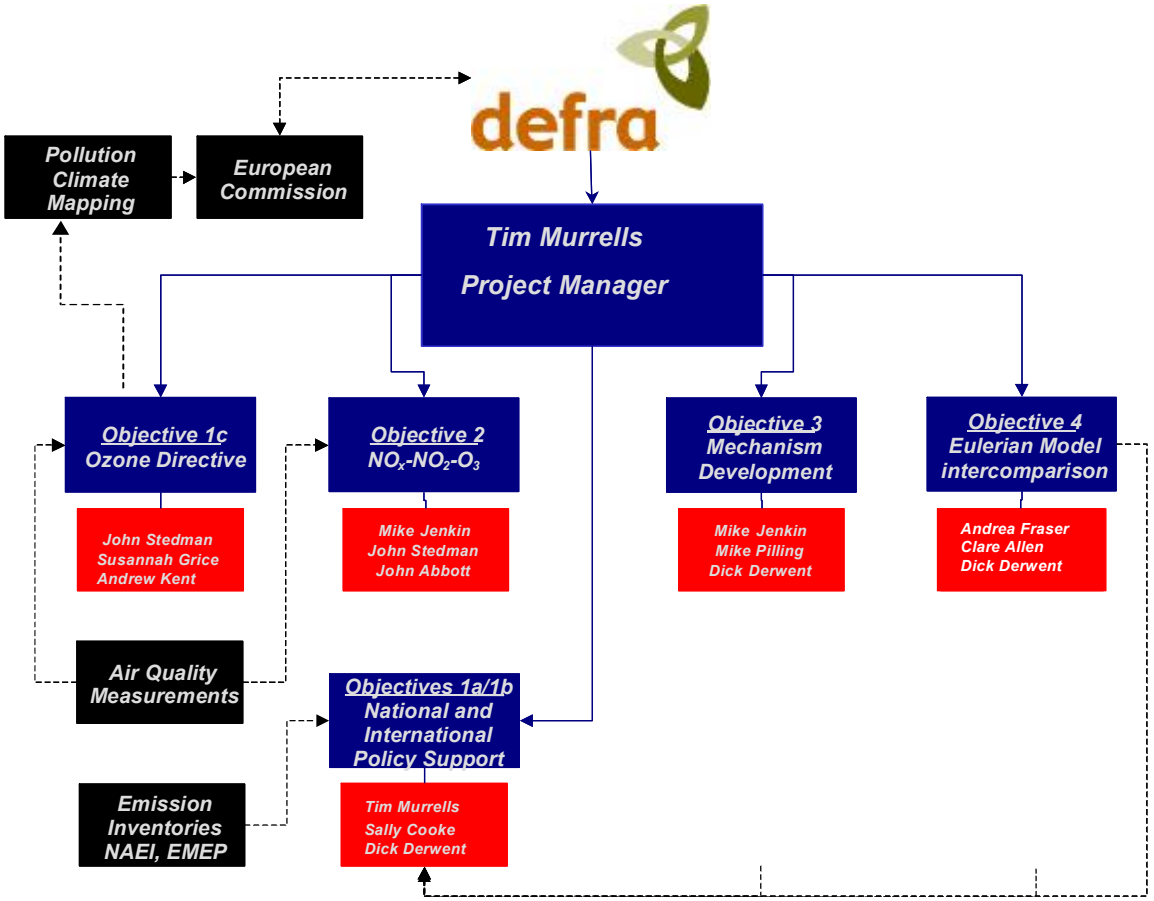

Figure 2.3: Project schedule

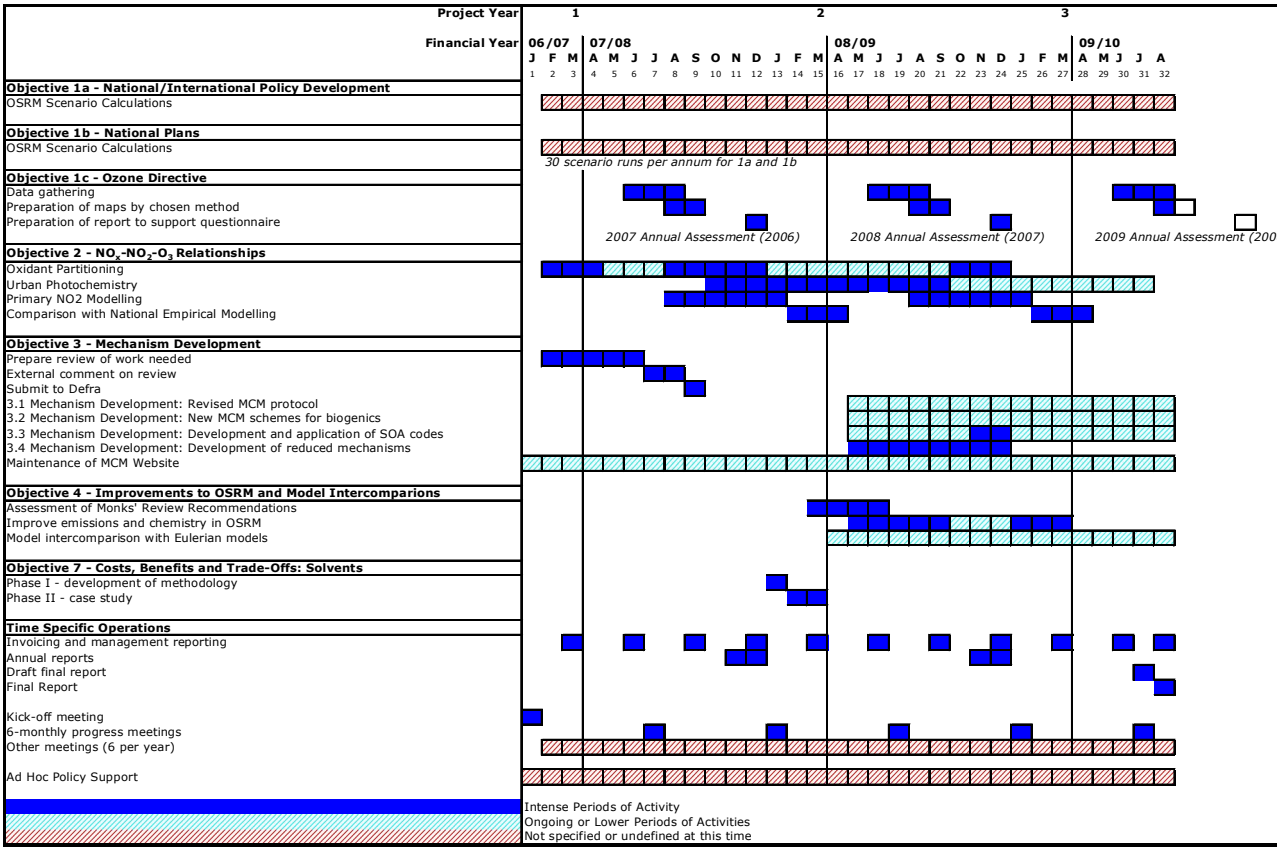

3 Overview of the Ozone Source Receptor Model

The Ozone Source Receptor Model (OSRM) is model developed to describe photochemical ozone production in the UK (Hayman *et al.*, 2002, 2005; 2006a). The OSRM covers the EMEP model domain and uses global meteorological datasets provided by the Met Office to derive 96-hour back trajectories to specified receptor sites (UK/EMEP monitoring sites or a 10km x 10km grid covering the UK). The chemical scheme is based on that used in the STOCHEM model. The mechanism has ~70 chemical species involved in ~180 thermal and photochemical reactions. The mechanism represents ozone formation using 12 VOCs, which provides an appropriate description of ozone formation on the regional scale. The emission inventories are taken from EMEP for Europe with the option to use National Atmospheric Emissions Inventory (NAEI) data for the UK, which have been aggregated to 10 km x 10 km and into 8 key sectors. A slightly fuller description of the model is given in Box 3.1.

The OSRM describes the boundary layer by a single box and assumes that this is well mixed. When the model is required to handle and generate concentrations of species near to the surface, account must be taken of surface removal processes (dry deposition and chemical reactions) and emissions that will generate gradients in the concentrations of ozone and oxides of nitrogen. This will result in lower and higher concentrations, respectively, of these species compared to their corresponding mid-boundary layer concentrations. These effects are of particular significance in urban areas. An algorithm has been developed and implemented in an OSRM post-processor to convert the hourly mid-boundary layer concentrations to surface concentrations. The algorithm uses the meteorological parameters characterising the boundary layer, surface roughness appropriate for the surface types considered, resistance parameters for O_3 and NO_2, the local NO_x emission rates and a simple NO-NO_2-O_3 photostationary state chemistry.

From the hourly concentrations, the post-processor calculates a large number of different metrics for ozone and nitrogen dioxide and produces output datafiles for generating maps of these metrics.

The OSRM has been tested by comparison with results from monitoring data. More details of the model performance are given in Hayman et al (2006a). Overall, the OSRM is a model which has a robust and flexible construction that makes it ideal for the demands of assisting in the development of policy. The improvements made to the OSRM during the previous modelling contract produced a model that is able to reproduce boundary-layer concentrations of ozone and oxides of nitrogen, representative of the UK.

In the context of ozone formation, the OSRM and UK Photochemical Trajectory Model were found to give identical output and responses, on a like-for-like basis. For the determination of surface concentrations of ozone and oxides of nitrogen, the OSRM has post-processor options, which take account of local emissions and removal processes. The comparison of the OSRM with the ADMS Urban model gave similar responses and showed similar spatial patterns. These comparisons demonstrate that, through the successful development to the current version, the OSRM provides a consistent and robust modelling tool, able to support the Department in the development of policy based upon strong science.

Box 3.1: Description of the Ozone Source Receptor Model

The OSRM is similar in concept to the UK Photochemical Trajectory Model (UK PTM) [Derwent *et al.*, 1998, 2004] in that it simulates the chemical development of species in an air parcel moving along a trajectory and to the ELMO source-receptor model [Metcalfe *et al.*, 2002] in that calculations can be undertaken to a 10 km x 10 km grid covering the UK. The OSRM (version 2.2a) has a number of features:

- **Air Mass Trajectories**: Realistic two-dimensional air mass trajectories are derived from wind fields extracted from meteorological datasets. Meteorological datasets are available for use with the OSRM for the years 1995 to 2007;
- **Meteorology**: The boundary layer depth and other meteorological parameters characterising the boundary layer are interpolated in space and time from the input meteorological datasets;
- **Chemical Mechanisms**: Three chemical mechanisms have been developed for use in the OSRM (a) the chemical mechanism used in the ELMO or STOCHEM models, (b) a modified and extended version of chemical mechanism used in the ELMO or STOCHEM models. The chemical mechanism has been modified to include the formation of HONO and organic nitrates and a more extensive chemistry of NO_3, (c) version 1 of the Common Reactive Intermediate mechanism and (d) a reduced version of the Common Reactive Intermediate mechanism where the CRI concept has been used for the VOCs used in the mechanism. The modified STOCHEM mechanism is currently used in the OSRM. The table below provides details of these chemical mechanisms;

Table: *Details of the Chemical Mechanisms used in the OSRM.*

	STOCHEM	Modified STOCHEM	Mini-CRI	Mini-CRI
# of Species	70	70	70	280
# of Reactions	154	180	198	
# of VOCs	12	12	12	125
Emitted VOCs	➢ **alkanes** (ethane, propane, *n*-butane) ➢ **alkenes** (ethene, propene) ➢ **aromatics** (toluene, *o*-xylene) ➢ **oxygenated VOCs** (methanol, acetone, methyl ethyl ketone, formaldehyde, acetaldehyde)	➢ **alkanes** (ethane, propane, *n*-butane) ➢ **alkenes** (ethene, propene) ➢ **aromatics** (toluene, *o*-xylene) ➢ **oxygenated VOCs** (methanol, acetone, methyl ethyl ketone, formaldehyde, acetaldehyde)	➢ **alkanes** (ethane, propane, *n*-butane) ➢ **alkenes** (ethene, propene) ➢ **aromatics** (toluene, *o*-xylene) ➢ **oxygenated VOCs** (methanol, acetone, methyl ethyl ketone, formaldehyde, acetaldehyde)	➢ **alkanes** ➢ **alkenes** ➢ **dienes** ➢ **alkynes** ➢ **aromatics** ➢ **oxygenated VOCs** ➢ **chlorinated VOCs** ➢ **biogenic VOCs**
Biogenic VOCs	Isoprene	isoprene	isoprene	isoprene, pinene
VOC speciation	NAEI 1998	NAEI 1998	NAEI 1998	NAEI 1998, 2000

- **Photolysis Rates**: Photolysis rates have been calculated off line using a modified version of the PHOTOL code. The input database contains the dependence of photolysis rates for 17 species on zenith angle, cloud cover, land surface type and column ozone;
- **Emissions:** The model uses up-to-date emission inventories for nitrogen oxides, volatile organic compounds, carbon monoxide and sulphur dioxide taken from UK (National Atmospheric Emission Inventory) and European (EMEP) sources. The emissions of each pollutant have been divided into to 8 broad source categories (solvent usage, road transport, industrial processes, power generation, fossil fuel extraction and delivery, domestic combustion, natural and other). The assignment of the ~600 VOCs in the UK speciated VOC emission inventory to the 13 model VOCs was based on reactivity and structural considerations.
- **Temporal Emission Factors**: The OSRM converts the annual emission estimates to instantaneous emission rates using temporal profiles for the emissions of NO_x, VOCs, SO_2 and CO generated by Jenkin *et al.* [2000a]. These profiles were derived either from real activity data or by using one of small set of default profiles.
- **Biogenic VOC Emissions:** An additional emission term is added to the emission rate of isoprene to represent the natural biogenic emissions from European forests and agricultural crops. The emission estimates can either be the same as those used in the UK PTM and taken from Simpson *et al.* [1995] or

the new biogenic inventory produced using the PELCOM land cover dataset and the TNO tree species inventory;

- **Dry Deposition**: Dry deposition processes are represented using a conventional resistance approach, in which the rate of dry deposition is characterised by a deposition velocity. Different deposition velocities are used over land and sea. The ozone deposition velocity over land has an imposed diurnal and seasonal cycle.
- **Initialisation**: The concentrations of O_3, CO, CH_4, C_2H_6, HNO_3 and PAN are initialised on each OSRM trajectory using output from the global tropospheric STOCHEM model.

A single trajectory calculation using the backwards-iterative EULER solver with a chemical timestep of 240s takes ~0.025 s (i.e., ~40 trajectories per second) using a Dell Precision Workstation 650 MiniTower (containing dual Intel® Xeon 3.06GHz processors). Making use of the two available processors on the workstation gives a runtime of ~4.5 days for a UK-scale model run to ~3,000 receptor sites for a calendar year.

4 Ozone in the UK: 2007 - Modelling Support for the Third Daughter Directive (Objective 1c)

Directive 96/62/EC on Ambient Air Quality Assessment and Management (the Framework Directive) establishes a framework under which the EU sets limit values or target values for the concentrations of specified air pollutants. Directive 2002/3/EC (the third Daughter Directive) sets Target Values (TVs) and Long-term Objectives (LTOs) to be achieved for ozone.

2007 is the fourth year for which an annual air quality assessment for the third Daughter Directive pollutants is required. A questionnaire has been completed for submission to the EU containing the results of this air quality assessment along with those required for the first and second Daughter Directives. The assessment takes the form of comparisons of measured and modelled air pollutant concentrations with the Target Values and Long-term Objectives set out in the Directives.

Air quality modelling of ozone is necessary to supplement the information available from the UK national air quality monitoring networks. In the previous tropospheric ozone modelling contract, AEA submitted a report evaluating the suitability of the OSRM and an empirical model calibrated to ozone data from network monitoring sites for providing the supplementary modelling data. It was proposed then and confirmed for this contract that the empirical modelling approach should continue to be used to provide the supplementary modelling data for the Commission as this provides better agreement with monitoring data for the key ozone metrics, but that each year the performance of the OSRM would be re-evaluated against the outputs from the empirical model.

The empirical modelling is based on assessments of ozone monitoring data for the relevant calendar year. The OSRM calculates ozone concentrations from relevant emissions data and real meteorological data for the relevant calendar year. Completion of the air quality questionnaire specified by the Commission and based on the monitoring data and empirical model results is carried out under AEA's Pollution Climate Mapping contract with Defra. The questionnaire submitted each year is accompanied by a report on the Supplementary Assessment Modelling for the 3rd Daughter Directive on Ozone Reporting. The Third Daughter Directive report that relates to ozone is written separately from, but in parallel with, the report covering the other Daughter Directive pollutants. The Third Daughter Directive report details the modelling methodology used to derive 1x1 km resolution maps of ambient air quality for ozone over the UK and presents modelled and measured data to illustrate instances where the European objectives have been exceeded.

The Supplementary Report for 2007 based on the empirical modelling has been prepared (Kent and Stedman, 2008a). The metrics covered by the report include:

- Days greater than 120 $\mu g\ m^{-3}$ (2006) (Long Term Objective for Human Health)
- Days greater than 120 $\mu g\ m^{-3}$ (2004-2006) (Target Value for Human Health)
- AOT40 (2006) (Long Term Objective for Vegetation)
- AOT40 (2002-2006) (Target Value for Vegetation)

This is the third year for which data from Gibraltar has been included in this report. Although no modelling is performed for Gibraltar, measured data from the continuous automatic air monitoring campaign is used in the assessment.

Section 4.1 summarises the empirical modelling approach and the results submitted to the Commission for 2007. Section 4.2 provides model results from the OSRM for 2007 and compares results with those from the empirical modelling method.

4.1 Empirical Modelling of Ozone in the UK in 2007

4.1.1 Methodology

The modelling and mapping for 2007 used the same methodology as for 2006. Measured ozone concentrations from rural monitoring sites in the UK's national networks are used to interpolate a rural background map of ozone concentrations for each metric. This map will overestimate concentrations in urban and roadside locations where titration with NO_x will lower ozone concentrations. The scavenging influence of NO_x concentrations is accounted for by calculating a percentage decrement that represents the changing ozone concentrations with changing NO_x concentrations. This decrement is subtracted from the interpolated rural map.

This method more easily facilitates alterations to the different model components, making the model more flexible and tailored for future scenario based work.

The preliminary assessment carried for the First Air Quality Daughter Directive (AQDD1) defined a set of zones to be used for air quality assessments in the UK based on population and urban areas data from the 1991 UK Census. These data have now been updated using information on populations from the 2001 Census and land-use data from the Devolved Administrations. Information on the definition of zones is included in Form 2 of the questionnaire. The zones are of two types: agglomeration zones (continuous urban areas with a population in excess of 250,000) and non-agglomeration zones. There are 28 agglomeration zones and 15 non-agglomeration zones, giving a total of 43 zones in the UK. The non-agglomeration zones in England correspond to the Government Office Regions, while those in Scotland, Wales and Northern Ireland were defined in conjunction with the Devolved Administrations.

The preliminary assessment for ozone also defined the monitoring and modelling requirements for each zone based on an assessment of concentrations in relation to Target Values (TVs) and Long Term Objectives (LTOs) specified by the Third Air Quality Daughter Directive. The minimum monitoring requirement for ozone and NO_x in the majority of zones was found to be at least one monitoring site per zone, with the monitoring results to be supplemented with information from modelling studies.

4.1.2 Results from Empirical Modelling

The summary of the report results is presented in Tables 4.1 to 4.4 below that show the number of zones exceeding the Directive objectives using both the monitoring data and the model results. Further details are given in Kent and Stedman (2008a).

Table 4.1: UK summary results of air quality assessment relative to the Target Values for ozone for 2010

Target Value	*Number of zones exceeding*
Max Daily 8-hour mean Target Value	none
AOT40 Target Value	none

Table 4.1 is a summary of the number of UK zones and agglomerations exceeding the Target Value for ozone. The Target Values are based on multi-year metrics for both health (averaged over 3 years) and vegetation (averaged over 5 years). Due to the averaging involved in the calculation of these metrics, even comparatively high ozone years can be averaged down by historic (often lower) data so these metrics tend to be less stringent than the corresponding single-year Long-Term Objectives. This assessment also incorporated monitoring data from the UK national networks.

Table 4.2: UK summary results of air quality assessment relative to the Long-term Objectives for ozone

Long-term Objective	Number of zones exceeding
Max Daily 8-hour mean Long-term Objective	41 zones (24 measured + 17 modelled)
AOT40 Long-term Objective	3 zones (1 measured + 2 modelled)

Table 4.2 is the corresponding summary table for the Long-Term Objective metrics for health and vegetation. These metrics are far more sensitive to high ozone years because they are based on only a single year of data and therefore there is no averaging out of high values. The year 2007 was a relatively low ozone year, but still shows zones exceeding the Long Term Objective.

Maps showing the Long Term Objective and Target Value ozone metrics for human health (days greater than 120 µgm^{-3}**)** and vegetation (AOT40) are shown in Figures 4.1 and 4.2. Figure 4.1 shows there were no areas in 2007 where the number of days with the maximum daily 8-hour mean exceeding 120 µg m^{-3} (the human health metric) was greater than the 2010 target threshold of 25 days. The areas with the most number of days exceeding the objective concentration threshold tended to be in the east of England. Averaged out over the 3 year period (2005-2007), the number of days of exceedences were higher in this region. This was because of the high ozone levels reached in 2006 (a high ozone year), but still nowhere exceeds the 25 day threshold.

Figure 4.2 shows that there were no areas that exceeded the AOT40 target threshold of 18,000 µg m^{-3} .hours in 2007, but there were areas in East Anglia and the south-east of England that exceeded the Long-Term Objective of 6,000 µg m^{-3} .hours. Averaged over the last 5 year period (2003-2007), the AOT40 values are generally higher than for the single year 2007, again because of including the high ozone year of 2006, but there were no areas exceeding the 18,000 µg m^{-3} .hours Target Value threshold, even when averaged over these years.

The corresponding summary results for Gibraltar are shown in Tables 4.3 and 4.4.

Table 4.3: Gibraltar summary results of air quality assessment relative to the Target Values for ozone for 2010

Target Value	*Number of zones exceeding*
Max Daily 8-hour mean Target Value	none
AOT40 Target Value	none

Table 4.4: Gibraltar summary results of air quality assessment relative to the Long-term Objectives for ozone

Long-term Objective	*Number of zones exceeding*
Max Daily 8-hour mean Long-term Objective	1 zone (measured)
AOT40 Long-term Objective	1 zone (measured)

4.1.3 Empirical Model verification

Tables 4.5 and 4.6 show the average measured and modelling concentrations at sites in the AURN (used to calibrate the model) and at verification sites (completely independent of the model).

Table 4.5: Summary statistics for comparison between modelled and measured number of days exceeding 120 µg m^{-3} as a maximum daily 8-hour mean

		Mean of measurements (days)	Mean of model estimates (days)	r^2	% outside data quality objectives	No. sites
National Network	2007	2.0	2.1	0.59	44	71
Verification Sites	2007	2.4	3.5	----- *	100	8
National Network	2005-7	6.1	6.0	0.76	20	71
Verification Sites	2005-7	8.3	7.2	0.24	24	17

* negative slope - r^2 not presented

Table 4.6: Summary statistics for comparison between modelled and measured AOT40 vegetation metric

		Mean of measurements (µg.hours)	Mean of model estimates (µg.hours)	r^2	% outside data quality objectives	No. sites
National Network	2007	2281	2321	0.73	24.4	78
Verification Sites	2007	3061	2856	----- *	12.5	8
National Network	2003-7	5138	4344	0.72	8.3	72
Verification Sites	2003-7	6347	4910	0.23	17.6	17

* negative slope - r^2 not presented

These statistics are standard Pollution Climate Mapping empirical model summary outputs that are also used for other pollutants modelled for the Daughter Directives. They show averages of the measured metric, corresponding averages of the modelled metric, the correlation coefficient of plotted measured *vs*. modelled concentrations (R^2, presented in verification plots in the main report), the number of sites used in the assessment and the percentage of these sites that fall outside the +/- 50% data quality objective (DQO) range. The table shows these for National Network sites (AURN sites used in the model) and for Verification sites (independent sites that are suitable for assessing model performance). Comparisons have been made for single years (corresponding to the Long Term Objectives (LTOs)) and for multiple years (corresponding to the Target Values).

In 2007, for the number of days exceeding 120 µg m^{-3} as a maximum daily 8-hour mean metric, half of the verification sites were under estimated, lying outside the +50% DQO and half were over estimated, lying outside the –50% DQO. Table 4.5 suggests that in general, the model over predicts concentrations across all sites with a difference of 1.1 between the number of measured and the number of modelled days above 120 µg m^{-3}. The r^2 value has not been presented in Table 4.5 for verification sites because the relationship is negative as a result of the Thanet rural site which was predicted with 9 days above 120 µg m^{-3} but which recorded zero in 2007. All of the verification sites in 2007 were outside the +/50% DQO range. The National network sites display much better agreement between measured and modelled figures because these sites were used to generate the relationships used in the model.

There is better model performance for the multi-year 2005-2007 (TV) model compared with the 2007 (LTO) model. This is because the model performs best in years where ozone concentrations are higher. In 2007 ozone concentrations were particularly low whereas the multi-year model still contains data from the high ozone year of 2006. Again, the model results for the National network sites are shown to closely match the corresponding measured values which is because these sites were used to generate the relationships used in the model. The verification sites in Table 4.5 illustrate a slight under estimation.

For AOT40, with the exception of the Thanet rural site the verification sites generally suggested a slight under estimation by the model for 2007. This is reflected in the Table 4.6 which presents the summary statistics for the comparison between modelled and measured ozone concentrations. However, the results for the AOT40 metric are more encouraging that those for the number of days greater than 120 µg m^{-3} and all but one of the verification sites (Thanet rural, for which the modelled value was significantly in excess of that measured) was located within the +/- 50% DQO range.

There was more variation in the multi-year metric (TV) and the under estimation was more notable in this metric than in the single year model (LTO), as shown in Table 4.6. More verification sites were available for comparison of this metric given the several years across which the metric is calculated. This explains the difference between the 8 sites used for 2007 and the 17 used for 2003-2007.

Figure 4.1: Long-term Objective (2007) and Target Value (2005-2007) for Human Health

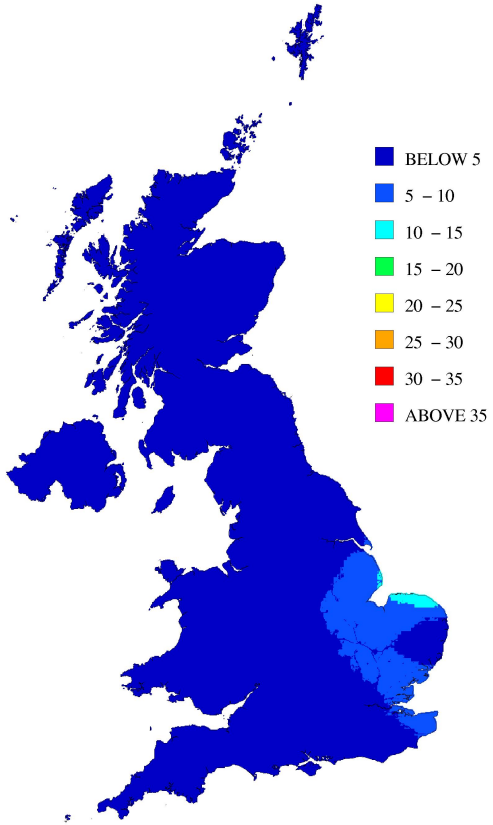

Days greater than 120 μg m^{-3} (2007)

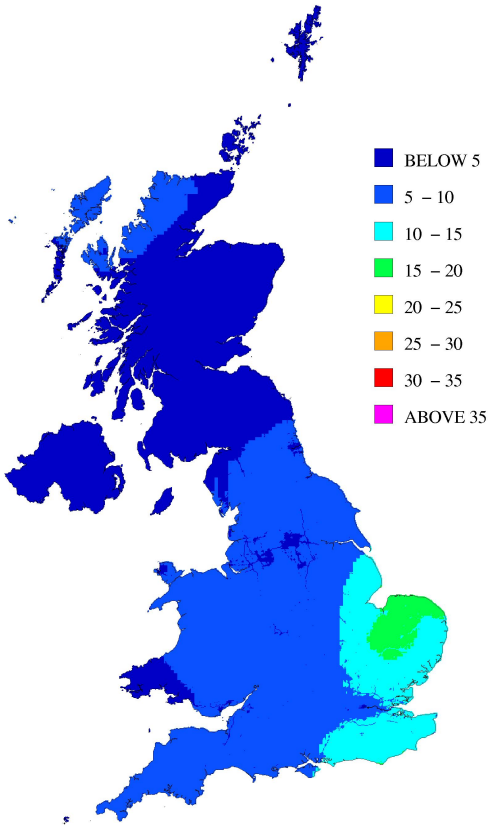

Days greater than 120 μg m^{-3} (2005-2007)

Figure 4.2: Long-term Objective (2007) and Target Value (2003-2007) for Vegetation

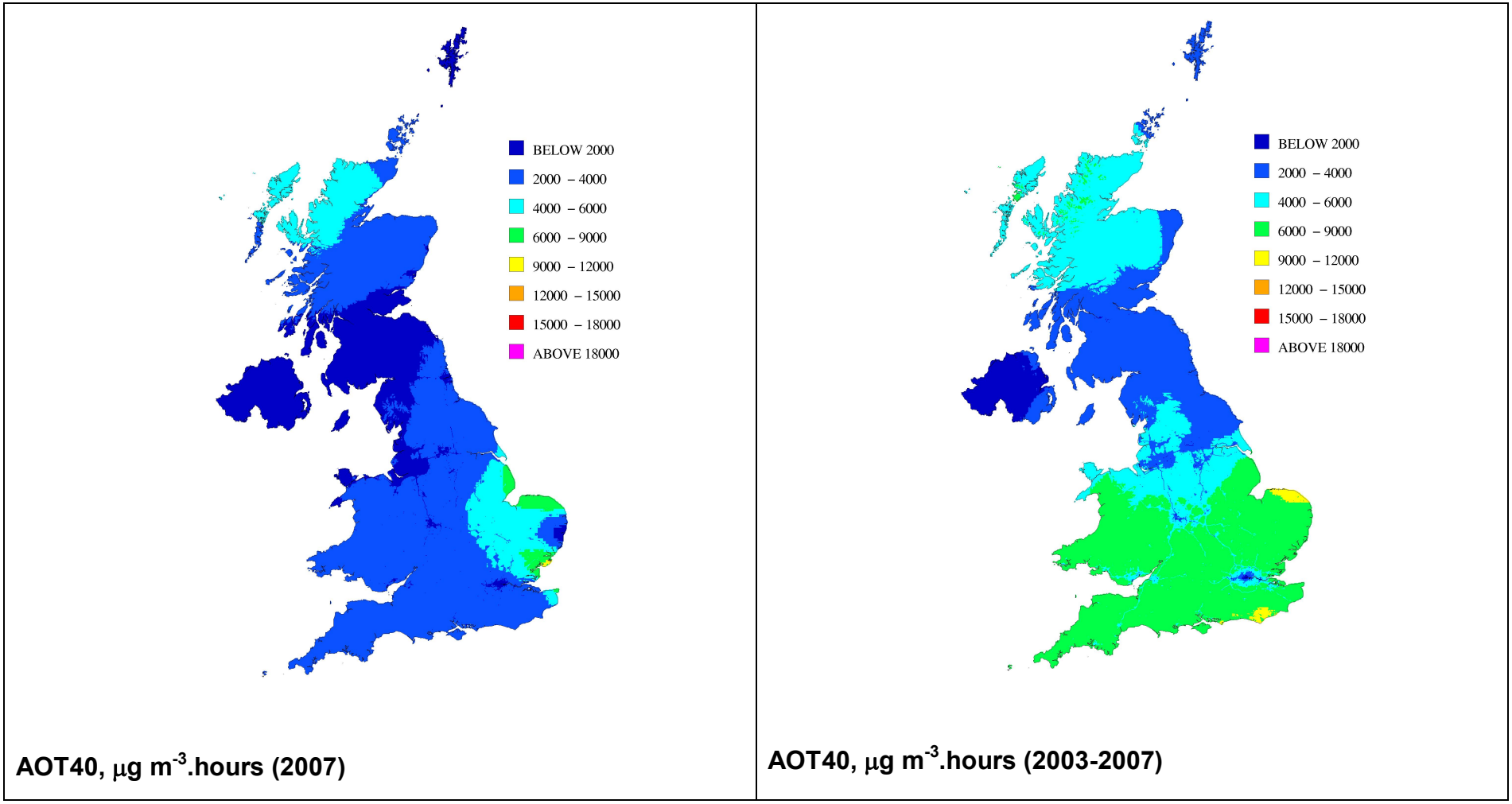

4.2 OSRM Modelling of Ozone in the UK in 2007 and Comparisons with the Empirical Model

The previous tropospheric ozone modelling contract had shown that the empirical modelling approach used in the Pollution Climate Mapping (PCM) model traditionally gives results for ozone concentration metrics that are more representative of the measured concentrations in model verification than corresponding outputs provided by the OSRM. Hence, the PCM empirical model is used to provide outputs submitted to the European Commission on behalf of Defra, as described in Section 4.1. The OSRM, on the other hand, has a stronger role to play in scenario analysis and policy development as the OSRM can model future emission scenarios.

The OSRM is a process-based Lagrangian model with a surface conversion post-processor using emissions and realistic meteorological data to calculate ozone concentrations so has the capability to be used for future year scenario modelling using alternative emissions and meteorological data fields.

The PCM is mainly an empirical model based on actual measurements data incorporating some process-based components, but is not so well suited for future scenario modelling.

Each year both models are verified against measured data to provide confidence in their performance. It is also useful to check the model results against each other in order to make clear and informed decisions about how best to use each model for their respective strengths. The two models have been compared in previous years, most recently for 2004 and 2005, which were noted as relatively "low ozone" years (Hayman et al, 2006a), and 2006 which was a relatievly "high ozone" year (Murrells et al, 2008). Ozone concentrations in 2007 were particularly low. The maximum hourly concentration in the UK was 168 µg m^{-3} (Blackpool Marton) in 2007, compared to 278 µg m^{-3} (Wicken Fen) in 2006.

The performance of the OSRM for 2007 was demonstrated using the two Long-Term Objective (LTO) metrics used in the Third Daughter Directive reporting that correspond to the specific calendar year 2007:

- Days greater than 120 µg m^{-3} as a maximum daily running mean (Long Term Objective for Human Health)
- AOT40 (Long Term Objective for Vegetation)

The multi-year Target Value metrics will not be as good an indicator of model performance during a low ozone year as the Long-Term Objective metrics because averaging over several years will lessen the contribution of ozone concentrations associated with a particular year. For this reason, the metrics that this report has concentrated on are the single year (2007) metrics for human health and vegetation.

OSRM runs for 2007 were made by implementing 6-hourly meteorological data provided by the Met Office and using UK emissions inventory data for 2007 based on projected figures from the the 2006 version of the NAEI.

4.2.1 Comparison of Maps of OSRM and PCM Outputs for Ozone Metrics in 2007

The maps that have been generated from the outputs of the OSRM and empirical PCM model for both the health and vegetation Long-Term Objective metrics are presented in Figures 4.3 to 4. 6. Figure 4.3 presents the map of the number of days exceeding 120 µg m^{-3} in 2007 from the OSRM and Figure 4.4 shows the same metric output from the PCM empirical model. Figure 4.5 shows the OSRM map for the AOT40 metric in 2007 and Figure 4.6 shows the corresponding map from the PCM empirical model. Figures 4.4 and 4.6 are the same as the PCM Long-term Objective (2007) maps shown in Figures 4.1 and 4.2, respectively.

Both the PCM and OSRM maps look broadly similar to maps produced for 2004. These are presented in a previous report (Hayman et al, 2006b). That year, 2004, was also a low ozone year and similar

effects, such as the high concentrations in Eastern Scotland, can be seen on those maps too, though the OSRM AOT40 map for 2007 shows generally higher concentrations than 2004.

With 2007 being a low ozone year, the NO_x titration effect is not as apparent as it had been in 2006. Only the OSRM and PCM AOT40 maps identify areas of ozone depletion due to NO_x titration in large city areas and major roads. The number of days above 120 µg m^{-3} metric maps do not show the NO_x titration effect as the values are too low. The PCM model has a finer resolution (1km) than the OSRM (10km), so it identifies areas such as larger cities and major roads more readily than the OSRM. The empirical model utilises a modelled NO_x map (described in Kent and Stedman, 2008b) with a coefficient to describe the decrement in ozone concentrations with increased NO_x. The OSRM uses the surface conversion post-processor in conjunction with NAEI NO_x emission maps to account for the effects of NO_x titration on local ozone concentrations.

The typical gradient seen in previous years, decreasing from higher concentrations in the south to lower concentrations in the north cannot be seen in any of the maps of the metrics for 2007 because the concentrations were so low. In both the OSRM and PCM maps for the number of days above 120 µg m^{-3} most of the UK is below 5 (the lowest division on the mapped scale). The usual pattern is a natural feature of the increase frequency and magnitude of photochemical events in the more southerly and easterly areas of the UK. It has been suggested (Hayman et al, 2006b) that the relatively high concentrations in the north of Scotland may be the result of higher hemispheric background ozone concentrations here being represented in the model or intrusions of stratospheric ozone. This seems to have a relatively large effect on the OSRM results in 2007.

The OSRM shows broadly similar patterns to the empirical maps, however there are some specific spatial differences. The OSRM maps estimate notably higher concentrations of ozone in the south west of the country over Cornwall that have not been captured in the corresponding empirical maps. Both models show a higher number of days greater than 120 µg m^{-3} caused by higher concentrations in East Anglia than most of the rest of the UK. The majority of the higher ozone concentration areas identified by OSRM in 2007 are in coastal fringe areas. This is consistent with OSRM outputs from previous years. The PCM map for the AOT40 metric differs from 2004, but is similar to 2005 (the slightly higher ozone year) in that there are higher concentrations predicted in north-west Scotland. An unusual feature of the OSRM output is that coastal regions of north-eastern Scotland together with the Orkney and Shetland Islands are estimated to have high concentrations. This is unlikely given the latitude of these regions. This effect had been seen in previous OSRM modelled years and it has been suggested by Hayman et al (2006b) that this coastal 'edge effect' might be the result of the lack of ozone deposition over the sea surface or limitations of meteorological datasets. 2007 was a low ozone year and this effect is even more visible than in the higher ozone year (2006).

The highest modelled value of both the AOT40 and the days greater than 120 µg m^{-3} metrics in the empirical map were located in East Anglia and resulted from the high measured concentrations from the Wicken Fen monitoring site. The highest AOT40 and days greater than 120 µg m^{-3} values on the OSRM map are in north-west Scotland, possibly as a result of the higher hemispheric background and intrusions of stratospheric ozone accounted for in the model. On the OSRM map for the days greater than 120 µg m^{-3} metric some coastal locations display higher concentrations than inland (Scottish coast and Orkneys and Shetlands). The OSRM map for the AOT40 metric is quite different to the PCM map. The highest concentrations are in coastal north-east Scotland and south-west England.

Figure 4.3. Number of days exceeding 120 µg m^{-3} (2007) (OSRM map)

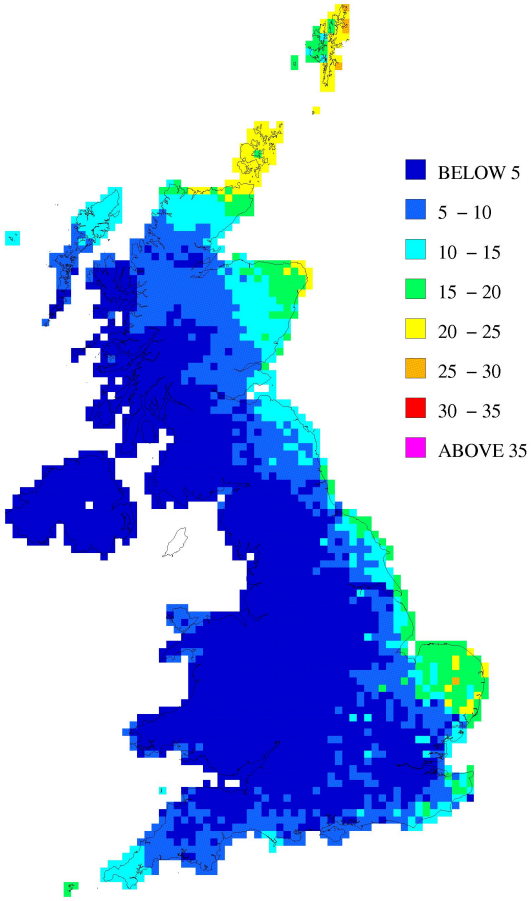

Figure 4.4. Number of days exceeding 120 µg m^{-3} (2007) (PCM empirical map)

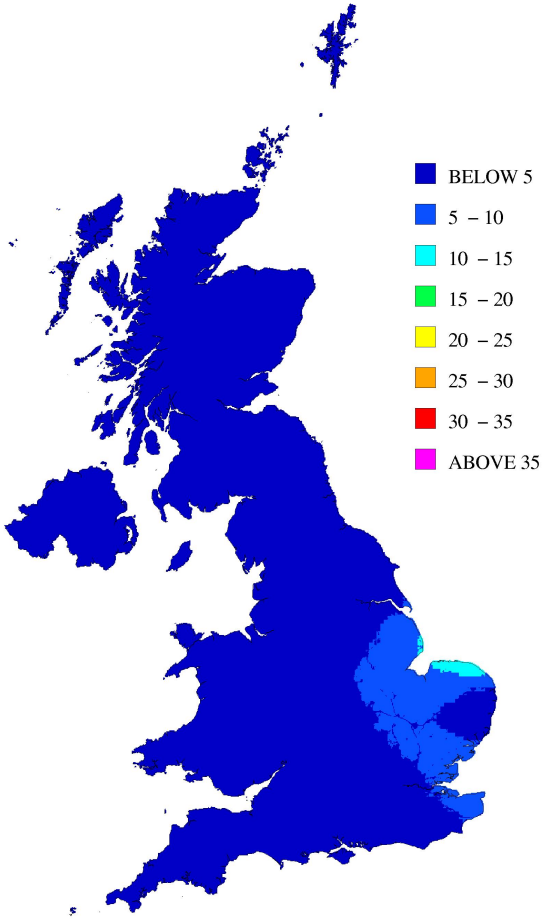

Figure 4.5. AOT40 (µg m^{-3}.hours) (2007) (OSRM map)

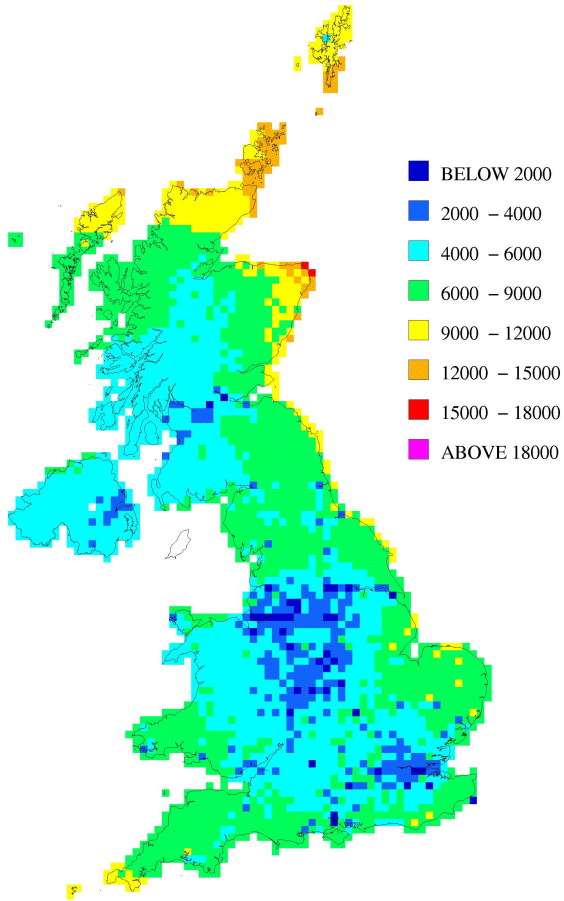

Figure 4.6. AOT40 (2007) (µg m^{-3}.hours) (PCM empirical map)

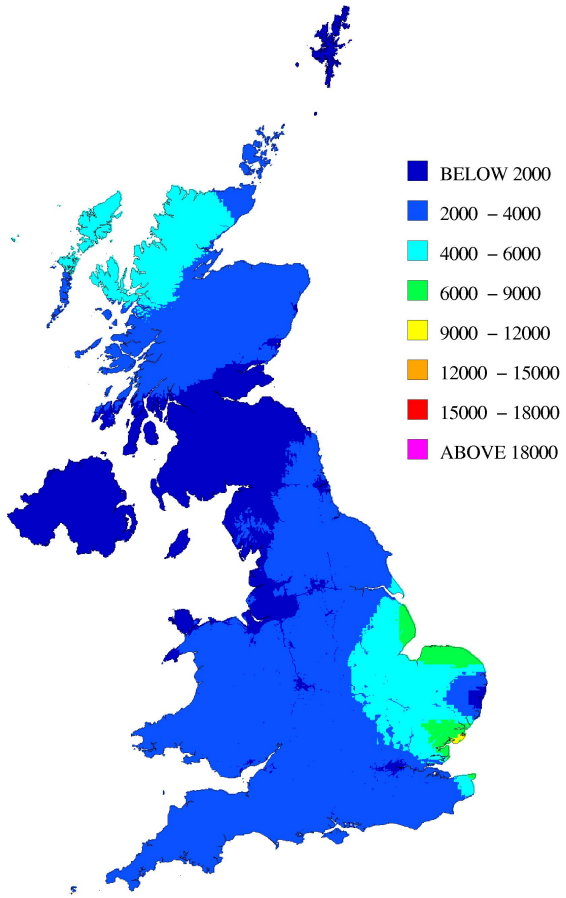

4.2.2 Verification of OSRM and PCM Outputs for Ozone Metrics in 2007

An evaluation of OSRM and PCM model performance has been undertaken, comparing model results for 2007 with measured concentrations from monitoring campaigns around the UK and against each other.

The model verification is represented in scatter plots comparing the model outputs with the corresponding measured metrics at ozone monitoring sites around the UK (Figures 4.7-4.10) for OSRM and the PCM empirical model for the same health- and vegetation-based Long-Term Objective metrics as compared in the maps. Two groups of sites are presented in the verification charts and summary tables:

- national network (AURN) monitoring sites
- verification sites

The AURN sites were used as a direct input to the PCM empirical model and therefore provide a useful check during the verification process, but are not able to provide a completely independent representation of model performance. For this reason there are a separate group of sites labelled 'verification sites' that are completely independent from the model. These typically come from local authorities, research institutions and *ad-hoc* monitoring campaigns for which AEA holds and ratifies the data. These monitoring data are ratified to the same standard as the AURN. Both groups of sites provide an independent verification of the OSRM because this is a process model which does not use monitoring data as an input or a calibration method. A data capture threshold of 75% has been applied to the monitoring data prior to analysis.

The verification charts also present a 1:1 line and lines representing the data quality objectives (DQO) defined in the third Daughter Directive (+/- 50%).

Corresponding summary tables (Tables 4.7 to 4.10) are also provided which display the average of measured concentrations, the average of the modelled estimates, the R^2 of the fit line, the number of monitoring sites used and the percentage of these monitoring sites that fall outside the DQO.

The OSRM days greater than 120 µg m^{-3} verification presented in Figure 4.7 and Table 4.7, show that there is a high degree of scatter across all sites in 2007. **In general the OSRM over predicted the measured metric**. Table 4.7 suggests that the model performance was better for the national network sites than the verification sites, but there is a high degree of scatter in both groups of sites. The percentage of sites outside the DQO range was high (62.5%) for the verification sites and less high (39.4%) for national network sites.

Figure 4.8 shows that the PCM empirical map of the days greater than 120 µg m^{-3} metric showed no obvious bias. However, the percentage of sites outside the data quality objective for both the national network (43.7%) and verification sites (100%) is larger than for the OSRM map. Table 4.8 shows that the average modelled and measured results are similar for both the national network sites and fairly similar for the independent verification sites that provide a more meaningful indicator of model performance.

For the AOT40 metric, the OSRM (Figure 4.9 and Table 4.9) **generally over predicted concentrations** and the PCM empirical map (Figure 4.10 and Table 4.10) performed better.

There were negative R^2 values for some of the correlations. The negative R^2 values for the verification sites for PCM were due to the Thanet rural site. The modelled days greater than 120 µg m^{-3} and AOT40 metrics are far greater than the values measured at this site. The cause of the negative R^2 value for the days greater than 120 µg m^{-3} metric modelled by OSRM for the verification sites is again due to Thanet rural site.

Figure 4.7 OSRM verification (Days greater than 120 µg m^{-3})

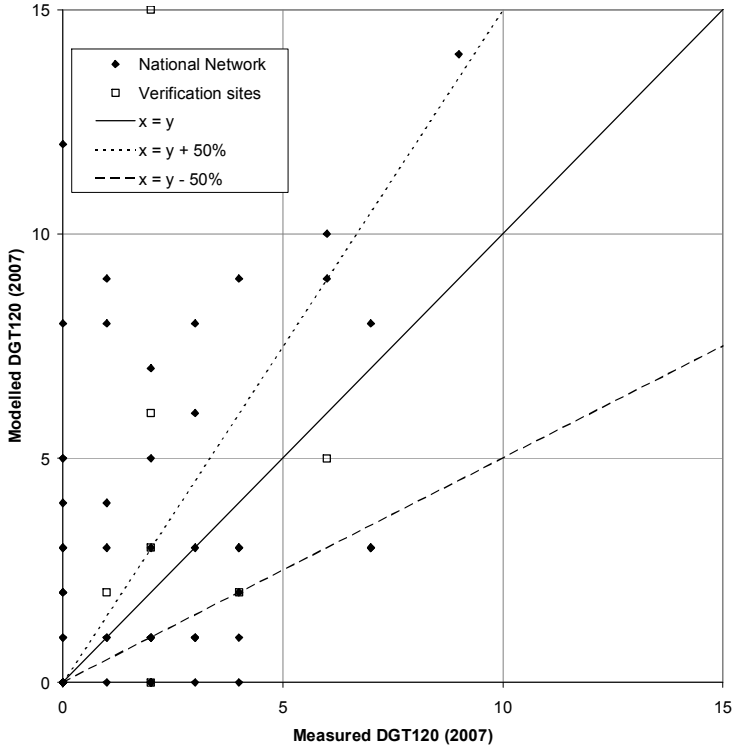

Figure 4.8 PCM empirical model verification (Days greater than 120 µg m^{-3})

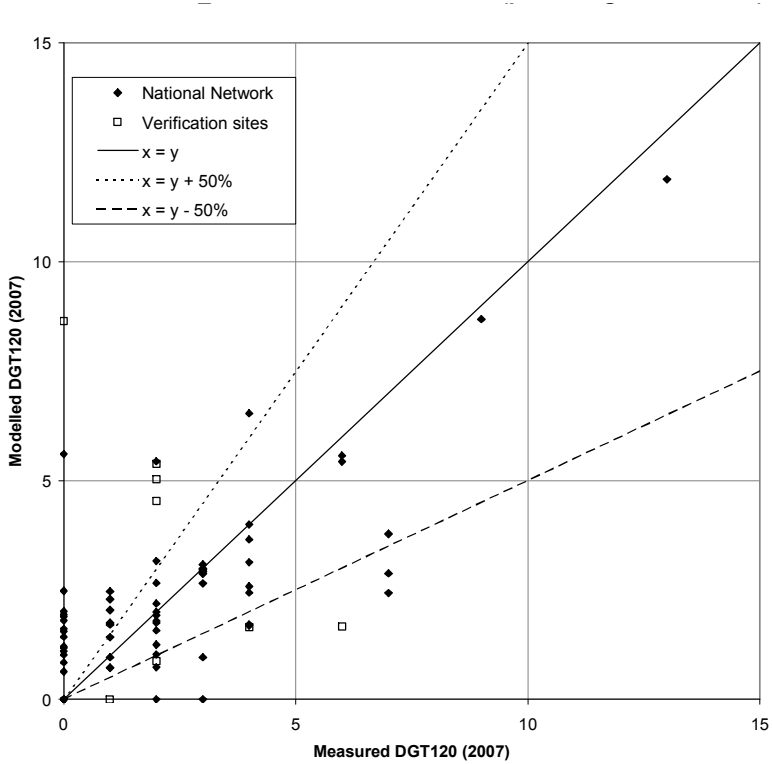

Figure 4.9. OSRM verification (AOT40, µg m^{-3}.hours)

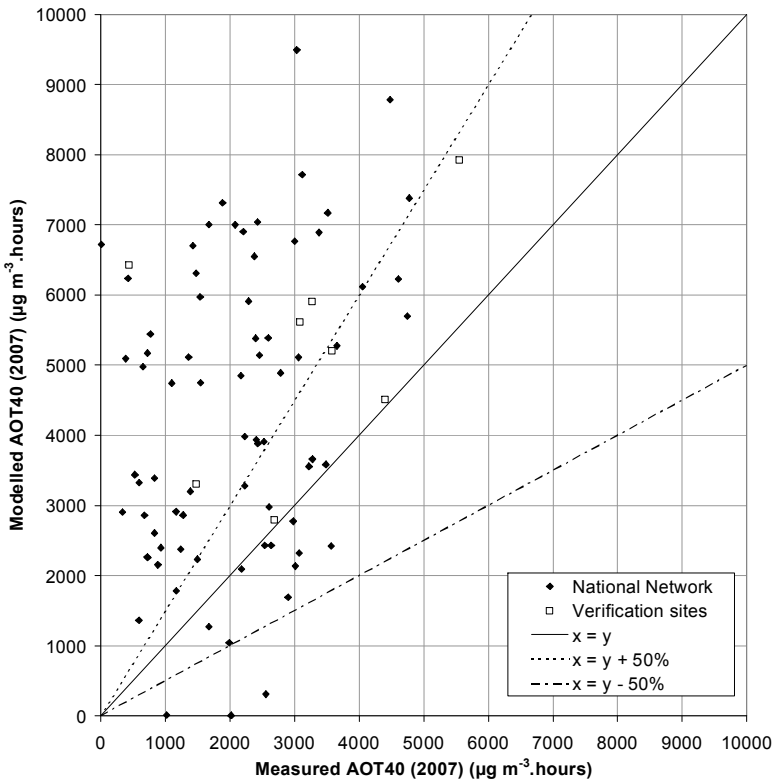

Figure 4.10. PCM empirical model verification (AOT40, µg m^{-3}.hours)

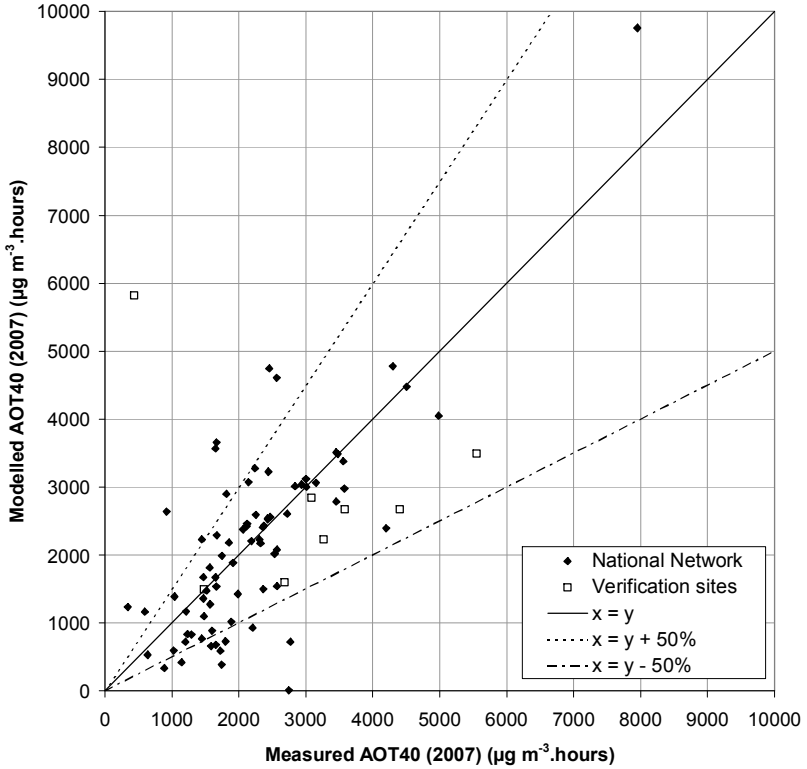

Table 4.7: OSRM verification summary, days greater than 120 µg m^{-3} (2007)

DGT 120 metric	Year	Mean of measurements (days)	Mean of model estimates (days)	R^2	% outside DQO	No. sites used in assessment
National network	2007	2.0	3.9	0.16	39.4	71
Verification sites	2007	2.4	6.1	----- *	62.5	8

* negative slope - r^2 not presented

Table 4.8: PCM empirical model verification summary, days greater than 120 µg m^{-3} (2007)

DGT 120 metric	Year	Mean of measurements (days)	Mean of model estimates (days)	R^2	% outside DQO	No. sites used in assessment
National network	2007	2.0	2.1	0.59	43.7	71
Verification sites	2007	2.4	3.5	----- *	100	8

* negative slope - r^2 not presented

Table 4.9: OSRM verification summary – AOT40 metric (2007)

AOT40 metric	Year	Mean of measurements (µg m^{-3}.hours)	Mean of model estimates (µg m^{-3}.hours)	R^2	% outside DQO	No. sites used in assessment
National network	2007	2281	4503	0.15	69.2	78
Verification sites	2007	3061	5211	0.13	50.0	8

Table 4.10: PCM empirical model verification summary – AOT40 metric (2007)

AOT40 metric	Year	Mean of measurements (µg m^{-3}.hours)	Mean of model estimates (µg m^{-3}.hours)	R^2	% outside DQO	No. sites used in assessment
National network	2007	2281	2321	0.73	24.4	78
Verification sites	2007	3061	2856	----- *	12.5	8

In addition to the verification plots, the model outputs from the OSRM and the PCM empirical model at each monitoring station have been plotted against one another for both metrics as shown in Figures 4.11 and 4.12. Figure 4.11 (the days greater than 120 µg m^{-3} metric) and Figure 4.12 (AOT40 metric) show that OSRM estimates higher concentrations than the PCM empirical model in both the national network and verification sites.

Past analysis (Hayman et al, 2006b) has shown that the OSRM has slightly under predicted measured concentrations in some cases and slightly over predicted measured concentrations in others. In general, it has underpredicted ozone metrics in high ozone years (e.g. 2003 and 2006) and slightly overpredicted ozone metrics in low ozone years (2004 and 2005) (Murrells et al, 2008).

Tables 4.11 and 4.12 below present the average measured and averaged modelled results from OSRM for the years 2004, 2005, 2006 and 2007. These illustrate the model performance during high (2006) and low (2004, 2005, 2007) years in both metrics. The difference between the concentrations predicted by the OSRM and the measured concentrations is larger for 2006 than for 2004, 2005 and 2007.

Figure 4.11. Comparison of OSRM against PCM empirical model (Days greater than 120 µg m^{-3})

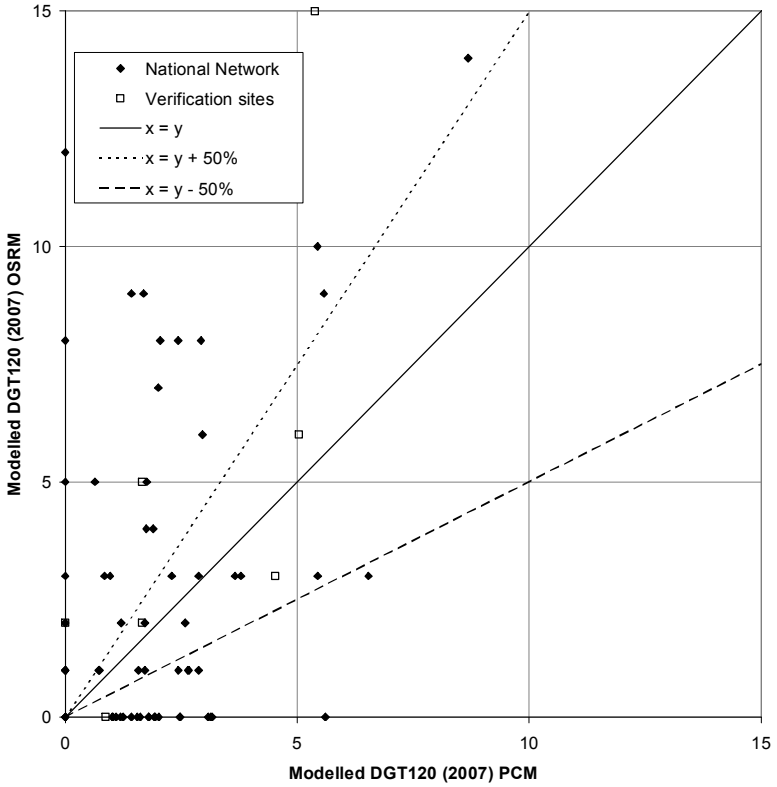

Figure 4.12. Comparison of OSRM against PCM empirical model (AOT40, µg m^{-3}.hours)

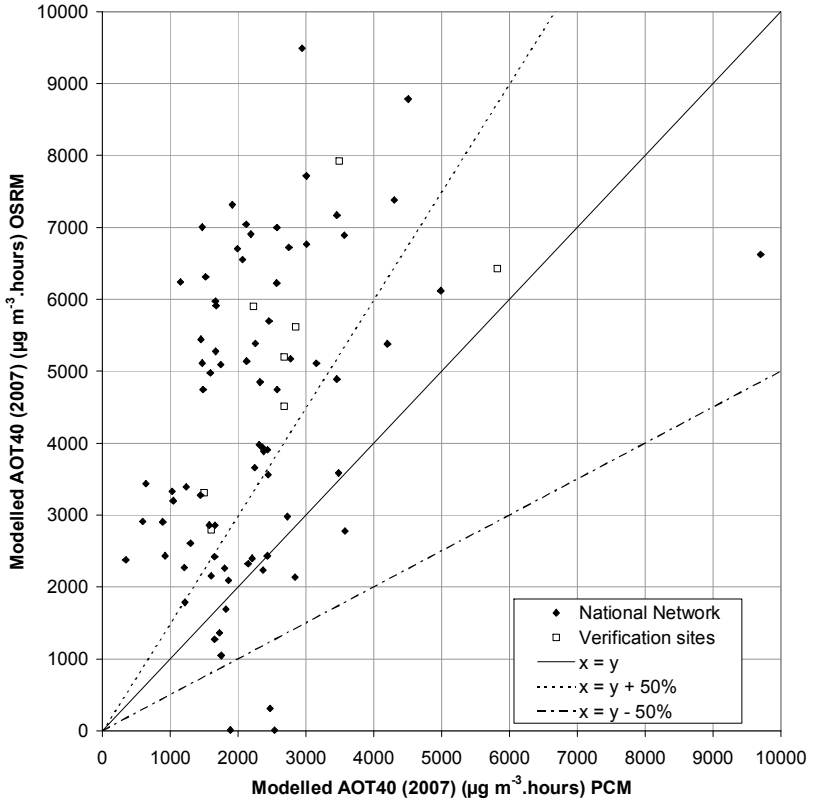

Table 4.11. Days greater than 120 µg m^{-3} OSRM results from 2004-2007

		National network		Verification sites	
Year modelled	**NAEI Year**	**Mean of measured**	**Mean of modelled**	**Mean of measured**	**Mean of modelled**
2004	**2004**	13	12	7	6
2005	**2004**	3	6	4	5
2005	**2005**	3	6	4	5
2006	**2005**	13	8	8	8
2007	**2006**	2	4	2	6

Table 4.12. AOT40 (µg m^{-3}.hours) OSRM results from 2004-2007

		National network		Verification sites	
Year modelled	**NAEI Year**	**Mean of measured**	**Mean of modelled**	**Mean of measured**	**Mean of modelled**
2004	**2004**	2888	2056	3681	2256
2005	**2004**	3650	4165	3810	3088
2005	**2005**	3650	4099	3810	3372
2006	**2005**	10497	5043	5061	6574
2007	**2006**	2281	4503	3061	5211

4.2.3 Conclusions for OSRM Performance in Modelling 2007 Ozone

- The OSRM in 2007 has generally overestimated Third Daughter Directive ozone metrics compared with measured data.
- This continues the trend found previously that indicates the OSRM overestimates these ozone metrics in low ozone years (2004, 2005 and 2007) and underestimates them in high ozone years (2003 and 2006) compared with measured data.
- The PCM empirical model continues to produce results that are closer to the measured concentrations than the OSRM and should continue to be used in its current capacity (contributing modelled data in fulfilment of UK reporting obligations to the European Commission.

5 Modelling for Policy Support (Objective 1)

Work carried out for this objective is of an *ad-hoc* nature involving using available tools to show impacts of planned and proposed policies on ozone levels, to understand past and future trends and the contribution made by emission sources to ozone in the UK.

Three main policy-related areas directly and indirectly related to ozone were examined in the past year, all using the UK Photochemical Trajectory Model (UK PTM).

- Trends in episodic peak and annual mean ozone metrics based on UK and European NO_x and VOC emissions
- The contribution to ozone formation from solvents
- Development of a PM Closure Model.

5.1 Modelling UK Ozone Trends 1990 – 2010

The UK PTM has been set up to study both episodic peak and annual mean of the daily maximum ozone metrics using UK and European NO_x and VOC precursor emissions for the years 1990, 1993, 1996, 1999, 2002 and 2005. The calculations were initialised using the observed baseline ozone concentrations for each year taken from the Mace Head historical record to simulate the year-by-year variations in intercontinental trans-Atlantic ozone transport. Studies of the episodic peak ozone metric have used constant meteorology based on that for the PUMA Campaign in 1999 centred on a location in the West Midlands of the UK at the University of Birmingham. Those for the annual mean metric have used the daily meteorology for the full year 2005 based on the rural location in the South Midlands at Harwell, Oxfordshire. All meteorological data has been prepared by the Met Office using the NAME model. The aim has been to determine the contribution to the observed trends in the ozone metrics from:

- NO_x and VOC precursor emission reductions
- intercontinental trans-Atlantic ozone transport
- non-linearities in ozone formation
- the ambition level achieved in international policy negotiations.

5.1.1 Episodic peak ozone levels

Figure 5.1 illustrates the UK PTM model results for episodic peak ozone over the period from 1990 – 2010 using three different chemical mechanisms; MCMv3.1, MCM CRIv2.0 and CBM4 (further details of chemical mechanisms used in ozone modelling are given in Chapter 7). There appears to be no significant differences between the year-by-year trends as a result of the choice of mechanism. The model appears to be able to reproduce well the observed trends in episodic peak ozone at the Harwell and Aston Hill locations using constant 1999 PUMA meteorology. This shows that there has been a strong influence of UK and European NO_x and VOC emission reductions on episodic peak ozone levels. Two years, however, stand out as exceptional in Figure 5.1, 2003 and 2006. These years have been strongly influenced by biomass burning in Portugal and the Russian Federation.

By setting the model initialisations to the 2005 values and repeating the model calculations, a small decrease in the model trends was found that was not significant. This means that it is unlikely that year-by-year increases in baseline ozone have off-set significantly the decreases due to UK and European precursor emission controls. This is because baseline ozone levels make a small

Figure 5.1. Observed and model trends from 1990 through to 2010 in episodic peak ozone for locations in the Midlands showing the influence of emission reductions.

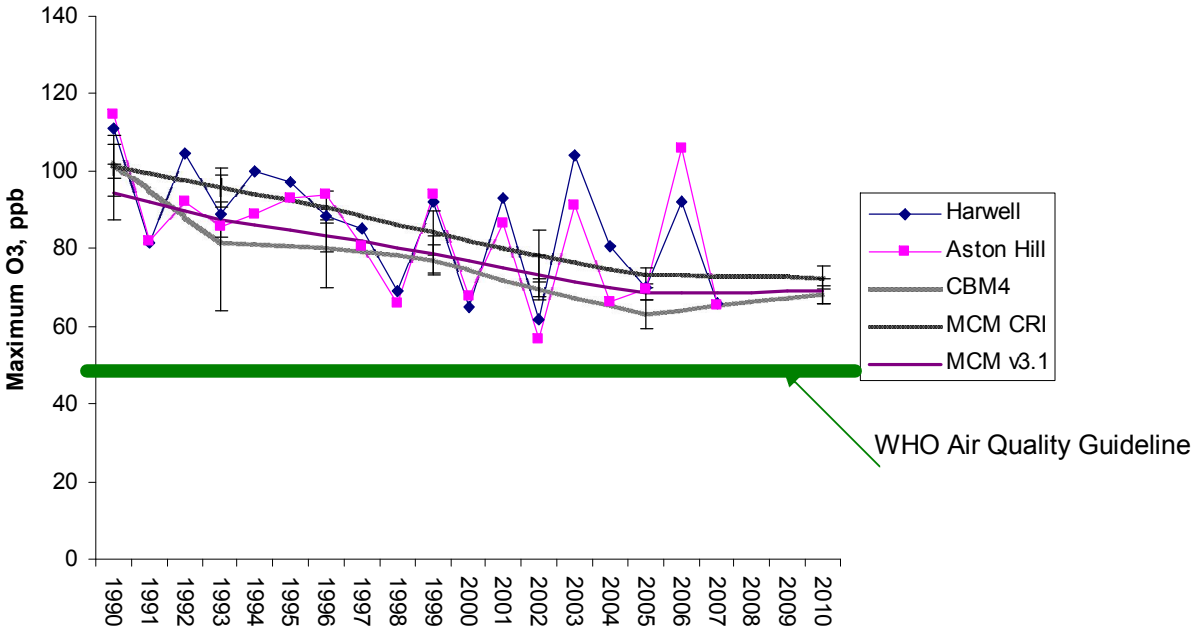

contribution to ozone levels during the summertime when regional-scale photochemical ozone production and destruction are at their most efficient.

There has been a strong influence from non-linearity between NO_x and VOC. This is apparent because NO_x and VOC emissions have declined by about 40-60% yet peak ozone levels have declined by only 28%. Peak ozone levels fail to reach the 50 ppb level, a level recommended by the WHO as an Air Quality Guideline, showing that the level of ambition agreed by the policy-makers has not been adequate and this has had a major impact on the observed downwards trend.

5.1.2 Annual mean of the daily maximum ozone levels

Figure 5.2 illustrates the UK PTM model results for the annual mean of the mid-afternoon maximum ozone concentrations using the MCM CRIv2.0 and CBM4 mechanisms. There appears to be no significant difference in the model trends resulting from the choice of chemical mechanism. Year-by-year variability ('with' in Figure 5.2) in intercontinental transport has completely overwhelmed the slight downwards trend ('without' in Figure 5.2) due to the reduction in precursor emissions from 1990 to 2005. This latter trend is only slight because of the limited ambition level of the UK and European NO_x and VOC emission reductions agreed.

5.1.3 Summary

The balance between the contributions to the observed trends from:

- NO_x and VOC precursor emission reductions
- intercontinental trans-Atlantic ozone transport
- non-linearities in ozone formation
- the ambition level achieved in international policy negotiations,

based on the UKPTM modelling results appear to be significantly different for the episodic peak and annual mean ozone metrics. All four influences appear to be important to one or other of the ozone metrics.

Figure 5.2. Observed and model trends in the annual mean of the daily ozone maximum concentrations from 1990 – 2010 for locations in the Midlands and South-East England (Lullingtom Heath) showing the influence of year-by-year variations in intercontinental transport. 'With' means with varying intercontinental transport and 'without' means constant intercontinental transport.

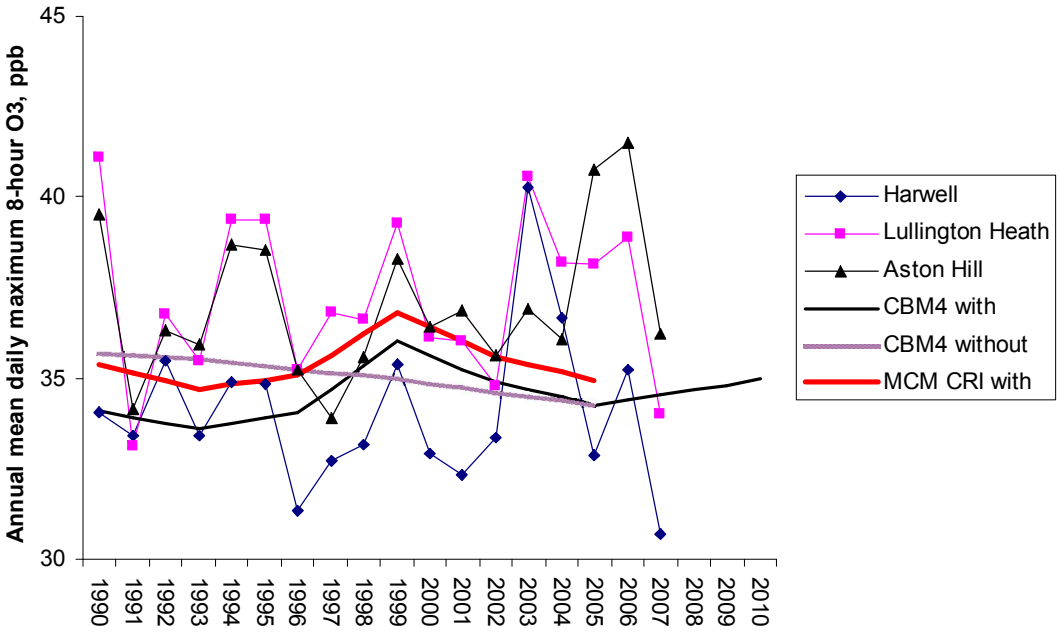

5.2 Modelling the Contribution to Ozone Formation from Solvents

The UK PTM model has been used to evaluate the contribution to ozone formation from solvents. In this study, a detailed breakdown of the composition of VOC emissions from 248 VOC emission source categories has been employed based on the National Atmospheric Emission Inventory (NAEI). We have also adopted the Master Chemical Mechanism (MCM) to describe the ozone formation from 175 VOC species, taking part in 12 871 chemical reactions.

Based on our results, Table 5.1 presents the contribution to ozone formation from the major VOC emission source sectors for the year 2000, a commonly used base year for the consideration of air quality policies stretching to 2010 and beyond to 2020. Interestingly, the contributions from road transport are only slightly higher than those from the usage of solvents and other products such as aerosol sprays.

A wide range of organic solvents is in use today. As a result, it has not been possible to generalise the different applications because each relies on a specific property of the organic solvent such as evaporation rate, boiling point, viscosity, surface tension as well as whether some particular compound dissolves in it or not. Each different type of solvent application requires a different type of solvent and each solvent has a different atmospheric chemical reactivity and hence a different potential for forming ozone photochemically.

Table 5.1. Summary of the major VOC emission sectors and their contribution to episodic peak ozone contrations in 2000.

Sector	Ozone contribution/ ppb
Road transport - exhaust	11.4
Road transport – petrol evaporation	1.6
Solvent and other product usage	10.6
Extraction and distribution of fossil fuels	7.2
Production processes	3.6
Off-road	1.8
Combustion	1.3
Agriculture	0.3
Wastes	0.2

Our approach addresses all these issues because it uses an accurately speciated VOC inventory and a fully explicit chemical mechanism that handles all the complex atmospheric chemistry for individual types of VOCs. Figure 5.3 shows the contribution to episodic ozone from all 53 sub-sectors that make up the solvent and other product usage sector. There is no one sector that dominates overall. Indeed, the top 10 most prolific sectors account for only 60% of the ozone formation from all 53 sub-sectors combined.

The sub-sector that makes the largest contribution, 'other solvent usage', is itself a catch-all category that represents a myriad of minor solvent applications. Large contributions are given by the aerosol sub-sectors involving cosmetics, toiletries and car-care products. Decorative paint usage accounts for over a ppb when the trade and retail sub-sectors are combined together. Industrial coatings and adhesives and surface cleaning operations using hydrocarbons and trichloroethylene are also large sources of reactive organic solvents. The picture is one of detail and complexity, with many different activities and applications and no dominant activity or process upon which to focus policy.

A paper on this topic has appeared as a publication in the journal "Chemistry and Industry" (Derwent et al, 2008a). The work was also used to inform the work undertaken for Objective 7 (Cost-Benefit Anlaysis of Solvent eduction) described in Chapter 9

5.3 Development of a PM Closure Model

Whilst this project is primarily focused on modelling of tropospheric ozone, there is considerable overlap with modelling approaches and methods used to model secondary particulate matter (PM), namely sulphate, nitrate and ammonium aerosol formed from precursor NO_x, SO_2 and NH_3 emissions as well as secondary organic aerosols generated by a complex sequence of photochemical reactions analogous to those involved in the production of ozone. Like ozone, secondary PM is a transboundary air pollutant and affects local concentrations of PM_{10} made up of primary emitted PM_{10}, secondary organic and inorganic aerosol and coarse PM. Process models for forecasting the response of secondary PM formation to changes in precursor emissions (NO_x, SO_2, NH_3, NMVOCs) require similar chemical transport models to the types used for predicting ozone concentrations and there is overlap in terms of evaluating policies affecting the formation of both pollutants. Modelling of both secondary PM and ozone benefit from good description of the chemical mechanisms and meteorological processes, much of which are common to both pollutants.

Empirically-based mapping models have played a significant role in policy development for $PM_{2.5}$ and PM_{10} in the United Kingdom (AQEG, 2005). Stedman et al. (2007) have used these models to prepare UK maps for $PM_{2.5}$ and PM_{10} for a base year 2004 and for 2010 and 2020, on the basis of current policies. These predicted maps for 2010 and 2020 have been used to check future compliance with air quality regulations. Whilst forecasting the future primary PM component in empirical models is relatively straightforward if accurate primary PM emission inventories are available for the present and future years, dealing with secondary PM is more difficult. Currently,

Figure 5.3. The contribution to ozone formation from each of the 53 sub-sectors that make up the solvent and other product usage sector.

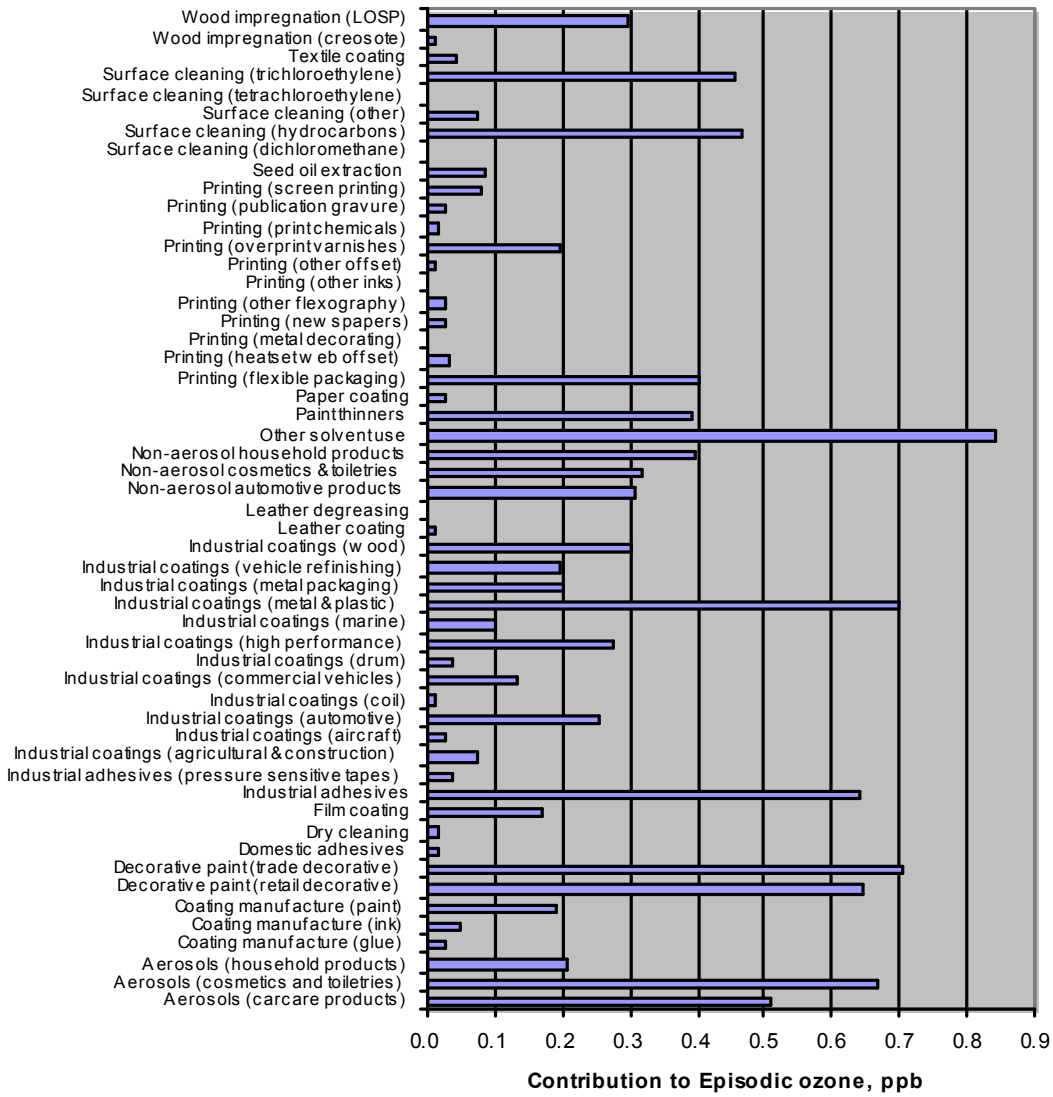

empirical models use outputs from the EMEP model, which explicitly models the formation of secondary inorganic aerosols, to provide single UK wide scaling factors for use in the empirical Pollution Climate Mapping (PCM) model. However, there is currently some uncertainty in how robust this method was.

Previous work was undertaken in this project using the Photochemical Trajectory Model (PTM) and the Met Office NAME model to assist in understanding the behaviour of secondary particulates as the emissions of their primary precursors decline and to examine the sensitivity of secondary PM component concentrations to changes in the emissions of PM precursors. The PTM was used to develop sensitivity coefficients for each secondary PM component, showing the likely importance of non-linearities in the atmospheric chemistry of secondary PM formation, that could be used in the PCM to gauge the importance of these non-linearities for policy-making in realtion to changes in precursor emissions. This work was reported in the last annual project report (Murrells et al, 2008). This work has been further developed in this year of the project.

The UK PTM model has been extended to provide an estimate of the mass concentrations of all the major $PM_{2.5}$ components for Harwell, Oxfordshire. The PTM describes the formation of the secondary fine PM sulphate, ammonium, nitrate and organic carbon in addition to primary carbonaceous PM. The formation of coarse PM nitrate by sea-salt displacement reactions has also been included. The

model has been used to estimate the mid-afternoon mass concentrations of each component of the suspended particulate matter (PM) for each day of 2006 for a rural location, Harwell, Oxfordshire, in the southern UK. A large number of equally-probable and randomly selected 96-hour 3-dimensional air mass trajectories were used to describe the variability of the atmospheric transport paths during each day. A chemical kinetic description was given for the major PM formation processes. Model performance was evaluated against gravimetric $PM_{2.5}$ observations, taking into account a 7 μg m^{-3} offset, and is illustrated in Figure 5.4 below.

Figure 5.4. Comparison of the model and observed $PM_{2.5}$ concentrations for Harwell, Oxfordshire for each day of 2006, showing the daily bias (model – observation).

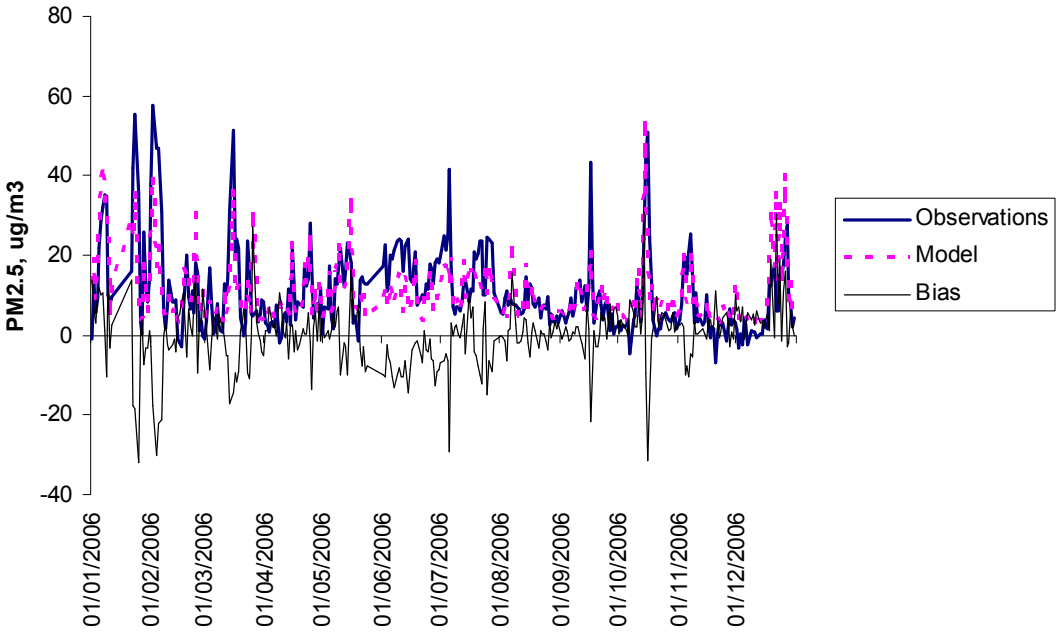

The linearity of the chemical production pathways forming the secondary PM components was examined by sensitivity studies to reductions in SO_2, NO_x, NH_3, VOC and CO emissions, reduced by 30% across-the-board, relative to the base case emissions. The annual mean PM component concentrations are shown in Table 5.2 for these sensitivity cases which were performed with initial and boundary concentrations set to zero.

Sensitivity coefficients, E_{ij}, were then calculated for PM component, i, for changes in the emissions of precursor pollutant, j, as follows:

$$E_{ij} = \frac{\dfrac{\text{Change in PM component, i, concentration}}{\text{Base case PM component, i, concentration}}}{\dfrac{\text{Change in emissions of pollutant, j}}{\text{Base case emission of pollutant, j}}}$$

They represent the sensitivity of the mass concentrations of the PM component to across-the-board emission changes, that is, to emission changes both in the United Kingdom and in the rest of Europe.

Table 5.2. Emission sensitivity coefficients for the different PM components calculated with the UK PTM model for 30% across-the-board emission reductions.

Scenario case	PM SO_4 , µg m^{-3}	Fine PM NO_3, µg m^{-3}	PM NH_4, µg m^{-3}	$PM_{2.5}$, µg m^{-3}	Coarse PM NO_3, µg m^{-3}
Across-the-board cases					
30% SO_2 case	1.0	-0.32	0.20	0.21	0.07
30% NO_x case	-0.15	0.63	0.28	0.13	0.72
30% NH_3 case	0	1.0	0.71	0.30	-0.21
30% VOC case	0.05	0.02	0.02	0.02	0.22
30% CO case	-0.005	0.003	0	0	0.01
UK-only cases					
30% SO_2 case	0.51	-0.12	0.05	0.11	0.02
30% NO_x case	-0.11	0.24	0.10	0.03	0.26
30% NH_3 case	0	0.44	0.33	0.13	-0.05
30% VOC case	0.03	0.005	0.007	0.01	0.13
30% CO case	-0.002	0	0	0	0.004
Rest of Europe-only cases					
30% SO_2 case	0.49	-0.20	0.15	0.10	0.05
30% NO_x case	-0.05	0.38	0.18	0.09	0.46
30% NH_3 case	0	0.57	0.37	0.16	-0.16
30% VOC case	0.02	0.12	0.01	0.01	0.09
30% CO case	-0.003	0.002	0	0	0.006

The chemical environment revealed by these sensitivity studies appeared to be 'ammonia-limited'. Consequently, PM mass concentrations appeared to be markedly non-linear with PM precursor emissions. Policy strategies for $PM_{2.5}$ therefore need to take into account emission reductions for a wide range of primary PM components and secondary PM precursors and to focus primarily on the abatement of NH_3. This complex interlinking may help to explain why PM levels have remained constant despite falling primary PM emissions.

This work has been published in the peer-reviewed journal '*Atmospheric Environment'* (Derwent et al, 2008b)

6 Detailed Assessment of Relationship Between Ozone, Nitrogen Oxide and Nitrogen Dioxide Levels, and Factors Controlling Them (Objective 2)

It is well-established that the behaviour of ozone (O_3), NO and NO_2 in the atmosphere is coupled by the following reactions,

$$NO + O_3 \rightarrow NO_2 + O_2 \quad (1)$$

$$NO_2 + \text{sunlight} (+ O_2) \rightarrow NO + O_3 \quad (2)$$

and it is because of this strong chemical coupling that the term "oxidant" is sometimes used as a collective term for NO_2 and O_3. This reaction cycle partitions NO_X between its component forms of NO and NO_2, and oxidant between its component forms of O_3 and NO_2, but conserves both NO_X and oxidant. As a result, oxidant derived from background O_3 is partitioned between the forms of NO_2 and O_3, with a progressively greater proportion in the form of NO_2 as NO_X increases as a result of received emissions. In urban areas, oxidant can also be derived significantly from directly emitted NO_2, and this is also partitioned between the forms of NO_2 and O_3, with a progressively greater proportion in the form of O_3 as NO_X decreases with dilution.

Owing to this local-scale chemical coupling of O_3 and NO_X, ambient levels of O_3 and NO_2 are inextricably linked. Consequently, the response to reductions in the emissions of NO_X is highly non-linear (e.g. AQEG, 2004; 2007), and any resultant reduction in the level of NO_2 is invariably accompanied by an increase in the level of O_3. It is therefore necessary to have a complete understanding of the relationships between O_3, NO and NO_2 under atmospheric conditions, if the success of proposed control strategies is to be fully assessed. Previous analyses have shown that consideration of O_3, NO and NO_2 as a set of chemically coupled species (rather than NO and NO_2 alone) provides additional information to assist the prediction and interpretation of how the levels of NO_2 and O_3 vary with that of NOx (Jenkin, 2004a). The method involves defining (i) linear expressions describing how the level of oxidant varies with the level of NOx, and (ii) algebraic expressions describing how the fractional contribution of NO_2 to oxidant (i.e., $[NO_2]/[\text{oxidant}]$) varies with NOx. The product of these two quantities yields the dependence of NO_2 levels as a function of NOx. The advantage of this semi-empirical approach (usually termed the "*oxidant partitioning model*") is that it allows the derived NO_2 vs NOx relationships to be rationalised in terms of sources of oxidant and well-understood chemical processes. In this way it also enables predictions that take account of possible changes in the magnitudes of oxidant sources, such as the background O_3 level or the fractional contribution of NO_2 to NOx emissions (i.e. "primary NO_2").

In the first year of the programme, activities included the recommendation of improved expressions to describe the NOx-dependence of the partitioning of oxidant into its component forms of NO_2 and O_3, based on a detailed analysis of annual mean $[NO_2]/[\text{oxidant}]$ ratios at 75 urban and 13 rural UK sites where the necessary co-located measurements are made, considering data up to 2006. In the present report, focus is placed on factors which influence total level of oxidant which is available to partition, and contributions to this oxidant which derive from processes on a range of geographical scales. The outputs of these analyses are being used to improve and update the representation of the oxidant partitioning method in the Pollution Climate Model (PCM), in relation to assessments of annual mean NO_2 and O_3 levels. Additional work has also been carried out using the Netcen Primary NO_2 Model to examine trends in the fraction of NO_x emitted as primary NO_2 by analysis of monitoring data.

6.1 Spatial Trends in Annual Mean Background Oxidant in the UK

The level of oxidant (denoted [OX]), at a given location in the UK is made up of a combination of a background (NOx-independent) source and a local, (NOx-dependent) source (e.g., Clapp and Jenkin, 2001; Jenkin 2004a), denoted here as $[OX]_B$ and $[OX]_L$, respectively:

$$[OX] = [OX]_B + [OX]_L \quad \text{(i)}$$

$[OX]_L$ is derived from primary emissions of NO_2, and can be represented by the term $f_{NO2}[NOx]$, where f_{NO2} is the fraction of NOx emitted as NO_2 (AQEG 2007). $[OX]_B$ provides a quantification of the ozone concentration which would exist at the given location in the notional absence of NOx, i.e. when the local-scale chemical coupling described above cannot occur.

It is well established that $[OX]_B$ must be greatly influenced by baseline surface ozone concentrations entering the British Isles from the north Atlantic under prevailing meteorological conditions (e.g., Derwent et al., 2007a). However, it may also be modified by processes occurring regionally over the UK and north-west Europe, which may be both positive (i.e., production from regional-scale chemistry) or negative (i.e., removal by deposition). In the present analysis, annual mean data from 17 UK sites (listed in Table 6.1) for the period 2001-2006, have been examined to estimate the contribution to $[OX]_B$ which derives from the hemispheric baseline, and the impact of regional-scale processes in modifying this baseline. This allows the geographical dependence of annual mean $[OX]_B$ over the UK to be investigated, and parameterisations to be recommended for use in empirical modelling studies applied to ozone and NO_2.

Table 6.1: Summary of background oxidant contributions determined for the sites considered in the present analysis (based on the mean of 2001-2006 data) and the distance parameters used to describe their geographical dependence (see text).

Site[a]	$[OX]_H$	$[OX]_R$	$[OX]_B$	d_1 [b]	d_2 [c]	d_3 [d]
	ppb	ppb	ppb	km	km	km
Port Talbot	35.5	-0.3	35.2	2.0	255.9	330.2
Rochester	33.5	1.0	34.5	82.6	18.6	6.9
Strath Vaich	35.9	-0.5	35.4	82.6	751.9	130.7
London Teddington	34.1	2.0	36.1	113.5	82.6	178.9
London Eltham	33.9	1.1	35.0	127.3	64.7	165.1
Lullington Heath	34.4	0.7	35.0	130.0	0.0	96.3
London Brent	33.2	1.1	34.4	134.1	87.4	178.9
Bolton	35.2	1.4	36.5	137.6	133.5	220.1
Harwell	32.7	0.4	33.1	137.6	346.7	151.3
Wolverhampton Centre	33.1	0.4	33.5	165.1	245.6	185.7
Newcastle	33.4	1.1	34.5	168.5	408.6	11.0
Cardiff Centre	35.3	0.3	35.6	175.4	217.4	309.6
Middlesbrough	33.6	1.2	34.8	236.0	362.5	17.2
Redcar	33.7	1.3	35.0	249.7	362.5	1.0
Ladybower	30.9	0.7	31.6	257.3	296.5	137.6
Wicken Fen	30.7	0.9	31.6	268.3	108.0	90.8
Norwich Centre	30.4	1.6	31.9	319.2	103.9	29.6

Notes

a: Sites are listed in order of their d_1 values. b: Distance across land from the Atlantic in a south-west to north-east direction. Includes contributions from Ireland and north-west France where appropriate. c: Distance on a north-westerly co-ordinate relative to Lullington Heath. d: Distance across land from the North Sea in a north-east to south-west direction.

6.1.1 Method

Annual and monthly mean [OX] and [NOx] were obtained for each of the 17 sites using O_3, NO and NO_2 data obtained from the National Air Quality Information Archive (http://www.airquality.co.uk). Corresponding values of $[OX]_B$ were determined from the following expression, rearranged from

equation (i) above, where "$f_{NO2}[NOx]$" represents a correction for the $[OX]_L$ source derived from primary NO_2 emissions.

$$[OX]_B = [OX] - f_{NO2}[NOx] \quad \text{(ii)}$$

The sites chosen for the analysis are either rural sites or comparatively unpolluted urban sites, such that the $[OX]_L$ correction amounted to less than 2.5 ppb in each case. The values of f_{NO2} for the urban sites were taken from Jenkin (2004a), with the average value of 0.093, reported in the same study, applied to rural sites.

$[OX]_B$ was further separated into an estimate of the hemispheric baseline, $[OX]_H$, and a regional modification to this baseline, $[OX]_R$, on the basis of site specific air mass histories described by four-day back trajectories (from the British Atmospheric Data Centre, ECMWF, 2007) starting at noon for each day of the period:

$$[OX]_B = [OX]_H + [OX]_R \quad \text{(iii)}$$

Air masses which were calculated to be at a longitude to the west of the arrival point for the entire four-day period were used to define the baseline, $[OX]_H$, with the regional modification, $[OX]_R$, being obtained from the deviation from $[OX]_B$, in accordance with equation (iii). The resultant values of $[OX]_H$, $[OX]_R$ and $[OX]_B$ are listed in Table 6.1.

6.1.2 Results and analysis

Geographical dependence of $[OX]_H$: The values determined for $[OX]_H$, based on the average of data over the period 2001-2006, were found to vary over the range 30.4 – 35.9 ppb , depending on location within the UK (see Table 6.1). This indicates that the true hemispheric baseline is modified during passage of air across the UK, most likely due to removal of ozone through deposition to the ground. The screened air mass trajectories used to determine $[OX]_H$ were dominated by the prevailing south-westerlies, and a generally good anti-correlation between $[OX]_H$ and the distance across land from the Atlantic to each site from a south-westerly direction (d_1 in Table 6.1) was found. This was further improved by an adjustment to the south-west land distance being made to account for the progressively greater wind speeds towards the north and west of the British Isles (i.e., shorter contact time with land per unit distance). This was done on the basis of a north-westerly co-ordinate defined relative to the most south-easterly site, Lullington Heath (d_2 in Table 6.1). On this basis, the following optimized expression for $[OX]_H$, in ppb, was determined:

$$[OX]_H = [OX]_H^\circ \exp(-6.51 \times 10^{-4}\, d_{1^\circ}) \quad \text{(iv)}$$

where $[OX]_H^\circ = 36.16$ ppb and $d_{1^\circ} = d_1 \exp(-1.57 \times 10^{-3}\, d_2)$. The correlation is shown in Figure 6.1, and the values of $[OX]_H$ calculated for the 17 sites using this expression are compared with those derived from the observed data in Figure 6.2 (upper panel).

The altitudes of the sites considered in the analysis vary over the range 4–360 m, and any influence resulting from this was also considered. However, no clear dependence of $[OX]_H$ on altitude was apparent. This suggests that any decreasing deposition trend with increasing altitude is not observable for the range of altitude considered here, and that the altitude dependence reported previously for ozone by PORG (1997) may have been due primarily to loss of ozone at lower altitudes through relatively increased oxidant partitioning via reactions (1) and (2).

Figure 6.1: Correlation of $[OX]_H$ with adjusted distance across land from the south-west (see text).

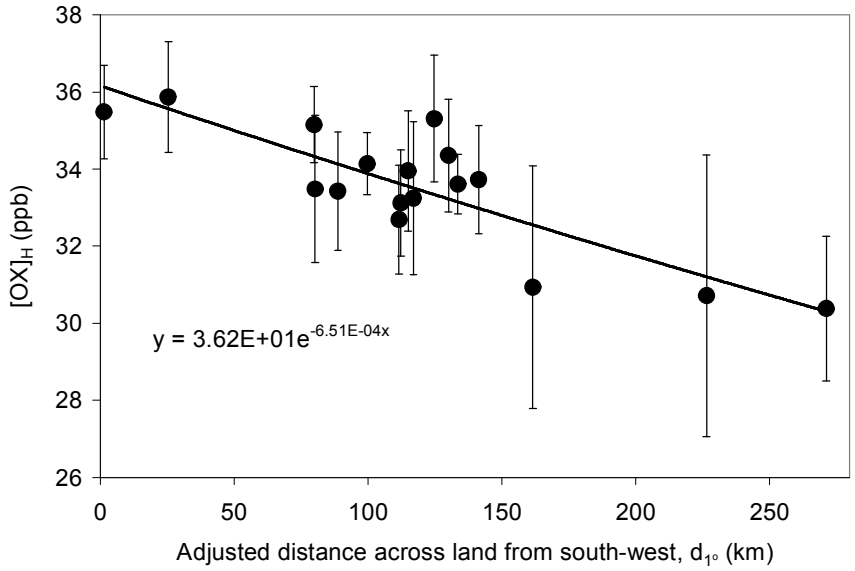

Figure 6.2: Comparison of background oxidant components determined from observational data from the 17 UK sites with those simulated using the optimised expressions in equations (iv) and (v). The sites are listed in order of increasing values of the distance parameter d_1 (see Table 6.1).

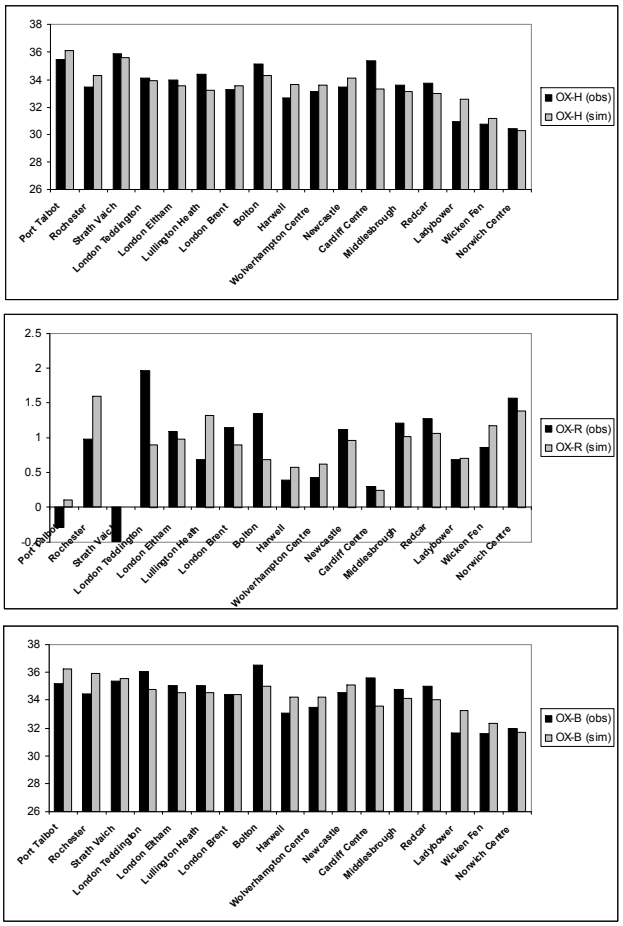

Geographical dependence of [OX]$_R$: The values determined for the regional modification ([OX]$_R$), based on the average of data over the period 2001-2006, were found to vary over the range -0.5 – 2.0 ppb , depending on location within the UK (see Table 6.1). Previous analyses have shown that annual maximum hourly-mean ozone concentrations and public information threshold exceedence statistics for ozone tend to show a south-easterly to north-westerly gradient (see first annual report (Murrells et al, 2008) and Jenkin, 2008), suggesting that the contribution to [OX]$_R$ made by regional-scale photochemical oxidant production should display a similar trait. However, it is also clear that other factors operate when annual mean data are being considered. In particular, it is clear that southerly sites on the west of the country (e.g. Port Talbot and Cardiff Centre) have low values of [OX]$_R$ (even though photochemical oxidant production is expected to be reasonably high) whereas those near the coast of north-east England (i.e., Newcastle Centre, Middlesbrough and Redcar) have comparatively high values. Examination of the "easterly" air mass trajectories which were screened out for the [OX]$_H$ analysis, indicates a general prevalence for air from the north-east sector (arriving in the UK from across the North Sea) when annual data are considered. The possible role of oxidant loss through deposition during north-east to south-west transit across the UK was therefore considered, the relevant distance being defined as d_3 in Table 6.1. A multiple regression of the data indicated that [OX]$_R$, in ppb, can be reasonably well described by the expression,

$$[OX]_R = F.[OX]_{R\ chem} + [OX]_{R\ dep} \qquad (v)$$

where $[OX]_{R\ chem} = (1.65 - (1.59 \times 10^{-3}\ d_2))$ and $[OX]_{R\ dep} = (-3.43 \times 10^{-3}\ d_3)$, the former being the photochemical production contribution and the latter being the deposition contribution. The parameter F

Figure 6.3: Seasonal variation of regional oxidant modifications, [OX]$_R$, determined for selected UK sites, based on 2001-2006 data.

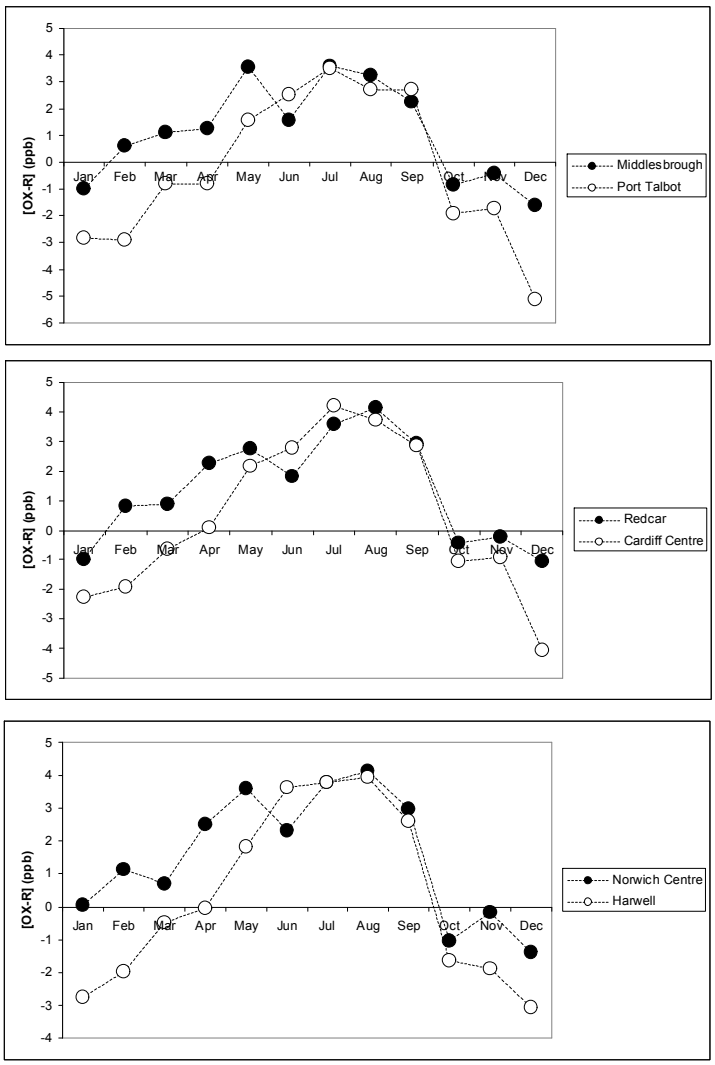

is a scaling factor to account for variations in the level of photochemical pollution, which has a value of unity in the present reference case. Figure 6.2 (middle panel) shows the values of $[OX]_R$ calculated for the 17 sites using this expression, compared with those derived from the observed data. The lower panel in the figure presents the comparison for $[OX]_B$.

The balance between oxidant production through photochemistry and loss through deposition can be clearly illustrated by examination of the seasonal variation of $[OX]_R$ (see Figure 6.3). The majority of sites display positive values during the summer months, when photochemical production is greater than loss through deposition, and negative values during the winter when the reverse is true. The comparison of sites near the North Sea coast with those further south-west (Figure 6.3), indicates that the sites near the coast have a much smaller influence from deposition.

6.1.3 Calculation of background oxidant components for empirical modelling

In principle, the expressions in equations (iv) and (v) can be used to determine background oxidant levels on an annual mean basis for any location in the UK, and the contributions of $[OX]_H$ and $[OX]_R$ to those levels, provided values of the distance parameters d_1, d_2 and d_3 are available. Example maps of average $[OX]_H$, $[OX]_R$ and $[OX]_B$ for the UK over the period 2001-2006 are illustrated in Figure 6.4, with values calculated for each 100 km Ordnance Survey grid square, based on the co-ordinates of the grid square centres. Recognising that the centre points are not always representative of the entire grid square, this does nonetheless allow the general geographical trends of the various factors influencing $[OX]_B$ to be illustrated.

The same data are tabulated in Table 6.2, with $[OX]_R$ further broken down into the photochemical production and deposition components, $[OX]_{R\ chem}$ and $[OX]_{R\ dep}$. These data can therefore potentially be used to generate maps with $[OX]_{R\ chem}$ and/or the hemispheric baseline contribution, $[OX]_H$, scaled to generate different scenarios. Alternatively, the complete removal of deposition impacts would lead to values of $[OX]_B$ equal to 36.16 + $[OX]_{R\ chem}$.

6.1.4 Assignment of year-specific parameters for empirical modelling

It is recognised that the oxidant components described above show year-to-year variability, by virtue of variations in the magnitude of regional and global scale influences on emissions and chemical processing (e.g., Derwent et al., 2007a; Jenkin, 2008). Modelling of annual mean data for individual years therefore ideally requires year-specific values of $[OX]_H°$ and $[OX]_R$.

The full spatial analysis described above was carried on the basis of average data for 2001-2006, leading to the value of $[OX]_H°$ = 36.16 ppb. In order to generate year-specific data for this period, the values of $[OX]_H$ for each site in each year were used in conjunction with equation (iv) to obtain an estimates of $[OX]_H°$. The values obtained for all the sites in each year were then averaged to obtain the values of $[OX]_H°$ in Table 6.3 for the individual years in the 2001-2006 sequence. An estimate of $[OX]_H°$ for 2007 is also included, based on a correlation of $[OX]_H°$ vs [OX] at the Strath Vaich remote site, and the value of [OX] at Strath Vaich in 2007.

Figure 6.4: Illustration of the spatial variation of the hemispheric and regional oxidant components, $[OX]_H$ and $[OX]_R$, and the summed background oxidant, $[OX]_B$, over the UK (in ppb). Values are assigned to each 100 km Ordnance Survey grid square, based on the co-ordinates of the grid square centres, and are based on an average over the period 2001-2006.

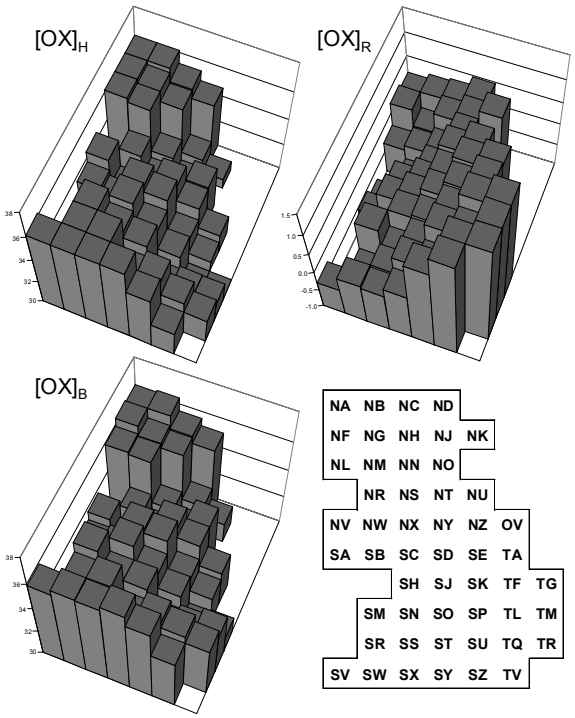

Table 6.2: Parameterized values of the oxidant components (2001-2006 average) for the 100 km OS grid squares, based on the co-ordinates of the grid square centres. $[OX]_R$ is subdivided into the photochemical production ($[OX]_{R\ chem}$) and deposition ($[OX]_{R\ dep}$)components. $[OX]_B$ is given by the sum of the three other columns.

OS Grid	$[OX]_H$	$[OX]_R$		$[OX]_B$
		$[OX]_{R\ chem}$	$[OX]_{R\ dep}$	
NA	36.16	0.13	0.00	36.29
NB	36.16	0.24	0.00	36.40
NC	35.25	0.35	-0.07	35.53
ND	34.59	0.47	0.00	35.06
NF	36.16	0.24	0.00	36.40
NG	35.88	0.35	-0.49	35.75
NH	35.14	0.47	-0.15	35.46
NJ	31.77	0.58	-0.10	32.25
NK	30.73	0.69	0.00	31.42
NL	36.16	0.35	-0.63	35.88
NM	35.90	0.47	-0.63	35.74
NN	32.80	0.58	-0.58	32.80
NO	31.12	0.69	-0.17	31.64
NR	33.86	0.58	-1.07	33.38
NS	32.25	0.69	-0.65	32.29
NT	31.63	0.80	-0.13	32.30
NU	33.29	0.92	0.00	34.21
NW	32.48	0.69	-0.75	32.42
NX	32.92	0.80	-0.62	33.11
NY	34.43	0.92	-0.34	35.00
NZ	33.22	1.03	0.00	34.25
OV	31.53	1.14	0.00	32.67
SC	35.36	0.92	-0.58	35.70
SD	34.92	1.03	-0.44	35.51
SE	32.24	1.14	-0.19	33.19
TA	30.95	1.25	0.00	32.20
SH	35.62	1.03	-0.63	36.02
SJ	34.09	1.14	-0.68	34.55
SK	32.53	1.25	-0.36	33.42
TF	29.76	1.37	0.00	31.13
TG	29.77	1.48	0.00	31.25
SM	36.16	1.03	-0.63	36.56
SN	35.05	1.14	-1.16	35.03
SO	34.62	1.25	-0.85	35.02
SP	31.46	1.37	-0.39	32.44
TL	31.68	1.48	-0.39	32.77
TM	31.63	1.59	0.00	33.22
SR	36.16	1.14	-1.43	35.87
SS	36.16	1.25	-1.19	36.23
ST	33.73	1.37	-0.87	34.22
SU	34.24	1.48	-0.87	34.85
TQ	33.04	1.59	-0.19	34.43
TR	32.18	1.70	0.00	33.89
SV	36.16	1.14	-1.43	35.87
SW	36.16	1.25	-1.19	36.23
SX	36.16	1.37	-1.36	36.17
SY	36.16	1.48	-1.26	36.38
SZ	34.53	1.59	-0.49	35.64
TV	32.18	1.70	0.00	33.89
NV	34.47	0.58	-1.31	33.74
SA	33.67	0.69	-1.24	33.12
SB	33.25	0.80	-0.71	33.34

Table 6.3: Year-specific annual mean values of $[OX]_H°$ and F for use in empirical modelling. Values for 2001-2006 are based on data for the oxidant components in each year. The 2007 values are inferred as described in the text.

Year	2001	2002	2003	2004	2005	2006	2007
$[OX]_H°$	35.00	35.79	38.16	36.27	35.50	36.32	*35.29*
F	0.859	0.816	1.334	0.988	0.581	1.422	*0.25*

To obtain year-specific values of $[OX]_R$, it was first assumed that $[OX]_{R\ dep}$ remains constant at a given location, such that any variability is due to variations in the regional photochemistry component, $[OX]_{R\ chem}$. $[OX]_R$ data for each site in each year were then used in conjunction with the values $[OX]_{R\ dep}$ to generate estimates of $[OX]_{R\ chem}$. The values obtained for all the sites in each year were then averaged to obtain year-specific average values of $[OX]_{R\ chem}$, which were divided by the 2001-2006 average value to obtain year-dependent values of the scaling factor F in equation (v). The resultant values of F are shown in Table 6.3 for the individual years in the 2001-2006 sequence.

An estimate of F for 2007 is also included, based on consideration of the variation of a number of elevated ozone and related metrics (e.g., maximum hourly-mean ozone at long-running rural sites; hours $\geq$ 90 ppb ozone at long running sites; average summer temperature) over the 2001-2006 period, in comparison with that of F. These analyses suggested that the value of F in 2007 should lie between zero and 0.5. It is noted that the available metrics give a very clear message in high photochemistry years like 2003 and 2006, but are also significantly influenced by other factors in low photochemistry years leading to scatter in the key region of interest for 2007. Nevertheless, it was clear from the analysis that F should be lower in 2007 than in any of the years 2001-2006, and should therefore be the lowest of the years considered to date. Based on the range given above, a value of F = 0.25 is assigned to 2007. This level of uncertainty in F influences the estimated $[OX]_B$ value by about $\pm$ 0.4 ppb in the south-east UK, and by smaller amounts elsewhere.

6.2 Trends in f-NO_2 at UK Monitoring Sites Calculated Using the Netcen Primary NO_2 Model

Two different approaches to controlling oxides of nitrogen in air have resulted in a legislation gap where vehicle manufacturers have reduced NO_X emissions in compliance with the Euro standards and other directives without yielding a corresponding reduction in ambient NO_2 concentrations to below the EU First Daughter Directive limit values for NO_2 in many locations.

One possible reason for this gap relates to the proportion of NO_X emitted directly as NO_2 from vehicle exhausts (this is the primary NO_2 fraction, f-NO_2, often expressed as a percentage).
f-NO_2 in many locations in the UK may be rising as a result of changes in the composition of the national vehicle fleet and the introduction of new exhaust technologies that have been brought in to meet the emission limits for various pollutants. For petrol-fuelled vehicles f-NO_2 is less than 5%, whereas f-NO_2 in diesel vehicles not fitted with new exhaust treatment technology is higher. The continuing increase in the proportion of diesel-engine vehicles in the national fleet will therefore have a significant impact on the ambient NO_2 concentrations, particularly in roadside environments. Furthermore, the pressure to fit diesel vehicles with after exhaust treatment technology such as particulate traps and oxidation catalysts is likely to further increase f-NO_2. Some catalyst-based particulate filters achieve the catalytic action by oxidising a portion of the NO in the exhaust to NO_2 in order to promote the oxidation of soot collected in the filter and so potentially emit a higher proportion of NO_X as NO_2.

The potential implications of increases in f-NO_2 within the UK on likely compliance with the ambient NO_2 limit values in 2010 mean there is a growing interest in identifying and understanding trends in f-NO_2. Understanding how f-NO_2 is changing and having up-to-date information on f-NO_2 levels is particularly important for incorporating f-NO_2 into models designed to predict future ambient NO_2 concentrations (e.g. the PCM model) and models for predicting ozone in urban areas (e.g. OSRM) where there are significant interactions with local NO_x sources.

In this project, trends in f-NO_2 have been calculated for a selection of roadside monitoring sites across the UK, from several different networks, using the Netcen Primary NO_2 model. Analysis of how modelled f-NO_2 varies geographically across the UK and how f-NO_2 trends have changed in the past few years is presented.

6.2.1 Methodology

To carry out the modelling, the Netcen Primary NO_2 model has been used combined with monitoring data from a selection of roadside and background monitoring sites.

6.2.1.1 The Netcen Primary NO_2 Model

The Netcen Primary NO_2 Model is a one-dimensional model of the relationships between f-NO_2 and NO_X, NO_2 and O_3 concentrations at roadside locations. Abbott (2005) gives a detailed description of the model and an example of its application using data at a selection of UK AURN monitoring sites.

Several relationships and assumptions underpin the model. These include:

- A background site can be chosen to be 'paired' with each roadside monitoring site such that the NO_x, NO_2 and O_3 measured at the background site are representative of the background concentrations at the roadside site.
- Total oxidant at roadside locations $[Ox] = [O_3] + [NO_2]$;
- $[Ox]_1 - [Ox]_0 = A([NO_x]_1 - [NO_x]_0) + B^*$ where A is the primary NO_2 ratio, Ox is the total oxidant (the subscript 1 is for roadside, 0 is for background) and B* represents the net effect of other reactions and deposition and excludes the background oxidant concentration.

The model has three modules depending on what input data is available and what output information is needed. Two of these modules are used in the analysis of recent trends in f-NO_2 presented here. These are:

Module 1: The analysis module. This calculates f-NO_2 for roadside monitoring sites using hourly NO_X, NO_2 and O_3 measurements from this site and hourly NO_X, NO_2 and O_3 measurements from its paired background site. The annual f-NO_2 component is derived directly from the monitoring data by regressing the hourly roadside increment of oxidant (dependant variable) against the hourly roadside increment of NO_X (independent variable). The annual f-NO_2 is calculated as the gradient of the regression line.

Module 2: The ozone module. The ozone concentration at the roadside is calculated using a one-dimensional finite difference model of the chemistry and turbulent diffusion in the surface boundary layer. f-NO_2 is then derived from the monitoring data by regression analysis as in the analysis module. There are relatively few roadside monitoring sites across the UK where ozone is measured. The ozone module has therefore been used in the analysis of recent time series data so as to prevent being limited to analysing roadside sites with ozone monitoring.

6.2.1.2 Model Set-Up

When running the analysis and ozone modules, the model loops through each hour of the year and then calculates the annual mean f-NO_2 through regression analysis of hourly f-NO_2 for all the hours modelled. The model requires the following data channels to run: measured NO_X, NO_2 and O_3 at the background site and measured NO_X, NO_2 and O_3 (or modelled O_3 if the ozone module is in use) at the roadside site. If any input data is missing for any hour that hour will not be modelled. The model is currently configured to use default met data settings in the ozone module if met data is missing for a given hour. If the modelled f-NO_2 >100% for any given hour, this hour is not included in the regression analysis. This is because f-NO_2 >100% is not physically realistic because the maximum possible proportion of NO_X that can be NO_2 is 100%. Where f-NO_2 >100% occurs, it suggests that the model assumptions are not holding true. This may occur as a result of reactions occurring between the background and roadside site that added extra total oxidant to the air mass. It is also possible, for any

given hour that the air mass at the background site is not representative of the behaviour of the non-traffic related component of the roadside site.

The analysis module performs better where there is a significant NO_X roadside increment as a higher NO_X roadside increment means there is a bigger f-NO_2 signal for the model to detect. Therefore, a minimum roadside increment was set at 10µg m^{-3}. For hours with a roadside increment less than this, the model did not run and no result was included in the regression analysis to calculate the annual f-NO_2.

6.2.1.3 Model Runs

For the model runs carried out for the analysis presented here, monitoring data has been used from sites from a range of networks including the AURN, LAQN and other contract sites managed by AEA. Details of which roadside sites have been used in the model and the background sites they have been paired with are given on the graphs presented in the results section.

For all sites Waddington met data has been used in the ozone module.

Model runs have been carried out for years with available data up to and including 2007.

6.2.2 Results of f-NO_2 Trends

Figures 6.5-6.11 present plots of modelled f-NO_2 for a selection of sites across different regions in England. Figures 6.12-6.14 present similar plots for selected sites in Wales, Scotland and Northern Ireland. Each point on the graphs represents an annual average f-NO_2 at the roadside site being modelled. Black points have a data capture of >30% and are therefore considered reliable for this modelling. Points with data capture of between 10 and 30% are shaded grey and points with less than 10% data capture are coloured white. The name of the paired background site assumed to represent background concentrations at each roadside site is given in brackets after the roadside site name.

6.2.2.1 London

Figures 6.5 and 6.6 show a general upwards trend in f-NO_2 at most of the sites modelled in London. However at some, but not all sites, there is evidence of a levelling off or even slight decrease in f-NO_2 levels between 2006 and 2007. Compared with other sites across the UK, f-NO_2 at sites in London has generally shown greater upward trends in recent years and is therefore generally higher by 2006, although there are some exceptions to this.

AURN sites (Figure 6.5) with particularly noteworthy trends include London Marylebone Road where there is clear evidence of step change in f-NO_2 between 2002 and 2003. f-NO_2 levels at this site then continued to rise until 2005 where f-NO_2 peaked at 27.1% before dropping slightly in 2006 to 25.1%. In 2007 levels rose marginally to 25.4%.

At London A3 roadside, the maximum modelled f-NO_2 was 19.1% in 2007. While this is not particularly high relative to other London sites, modelled f-NO_2 up to 2000 did not exceed 3% so there has been a very significant increase in f-NO_2 over the past 7 years at this site. By contrast, London Cromwell Road 2 is noteworthy because it had unusually high f-NO_2 in the late 1990s with f-NO_2 as high as 18.1% in 1998. f-NO_2 levels at this site have increased to 23.1% by 2006, but the upwards trend shows evidence of levelling off.

The highest modelled f-NO_2 from LAQN sites (Figure 6.6) selected occurred at Lambeth 4, where the three years with good data capture show a slight upward trend from 28.5% in 2004 to 34.6% in 2007. Other sites with high f-NO_2 values include Barnet 1 – Tally Ho Corner, which showed a very steep increase in f-NO_2 between 2000 and 2003, after which the rate of increase has slowed significantly. The maximum modelled f-NO_2 value at this site was 32.0% in 2007. f-NO_2 at Croydon 4 – George Street also reached a high level in 2006 of 27.1% before dropping to 20.7% in 2007.

Several of the LAQN sites show evidence of a slight down turn in f-NO_2 in 2007 relative to 2006 (e.g. Croydon 4 – George Street, Ealing 2 – Acton Town Hall, Lewisham 2 – New Cross). This change in trend is not apparent at many of the AURN sites in London.

Three of the LAQN sites that showed a sharp decrease in f-NO_2 between 2005 and 2006 showed little to no change between 2006 and 2007. These sites are Hounslow 4 – Chiswick High Rd, Islington 2 – Holloway Road and Redbridge 3 – Fulwell Cross.

6.2.2.2 The South East

Both AURN sites in the South East, Brighton Roadside and Hove Roadside, (Figure 6.7) showed an increase in f-NO_2 between the first year of measurements and 2007, without ever exceeding 20% f-NO_2. Canterbury Roadside reached the highest f-NO_2 of the sites modelled in the South East with a big increase from 17.6% in 2005 to 35.6% in 2006. In 2007 levels returned to 9.4% suggesting that the high year in 2006 was either caused by a model artefact or by a temporary local feature at the site.

f-NO_2 at some contract sites does show evidence of remaining constant with time (e.g. Gravesham A2 Roadside, Maidstone A229 Kerbside). At the majority of the other sites modelled in the South East, there are insufficient years of data to pick out any strong trends. f-NO_2 values between 10 and 20% in the South East region seem to be typical.

6.2.2.3 The South West

There is clear evidence of an upward trend in f-NO_2 at all three sites (all AURN) modelled in the South West region (Figure 6.8). However, this trend has been relatively gentle at Bath Roadside and Bristol Old Market where modelled f-NO_2 had not reached 20.0% by 2007. The upward trend at Exeter Roadside between 2001 and 2006 has been steeper with a maximum modelled f-NO_2 of 24.1% in 2006 before decreasing to 15.1% in 2007.

6.2.2.4 The Midlands

Figure 6.9 shows that f-NO_2 has gradually increased at Oxford Centre Roadside from 5.9% in 1999 to 17.4% in 2007. This increase is not apparent at the nearby contract site, Oxford High St. The modelled f-NO_2 at West Chipping Norton in 2006 is relatively high at 28.8%.

6.2.2.5 East Anglia

The sites in East Anglia (Figure 6.10) show little evidence of any significant increase in f-NO_2 although there is a slight upwards trend at two of them. The model suggests there was a very high f-NO_2 at Cambridge Silver Street in 2002/2003, but it is unclear as to why this occurred or whether it is actually an artefact of the model. The two other roadside sites in Cambridge do not show such high f-NO_2 levels.

6.2.2.6 The North

Figure 6.11 shows modelled f-NO_2 at Bury Roadside increased very gradually between 1997 and 2004 from 4.6 - 8.2% before increasing more rapidly to 18.2% in 2006. Rotherham Wales and Wakefield Horbury Road (excluding the peak in 2004) also both show an upward trend in recent years. By contrast Stockton-on Tees Yarm shows a very flat trend.

6.2.2.7 Wales

Modelled f-NO_2 at sites selected in Wales (Figure 6.12) is generally relatively low in comparison with many other sites across the UK. There is a slight upward trend evident and the Cardiff and Swansea sites, but f-NO_2 at these sites remains below 15% in 2007.

Data capture of modelled f-NO_2 was relatively poor for at least some of the years at the majority of Welsh sites included in the modelling (a lot of the data points have less than 30% data capture). This may be caused by a relatively low NO_X roadside increment at some of these sites. The model is set up to only run for hours when the roadside increment is at least 10µg m^{-3} because at lower roadside increments the f-NO_2 signal is not sufficiently clear for the model to detect.

6.2.2.8 Scotland

Of the Scottish sites where f-NO_2 has been modelled (Figure 6.13), only Inverness shows any clear upward trend. This site has very low data capture – probably reflecting the low NO_X roadside increment at the roadside site – and only reached a maximum f-NO_2 of 13.7% in 2005. The only Scottish site with good data capture over a period of years, Glasgow Kerbside has a very flat trend in f-NO_2 from 1999 until 2006. In 2007 f-NO_2 increased to 12.8% compared with 9.5% in 2006. Generally f-NO_2 at the small selection of sites modelled did not exceed 15%

6.2.2.9 Northern Ireland

In Northern Ireland (Figure 6.14), as in Wales and Scotland, there are issues with reliability of the model results at many of the sites considered due to low data capture. This again probably results from the relatively low NO_X roadside increment experienced along the roads on which the monitoring sites are located. The general picture from the results, however, suggests that f-NO_2 on many roads remains low with small upward trends apparent in some locations and no trend apparent in others. Derry Dales Corner (maximum modelled f-NO_2 of 28.8%), Belfast Roadside (maximum f-NO_2 of 19.2%), North Down Holywood A2 (maximum f-NO_2 of 17.6%) and Castlereagh Lough View Drive (maximum f-NO_2 of 17.3%) have the highest modelled f-NO_2 from the sites modelled in Northern Ireland. Otherwise modelled f-NO_2 values are typically in the region of approximately 10%.

6.2.3 Discussion on f-NO_2 Trends

6.2.3.1 Geographical Distribution of f-NO_2

The results presented above provide evidence of regional geographical variations across the UK in terms of f-NO_2 at roadside locations. The highest f-NO_2 values tend to be found in London, which also contains many of the sites where the steepest upward trends in f-NO_2 have been modelled. Many, but not all, sites considered in this analysis across the South of England, the Midlands and East Anglia also exhibit upward trends in f-NO_2, although the maximum modelled f-NO_2 at these sites do not typically reach the levels found at some of the higher sites in London. The sites selected in the North of England, Wales, Scotland and Northern Ireland collectively suggest there is less of a general increase in roadside f-NO_2 in these areas, although there are a few sites within these regions where f-NO_2 has risen significantly in the past few years.

It is important to note that there are a number of caveats that should be applied to the general geographical distribution of f-NO_2 described above. Firstly, the model is a local scale model, which applies only in the immediate vicinity of the roadside monitoring site for which it has been run. For example, the two Oxford sites are located on adjoining roads in the city centre, but f-NO_2 at these sites from 2003-2007 has increased at one without showing a clear trend at the other (although the absolute f-NO_2 values are broadly similar at the two sites). Given the different behaviours of sites within the same cities/regions (e.g. within London and within Cambridge), it is difficult to generalise f-NO_2 results, even across roads within a very small area.

Secondly, the coverage of the sites used in this modelling exercise in some regions is relatively poor and there are large areas across the country that are not represented by even one site. Where there are a good number of sites in a region, often the length of time series is insufficient to detect trends in the modelled f-NO_2.

Thirdly, particularly at sites in Scotland, Northern Ireland and to a lesser extent Wales, low data capture has been an issue in this modelling exercise because of the relatively low roadside increment on roads next to the monitoring sites. Points with low data capture are more uncertain and therefore less confidence can be placed in these results.

6.2.3.2 Trends in f-NO_2 up to and including 2007

At sites where the model suggests f-NO_2 has increased over time, it is possible to identify three groups of sites:

- Sites where f-NO_2 has continued to rise between 2006 and 2007
- Sites where f-NO_2 has levelled off
- Sites where f-NO_2 has fallen between 2006 and 2007

Sites where f-NO_2 has continued to rise between 2006 and 2007 include sites where significant increases are still occurring (e.g. Camden Kerbside, Tower Hamlets Roadside). f-NO_2 at other sites (e.g. Brighton Roadside) has risen more slowly, while at some sites (e.g. London Marylebone Road) f-NO_2 increases have levelled off entirely. A significant number of the sites modelled in London from the LAQN network suggest f-NO_2 has peaked in 2005-2006 and now declining again (e.g. Islington 2 – Holloway Road, Hammersmith and Fulham 1 - Broadway).

Figure 6.5. f-NO_2 trends at selected sites in England – London (AURN sites).
Labelling convention Network: roadside site name (paired background site name)
Black points denote >30% data capture; grey points <30% and >10% data capture; and white points <10% data capture

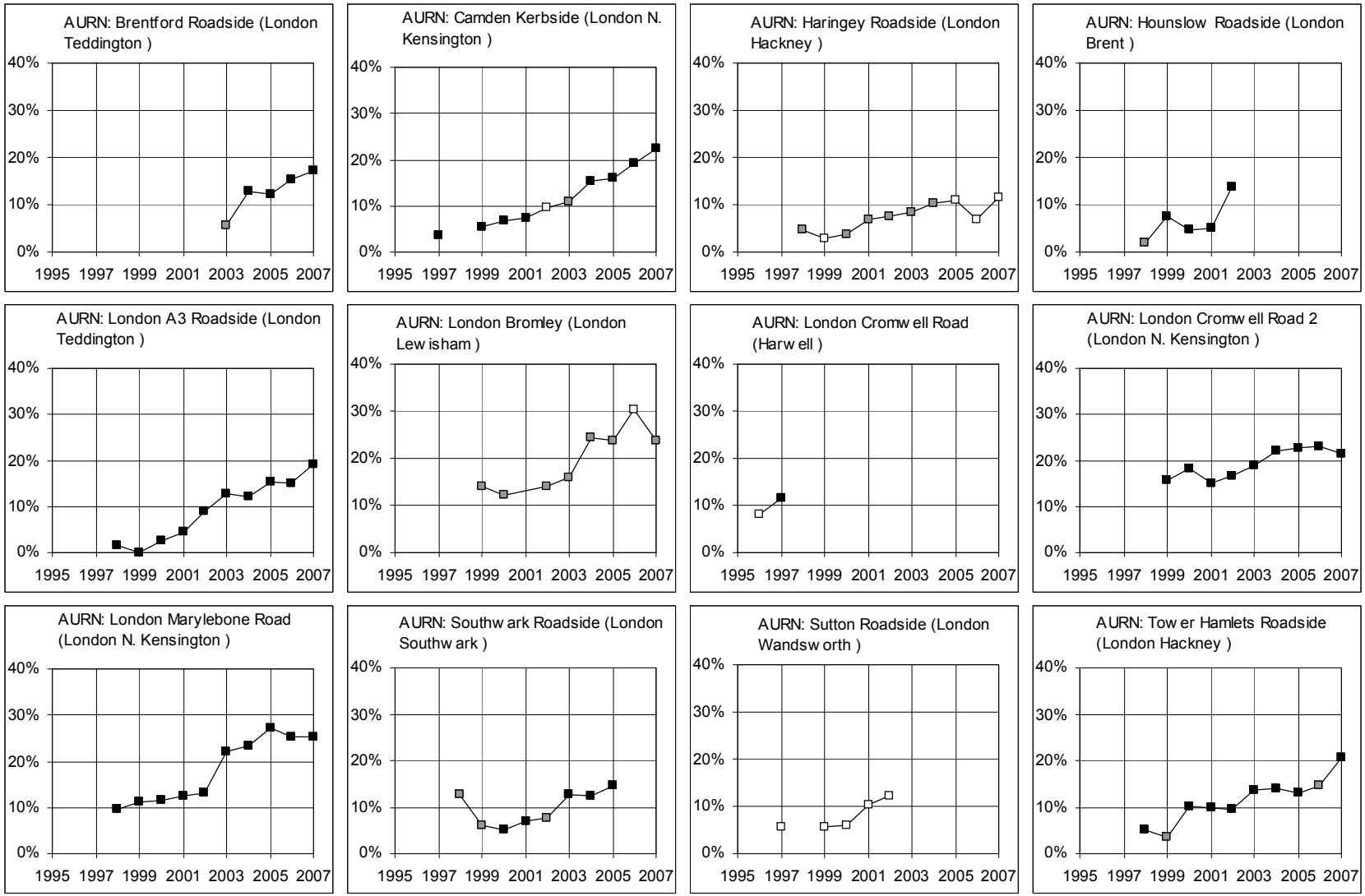

Figure 6.6. f-NO_2 trends at selected sites in England – London (LAQN sites).
Labelling convention Network: roadside site name (paired background site name)
Black points denote >30% data capture; grey points <30% and >10% data capture; and white points <10% data capture

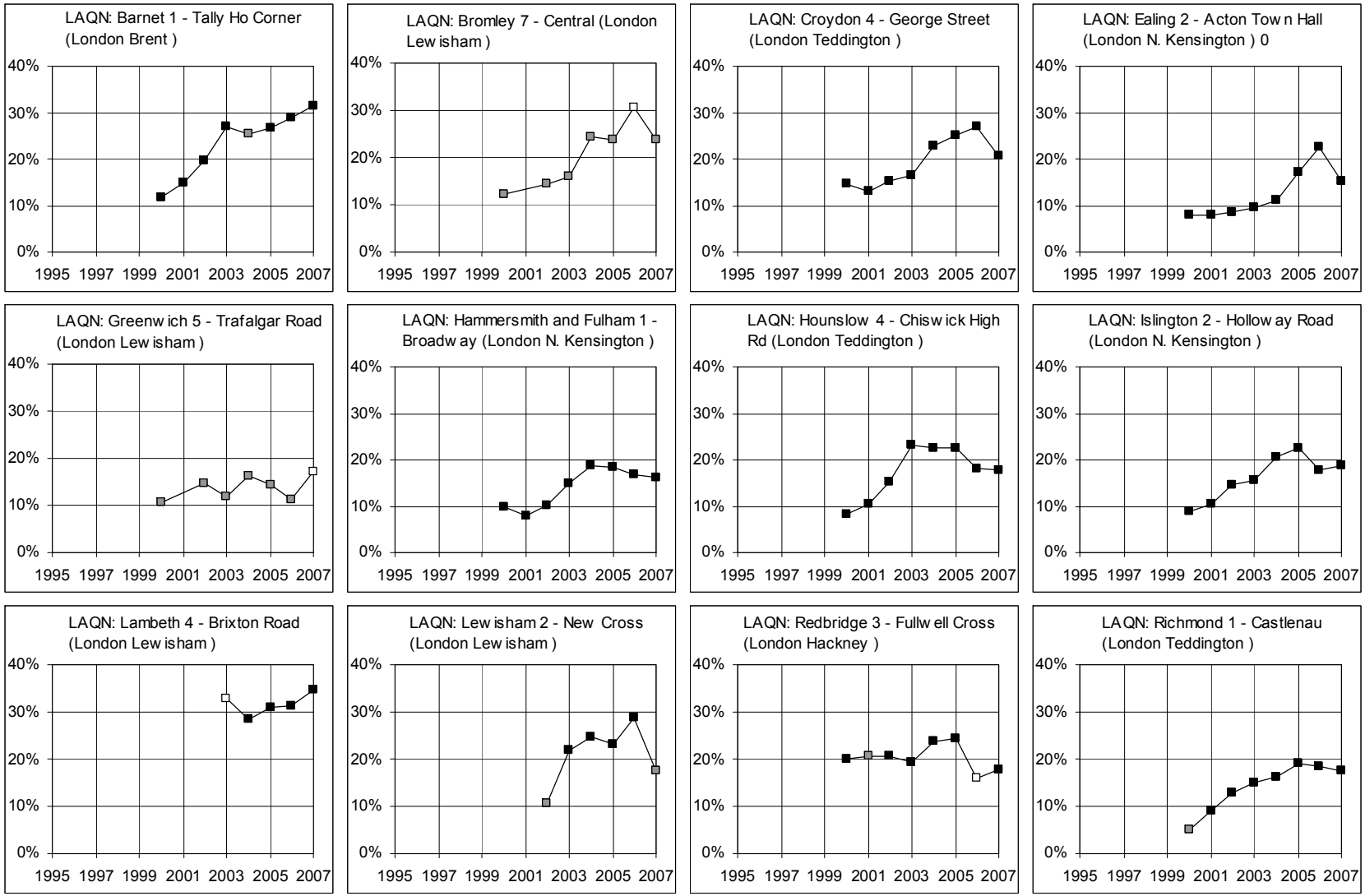

Figure 6.7. f-NO_2 trends at selected sites in England – The South East
Labelling convention Network: roadside site name (paired background site name)
Black points denote >30% data capture; grey points <30% and >10% data capture; and white points <10% data capture

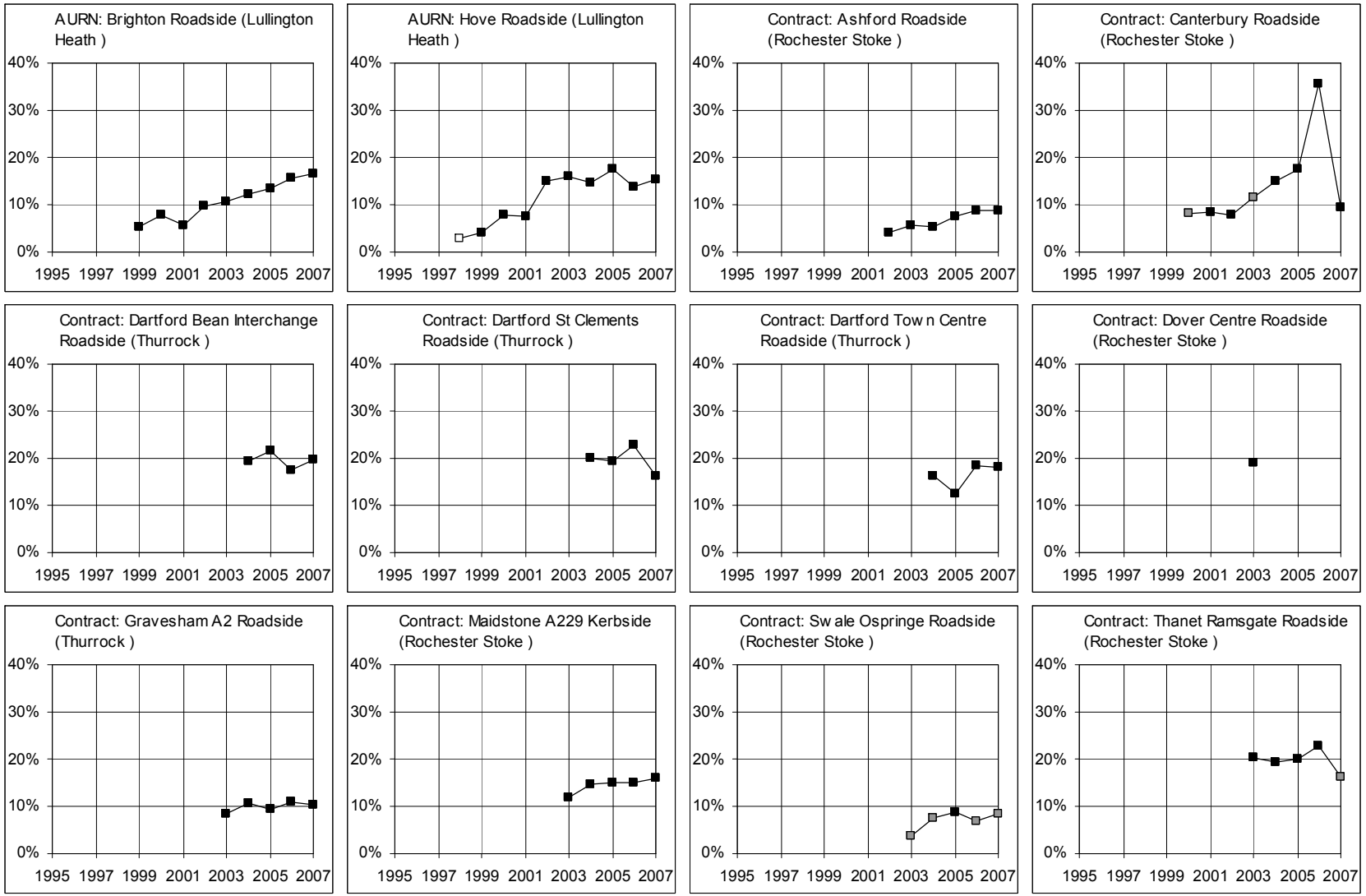

Figure 6.8. f-NO_2 trends at selected sites in England – The South West
Labelling convention Network: roadside site name (paired background site name)
Black points denote >30% data capture; grey points <30% and >10% data capture; and white points <10% data capture

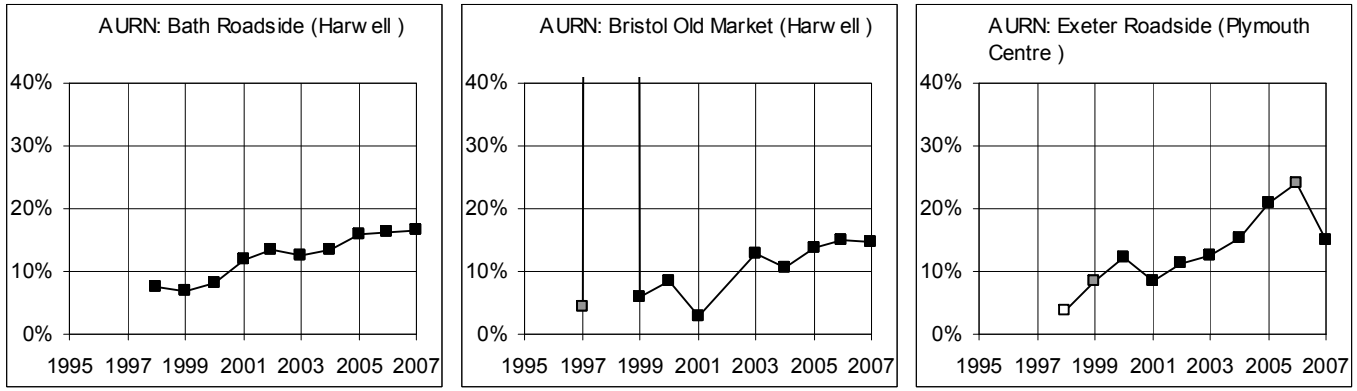

Figure 6.9. f-NO_2 trends at selected sites in England – The Midlands
Labelling convention Network: roadside site name (paired background site name)
Black points denote >30% data capture; grey points <30% and >10% data capture; and white points <10% data capture

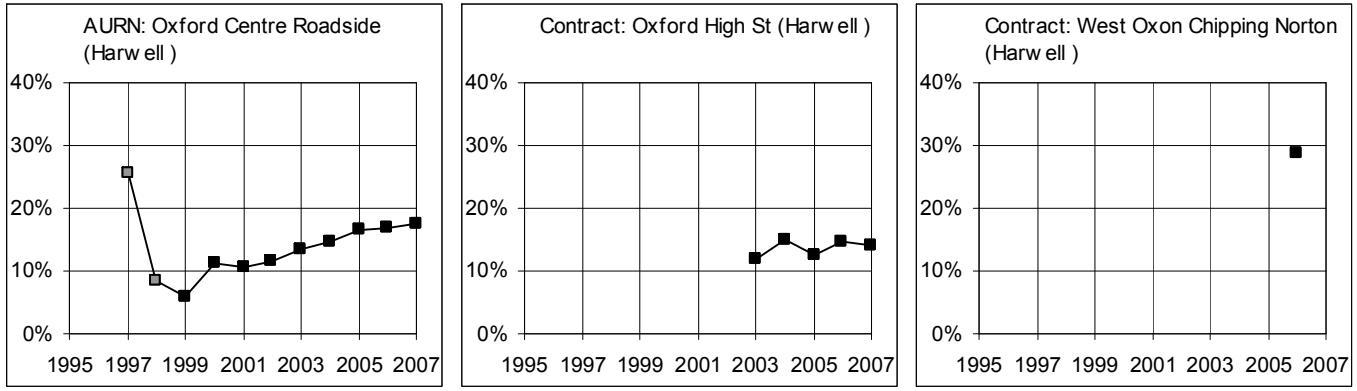

Figure 6.10. f-NO_2 trends at selected sites in England –East Anglia
Labelling convention Network: roadside site name (paired background site name)
Black points denote >30% data capture; grey points <30% and >10% data capture; and white points <10% data capture

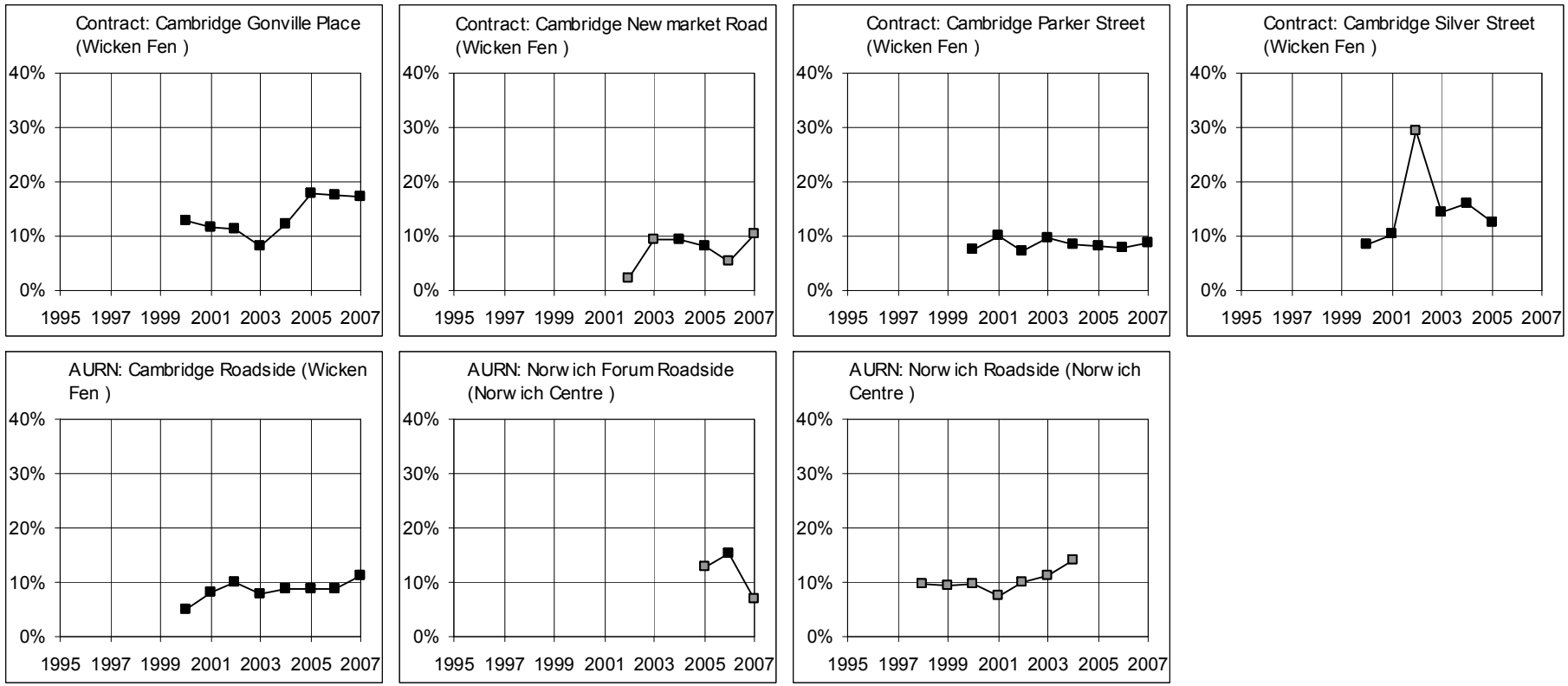

Figure 6.11. f-NO_2 trends at selected sites in England – The North
Labelling convention Network: roadside site name (paired background site name)
Black points denote >30% data capture; grey points <30% and >10% data capture; and white points <10% data capture

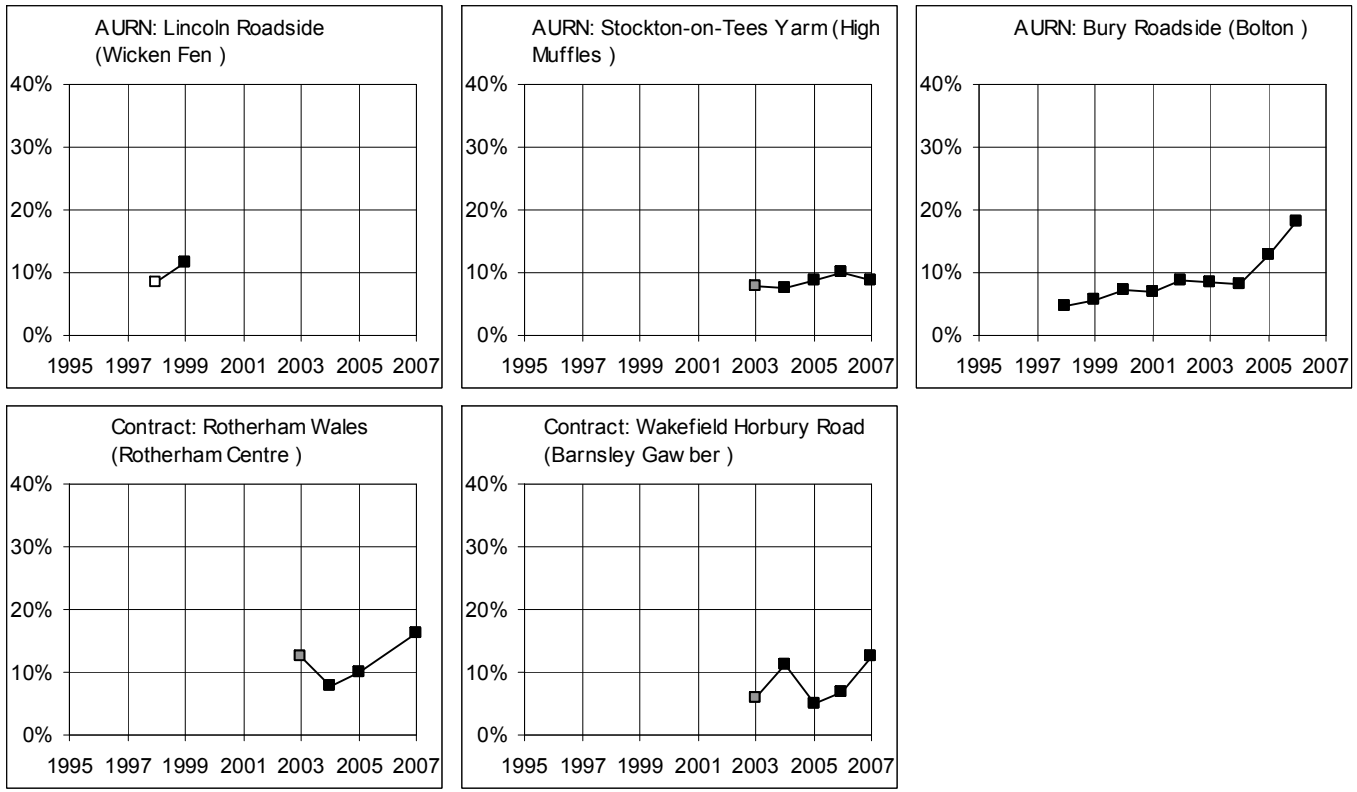

Figure 6.12. f-NO_2 trends at selected sites in Wales
Labelling convention Network: roadside site name (paired background site name)
Black points denote >30% data capture; grey points <30% and >10% data capture; and white points <10% data capture

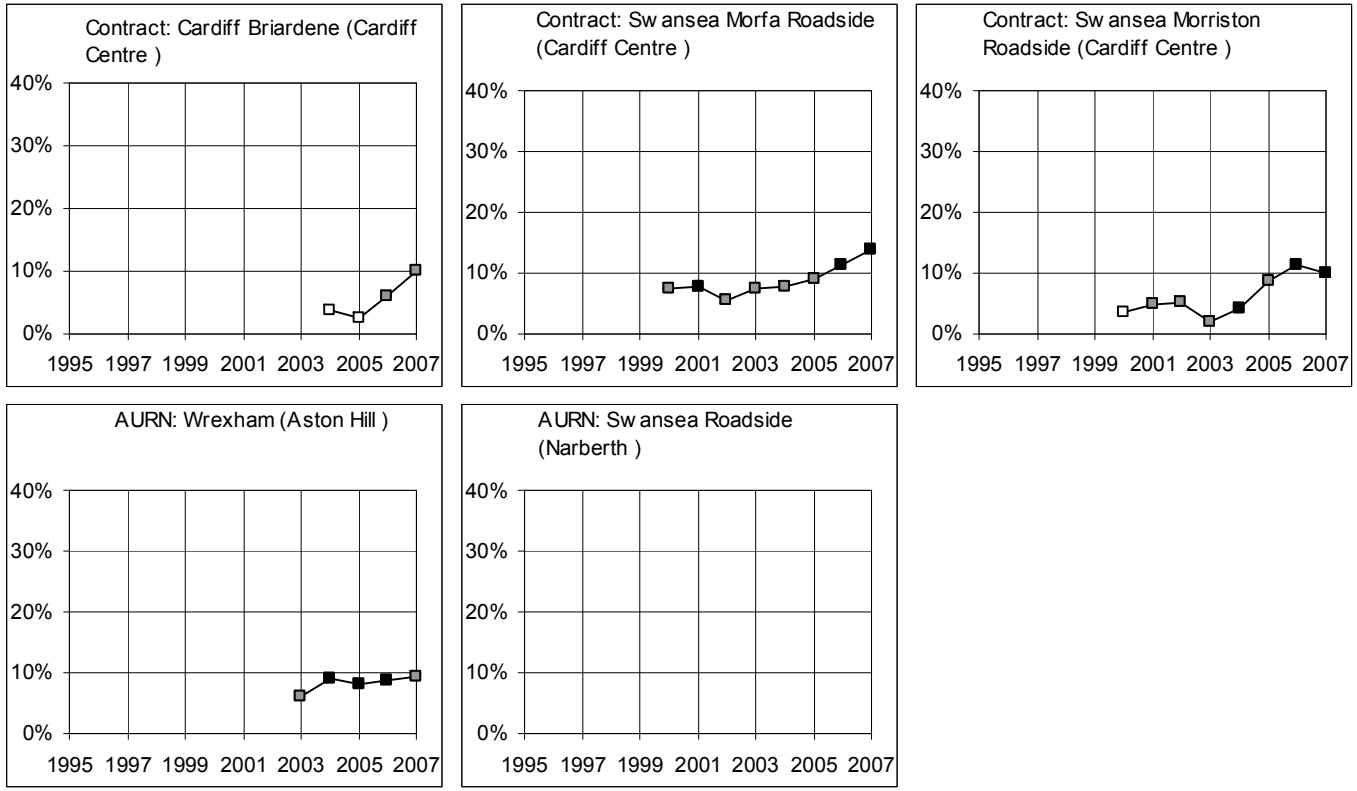

Figure 6.13. f-NO_2 trends at selected sites in Scotland
Labelling convention Network: roadside site name (paired background site name)
Black points denote >30% data capture; grey points <30% and >10% data capture; and white points <10% data capture

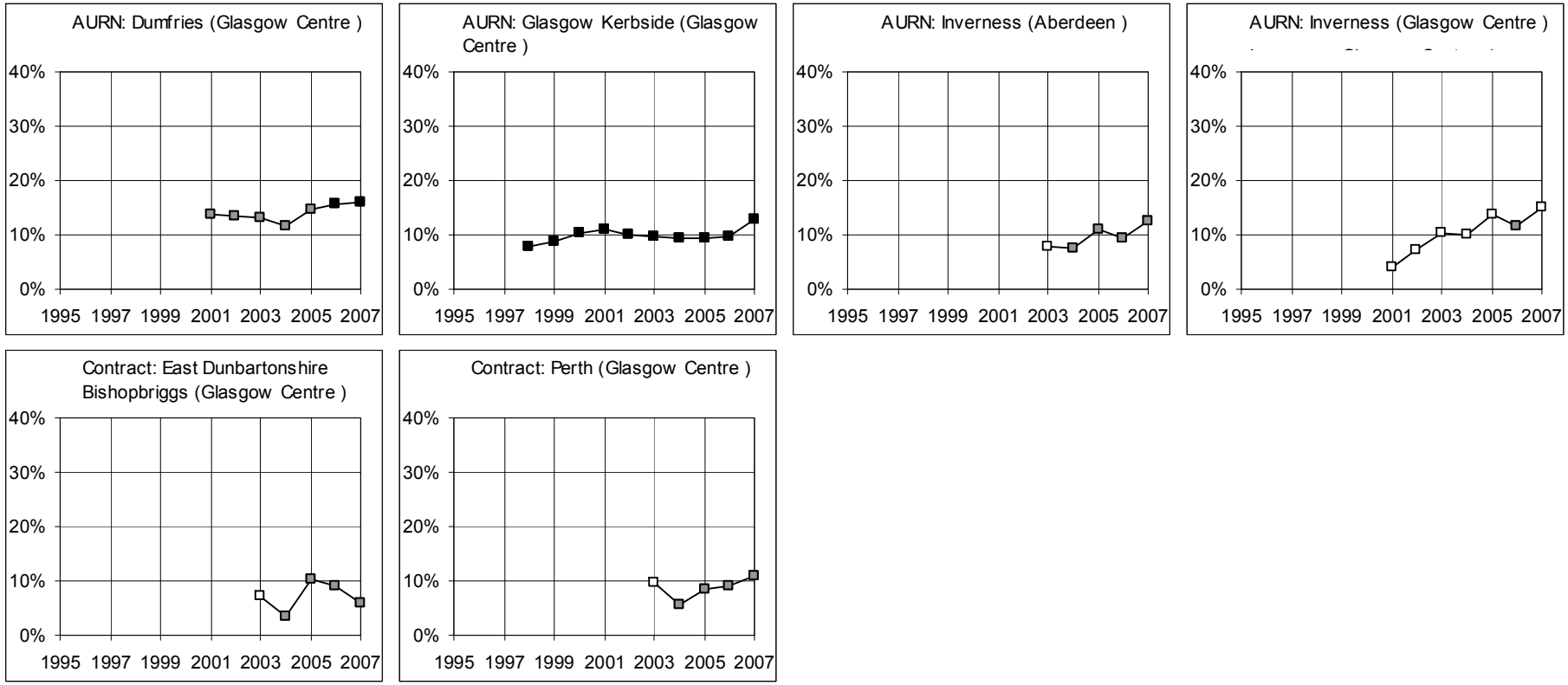

Figure 6.14. f-NO_2 trends at selected sites in Northern Ireland
Labelling convention Network: roadside site name (paired background site name)
Black points denote >30% data capture; grey points <30% and >10% data capture; and white points <10% data capture

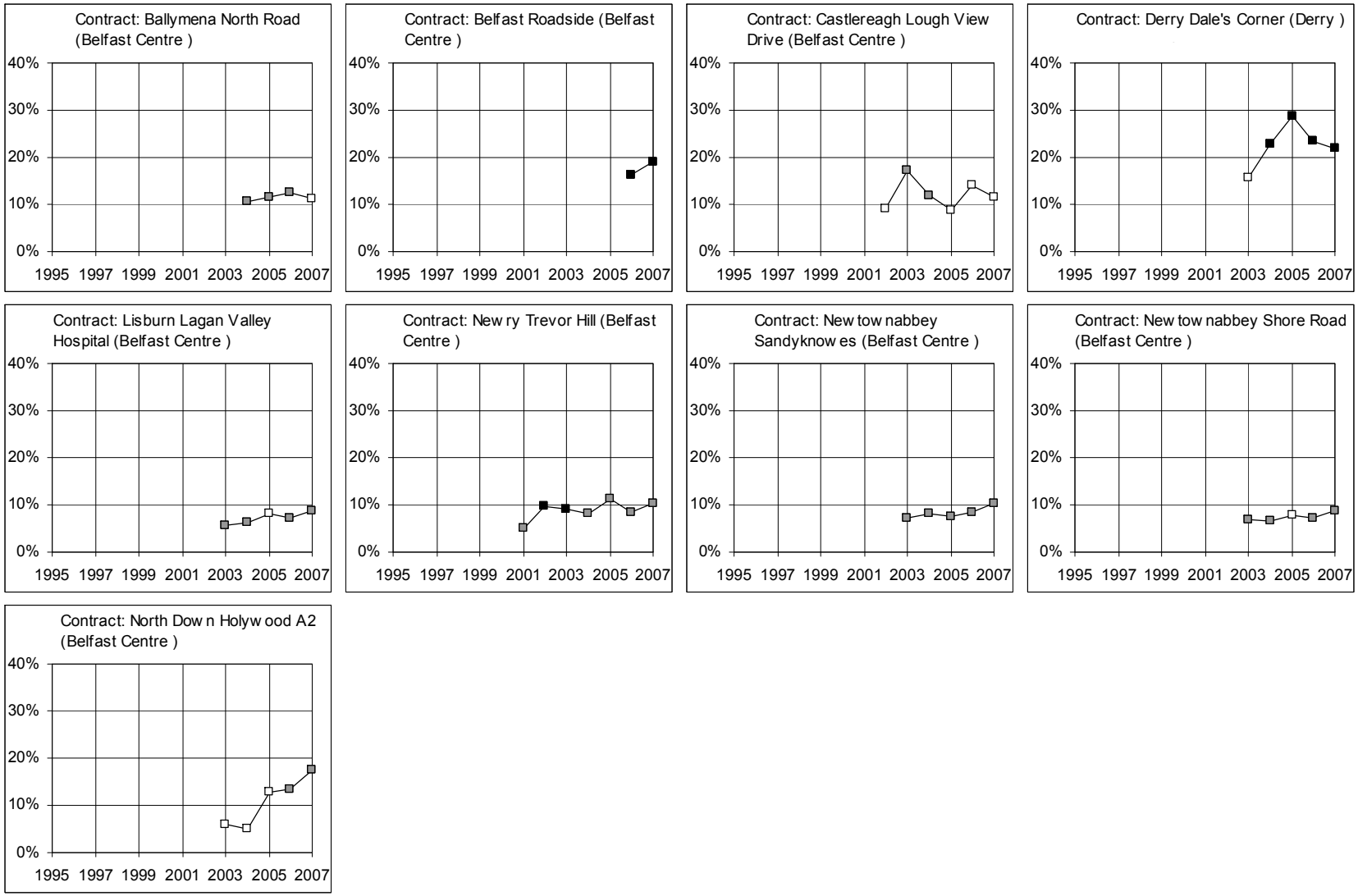

The modelling presented above therefore presents a very mixed picture in terms of how f-NO_2 has changed in the past year or so. This suggests that predicting future changes in f-NO_2 across the UK for national scale models like the PCM model will be difficult as f-NO_2 is increasing in some places, but decreasing in others.

6.2.3.3 Comparison of modelled f-NO_2 with f-NO_2 derived using an emissions inventory

One alternative method to estimating f-NO_2 is to generate an NO_2 specific inventory. This has been calculated by the NAEI for use in the Technical Guidance 08 (TG(08)). On the basis of the NO_X emissions inventory for the traffic combined with f-NO_2 values for different vehicle categories based on exhaust emission measurements, fleet-average f-NO_2 values across the UK for all traffic, all London traffic, all other urban traffic, all non-urban traffic and for specific vehicle types have been calculated in TG(08).

A time-series of f-NO_2 values is shown in Figure 6.15. The time-series reflects changes in the traffic mix in each area and the mix of vehicle emission control technologies (Euro standards) since f-NO_2 values for a given vehicle type depend on these. This shows f-NO_2 for all London traffic is expected to increase to around 23% by 2015 and then level off. For all other UK urban traffic f-NO_2 is expected to continue to rise until 2025, but only to reach a maximum value of around 15%.

Given the cross-section of roads that the f-NO_2 values represent – both in London and those from across other urban areas in the UK – this graph seems to broadly agree with the general trend of increasing f-NO_2 at many roadside locations in the UK. However, a comparison between the UK urban roads trend shown in Figure 6.15 and the trends at individual sites in Figures 6.5-6.14 does illustrate the extent to which f-NO_2 on individual roads may not be adequately represented by the national average, especially in London.

Figure 6.15. f-NO_2 estimates from the NAEI for use in TG(08)

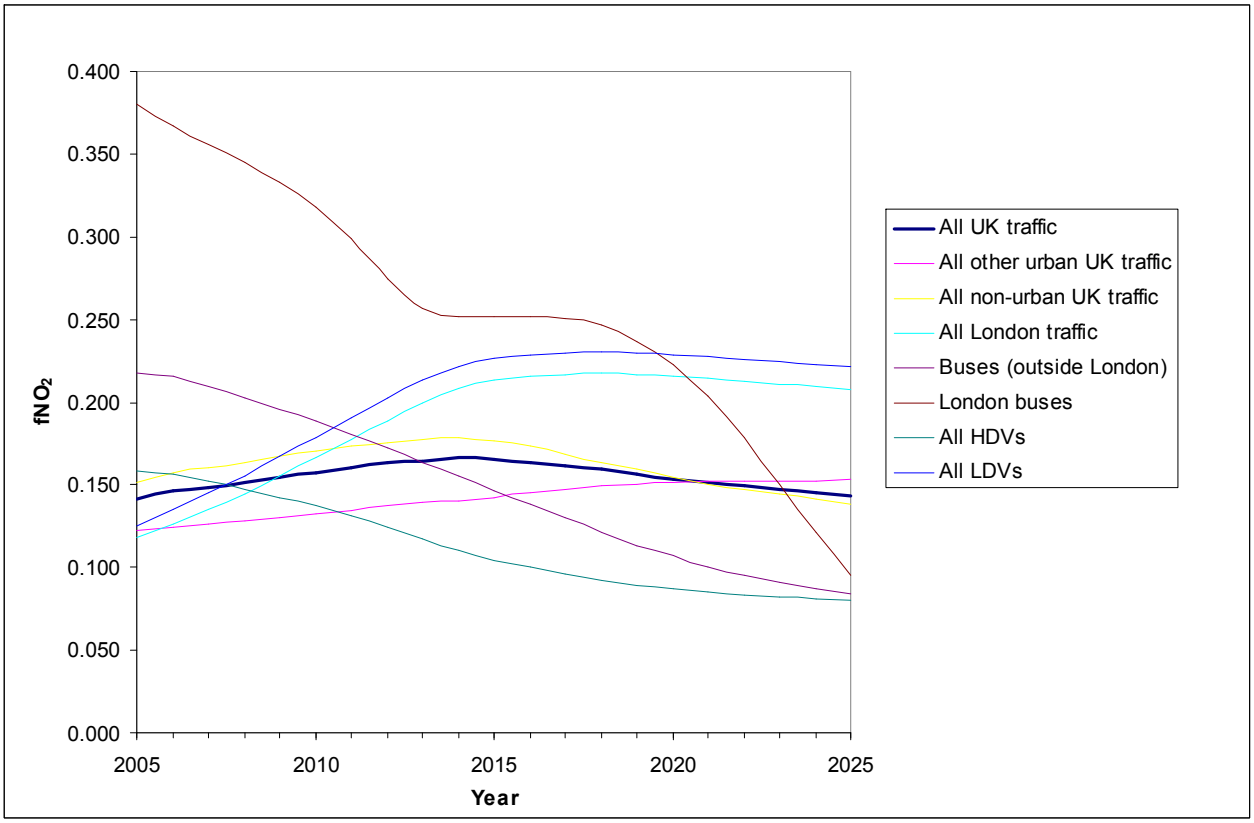

6.3 Conclusions on NO_x-NO_2-O_3 Relationships

The focus of the research for this objective has been on the analysis and interpretation of ozone, NO_x and NO_2 monitoring data to gain further insight into the geographical dependence of the hemispheric baseline contributions and regional modifications to the background oxidant (ozone plus NO_2) concentrations in the UK. This has enabled the development of expressions describing the spatial variation in the hemispheric and regional oxidant components and year-specific parameters for use in empirical modelling of annual mean background oxidant concentrations in the UK. The outputs of these analyses are being used to improve and update the representation of the oxidant partitioning method in the Pollution Climate Model (PCM), in relation to assessments of annual mean NO_2 and O_3 levels. Further analysis of oxidant at roadside monitoring sites using the Netcen Primary NO_2 Model, extended to 2007, has yielded further information on regional variations in trends in primary NO_2 emissions to compare directly with trends predicted by the national emissions inventory.

An analysis of hourly-mean O_3 and NO_X data from a series of historical photochemical episodes in the UK has commenced, with the aim of evaluating urban-scale oxidant production in the London conurbation. The analysis will examine whether there is evidence for an apparent increase in the background oxidant level, $[OX]_B$, during east-to-west passage over the London conurbation. The results of this analysis will be reported in subsequent project reports.

7 Improvements to Photochemical Reaction Schemes (Objective 3)

There are a large number of volatile organic compounds emitted from both anthropogenic and natural sources which contribute to ground-level ozone production. For instance, the 2000 UK VOC emission inventory considered 664 VOCs emitted from 249 source sectors. The contributions of individual compounds to ozone formation vary, a result of differing chemical reactivities and structures. VOC control policies will be more effective from the point of view of reducing ozone formation if they are based on assessments using models that can take full account of the different reactivities of different VOC species. A major thrust in development of ozone models has been to improve and/or expand the information available on key groups of compounds contributing to ozone formation

The Department's Ozone Research Programme has supported the development of detailed chemical mechanisms representing the breakdown of individual volatile organic compounds in the atmosphere. This has culminated in the **Master Chemical Mechanism (MCM)**, the latest version of which treats 135 emitted volatile organic compounds from both manmade and natural sources, producing ~5,900 chemical species involved in nearly 13,500 thermal and photochemical reactions. Generally speaking, the purpose of a chemical mechanism in any policy modelling tool addressing ozone or other air pollutants is to convert the emissions of the organic compounds into estimates of the concentrations of the pollutants. The modelling tool itself may address the urban, regional or global atmosphere and the damaging pollutants addressed may be ozone and the other atmospheric oxidants, together with fine particulate matter. In each case, the chemical mechanism is required to quantify the conversion rates of the emitted organic compounds into ozone, other oxidants and fine particulate matter and, in turn, to describe quantitatively their atmospheric destruction and removal rates.

The MCM has played a critical role in the development of the Photochemical Ozone Creation Potential (POCP) concept, an index to rank the contribution of individual VOCs to ozone formation, and the calculation of POCPs on different timescales including multi-day timescales characteristic of photochemical episodes in Europe.

Using the knowledge and understanding gained from developing the MCM, a reduced mechanism - the Common Representative Intermediate (CRI) mechanism - has been derived from the Master Chemical Mechanism, v3.1. Models such as the OSRM currently use other reduced chemical mechanisms not linked directly to the MCM.

In the previous year of the current tropospheric ozone modelling project (2007), a comprehensive review of the MCM was undertaken (Derwent et al, 2007b and see also Murrells et al, 2008). The initial assessment of the MCM was independently peer-reviewed and following this a series of recommendations were made on future development work. A work programme was agreed with the Department aimed at improving and maintaining the status of the MCM and related mechanisms and assessing and guiding the improvement of the representation of organic chemistry in atmospheric models used in policy applications. The four main tasks to be carried out are:

- Development of a hierarchy of traceable reduced mechanisms from the MCM
- Development of new MCM schemes
- A major revision of the MCM protocol
- Development and application of a secondary organic aerosol (SOA) code

In addition to this, and in support of these tasks, the maintenance of the MCM on the internet website by the University of Leeds would continue.

This section reports on developments in each of these tasks.

7.1 Development of a Hierarchy of Traceable Reduced Mechanisms

7.1.1 Introduction

The many hundreds of VOCs that are emitted (e.g. Dore et al, 2003a) possess a variety of physico-chemical properties by virtue of differences in structure and functional group content. It is because these factors influence the reactivity (i.e., the rate of oxidation in the atmosphere) and the oxidation pathways available (i.e., the degradation mechanism) that the propensities of VOCs to form secondary pollutants such as ozone and SOA varies from one compound to another (e.g., Derwent and Jenkin, 1991; Carter, 1994; Grosjean and Seinfeld, 1989). Modelling studies using detailed emitted VOC speciations and comprehensive descriptions of VOC degradation chemistry have thus provided a means of quantifying the roles played by VOCs (both individually and collectively) in atmospheric chemistry, thereby allowing detailed appraisals of the contributions made by individual VOCs, or VOC classes, to ozone formation (e.g., Derwent et al., 2007c). Those studies made use of the **MCM v3.1**, which represents a direct utilisation and application of the results of studies of elementary chemical processes. The MCM is therefore conceptually simple, since it contains almost no empirical lumping or surrogate species. As a result, however, the mechanism contains many thousands of chemical species and reactions, and it is recognised that the development of less-detailed schemes is essential for many applications where greater computational efficiency is required.

The development of a traceable reduced mechanism to describe the formation of ozone from the oxidation of methane and 115 emitted hydrocarbons and oxygenated VOCs (112 anthropogenic and 3 biogenic) was carried out in a preceding project, the mechanism being known as version 2 of the Common Representative Intermediates mechanism, CRI v2 (Jenkin et al., 2008). The mechanism was built up on a compound-by-compound basis, with the performance of its chemistry optimised for each compound in turn by comparison with that of MCM v3.1, using a series of five-day box model simulations. The resultant mechanism contains 1183 reactions of 434 chemical species, which is about 10 % of the number of reactions and species required to degrade the same set of VOCs in MCM v3.1. A key assumption in the CRI v2 construction methodology is that the potential for ozone formation from a given volatile organic compound (VOC) is related to the number of reactive (i.e., C-C and C-H) bonds it contains. This index allowed a series of generic intermediates to be defined, with each being used as a “common representative” for a large set of species possessing the same index, as formed in detailed mechanisms such as the MCM.

In the following section, a description of the validation of CRI v2 is provided, through comparison of its performance with that of MCM v3.1 for a wide range of ambient conditions. These consider variations in VOC/NOx emissions ratio over ranges of 32 and 400 for anthropogenic and biogenic VOCs, respectively, in box model simulations, and simulations of the TORCH 2003 campaign in the southern UK using the PTM, which consider notable ranges in the relative and absolute emissions of NOx and VOCs, and in the relative contributions of anthropogenic and biogenic species to the VOC total.

CRI v2 is a reduced mechanism of intermediate complexity, which is traceable to MCM v3.1, and which provides the basis for further systematic reduction. The further reduction of CRI v2 through systematic emissions lumping is described in Section 7.1.3, yielding a traceable set of further reduced CRI mechanisms. The development and assessment of an associated SOA module, for application with CRI v2 and its reduced variants, has also been carried out and is described further below in Section 7.4.4.

7.1.2 Testing of CRI v2

Initial testing was carried out using a series of five-day box model simulations. The box model represents a well-mixed boundary layer box, 1 km in depth, which receives emissions of NO_X, CO, SO_2, methane and non-methane VOCs, based on average emission densities in the UK in 2001 (Dore et al., 2003a), but with appropriate diurnal and seasonal variations superimposed, as presented by Utembe et al. (2005). The model was run for conditions appropriate to a latitude of 51.5 °N on June 21, under clear sky conditions.

Figure 7.1 shows a comparison of ozone profiles simulated with CRI v2 and MCM v3.1 throughout the five day period for a speciation of 112 non-methane anthropogenic VOCs, based on the UK NAEI. Simulations were carried out for the standard emissions densities, and with the VOC/NOx emission ratio varied over a range of 32 by scaling the NOx emissions by factors between 0.125 and 4. This allowed the transition from VOC-limited to NOx-limited conditions to be examined, which is presented in terms of the VOC/NOx ratio relative to the base case, $(VOC/NOx)_{rel}$, in Figure 7.1. The ozone profiles simulated with CRI v2 are in good agreement with the MCM v3.1 profiles for the complete range of VOC/NOx emission ratio. The base case profile, denoted $VOC/NO_x = 1$ in Figure 7.1, shows a tendency to overestimation (by ca. 5%) in the latter stages of the simulation, with a better level of agreement in all the other scenarios.

Figure 7.1: Comparison of ozone mixing ratios simulated from anthropogenic VOC degradation over a five day period with MCM v3.1 (○) and CRI v2 (—) for a range of 32 in VOC/NOx emission ratio (June 21 conditions, 51.5° Lat). The base case simulation was based on average 2001 UK emission densities for anthropogenic VOCs and NOx, using the NAEI VOC speciation (see text), the applied daily average densities being 15.4 kg km^{-2} day^{-1} for VOCs and 18.3 kg km^{-2} day^{-1} for NOx. The range in VOC/NOx was achieved by scaling the NOx emissions, and is displayed relative to the base case, denoted $(VOC/NOx)_{rel}$. The inset shows a comparison of the simulated mean ozone mixing ratios.

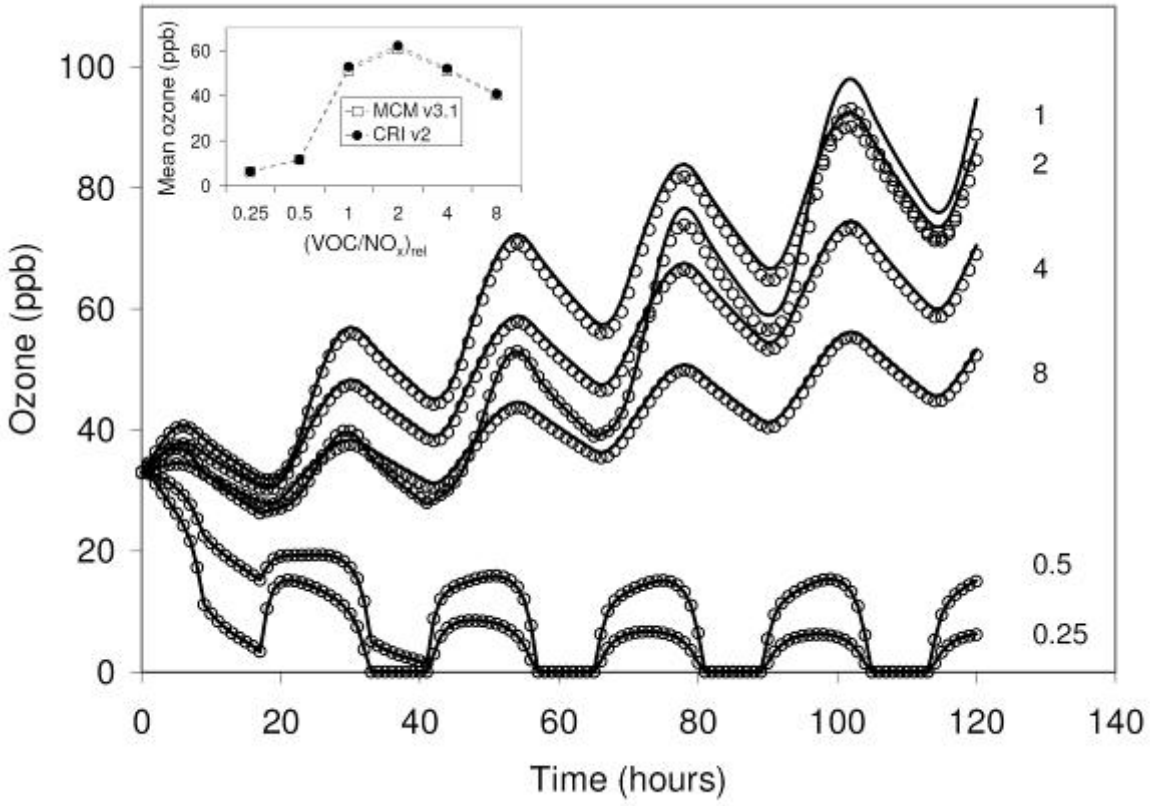

Wider testing of the performance of CRI v2 has also been carried out in relation to simulations of ozone, NO, NO_2, OH, HO_2 RO_2, NO_3, HNO_3, H_2O_2 and HCHO. This has been done for the complete anthropogenic VOC speciation, and also for VOC emissions entirely as alkanes, alkenes, aromatics and oxygenates, whilst maintaining the relative speciation within these categories in line with the NAEI. In each case, variation of the VOC/NOx emissions ratio over at least a range of four has been considered. This has demonstrated a generally good performance over a wide range of conditions, with the simulations of ozone typically agreeing to better than 10 % for the simulations in which VOC emissions were emitted entirely as aromatics, and to better than 5 % in all other cases. The example comparisons shown in Figures 7.2 and 7.3a demonstrate that the simulated levels of OH and HCHO for the full anthropogenic VOC mix also typically agree to better than 5 % for the complete range of VOC/NOx emissions ratio discussed above.

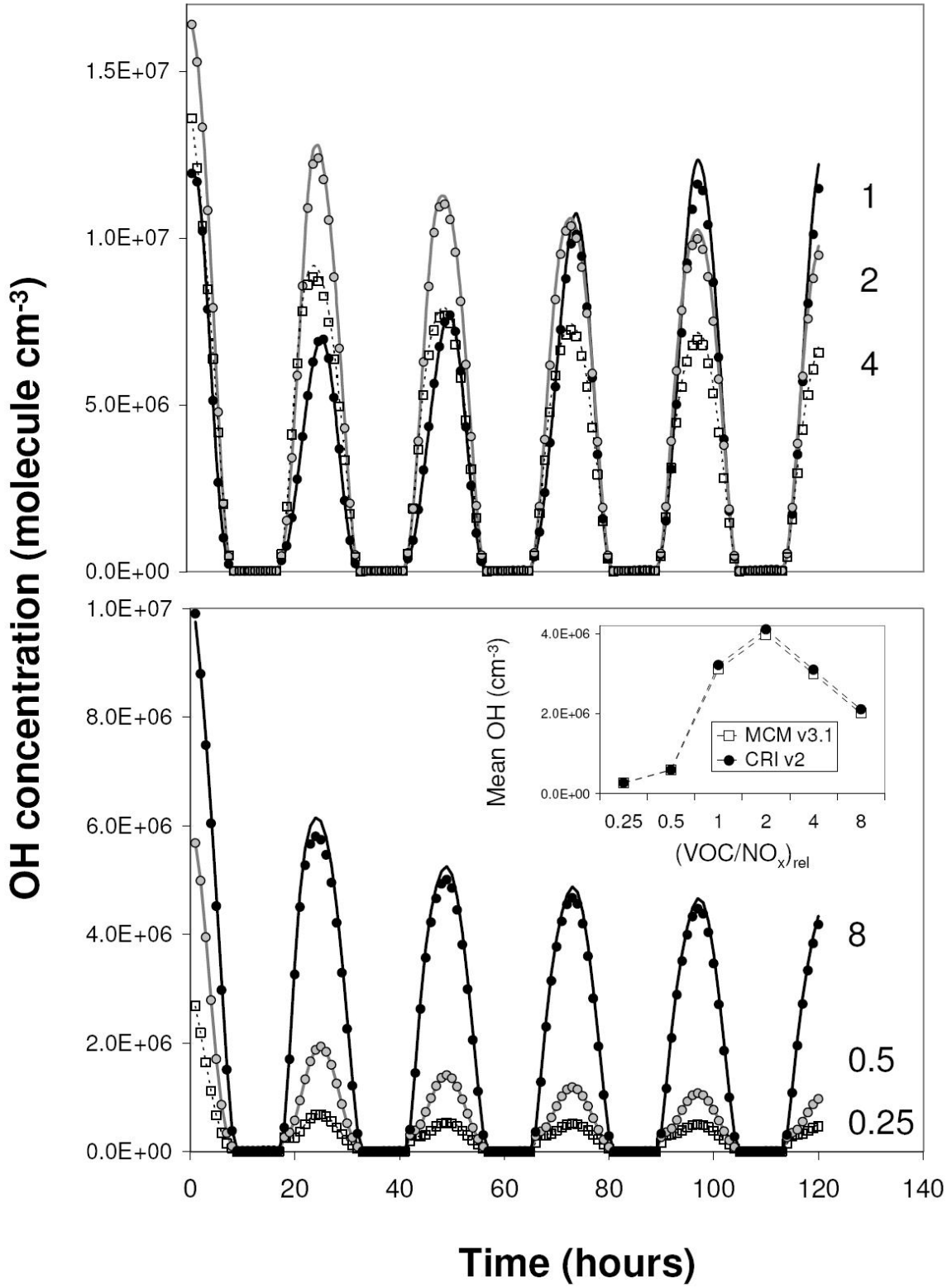

Figure 7.2: Comparison of OH concentrations simulated over a five day period with MCM v3.1 (points) and CRI v2 (lines), for the conditions summarised in the Figure 7.1 caption. The lower panel inset shows a comparison of the simulated mean OH concentrations.

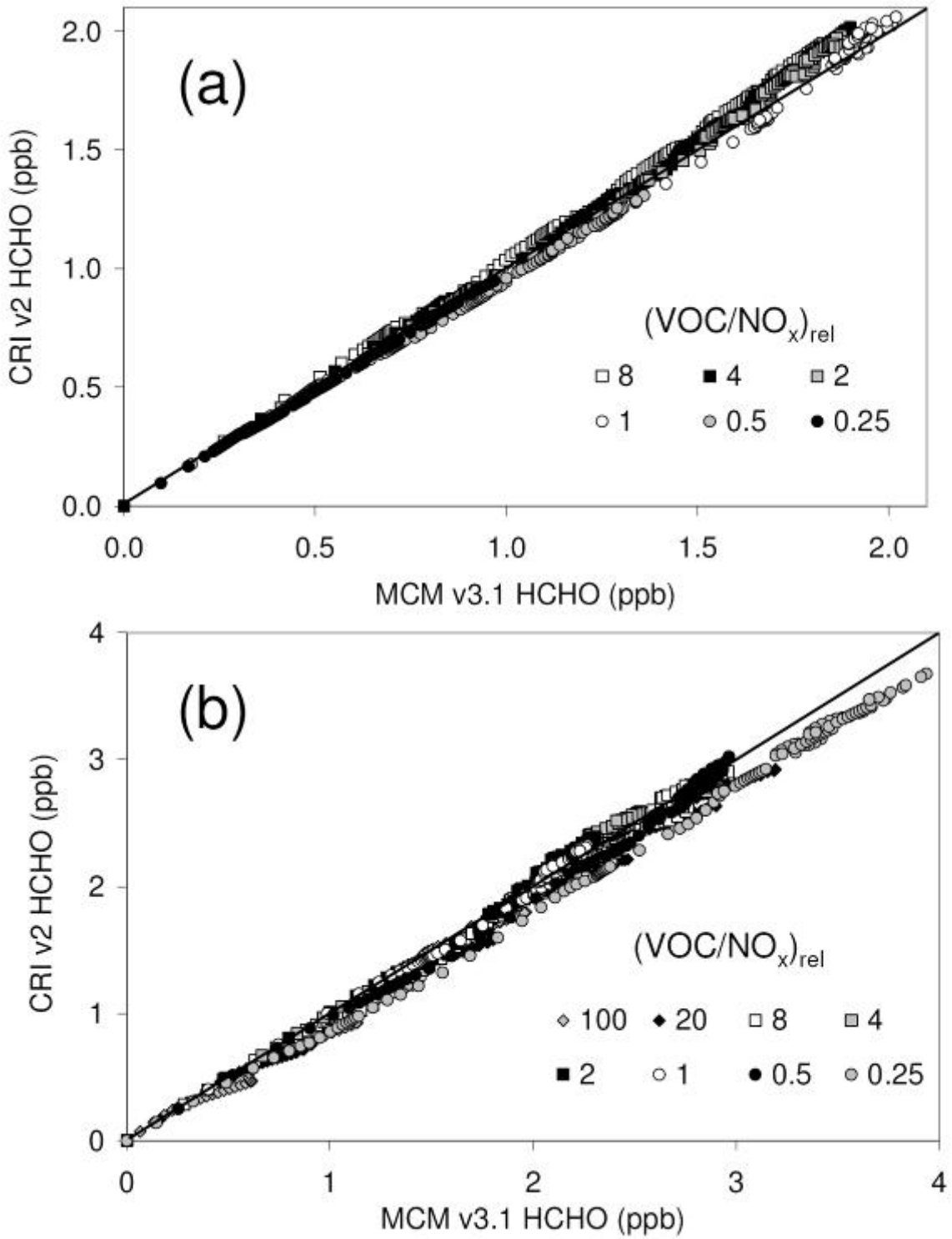

Figure 7.3: Correlation of HCHO mixing ratios generated from the processing of emitted VOCs over a five day period, simulated with MCM v3.1 and CRI v2. (a) Results using an anthropogenic VOC speciation, for the conditions summarised in the Figure 7.1 caption; (b) Results using a biogenic VOC speciation, for the conditions summarised in the Figure 7.4 caption. The 1:1 line in also shown in each panel.

Figure 7.4 shows a comparison of ozone profiles simulated with CRI v2 and MCM v3.1 for a range of VOC/NOx emissions ratios, using a previously applied biogenic hydrocarbon speciation for isoprene and the monoterpenes, α– and β–pinene (Utembe et al., 2005). For procedural consistency, the applied VOC emissions density was based on the UK anthropogenic total. Simulations were carried out for a substantially extended range of VOC/NOx emission ratios of 400 (obtained by scaling the NOx emissions by factors between 0.01 and 4), thus allowing the transition from VOC-limited through to highly NOx-limited conditions to be examined. As shown in Figure 7.4, the ozone profiles simulated with CRI v2 are once again in acceptable agreement with the MCM v3.1 profiles for the complete range of VOC/NOx emission ratio. Importantly, the abilities of the mechanisms to sequester NOx in the form of higher oxidised (inorganic and organic) nitrogen compounds was comparable across the VOC/NOx range, confirming that the biogenic mechanisms would have similar impacts on ozone chemistry under highly NOx-limited conditions characteristic of more remote locations where significant biogenic inputs occur. The formation of HCHO was also found to be in good agreement for the full VOC/NOx range (see Figure 7.3b), indicating that CRI v2 would provide an acceptable basis for interpretation of space-based HCHO measurements in relation to constraining VOC emissions, and their impacts, in remote and polluted environments (e.g., Fu et al., 2007; Palmer et al., 2007).

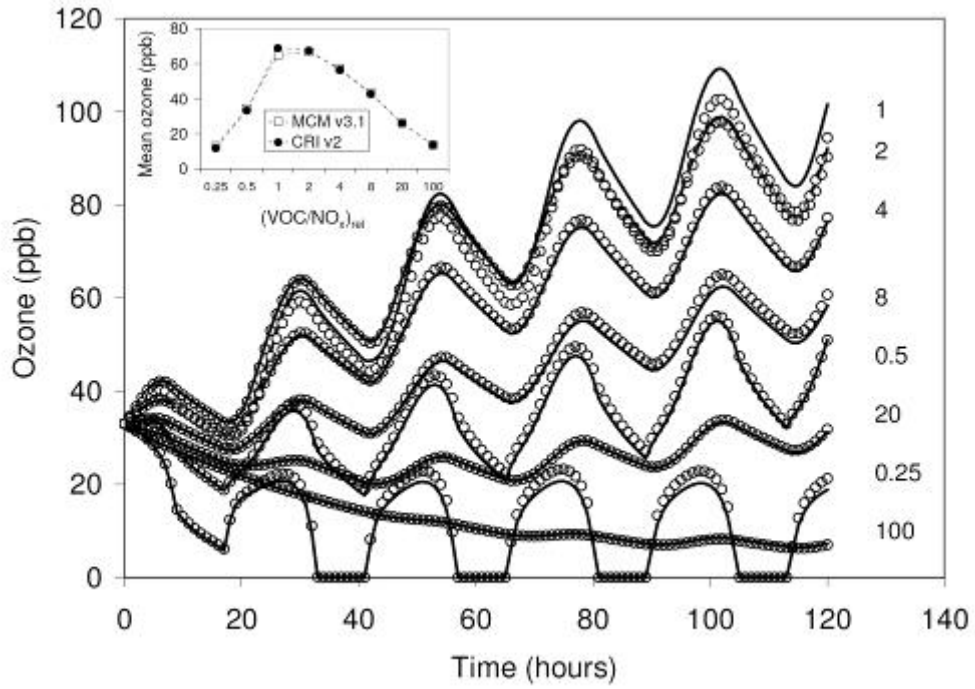

Figure 7.4: Comparison of ozone mixing ratios simulated from biogenic VOC degradation over a five day period with MCM v3.1 (○) and CRI v2 (—) for a range of 400 in VOC/NOx emission ratio (June 21 conditions, 51.5° Lat). VOCs were emitted as 50% isoprene, 30% α-pinene and 20% β-pinene. The range in VOC/NOx was achieved by scaling the NOx emissions, and is displayed relative to the base case, denoted $(VOC/NOx)_{rel}$. The inset shows a comparison of the simulated mean ozone mixing ratios.

The CRI v2 mechanism was finally tested to examine its ability to simulate ozone formation in comparison with MCM v3.1, in relation to observations made during the Tropospheric Organic Chemistry Experiment (TORCH) campaign at Writtle, Essex, UK (51.74°N; 0.42°E), a rural site approximately 40 km to the north-east of central London, during late July and August 2003 (a period which included a regional-scale air pollution event associated with a heat-wave). The PTM containing CRI v2 was used to simulate the chemical development of boundary layer air parcels being advected along 96-hour trajectories arriving at the Writtle site at hourly resolution for the entire campaign period. This made use of ca. 800 back-trajectories, which were obtained from the NOAA on-line trajectory service (Draxler and Rolph, 2003). An otherwise identical version of the PTM containing MCM v3.1 was also used to simulate 16 case study events during the campaign period.

The simulated ozone mixing ratios at the receptor are presented in Figure 7.5, along with the hourly-mean observations. The CRI v2 version of the model recreates the general features of the observed time series, including the elevated ozone levels which prevailed during a stable anticyclonic period of the campaign (3–12 August), indicating that the model is able to provide a reasonable representation of the conditions experienced. As indicated in the figure, the simulated ozone mixing ratios agree well with those simulated using the MCM v3.1 version of the model for 16 case study events. These case studies represent a variety of conditions, such that the inputs of VOCs and NOx each vary over a range of more than an order of magnitude, with the VOC/NOx ratios varying from ca. 0.8 to ca. 2, and with the fractional contribution of biogenic VOC to the VOC total varying from ca. 5 % to ca. 30 %.

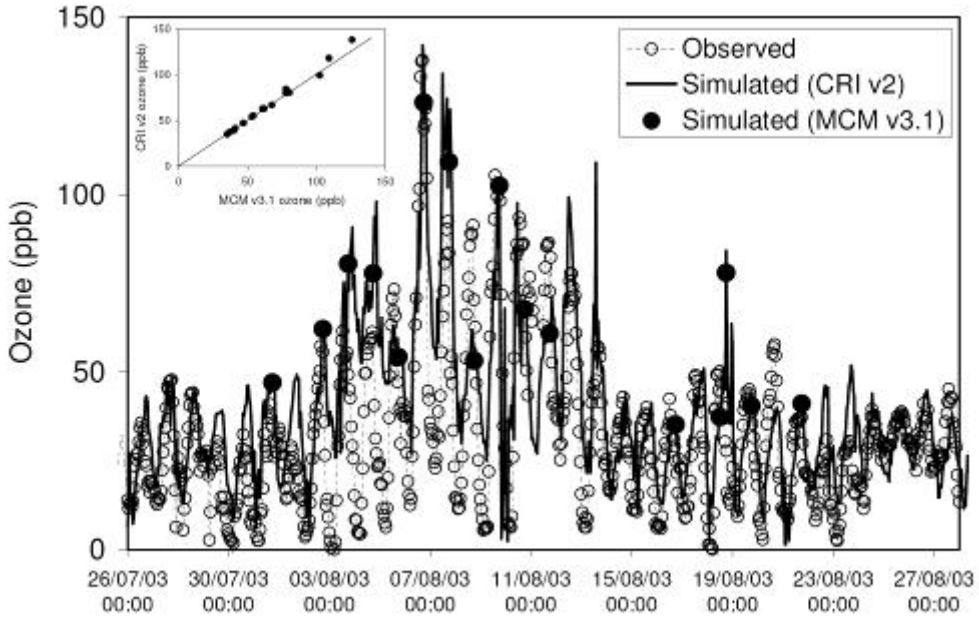

Figure 7.5: Comparison of observed hourly mean ozone mixing ratios with those simulated for the entire TORCH campaign with the PTM containing CRI v2, and for 16 case study trajectories with the PTM containing MCM v3.1. The ozone mixing ratios were measured by the University of York, as reported in Utembe et al. (2005).

7.1.3 Further reduction of CRI v2

Detailed, explicit chemical mechanisms for atmospheric applications are usually reduced either by (i) a systematic reduction in the complexity of the chemistry for the considered suite of VOCs or, (ii) the lumping of emissions so that the chemistry for one VOC can be used to represent that of a number of VOCs. CRI v2 was developed from MCM v3.1 using the first of these techniques (Jenkin et al., 2008). This method was successful in reducing the degradation chemistry for a large number of emitted VOCs while maintaining an accurate description of ozone production, with the resultant CRI v2 mechanism (1183 reactions of 434 chemical species) being smaller than MCM v3.1 by about an order of magnitude. Although CRI v2 is substantially smaller than MCM v3.1, it still contains too many reactions and species for application in models containing more detailed treatments of transport processes. This section presents a logical method for further reducing CRI v2 through systematic emitted species lumping techniques in order to create a series of reduced schemes. Focus is placed on reducing the number of emitted anthropogenic species by redistribution based on their chemical class and photochemical ozone creation potential (POCP), relative to a reference VOC speciation based on that reported by the UK NAEI.

VOC lumping was achieved by two general methods. In the first method, the redistribution of minor emitted VOCs into appropriate surrogates was carried out to maintain their chemical class within a number of VOC sub-categories (alkane, alkene, aromatic, alcohol/ether, aldehyde, ketone, ester/acid),

and aimed to preserve the ozone-forming ability of the redistributed VOCs in each category. The assessment of ozone-forming ability of the individual VOCs was based on the photochemical ozone creation potential (POCP) concept, developed by Derwent and co-workers (e.g., Derwent and Jenkin, 1991; Derwent et al., 1998). The POCP index provides a measure of the relative propensities of VOCs (per unit mass emission) to generate ozone over a timescale of five days, based on simulations using a photochemical trajectory model operating along an idealised trajectory travelling across north-west Europe to the UK. The POCP values are defined relative to a reference value of 100, which is assigned to ethene. For the present study, the POCP values for the non-aromatic and aromatic VOC were based on those calculated with MCM v3, as reported by Saunders et al. (2003) and Jenkin et al. (2003), respectively. This method was applied to generate a sequence of three reduced mechanisms (denoted CRI v2-R1, CRI v2-R2 and CRI v2-R3), with progressively increasing degrees of emissions lumping.

The second method made use of the non-methane VOC groups defined by the Global Emissions Inventory Activity (GEIA) to impose a more severe level of reduction through emissions lumping. In this case, more limited selections of VOCs were used to represent each VOC group, with the choice of species taking account of their POCP value, abundance in the detailed speciation, and the simplicity of the associated CRI v2 degradation mechanism. This method was applied to generate two further reduced mechanisms (denoted CRI v2-R4 and CRI v2-R5).

***VOC redistribution using method 1*:** The first method was applied in three phases to redistribute increasingly greater proportions (5%, 10% and 20%) of the anthropogenic VOC total into suitable surrogate species (as illustrated in Figure 7.6), the chosen surrogate in each case being the retained emitted VOC in the same class which possesses the closest POCP value. For each reduction phase, the given redistribution percentage was generally made up of those VOC with the lowest emissions, with the procedure allowing respective overall redistribution of 48, 60 and 73 VOCs, in the three reduction phases. However, a few VOCs with very low emissions (e.g., formic acid) are generated in CRI v2 as degradation products of VOCs with much higher emissions, and these species were therefore retained in the reduced mechanisms and emissions speciation.

The removal of the redundant species and their associated chemistry yielded the reduced mechanisms CRI v2-R1, CRI v2-R2 and CRI v2-R3, for which the resultant numbers of species and reactions are given in Table 7.1. As also shown in Table 7.1, the applied POCP-based methodology allowed the weighted POCP of the VOC mixture, and those of the broad VOC sub-classes, to be maintained at values which are very close to those of the starting VOC speciation. Accordingly, the box model simulations of ozone formation using the reduced mechanisms, with the associated VOC lumping, are in excellent agreement with that using CRI v2 with the full starting VOC speciation, for average UK emission densities of NOx and VOCs (see Figure 7.7). Logically, the deviation from the reference CRI v2 simulation tends to increase with extent of VOC redistribution and mechanism reduction, but even CRI v2-R3 deviates by $\leq$ 1.2 % throughout the simulation, with the ozone mixing ratios on the whole of the final day of the five day simulation agreeing to better than 0.1 %. This demonstrates that the POCP concept provides a good criterion for emissions lumping, provided the chemistry in the mechanism is consistent with that in the MCM (i.e., the mechanism used to generate the POCP scale).

As indicated in Table 7.1, the reduced variants generated by this procedure allowed reductions in run time by up to about 40 % compared with the full CRI v2. These mechanisms therefore provide more economical alternatives which can be applied more efficiently in selected applications. Because the associated VOC lumping preserves the average POCP values for the VOC sub-classes, these reduced mechanisms are potentially appropriate for applications which consider contributions to ozone formation made by specific emissions sectors or sources, provided the speciated VOC emissions within the sector or source are lumped in accordance with a similar methodology to that described above and summarised in Figure 7.6.

It is recognised that greater degrees of reduction are ideally required for many other applications, and extension of the above methodology to redistribute greater proportions of the VOC emissions total was explored. However, it was clear that the logic used for this method becomes less useful when attempting to redistribute a more significant portion of the emitted VOC mass emissions total. This is because a progressively limited series of species (and associated POCP values) remains in each of the VOC classes, such that the overall POCP of the VOC mixture in further reductions can only be preserved by redistribution of species to surrogates in other classes, or by offsetting a systematic error in the POCP of one VOC class with a compensating systematic error in another class. As a result, CRI v2-R3 is considered close to the limit of this method, which aims to retain a reasonably robust description of the composition and ozone forming ability of the VOC subclasses.

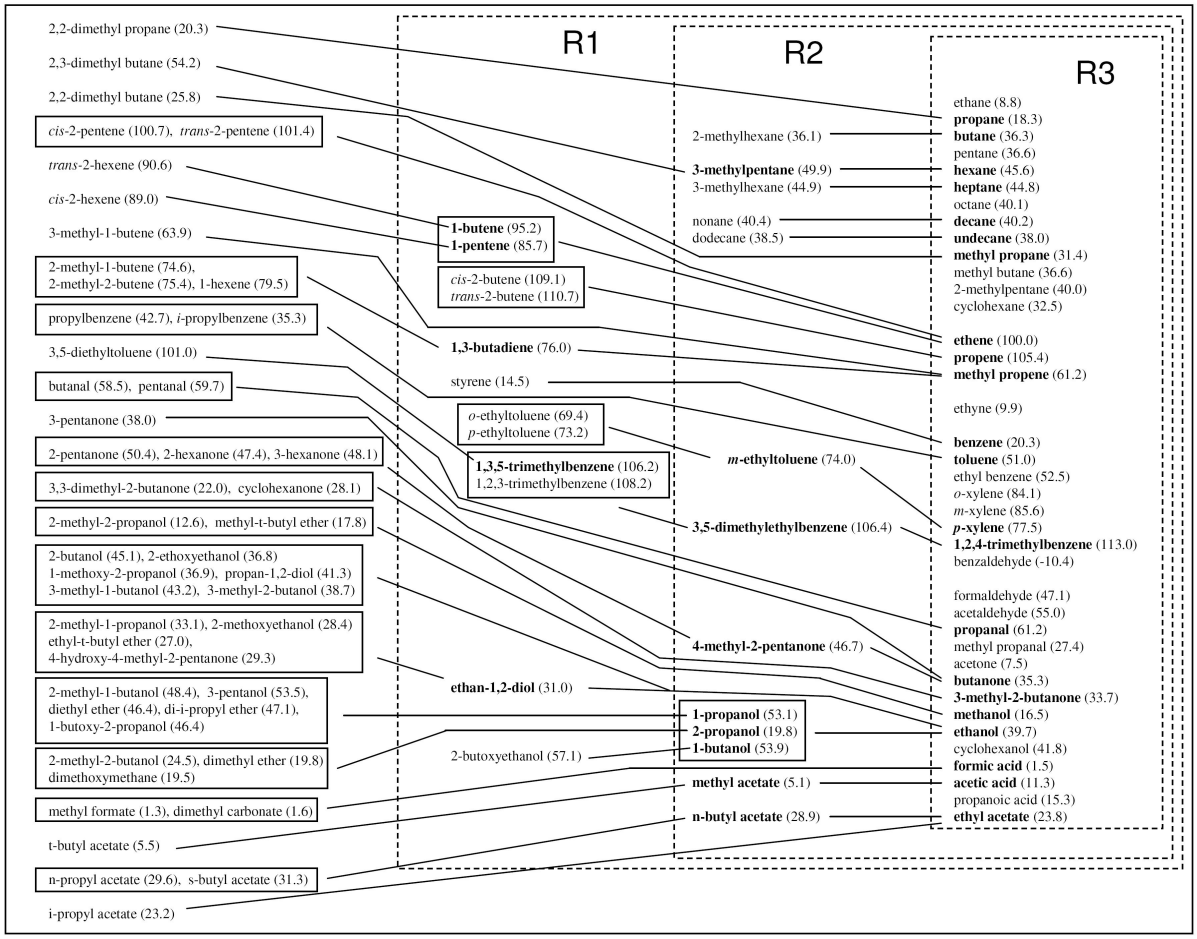

Figure 7.6: A list of anthropogenic VOCs treated in CRI v2, with their POCP values given in brackets. The VOCs treated in the progressive reduced versions, CRI v2-R1, CRI v2-R2 and CRI v2-R3, are shown in the respective internal boxes, such that the left hand column of VOCs were eliminated in the first stage of reduction (CRI v2 → CRI v2-R1) and so on. The linking solid lines indicate how emissions were lumped at each stage of reduction, with species shown in bold font being used as surrogates for those linked from the left. Each mechanism also retains the CRI v2 chemistry for isoprene, α-pinene and β-pinene.

VOC redistribution using method 2: To further reduce the number of emitted VOCs treated, experiments were performed to see if they could be lumped into groups similar to those defined by the Global Emissions Inventory Activity (GEIA) (http://www.mnp.nl/geia/data/NMVOC Groups/). As shown in Table 7.2, GEIA splits VOCs into 25 separate groups as determined by the Emission Database for Global Atmospheric Research (EDGAR 2.0) (Olivier et al., 1996), which is a collection of international statistics from the International Energy Agency (IEA), the United Nations (UN), and the Food and Agriculture Organisation (FAO).

Using the GEIA VOC groups as a guideline, 30 emitted anthropogenic species from CRI v2 were initially selected as surrogates to represent all the emitted non-methane VOCs in the mechanism, as shown in Table 7.2 (CRI v2-R4). The surrogates were chosen on the basis of POCP, abundance, and simplicity of mechanism. For example, 1,3,5-trimethylbenzene was chosen to represent all trimethylbenzenes, its degradation mechanism being simpler by virtue of its symmetry. Several of the GEIA categories were given more than one representative in CRI v2-R4, to provide some flexibility to account for widely varying POCP values within the group. For example, the category of esters was defined by both methyl formate and ethyl acetate, for which the respective POCP values are 1.3 and 23.8. As shown in Table 7.1, this approach to lumping VOCs in CRI v2-R4 was able to generate a more reduced mechanism than those described above.

Table 7.1: An overview of the properties of CRI v2 and the reduced variants (R1 – R5) developed in the present study.

CRI version [a]	v2	v2-R1	v2-R2	v2-R3	v2-R4	v2-R5
VOCs	115	67	55	42	33	22
Percentage redistribution [b]	0 %	5 %	10 %	20 %	33 %	44 %
Species	434 (4361)[c]	373 (3466)	352 (3099)	296 (2649)	219 (1983)	196 (1244)
Reactions	1183 (12775)[c]	1012 (10150)	988 (9099)	882 (7833)	643 (5884)	555 (3670)
$POCP_{VOC\ mix}$ [d]	46.45	46.51	46.51	46.47	47.02	46.53
$POCP_{alkane}$ [e]	34.55	34.54	34.54	34.45	36.42	33.19
$POCP_{alkene}$ [e]	85.35	85.21	84.36	84.36	89.80	93.04
$POCP_{aromatic}$ [e]	66.69	66.96	67.11	67.93	63.49	68.39
$POCP_{oxygenate}$ [e]	35.11	35.20	35.44	34.63	34.65	33.30
Run time [f]	1	0.75	0.64	0.60	0.33	0.29

Notes

[a] All mechanisms retain CRI v2 chemistry for isoprene, α–pinene and β–pinene, and this contributes to the number of VOCs, species and reactions given; [b] Percentage of anthropogenic mass emissions redistributed into surrogate VOC relative to starting speciation; [c] Figures in brackets indicate the number of species and reactions required to degrade the same set of VOCs in MCM v3.1; [d] Weighted mean POCP values based on the applied speciation of the emitted anthropogenic VOC mixture and the POCP values for the individual components; [e] Weighted mean POCP values for the anthropogenic VOC sub-classes based on the applied speciation within the given class and the total emissions of that class. The "alkene" category also incorporates acetylene; [f] Run time presented relative to that of CRI v2. For comparison, the full MCM v3.1 has a relative run time of 320.

Figure 7.7 shows that the simulated formation of ozone using CRI v2-R4, with the associated VOC emissions lumping optimised within the framework described above, is in excellent agreement with that using CRI v2 with the full starting VOC speciation, the ozone mixing ratios agreeing to better than 1% throughout the five day simulation. As shown in Table 7.1, this good agreement is also apparent from the consistent weighted POCP values of the VOC mixture in CRI v2 and CRI v2-R4. However, it is also clear that the greater level of simplification in the VOC speciation has inevitably required a level of compromise in the ozone-forming ability of the VOC subclasses to preserve the ozone-forming ability of the whole mixture, as discussed above. As a result, the average POCPs of the alkanes and alkenes treated in CRI v2-R4 are about 5-6% greater than those treated by CRI v2, whereas the average POCPs of the aromatics is smaller by about 5%.

A number of additional interim mechanistic variants have also been tested, leading to the most reduced version, CRI v2-R5. As shown in Tables 7.1 and 7.2, CRI v2-R5 treats the chemistry of 19 emitted anthropogenic VOC to represent the full speciation. The aim was to use an individual VOC to represent each GEIA group, with the assigned species also being relatively abundant and containing the most simple degradation scheme of the available options, where possible. However, two representatives were retained in each of a limited number of groups (see Table 7.2), because they are species generated in the mechanism from other emitted VOC, and which cannot therefore be removed from the mechanism (e.g., methanol and ethanol). As a consequence, this also provided some additional lumping options which allowed a good level of overall performance to be preserved for CRI v2-R5. As shown in Figure 7.7, the simulated formation of ozone using CRI v2-R5 once again agrees well with that of CRI v2, using average UK emission densities of NOx and VOCs. The deviation from CRI v2 is ≤ 2 % throughout the simulation, with the ozone mixing ratios for most of the final day of the five day simulation agreeing to better than 0.5 %. This good agreement is once again apparent from the consistent weighted POCP values of the VOC mixture in CRI v2 and CRI v2-R5 (see Table 7.1),

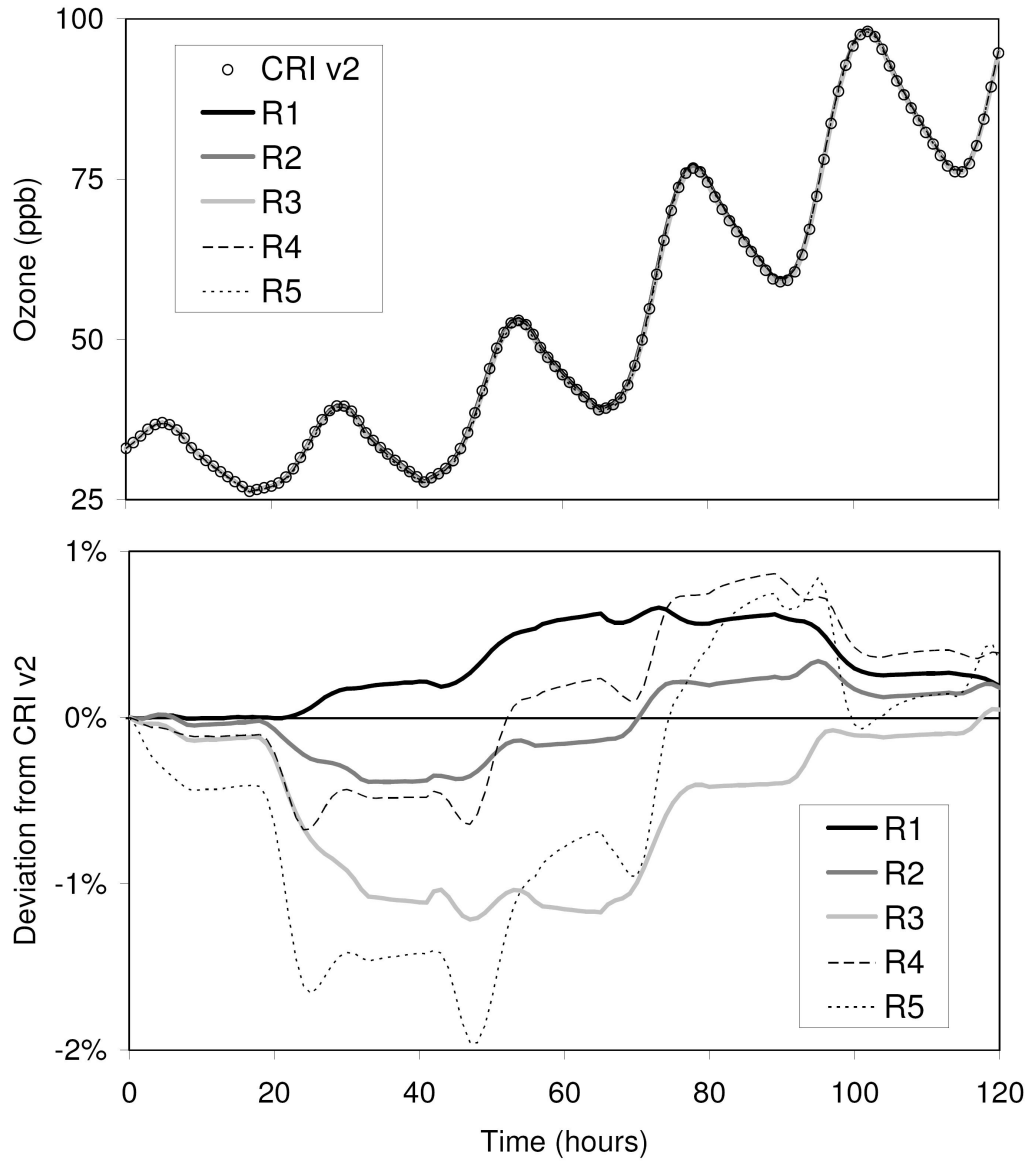

Figure 7.7: Comparison of ozone profiles simulated from anthropogenic VOC degradation over a five day period with the full CRI v2 and with the five reduced versions. The simulations were based on average 2001 UK emission densities for anthropogenic VOCs and NOx, the applied daily average densities being 15.4 and 18.3 kg km^{-2} day^{-1}, respectively. The applied VOC speciations were lumped as described in the text, Figure 7.6 and Table 7.2.

although there is an increased level of compromise in the ozone-forming ability of the VOC subclasses. In this case, the average POCPs of the alkenes and aromatics treated is greater than those treated by CRI v2 (by ca. 9% and 3%, respectively), whereas the average POCPs of the alkanes and oxygenates is smaller (by ca. 4% and 5%, respectively). Figure 7.8 illustrates how this compromise impacts on the fractional contributions made by the emitted VOC classes to ozone formation. Whereas the contributions of the four categories remain in close agreement for CRI v2-R1, -R2 and -R3, small but significant compensating systematic errors are apparent for CRI v2-R4 and -R5. Although this degree of compromise has some impact on mechanism performance (as discussed further below), it is nonetheless considered entirely acceptable for the level of mechanistic reduction achieved. The chemistry associated with anthropogenic VOC degradation in CRI v2-R5 is reduced by about a factor of about three compared with the full CRI v2, with the retained chemistry degrading the three biogenic VOC accounting for about 40% of the mechanism.

Table 7.2: A list of VOCs treated in the reduced mechanisms, CRI v2-R4 and CRI v2-R5, chosen to represent groups of compounds corresponding to GEIA categories.

GEIA VOC group (code) [a]	CRI v2-R4	CRI v2-R5
ethane (v02)	ethane	
propane (v03)	propane	
butanes (v04)	butane, methyl propane	butane
pentanes (v05)	pentane, methyl butane	
hexanes and higher alkanes (v06)	hexane	
ethene (v07)	ethene	
propene (v08)	propene	
other alkenes (v12)	1-butene, *trans*-2-butene	*trans*-2-butene
acetylene (v09)	acetylene	
benzene (v13)	benzene	
toluene (v14)	toluene	
xylenes (v15)	o-xylene	o-xylene
trimethylbenzenes (v16)	1,3,5-trimethylbenzene	
other aromatics (v17)	ethylbenzene	
formaldehyde (v21)	formaldehyde	
other aldehydes (v22)	acetaldehyde, propanal	
ketones (v23)	acetone, butanone	
alcohols (v01)	methanol, ethanol	methanol, ethanol
ethers (v19)	dimethylether, diethylether	
alkanoic acids (v24)	formic acid, acetic acid	formic acid, acetic acid
esters (v18)	methyl formate, ethyl acetate	
isoprene (v10) [b]	isoprene	
monoterpenes (v11) [b]	α–pinene, β–pinene	

Notes

[a] GEIA groups also include chlorinated hydrocarbons (v20) and other VOCs (v25), which are not considered in the present work; [b] The CRI v2 degradation chemistry to represent isoprene (v10) and monterpenes (v11) is retained unchanged in all the reduced mechanisms considered in the current work, but the associated emissions are not included in the presented simulations (see text).

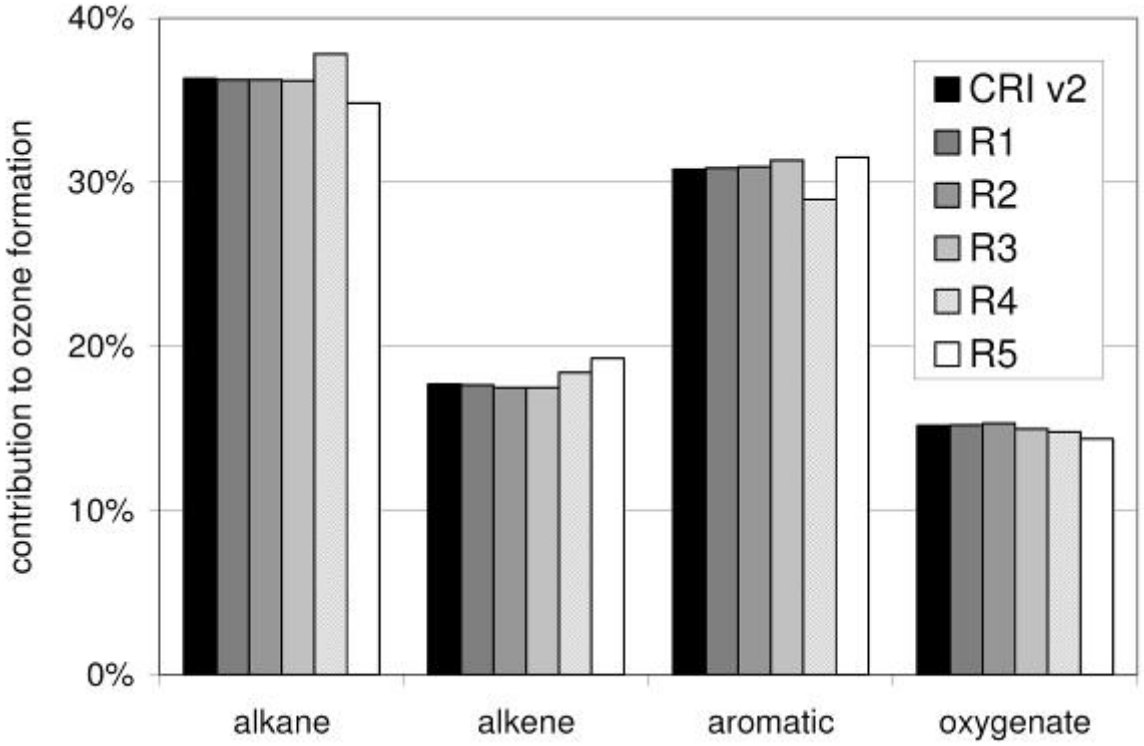

Figure 7.8: Contributions of emitted VOC classes to ozone formation under the base case scenario for CRI v2 and the five reduced variants with the associated emissions lumping. The displayed figures are based on the POCP-weighted mass emission of each class, determined using the average POCP value for each VOC class, shown in Table 7.1.

***Variation of VOC/NOx ratio*:** Additional simulations were carried out with all the reduced mechanisms (and associated VOC lumping measures) described above, with the VOC/NOx emission ratio varied over a range of 32 by scaling the NOx emissions by factors between 0.125 and 4. This allowed the transition from VOC-limited to NOx-limited conditions to be examined, which is presented in terms of the VOC/NOx ratio relative to the base case, $(VOC/NOx)_{rel}$, in Figures 7.9 and 7.10. Figure 7.9 (upper panel) presents the full ozone profiles simulated with the least reduced mechanism (CRI v2-R1) and the most reduced mechanism (CRI v2-R5), compared with those simulated using CRI v2, with the five day average results for all the mechanisms shown in the lower panel. Figure 7.10 shows a comparison of the five day average levels of a number of key radical and closed shell species, or groups of species, for all the mechanisms. The results in Figure 7.9 demonstrate that the production of ozone by all the mechanisms is comparable for the considered range of VOC/NOx. Logically, the deviation from CRI v2 is greatest for the most reduced variant, CRI v2-R5, with the associated VOC lumping. However, even in this case, the average ozone levels agree to better than 1% for $(VOC/NOx)_{rel} \geq 1$, but with a slightly greater degradation of performance apparent at the lower values, which correspond to NOx-inhibited conditions characteristic of polluted urban locations.

The comparisons for the radical and closed shell species shown in Figure 7.10 are also generally very good, although the results show some interesting traits resulting from the progressively increasing extent of emissions lumping. There is a general trend of slightly increasing $[HO_2]$ along the series, accompanied by an associated decrease in $[RO_2]$. This leads to a more notable trend in H_2O_2 levels, because it is generated mainly from the self reaction of HO_2, such that its production rate is proportional to $[HO_2]^2$. The more reduced mechanisms are more efficient at generating HO_2 (and therefore H_2O_2) because the minor emitted species (i.e., those that have been redistributed) tend to be further towards the high end of the homologous series of the considered VOC classes. As a result, the lumping procedure tends to redistribute larger species into smaller surrogate species, which generally have more direct routes to HO_2 formation upon degradation. This is particularly the case for oxygenated species containing hydroxy groups (e.g., alcohols and glycol ethers), where the degradation of smaller species (e.g., ethanol) following attack of OH radicals tends to be accompanied by a greater production rate of HO_2 relative to RO_2 than occurs for larger species (e.g., 2-methyl-1-butanol), even though their

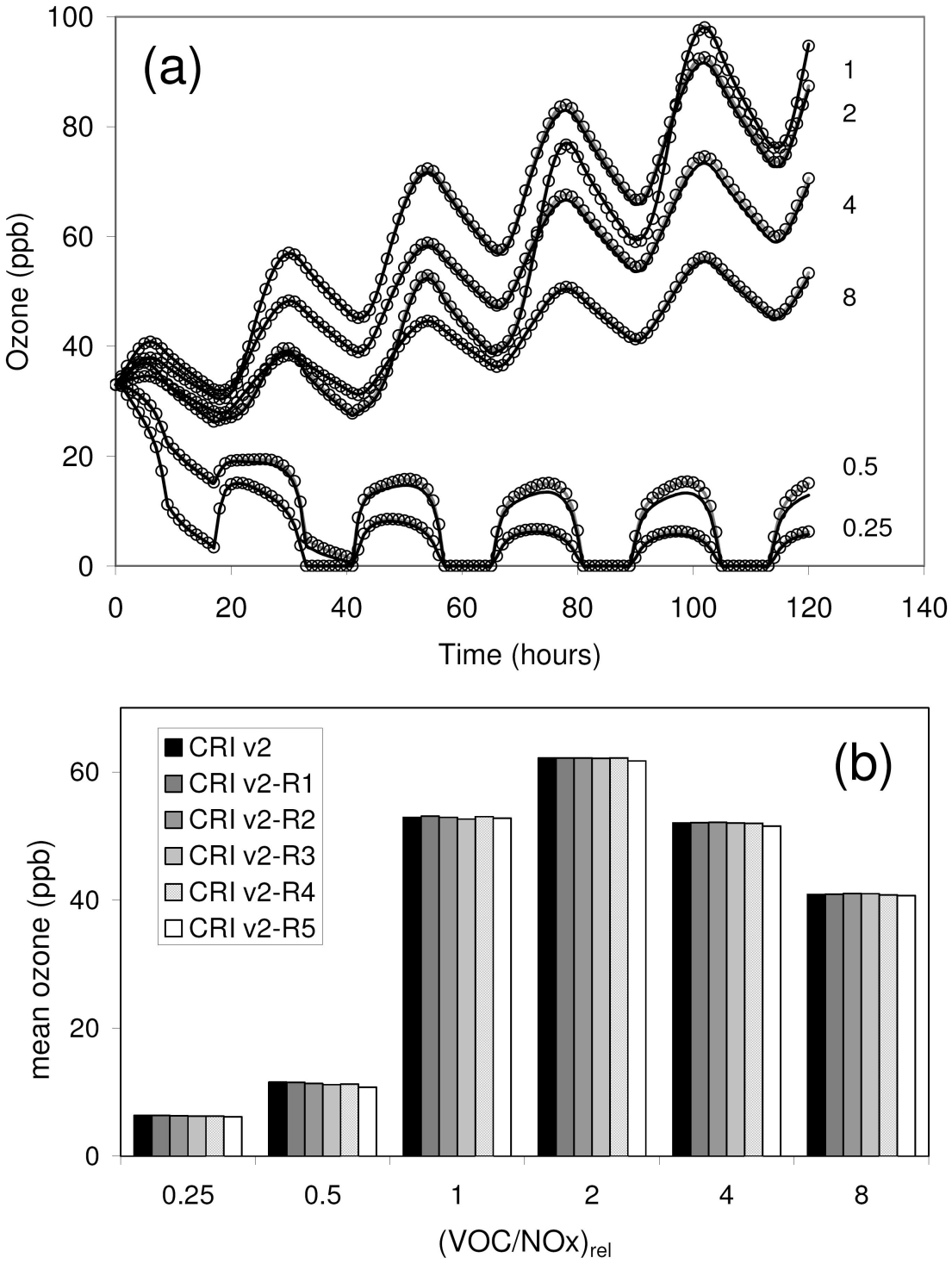

Figure 7.9: (a) Comparison of ozone mixing ratios simulated from anthropogenic VOC degradation over a five day period with CRI v2 (points), the least reduced variant CRI v2-R1 (grey line) and the most reduced variant CRI v2-R5 (black line) for a range of 32 in VOC/NOx emission ratio (June 21 conditions, 51.5° Lat). The base case simulation was based on average 2001 UK emission densities for anthropogenic VOCs and NOx, using the NAEI VOC speciation (see text), the applied daily average densities being 15.4 kg km^{-2} day^{-1} for VOCs and 18.3 kg km^{-2} day^{-1} for NOx. The range in VOC/NOx was achieved by scaling the NOx emissions, and is displayed relative to the base case, denoted $(VOC/NOx)_{rel}$. (b) Comparison of the simulated mean ozone mixing ratios over the five day period for CRI v2 and all the reduced variants for the considered range of $(VOC/NOx)_{rel}$.

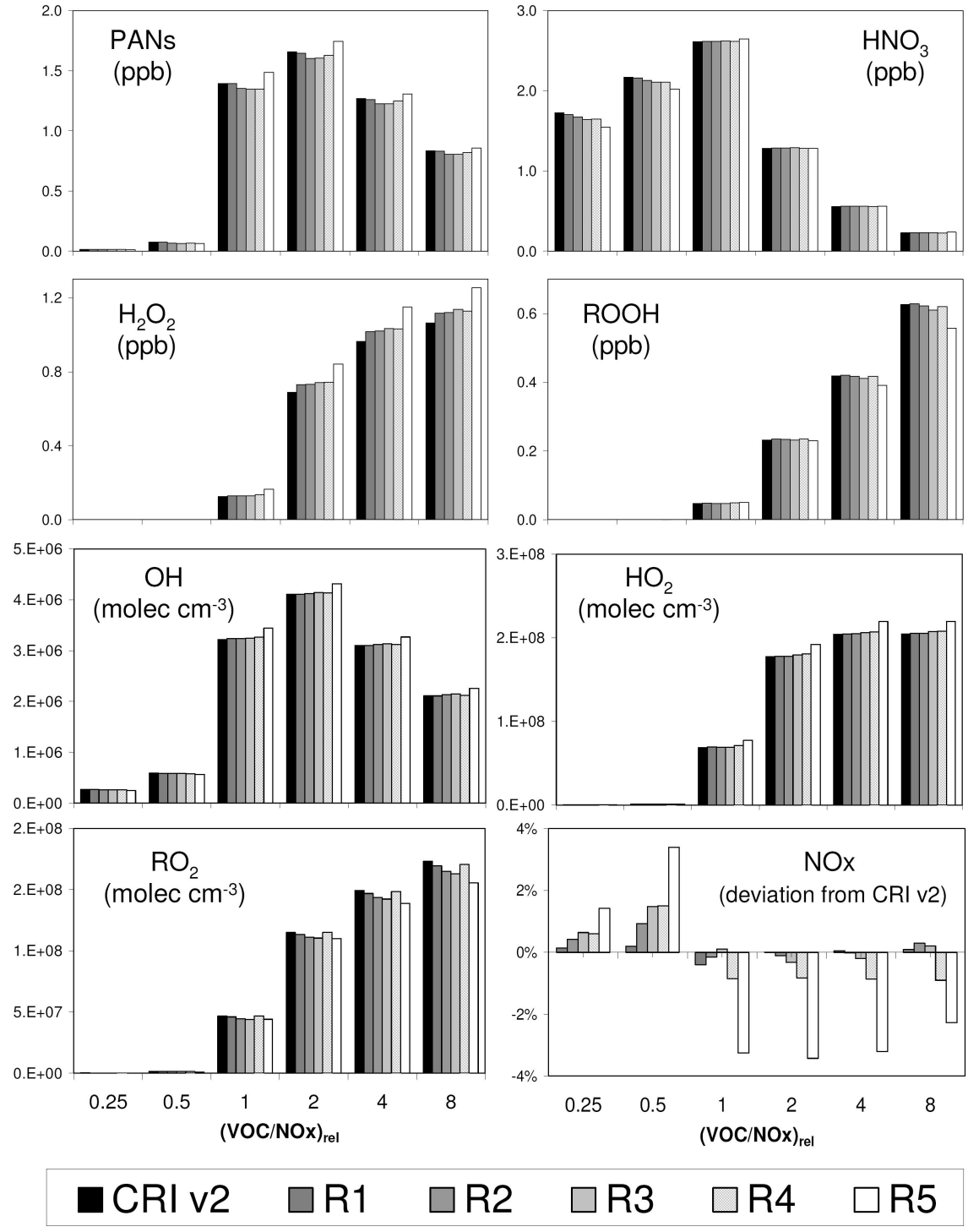

Figure 7.10: Comparison of mean mixing ratios or concentrations of a number of species or groups of species simulated over a five day period with CRI v2 and all the reduced variants (with associated VOC emissions lumping) for the considered range of $(VOC/NOx)_{rel}$. The simulated NOx is presented as a deviation from the CRI v2 simulation, for which the simulated mean mixing ratios in ppb were 89.0, 33.9, 3.88, 1.37, 0.782 and 0.460 for the $(VOC/NOx)_{rel}$ from 0.25 through to 8, respectively.

propensities to generate ozone (as quantified by the POCP concept) are similar. This is because OH attack generally occurs α to the hydroxy group with greater probability in smaller OH-substituted VOC that it does in larger ones:

$$OH + RCH(OH)R' \rightarrow RC(OH)R' + H_2O \quad (1)$$

$$RCH(OH)R' + O_2 \rightarrow RC(O)R' + HO_2 \quad (2)$$

The collective level of the related organic hydroperoxide species (denoted ROOH in Figure 7.10) shows a more subtle trend than that of H_2O_2, because the ROOH species are generated from reactions of HO_2 with RO_2 which, as indicated above, show compensating trends.

Superimposed on the general trends indicated above, are influences resulting from the compensating contributions of the different VOC classes to ozone formation (see Figure 7.8), which are most pronounced for CRI v2-R4 and -R5. As discussed in detail elsewhere (e.g., Carter, 1994; Jenkin and Hayman, 1999) the overall impact of a given VOC on ozone formation (as quantified, for example, by POCP value) results from a net effect of a combination of structure and reactivity influences. As a result, VOCs which possess similar POCP values, but which are from different classes, are likely to do so for a different combination of reasons. As shown in Figure 7.8, and discussed above, ozone formation from CRI v2-R5 possesses a slight bias towards the contributions made from alkene and aromatic degradation, at the expense of the alkane contribution. A resultant effect of the increased alkene contribution derives from radical formation from ozonolysis, which is generally not available for the other VOC classes. Consequently, CRI v2-R5 tends to be slightly more efficient at radical generation in scenarios where ozone levels are comparatively high, and this contributes to the elevated radical levels in the scenarios corresponding to $(VOC/NOx)_{rel} \geq 1$. This, in turn, leads to slightly more efficient processing of NOx and VOCs in general, leading to the associated decrease in NOx levels. The decreased contribution of alkanes to ozone formation, accompanied by the increased contribution of aromatics and alkenes in CRI v2-R5, also impacts on the relative formation of HO_2 and RO_2, because alkane degradation typically generates HO_2 radicals following propagation reactions via one or more RO_2 radicals, and is therefore comparatively less efficient at generating HO_2 and more efficient at generating RO_2 than the other classes. This exacerbates the progressive trends in H_2O_2 and ROOH discussed above. In CRI v2-R4, however, the opposite effect is apparent, because the contribution of alkane degradation to ozone formation is elevated at the expense of aromatic degradation (see Figure 7.8).

These general and specific traits discussed above demonstrate that mechanisms reduced through emissions lumping to maintain performance in relation to a specific target pollutant (in this case ozone) cannot always be guaranteed to recreate levels of all secondary pollutants to the same level of agreement, even though the level of agreement shown here for all the mechanisms (and associated emissions lumping) is still regarded as good.

The most reduced variant, CRI v2-R5, was finally tested in the PTM for the conditions of the TORCH campaign. The calculations using CRI v2 are described in the preceding section (and presented in Figure 7.5 in comparison with the observations). An otherwise identical version of the model, containing CRI v2-R5 with the associated emissions lumping, was also used to simulate the chemical development of boundary layer air parcels being advected along 96-hour trajectories to the campaign site at hourly resolution for the entire campaign period. The ozone mixing ratios simulated at the receptor using both mechanisms are in excellent agreement throughout the campaign period (see Figure 7.11), agreeing on average to 0.3 %, and with 99 % of the ca. 800 hourly ozone mixing ratios agreeing to better than 3 %. The hourly events represent a wide variety of conditions, such that the inputs of anthropogenic VOCs and NOx each vary over a range of more than two orders of magnitude, with the VOC/NOx ratios varying from ca. 0.1 to ca. 3 (mean = 1.15), and with the fractional contribution of biogenic VOC to the VOC total varying from less than 1 % to ca. 60 % (mean = 8.6 %).

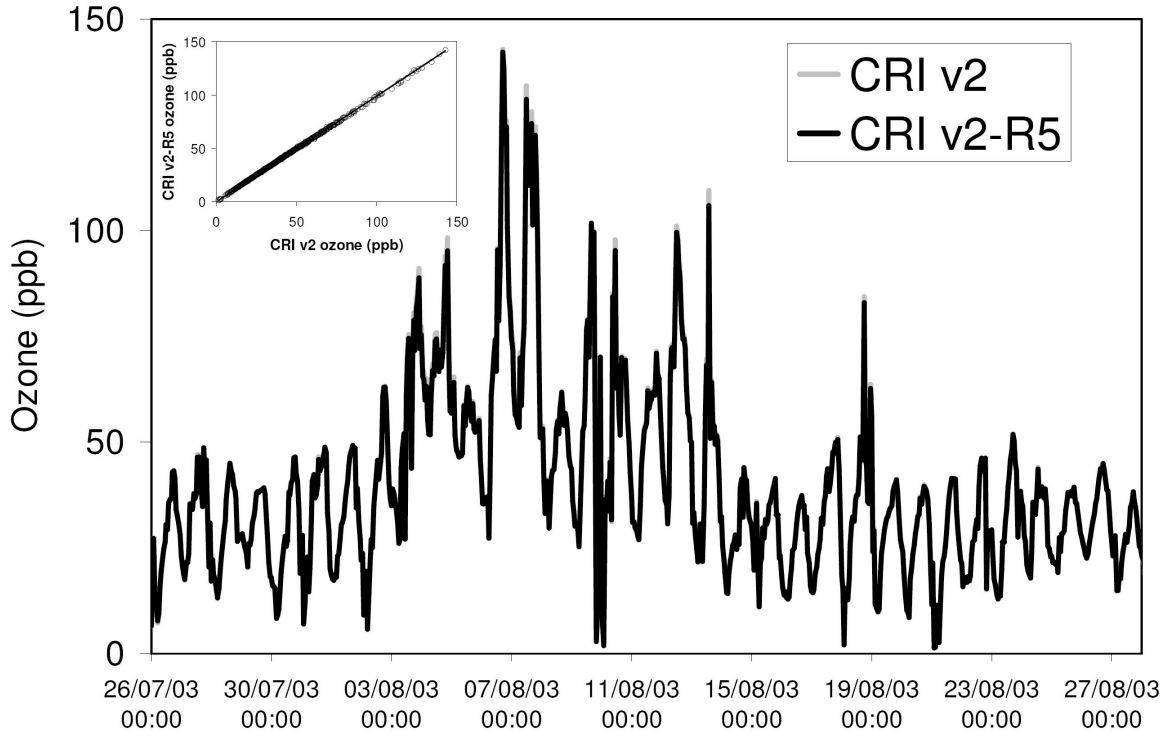

Figure 7.11: Comparison of hourly mean ozone mixing ratios simulated for the entire TORCH campaign using the PTM containing CRI v2 (with a speciation of 112 anthropogenic VOC) and CRI v2-R5 (with a speciation of 19 anthropogenic VOC). Biogenic emissions are represented by isoprene, α–pinene and β–pinene, which are treated by both mechanisms.

7.2 Development of New MCM Degradation Schemes

7.2.1 Introduction

The range of reactivity and structure of emitted anthropogenic VOCs (AVOC) is very well represented by the species degraded in the MCM. In contrast, there are only four biogenic VOCs (BVOC) treated, with most applications to date emitting three of these. In practice, the emitted speciation of BVOC includes contributions from isoprene, monoterpenes (isomeric formula $C_{10}H_{16}$), sesquiterpenes (isomeric formula, $C_{15}H_{24}$) and oxygenated VOCs (e.g., Owen et al., 2001), with typically more than 20 significant contributors identified in a given study. Owing to wide variations in reactivity, these species are oxidised on a variety of temporal and associated spatial scales in the atmosphere (lifetimes range from minutes to days), and detection of the more reactive BVOC (some monoterpenes and sesquiterpenes) is therefore non-trivial. The chemical structure of these compounds also has implications for degradation pathways, which can differ dramatically between BVOC, with corresponding variability in their ability to generate ozone. As a result of EU controls on AVOC emissions over the last decade, BVOC have an increasing relative impact on regional scale photochemistry in Europe, and have potential additional significance in relation to human-influenced activities such as biofuel production.

The general aim of this task is therefore to expand the MCM by inclusion of schemes for additional monoterpenes relevant to the UK and Europe, with the additional aim of increasing the reactivity range of the species represented. An initial survey of information on the speciation of emissions within the European region (e.g., Owen et al., 2001; Boissard et al., 2001; Jonsson et al., 2007) has identified limonene and myrcene as compounds for which schemes should be developed. As shown in Table 7.3, these compounds (along with α– and β–pinene which are already treated by the MCM) would ensure that representatives of four structural classes of monoterpene are treated, and which can therefore be used to represent a wider variety of species (examples are also shown in the table). Limonene and myrcene are also substantially more reactive than α– and β–pinene, such that the represented reactivity range is also increased (it is noted that limonene is

Table 7.3: Selected monoterpene categories and contributing species. Category representatives to be treated in MCM v3.2 are identified, with their lifetimes with respect to reaction with OH and ozone.

Category	Compounds (representative in bold)	OH reaction lifetime of representative[a,c]	O_3 reaction lifetime of representative[b,c]
Bicyclic monoterpene - endocyclic double bond	α–**pinene**, 2-carene, 3-carene	5.2 hours	4.3 hours
Bicyclic monoterpene - exocyclic double bond	β–**pinene**, camphene, sabinene	3.5 hours	1.0 days
Monocyclic diene monoterpene	**limonene**, terpinolene, β–phellandrene, γ–terpinene	1.6 hours	1.9 hours
Acyclic triene monoterpene	**myrcene**, ocimene	1.3 hours	47 minutes
a: [OH] = 10^6 molec. cm^{-3}; b: [O_3] = 7.5 x 10^{11} molec. cm^{-3} (ca. 30 ppb); c: Based on data from Calvert et al. (2000)			

also emitted from anthropogenic sources, appearing in the NAEI speciation under the pseudonym of "dipentene"). Further work is in progress to identify if other key species need to be treated (e.g., oxygenated biogenic VOC), and whether it is currently feasible to construct degradation schemes.

7.2.2 Limonene degradation scheme

The construction of a detailed, MCM-compatible, gas phase mechanism for limonene has been completed. The mechanism includes degradation initiated by reaction with OH radicals, ozone and NO_3 radicals, and contains 936 reactions of 337 new species which degrade limonene into species already present in MCM v3.1. The new species include limonene itself, 136 peroxy and oxy radical species and 200 new structurally complex oxygenated product species, typically containing between two and five oxygenated functional groups. These contain subset combinations of carbonyl, nitrate, peroxy nitrate, hydroxyl, hydroperoxy, carboxylic acid and peracid groups. A complete listing of the mechanism is provided in Appendix 1 in FACSIMILE format. Incorporation of this information into the MCM database is in progress, such that the information will be extractable and searchable along with the existing MCM code as part of MCM v3.2.

Figure 7.12 shows a highly simplified schematic of the OH-initiated degradation of limonene, as represented in the new mechanism. This figure includes only the main radical propagation routes (i.e., propagated by reactions of peroxy radicals with NO), which form the backbone of the chemistry under high-NOx conditions. This shows the formation of the major carbonyl and hydroxycarbonyl products which are generated through sequential oxidation of the double bonds in limonene, and also how fragmentation processes gradually lead to the breakdown of the carbon skeleton and the formation of smaller species already treated in the MCM. It is noted that the chemistry predicts the eventual formation of products normally regarded as markers of isoprene degradation (e.g., methacrolein, and the peroxy radicals denoted *ISOPDO2* and *HMVKBO2* in Figure 7.12).

Figure 7.13 shows examples of the types of chain terminating products which are also represented. At high NOx levels, these tend to be dominated by hydroxynitrates (i.e. species containing –OH and –ONO_2 groups), whereas at lower NOx, the formation of hydroxyhydroperoxides, hydroxycarbonyls and dihydroxy species becomes increasingly important. The acid species are formed from chain-terminating steps during the OH-initiated chemistry, from the further degradation of intermediate aldehydes. In practice, these acid species are also formed directly from the ozonolysis of either limonene itself, or from the ozonolysis of the unsaturated degradation products limononaldehyde and limonaketone (shown in Figure 7.12), and such processes are likely to represent the major sources of the carboxylic acid species.

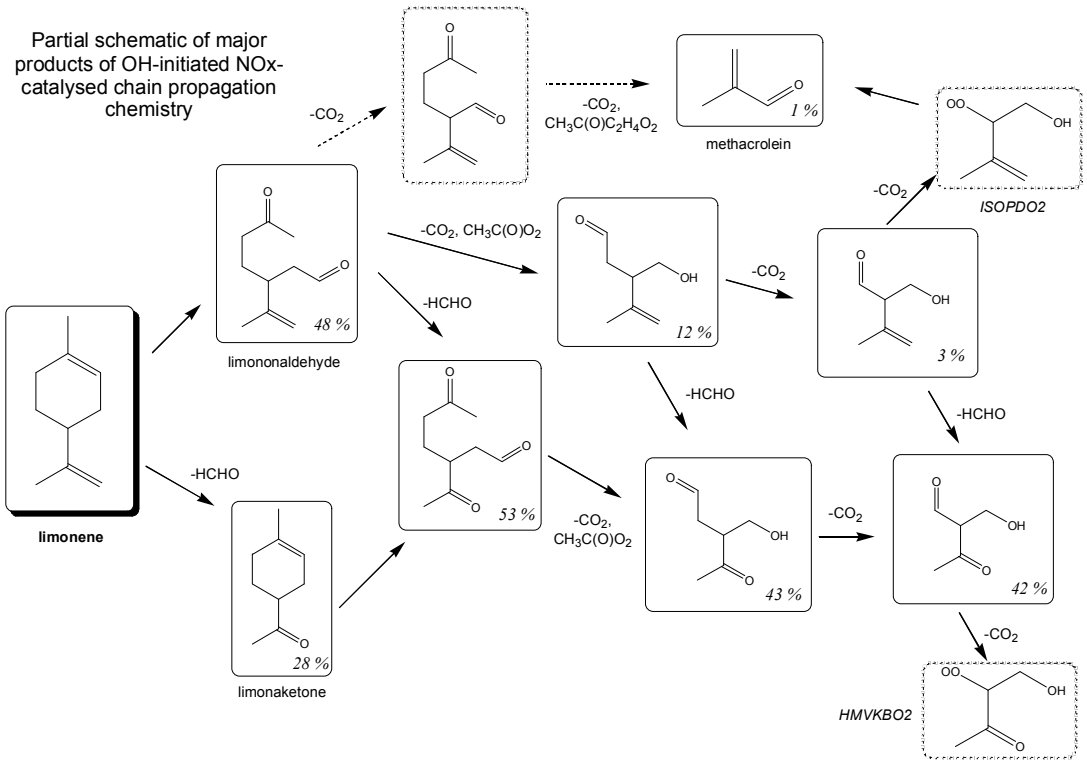

Figure 7.12: Simplified schematic of the OH-initiated degradation of limonene, as represented in the new mechanism. Only the main radical propagation routes are shown (see text).

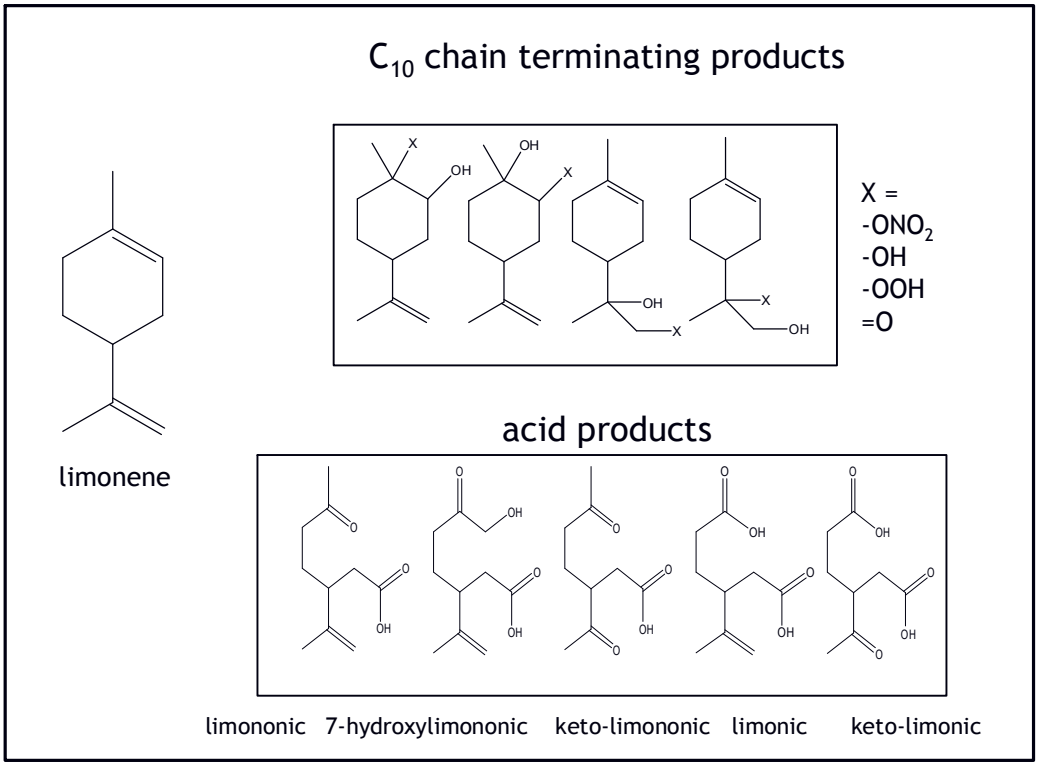

Figure 7.13: Selected chain terminating products represented in the early stages of the OH-initiated limonene degradation scheme. The acid products are also formed from the ozonolysis of limonene, limononaldehyde and limonaketone (see text).

7.3 Major Revision of the MCM Protocol

The method used to construct the MCM is broadly a two-stage process involving (i) the development of a "protocol" for mechanism construction, and (ii) application of the protocol to a series of emitted VOCs to develop the mechanism/database.

The protocol defines a set of rules which guide the development of the gas-phase degradation mechanisms, allowing two or more people to write consistent and compatible chemistry schemes. The flow chart in Figure 7.14 summarises the main types of reaction considered and classes of organic intermediate and product which are potentially generated. The chemistry of a given VOC is thus developed within this framework, based on the predefined set of rules (i.e. the protocol). The flow chart essentially represents the degradation of the given VOC into a set of "first generation products", which are themselves further degraded within the same general framework. This process is continued until the chemistry either yields the ultimate carbon-containing product, CO_2, or until an organic product or radical is generated for which the subsequent chemistry is already represented in the mechanism. The highlighted sections in Figure 7.14 contain the major free-radical propagated cycle shown in Figure 7.15, which illustrates the essential "hub" of reactions which form ozone in the atmosphere. The framework of the protocol thus allows this type of chemistry to be included explicitly for a large number of specific intermediates, whilst also representing relevant competing and supplementing processes in a rigorous and well-documented way.

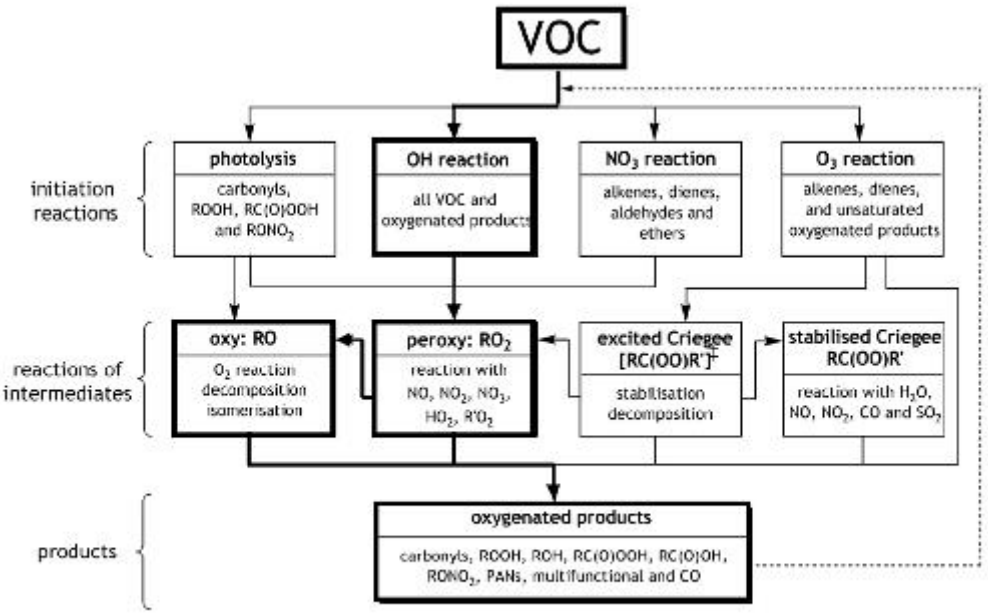

Figure 7.14: Flow chart indicating the major reactions, intermediate classes and product classes considered in the MCM protocol. The highlighted sections include the free-radical propagated chemistry shown in Figure 7.15.

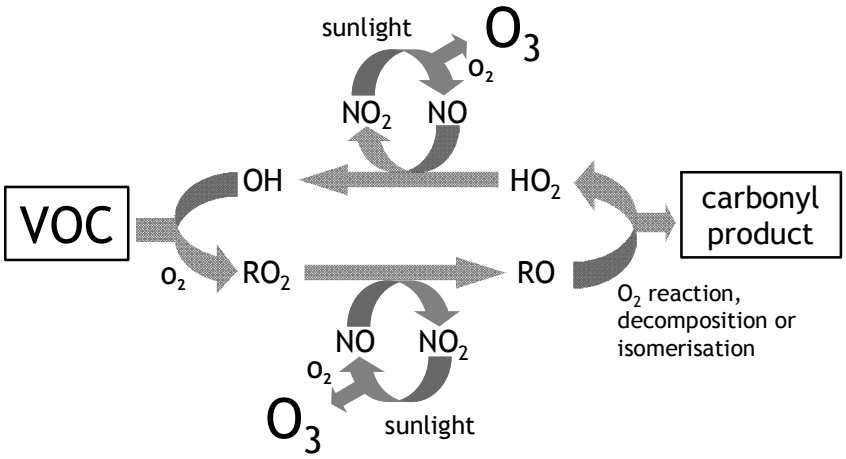

Figure 7.15: Generic free-radical propagated cycle, which illustrates the fast photochemical processes which form ozone.

Development of the updated MCM protocol has commenced, with subdivision into a number sections dealing with different facets of the degradation chemistry, as follows:

a) *Initiation reactions with OH and NO_3 (and Cl and Br)*: this is considering the kinetics and product radical distributions of the reactions of these radical and atomic species with relevant hydrocarbons and oxygenated organics, including those generated as degradation products (i.e. containing carbonyl, nitrate, peroxy nitrate, hydroxyl, hydroperoxy, acid, peracid, and anhydride groups, and multifunctional species containing two or more of these substituent groups).

b) *Initiation by photolysis*: this is considering the rates and product channels of photo-dissociation reactions for a relevant core set of species for which the necessary absorption cross-section and quantum yield data are available; and the use of these data to infer the rates and product channels for photo-dissociation reactions of a large number of degradation products.

c) *Initiation by reaction with O_3*: this is considering the kinetics of the reactions of O_3 with (predominantly unsaturated) organic compounds, and the subsequent reaction sequences leading to the generation of radical and closed-shell species for which the reactions are treated in other protocol sections. This section includes reactions of Criegee intermediates.

d) *Reactions of organic radicals with O_2*: this is considering the products of reactions with O_2 of carbon-centred radicals formed either from the above initiation reactions, or as a result of isomerisation of peroxy or oxy radical intermediates.

e) *Reactions of stabilised peroxy radicals (RO_2)*: this is considering the rates and product channels of bimolecular reactions of RO_2 with NO, NO_2, NO_3, HO_2 and $R'O_2$, and of unimolecular reactions of RO_2.

f) *Reactions of oxy radical intermediates (RO)*: this is considering the relative importance of reactions of RO radicals (reaction with O_2, decomposition and isomerisation) formed from propagating channels of RO_2 reactions.

The MCM construction methodology, as defined in the protocol, makes use of a number of sources of information, which are summarised in Table 7.4. Where possible, published experimental data for elementary reactions (e.g. rate coefficients; branching ratios) are generally applied, adopting parameters evaluated by expert groups, where available. However, only a comparatively small fraction of the required parameters have been studied experimentally, such that the MCM construction necessarily relies heavily on the use of parameters estimated using structure-activity relationships (SARs). This allows the kinetics and products of a large number of unstudied chemical reactions to be defined on the basis of the studied reactions of a smaller subset of similar chemical species, either using methods documented in the literature or on the basis of newly-defined methods which are presented in the protocol. It is proposed to publish the revised protocol in the scientific literature to ensure that all

methods used in the construction of the MCM are peer-reviewed and available to the scientific community.

A substantial number of the rate coefficients used in the MCM rely on evaluations, in particular those of the IUPAC Sub-Committee for Gas Kinetic Data Evaluation (http://www.iupac-kinetic.ch.cam.ac.uk/). A direct link between the MCM and the IUPAC database is being developed in parallel that will facilitate direct updating of the appropriate rate coefficients in the MCM.

Table 7.4: Approximate hierarchy of information sources used in the MCM protocol

Source of information	Description
1. Experimental data – evaluated	Parameters based on experimental studies of elementary reactions, which have been evaluated by an expert group such as the IUPAC subcommittee for gas kinetic data evaluation (http://www.iupac-kinetic.ch.cam.ac.uk/). Such evaluated data are based on all published measurements of a given parameter, and are thus likely to represent the most reliable values.
2. Experimental data – direct	Parameters taken directly from a published experimental study, or based on a group of experimental studies, when no independent evaluation is available. When only limited experimental data exist, a parameter based on an SAR[(a)] may be used in preference.
3. Structure-Activity Relationships (SARs)[(a)] – published	Parameters estimated on the basis of published methods which relate the parameter values to chemical structure.
4. Structure-Activity Relationships (SARs)[(a)] – defined in protocol	Parameters estimated on the basis of a newly-defined and justified method, which relates the parameter values to chemical structure.
5. Theoretical studies	Parameters for specific structures/reactions are occasionally based on theoretical studies of that structure/reaction. Such methods are not widely applied for practical reasons, although their accuracy has substantially improved in recent years
(a) A structure-activity relationship (SAR) allows parameters such as rate coefficients to be related to structural properties of chemical species, thereby providing a method of parameter estimation. SARs are developed from datasets of experimentally-determined parameters.	

7.4 Development and Application of Secondary Organic Aerosol (SOA) Codes for MCM v3.1 and CRI v2

7.4.1 Introduction

It is well documented that organic material is a significant and variable component of the tropospheric aerosol, accounting for between 10 % and 90 % of the mass of fine particles (e.g., Kanakidou et al., 2005). The organic component is usually categorised as either “primary organic aerosol (POA)”, defined as organic compounds which are emitted directly into the atmosphere in particulate form (e.g., from combustion sources), or “secondary organic aerosol (SOA)”, defined as semi- or non-volatile products of the gas-phase oxidation of emitted volatile organic compounds (VOCs) which have transferred from the gaseous to the aerosol-phase.

Because many hundreds of different VOCs are emitted (e.g., Dore et al., 2003a; Owen et al., 2001), and because the oxidation chemistry of those VOCs can be highly complex (e.g., Jenkin et al., 1997; Aumont et al., 2005), the atmosphere contains many thousands of structurally different organic oxygenates possessing a wide range of physicochemical properties, and therefore different propensities to undergo gas-to-particle transfer. In view of the chemical complexity of the system, representing the chemical processes that describe SOA formation in atmospheric models is a highly

challenging task. Kroll and Seinfeld (2008) have recently reviewed current understanding of the formation and evolution of low volatility products of VOC oxidation, identifying a number of facets to the problem which should ideally be represented or parameterised in atmospheric models. These highlighted the role of gas phase chemical processes (particularly those of the intermediate peroxy and oxy radicals) in determining product volatility, and also emphasised the need to understand and represent VOC oxidation chemistry over several generations. Accordingly, a number of previous studies have employed appropriately detailed representations of gas phase VOC oxidation chemistry, in conjunction with treatments of the gas-to-aerosol transfer of oxygenated products, to simulate the formation of SOA for both chamber and tropospheric conditions (Jenkin, 2004b; Johnson et al., 2004; 2005; 2006; Camredon et al., 2007; Capouet et al., 2008; Xia et al., 2008). Such studies have the advantage that the evolution of the oxygenated product distribution (and its propensity to form SOA) can be represented and examined in some detail, although it is recognised that the development of less-detailed SOA schemes is also essential for many applications where greater computational efficiency is required (e.g., Griffin et al., 2005).

In the following sections, the development and testing of an updated detailed representation of SOA formation for application with MCM v3.1 is described. As part of this work, the code implemented in the PTM has been used to assemble a comprehensive reference dataset of 50 case studies (comprised of 4,750 hourly air mass history events), which considers the base case ambient conditions and scenarios in which emissions of anthropogenic pollution have been reduced by factors of up to 100, which can been compared with, and validated against, ambient data from a variety of locations. This dataset is also used as a reference benchmark to enable the development and optimisation of a reduced SOA module for the CRI v2 mechanism, and its reduced variants, which is described in section 7.4.4.

7.4.2 Modelling method and SOA code development

The PTM was used to simulate the chemical development in well-mixed boundary layer air parcels being advected along four-day trajectories arriving at the TORCH campaign site at Writtle (Essex), a rural site approximately 40 km to the north-east of central London, during late July and August 2003 (a period which included a regional-scale air pollution event associated with a heat-wave). The trajectories were obtained from the NOAA on-line trajectory service (Draxler and Rolph, 2003) for the period 26 July – 2 September 2003 at hourly resolution. The air parcels received emissions of NO_X, CO, SO_2, methane and non-methane VOC, based on mapped emissions inventories covering the EMEP domain. The base case anthropogenic emissions were representative of the year 2003, and reductions by factors of up to 100 were considered in the current work to allow a wide range of ambient conditions to be considered. The speciation of the emitted anthropogenic non-methane VOCs was based on the UK National Atmospheric Emissions Inventory. Emissions of biogenic VOCs were represented by three species, isoprene and the monoterpenes α– and β–pinene, with the magnitude of the emissions taking account of variations in surface temperature and photosynthetically active radiation (PAR) along the applied trajectory paths, based on the method of Dore et al. (2003b).

Emissions of primary organic aerosol (POA) were defined relative to those of NO_X, according to observed correlations between NO_X mixing ratios and mass concentrations of fine organic particulate material (≤ 200 nm), at several urban locations (Allan et al., 2003; Alfarra, 2004). This approach was found to provide a good representation for the region of study (i.e., one in which anthropogenic combustion sources dominate NO_X and carbonaceous aerosol emissions, and with road transport being the major source), with support provided by the good agreement between the simulated concentrations of POA and those observed for a wide variety of conditions in the TORCH campaign period (McFiggans et al. 2005).

MCM v3.1 was used to describe the gas phase chemical processing of the emitted VOCs, and the further processing of intermediate oxygenated compounds containing carbonyl, nitrate, peroxy nitrate, hydroxyl, hydroperoxy, acid and peracid groups, and multifunctional species containing two or more of these substituent groups. Secondary organic aerosol (SOA) formation was represented in terms of the equilibrium partitioning of oxidation products between the gas-phase and the condensed organic phase,

$$C_a/C_g = K_p\, C_{om} \qquad \text{(i)}$$

where C_a is the concentration of a given species in the condensed organic-phase, C_g is its gas-phase concentration and C_{om} is the total mass concentration of condensed organic material ($\mu g\ m^{-3}$). The partitioning coefficients, Kp ($m^3\ \mu g^{-1}$), which characterise the extent of partitioning of the species, were

estimated for ca. 2,000 semi- and non-volatile closed-shell oxidation products in MCM v3.1 by Johnson et al. (2006) using the absorptive partitioning theory of Pankow (1994), and these values have also been applied in the present study. This required values of the liquid vapour pressure ($p_L°$) to be estimated for each of the partitioning species, which was achieved using an expanded, semi-empirical form of the Clausius-Clapeyron equation in conjunction with estimated values of species boiling temperatures (T_b) and vaporisation entropy changes at T_b ($\Delta S_{vap}(T_b)$). T_b values were estimated using the fragmentation method of Stein and Brown (1994), with values of $\Delta S_{vap}(T_b)$ estimated using the Trouton-Hildebrand-Everett rule with corrections for polar compounds and compounds with hydrogen-bonding capability, according to Vetere (see Baum, 1998).

Phase-partitioning was initially represented for the full suite of ca. 2,000 closed-shell species. On the basis of the results of 12 initial case studies carried out under base case conditions, and with anthropogenic pollution reduced by factors of up to 100, this was reduced to a representation of 365 partitioning species which were found to account for > 95 % of the simulated SOA mass concentration in all these initial case studies. This allowed a substantial reduction in model run-time (by more than an order of magnitude), and more efficient consideration of a large number of case study events. This model is hereafter referred to as "PTM-MCM v3.1".

Reduced representations of the gas phase chemistry were provided by CRI v2 and its reduced (lumped emissions speciation) variant CRI v2-R5, both of which are traceable to MCM v3.1 as described above. The development, optimisation and application of an SOA code for use with these reduced mechanisms is described below in Section 7.4.4. The versions of the model containing CRI v2 and CRI v2-R5 are hereafter referred to as "PTM-CRI v2" and "PTM-CRI v2-R5".

7.4.3 Optimisation and validation of MCM v3.1 SOA code

Concentrations of total organic aerosol (OA) mass were simulated for 15 selected case study events during the TORCH-2003 campaign using PTM-MCM v3.1 (see Figure 7.16). Consistent with a previous evaluation (Johnson et al. 2006), recreation of the observed concentrations of OA (also shown in Figure 7.16) required the implementation of two corrections. First, it was necessary to infer the presence of a regional background concentration of OA, for which the optimised value is 0.7 $\mu g\ m^{-3}$. This is interpreted as an aged OA component which is not derived from emissions collected along the back trajectories and which cannot therefore be generated by the model. It is believed to be a reasonable correction, with independent support for the existence of a nearly ubiquitous background fine OA concentration of the order of 1µg m^{-3} coming from measurements reported for a number of locations (e.g., Coe et al., 2006; Harrison and Yin, 2008). Secondly, it was necessary to increase the values of K_p for the partitioning species by a large species-independent factor, which was optimised to a value of 427 based on the TORCH observations (see Figure 7.16). The need for this large scaling factor reflects the possible occurrence of association or oligomerisation reactions between species absorbed into the organic aerosol-phase (such chemistry not being explicitly represented in the model), which would have the effect of apparently suppressing the vapour pressure of the absorbed species.

The contributions to OA made by the general source categories are illustrated for the 15 case study events in Figure 7.17, with the SOA contributions subdivided into anthropogenic and biogenic components on the basis of the detailed simulated composition. The results show a general dominance of SOA during the latter part of the anticyclonic (heat-wave) period, which persisted from 6 – 12 August, with important contributions from both anthropogenic and biogenic precursors, but also illustrate the necessity to include the background OA contribution to simulate events when low OA concentrations were observed (e.g., 16th August), when cleaner air was arriving from the northern sector.

Further simulations were carried out in which the emission rates of anthropogenic species (most notably NO_X, anthropogenic VOCs, and POA) were reduced by factors of 5, 10 and 100 for 11 of the case studies shown in Figure 7.16, and by a factor of 100 in a further two case studies, to generate a large reference dataset with arrival point data for 50 case study scenarios in total. These scenarios thus represent a very wide variety of conditions, with the fractional contribution of biogenic VOCs to the total VOC emissions collected along the 96-hour trajectories varying over the approximate range 5 – 98 %, and with total VOC/NO_X emissions ratios varying from ca. 0.8 to ca. 100. As shown in Figure 7.18, reduction in the anthropogenic input by factors of up to 100 had variable impacts on the simulated SOA concentrations, where the variation in anthropogenic input is presented in terms of the average mixing ratio of NO_X simulated over the 96-hour back-trajectory, $[NO_X]_{ave}$. For case studies in

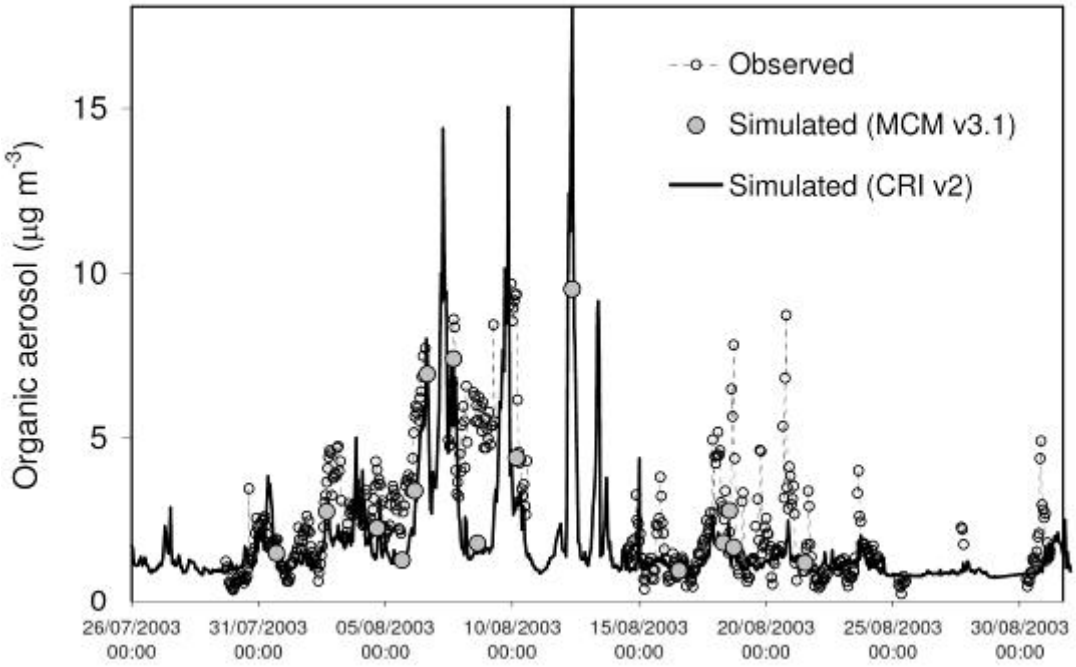

Figure 7.16: Comparison of observed hourly mean organic aerosol mass concentrations with those simulated for 15 case study trajectories with PTM-MCM v3.1. Those simulated for the entire TORCH campaign with PTM-CRI v2 are also shown (see Section 7.4.4). The observed organic aerosol mass concentrations were measured by the University of Manchester, as reported in Johnson et al. (2006).

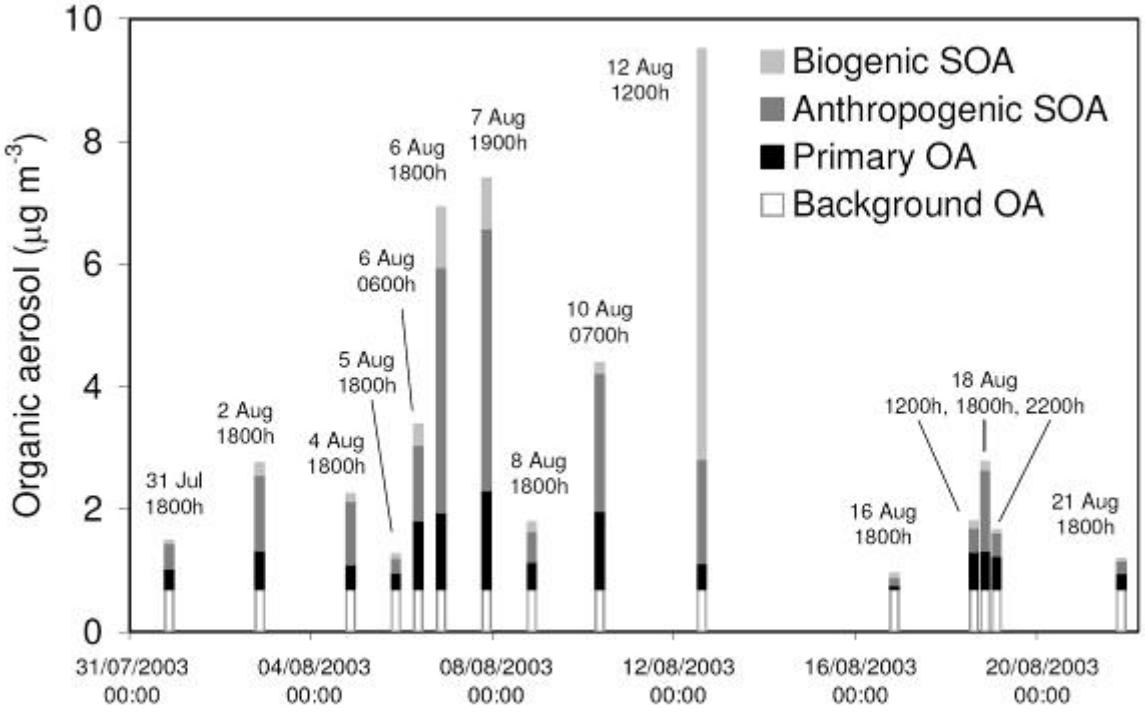

Figure 7.17: Organic aerosol mass concentrations simulated with PTM-MCM v3.1, broken down into component contributions, for 15 case study events in the TORCH campaign.

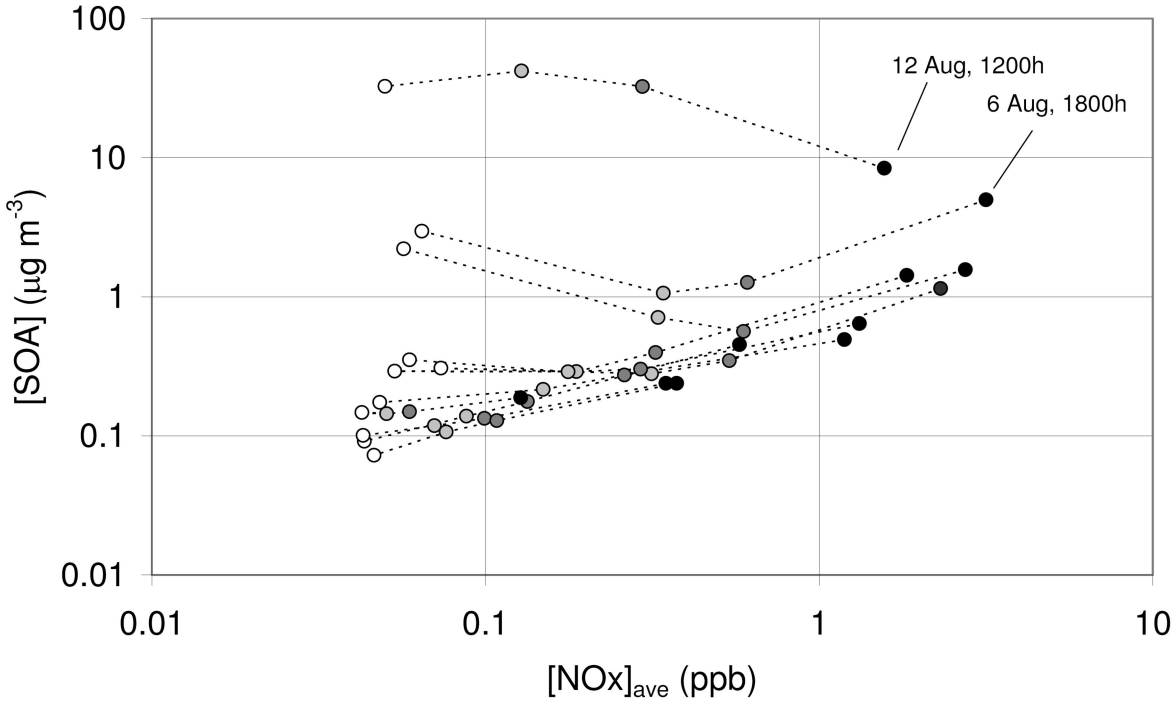

Figure 7.18: The impact of reduction in the anthropogenic input (presented in terms of the average mixing ratio of NOx over the 96-hour back-trajectory, $[NOx]_{ave}$) on SOA concentrations simulated using PTM-MCM v3.1 in 11 case study events. The filled black points represent the SOA concentrations simulated in the base case. Reductions of anthropogenic input by factors of 5 (dark grey points), 10 (light grey points) and 100 (open points) for each case study are connected by dotted lines.

which the base case SOA is predominantly anthropogenic, reduction of the anthropogenic input logically leads to a progressive reduction in the simulated SOA concentration, due to both the decrease in POA concentration (which acts as a partitioning medium for VOC oxidation products) and to the reduction in the emissions of anthropogenic VOCs which are precursors to the SOA. For case studies in which a notable concentration of predominantly biogenic SOA is formed in the base case (e.g., the 12 August 12:00 h event identified in Figure 7.18), reduction of the anthropogenic input leads to an increase in the simulated SOA concentration. As discussed below, this is because the detailed degradation chemistry is sensitive to the level of NO_X, becoming more efficient at generating lower volatility products as NO_X decreases. For case studies in which the base case SOA is made up of notable concentrations of anthropogenic and biogenic species (e.g., the 6 August 18:00 h event identified in Figure 7.18), a combination of the above effects occurs, leading to an initial reduction in SOA concentration with decrease of anthropogenic input, followed by an increase in SOA concentration with more severe anthropogenic reductions.

The effect of the variation of anthropogenic input on all the simulated OA component concentrations is illustrated further for the 6 August 18:00 h case study in Figure 7.19. The anthropogenic SOA component under base case conditions was simulated to be dominated by aromatic hydrocarbon degradation products, with major contributors being furan-2,5-dione, and its substituted analogues, and ring-retained oxygenated aromatics containing hydroxy and nitro groups, particularly the tri-substituted species, nitrocatechols and dinitrophenols. The biogenic contribution under base case conditions was dominated by species such as first-generation hydroxynitrates and multifunctional peroxynitrates from the oxidation of α– and β–pinene, and pinonic acid. When the anthropogenic pollution was reduced, the gas phase degradation of α– and β–pinene was simulated to produce a progressively more condensable distribution of species, with the biogenic SOA component containing increasing contributions from multifunctional hydroperoxides and acids. As shown in Figure 7.19, the resultant concentration of biogenic SOA generated in the lowest anthropogenic pollution scenario is a factor of three greater than that simulated in the base case, for the 6 August 18:00 h case study. This

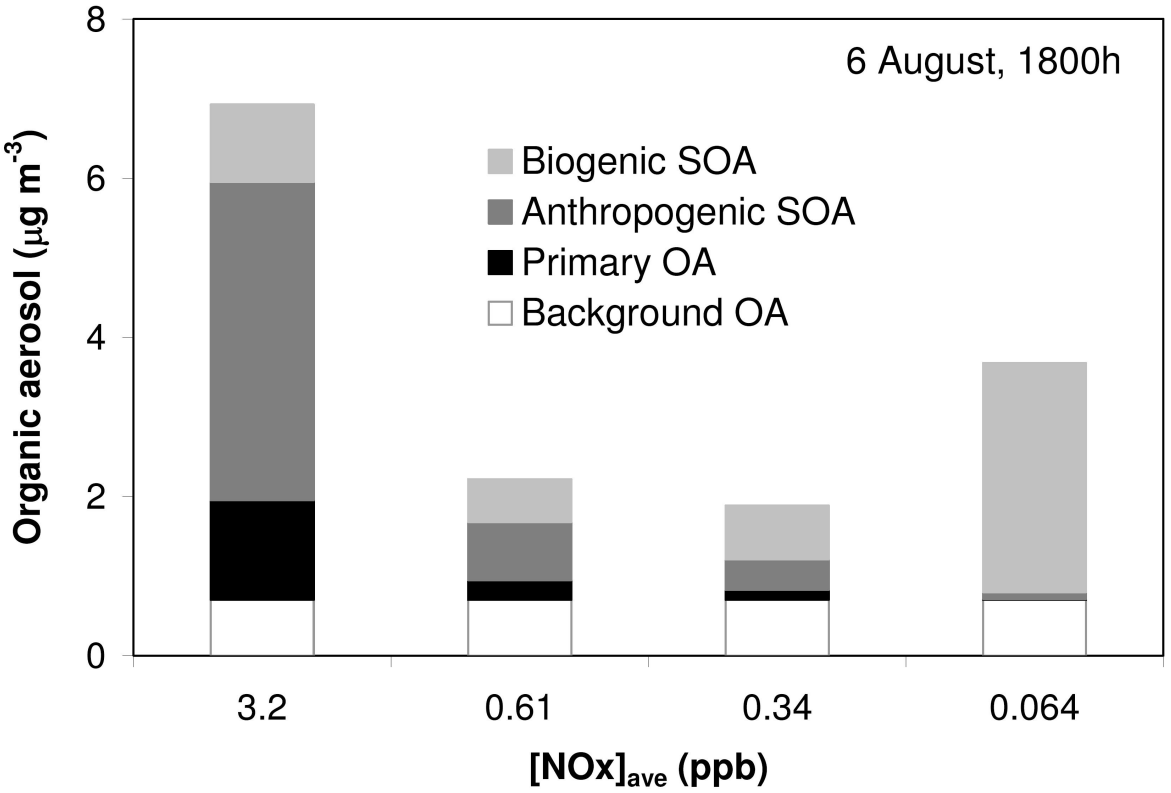

Figure 7.19: OA mass concentrations, broken down into component contributions, as simulated for the 6 August 18:00h case study using PTM-MCM v3.1. Results are shown for the base case, and for case study scenarios in which the inputs of anthropogenic species were reduced by factors of 5, 10 and 100, and are presented in terms of the average mixing ratio of NO_X over the 96-hour back-trajectory, $[NO_X]_{ave}$ (see text).

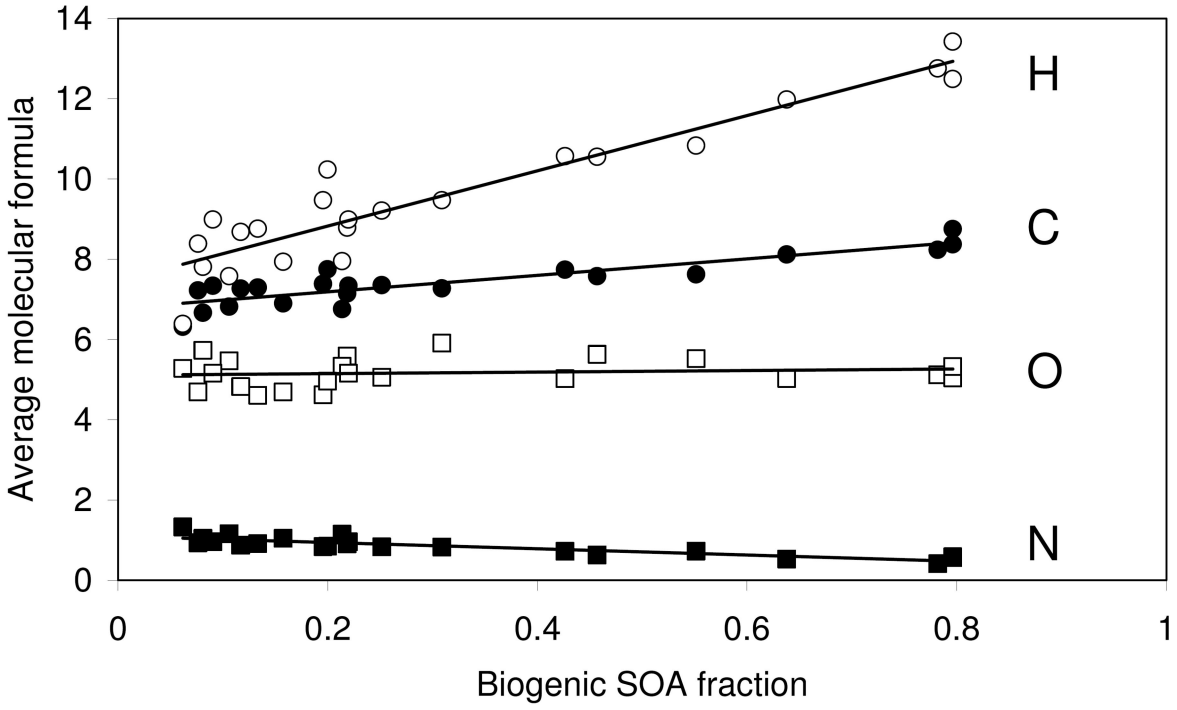

Figure 7.20: Average molecular formula of SOA simulated with PTM-MCM v3.1 as a function of the fractional biogenic content of the SOA, for case studies for which $[NO_X]_{ave}$ > 300 ppt.

increasing propensity of the monoterpenes to generate SOA with reduction of NO_X level is consistent with observations of SOA formation in a number of chamber investigations (e.g., Presto et al., 2005; Ng et al., 2007), and also with previous assessment of multifunctional acid formation from α–pinene degradation under representative ambient conditions using the MCM (Jenkin et al., 2000b).

In the lowest anthropogenic pollution scenarios, a small fractional contribution to the biogenic SOA (typically 1 %) was simulated to be comprised of products of isoprene oxidation. This contribution was dominated by C_5 species containing four polar substituents, predominantly isomers containing two hydroxy, one carbonyl and one hydroperoxy functionality. Such products are predicted to be formed, for example, from the further oxidation of the well-established first-generation C_5 hydroxycarbonyl products, 4-hydroxy-2-methyl-but-2-enal and 4-hydroxy-3-methyl-but-2-enal (e.g., Baker et al., 2005) at low NO_X levels, following attack of OH at the double bond.

Consistent with the above discussion, the average molecular formula of the simulated SOA in the 50 case study scenarios was found to depend on both the relative contributions of anthropogenic and biogenic species, and on the level of NO_X, particularly for the nitrogen content at very low $[NO_X]_{ave}$. Figure 7.20 shows data from 22 case study scenarios at relatively high $[NO_X]_{ave}$ (> 300 ppt), which corresponds to levels at which the NO_X-dependence of the nitrogen content is less-pronounced (see upper left panel of Figure 7.21), and which mainly comprise the base case scenarios and those with anthropogenic pollution reduced by a factor of five (see Figure 7.18). The data in Figure 7.20 show a well-defined dependence of the average molecular formula on the fractional biogenic content of the SOA. Linear regression of these data implies an average molecular formula of $C_{6.78}H_{7.45}O_{5.11}N_{1.10}$ (molecular weight = 186.0) for the anthropogenic SOA component (i.e., fractional biogenic content = 0), and $C_{8.83}H_{14.33}O_{5.31}N_{0.32}$ (molecular weight = 209.8) for the biogenic SOA component (i.e., fractional biogenic content = 1), where these average formulae and molecular weights correspond to the distribution of absorbed monomers generated by the MCM v3.1 gas phase chemistry. In Table 7.5, the corresponding simulated elemental ratios are compared with those reported for measurements of water-soluble organic compounds (WSOC) in fine aerosol at (mainly) rural locations in central and southern Europe (Krivácsi et al., 2001; Kiss et al., 2002; Pio et al., 2007; Salma et al., 2007). The reported ratios clearly show a greater correspondence with those simulated here for SOA with a high biogenic content, which is consistent with source-apportionment analysis reported for a subset of the same sites as part of the CARBOSOL project (Gelencér et al., 2007). In particular, the composition of the biogenic SOA component simulated here corresponds most closely with the observations from the remote site at the Jungfraujoch, Switzerland (Krivácsi et al., 2001), which were reported to contain important contributions from higher molecular weight humic-like substances (HULIS). This similarity therefore suggests that the present methodology provides a reasonable description of the production and gas-to-aerosol transfer of HULIS building blocks, and may also provide an indication that the persistent OA background required to simulate the ambient data is dominated by an aged, humic-like biogenic SOA component.

Table 7.5: Atomic ratios (relative to C) and OM/OC for SOA simulated with PTM-MCM v3.1 here and measurements reported for water soluble organic compounds (WSOC) at rural and urban sites in Europe.

		C	H	O	N	OM/OC
Jungfraujoch, CH (rural), Summer 1998 [a]	Krivácsy et al 2001	1.00	1.53	0.55	0.04	1.91
K-puszta, HU (rural), Jan-Sep 2000 [b]	Kiss et al., 2002	1.00	1.42	0.58	0.04	1.93
Aveiro, PT (rural), Summer 2002/2003 [c]	Pio et al., 2007	1.00	1.38	0.56	0.06	1.9
Winter 2002/2003 [c]		1.00	1.30	0.43	0.03	1.7
Budapest, HU (urban), April/May 2002 [d]	Salma et al., 2007	1.00	1.45	0.45	0.05	1.81
Simulated anthropogenic SOA [e]	This work	1.00	1.10	0.75	0.16	2.28
Simulated biogenic SOA [e]	This work	1.00	1.62	0.60	0.04	1.98

a: Elemental composition based on reported content, 52.3% C, 6.7% H, 38.5% O and 2.5% N. OM/OC calculated here. b: Elemental composition based on the reported ratios, C:H:O:N ≈ 24:34:14:1. OM/OC as reported. c: Citing data of Duarte (2006). Elemental composition based on the reported ratios, C:H:O:N = 16:22:9:1 (summer) and C:H:O:N = 30:39:13:1 (winter). OM/OC as reported. d: Elemental composition based on the reported ratios, C:H:O:N = 22:32:10:1. OM/OC as reported. e: Based on linear regression of data for $[NO_X]_{ave}$ > 300 ppt, as shown in Figure 7.20. Representative of south-eastern England in August 2003.

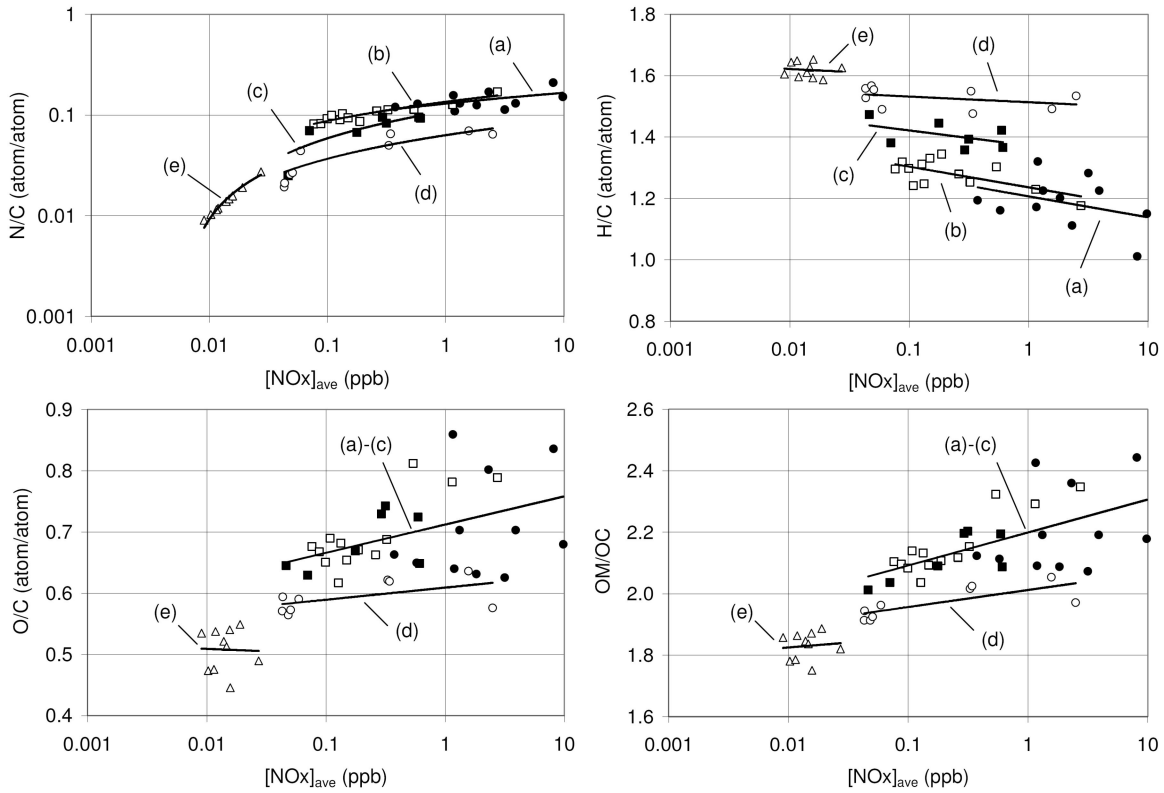

Figure 7.21: Atomic ratios, N/C, H/C and O/C and the ratio of the organic aerosol mass to organic carbon mass (OM/OC) of SOA simulated with PTM-MCM v3.1 as a function of $[NO_X]_{ave}$ and of the fractional biogenic content of the SOA. Biogenic content 0-20 % (filled black circles); 20-40 % (open squares); 40-60 % (filled black squares); 60-80 % (open circles); 80-100 % (open triangles). Lines denoted (a) – (e), are based on log-linear fits to the respective datasets and are intended to guide the eye only.

The NO_X dependences of the component element ratios in the simulated SOA, and the organic mass/organic carbon mass ratio (OM/OC), are presented in Figure 7.21, with the data also subdivided into a series of fractional biogenic content categories. This information demonstrates that, with the exception of the N/C ratio at low $[NO_X]_{ave}$, the simulated SOA empirical composition within the biogenic categories generally shows a comparatively mild trend with $[NO_X]_{ave}$ over the considered three orders of magnitude range. The simulated H/C ratio tends to increase with decreasing NO_X, whereas the O/C ratio tends to decrease, with the dependence in each case being more pronounced for SOA with a higher anthropogenic content. The N/C ratio falls away more rapidly at lower $[NO_X]_{ave}$, when the system becomes increasingly NO_X-limited and the formation of products containing oxidised nitrogen substituent groups (i.e., from the reactions of RO_2 radicals with NO and NO_2), becomes progressively less favoured. Under all conditions, oxygen accounts for the major non-carbon contribution to the SOA, such that the trends in the OM/OC values follow a similar pattern to those for the O/C ratios, varying between about 2.3 (on average) for anthropogenic SOA at the high end of the $[NO_X]_{ave}$ range (ca. 10 ppb) and about 1.8 (on average) for biogenic SOA at the low end of the $[NO_X]_{ave}$ range (ca. 10 ppt). The strong correlation between O/C and OM/OC simulated here is thus consistent with that reported recently by Aitken et al. (2008) for both chamber and ambient OA.

Table 7.6: Summary of species used to represent SOA formation from CRI v2 (and CRI v2-R5).

CRI v2 species	Description	Closest MCM v3.1 analogue(s)
Biogenic species		
RTN28OOH	First-generation α–pinene product containing *-OH* and *-OOH* groups	APINAOOH, APINBOOH, APINCOOH
RTN28NO3	First-generation α–pinene product containing *-OH* and *–ONO_2* groups	APINANO3, APINBNO3, APINCNO3
RTX28OOH	First-generation β–pinene product containing *-OH* and *-OOH* groups	BPINAOOH, BPINBOOH, BPINCOOH
RTX28NO3	First-generation β–pinene product containing *-OH* and *-ONO_2* groups	BPINANO3, BPINBNO3, BPINCNO3
RTN26OOH	Second-generation α–pinene product containing *-C(=O)-* (x2) and *-OOH* groups	PINALOOH, PERPINONIC
RTN26PAN	Second-generation α–pinene product containing *-C(=O)-* and *-C(=O)$OONO_2$* groups	C10PAN2
RTN25OOH	Second-/third-generation α–pinene product containing *-C(=O)-* and *-OOH* groups	C96OOH
RTN24OOH	Second-/third-generation α–pinene product containing *-OH, -C(=O)-* and *-OOH* groups	C97OOH
RTN23OOH	Second-/third-generation α–pinene product containing *-OH, -C(=O)-* (x2) and *-OOH* groups	C98OOH
RCOOH25	First-/second-generation α–pinene product containing *-C(=O)-* and *-C(=O)OH* groups	PINONIC
RU12OOH	Second-generation isoprene product containing *-OH* (x2), *-C(=O)-* and *-OOH* groups	C57OOH, C58OOH, C59OOH
Anthropogenic species		
ARNOH14	Second-generation benzene product containing *-OH* and *-ONO_2* groups	HOC6H4NO2
ARNOH17	Second-generation toluene product containing *-OH* and *-ONO_2* groups	TOL1OHNO2
ANHY	Second-generation cyclic anhydride product of aromatic oxidation	MALANHY and substituted analogues

7.4.4 Development of SOA capability for CRI v2

A limited number of species in the CRI v2 mechanism were identified to act as appropriate surrogates for sets of species contributing to SOA in the MCM v3.1 reference simulations. These were selected to ensure that a reasonable proportion of the simulated SOA mass concentration (typically at least 40 %) could be covered in case study scenarios over the full range of anthropogenic pollution conditions described above. On this basis, the 14 species listed in Table 7.6 were identified, made up of three aromatic hydrocarbon-derived anthropogenic species, ten terpene-derived biogenic species and one isoprene-derived biogenic species. The larger set of terpene-derived species was required because, as discussed above, terpenes were found to be important SOA precursors over the full range of pollution conditions, thereby necessitating inclusion of a variety of surrogate species formed at both

high and low NOx (i.e., containing oxidised nitrogen, hydroperoxide and acid functionalities), derived from both α– and β–pinene. In contrast, species derived from aromatic hydrocarbons and isoprene tended to be most significant under high and low pollution conditions, respectively, such that they could be represented reasonably using more limited sets of surrogates.

Gas-aerosol partitioning reactions were implemented into a version of the PTM containing CRI v2 for the 14 surrogate species in Table 7.6, using the same method as described for the MCM v3.1 species in Section 7.4.2. Values of K_p were initially assigned, based on those of the closest MCM v3.1 analogue species (including the scaling factor of 427). The values of K_p were further scaled for the anthropogenic, terpene-derived biogenic and isoprene-derived biogenic species independently to optimise agreement with the PTM-MCM v3.1 reference simulations, both in terms of total SOA mass concentration generated and the relative contributions of the three component categories for the range of simulated conditions. During the optimisation procedure, emphasis was placed on case study scenarios in which SOA concentrations of 1 μg m^{-3} or greater were generated. However, as shown in Figure 7.22, the method yielded a good correlation of the PTM-CRI v2 and PTM-MCM v3.1 results for all 50 case study scenarios at the trajectory end point, and also for the SOA concentrations generated at the 4,750 hourly time points along the considered trajectories prior to arrival. The total SOA concentrations at the end point agree to better than a factor of 2.5 for the whole dataset, with 60% of the data agreeing to better than a factor of 1.5.

The set of base case simulations using PTM-CRI v2 was expanded to consider ca. 800 hourly arrival events throughout the TORCH-2003 campaign. The simulated OA concentrations at the receptor are presented in Figure 7.16, in comparison with the observed concentrations and those simulated in the 15 case studies with PTM-MCM v3.1, as described above. PTM-CRI v2 is able to recreate the general features of the observed time series, with the highest observed and simulated OA concentrations occurring during the latter part of the stable anticyclonic period of the campaign (6-12 August). Figure 7.23 shows the same simulated OA data, broken down into the broad source categories. These data are clearly consistent with those shown for the PTM-MCM v3.1 case study simulations in Figure 7.17 (i.e., showing a general dominance of SOA during the anticyclonic period, with important contributions from both anthropogenic and biogenic precursors), but are able to extend the information to a description of the complete campaign period at hourly temporal resolution. As a result, a campaign mean OA concentration of 1.8 g m^{-3} can be calculated, which is made up of 38 % background OA, 24 % primary OA, 23 % anthropogenic SOA and 15 % biogenic SOA. The simulated contribution from anthropogenic SOA is logically higher than the range 4~13 %, reported by Gelencér et al. (2007) for fossil fuel-derived SOA at a transect of sites in central and southern Europe, which lie in regions that are more influenced by biogenic VOC emissions and also generally less impacted by anthropogenic VOC emissions than the region of north-west Europe considered in the present analysis. The proportion of the background OA to the simulated total is consistent with a major contribution from OA imported into the model domain. Although the present analysis can draw no direct conclusions about the composition of this background OA, the comparison of the detailed MCM v3.1 composition results with reported elemental ratios (discussed above), provides an indication that the background might be mainly an aged, humic-like biogenic SOA component.

The reduced SOA module was also implemented into a version of the PTM containing the CRI v2-R5 gas phase chemistry. Importantly, CRI v2-R5 contains all of the 14 partitioning species listed in Table 7.6 and is therefore fully compatible with the reduced SOA module. As shown in Figure 7.24, the hourly SOA concentrations simulated at the receptor under base case conditions using PTM-CRI v2 and PTM-CRI v2-R5 are in excellent agreement throughout the campaign period, for both the total SOA concentrations and for the collective concentrations of the anthropogenic and biogenic components. The total concentrations agree on average to 1.5 %, and with 99 % of the data agreeing to within 10 %. Reduction of the anthropogenic input by factors of 5, 10 and 100 results in a progressive improvement on these figures, because CRI v2 and CRI v2-R5 contain the same representation of biogenic chemistry.

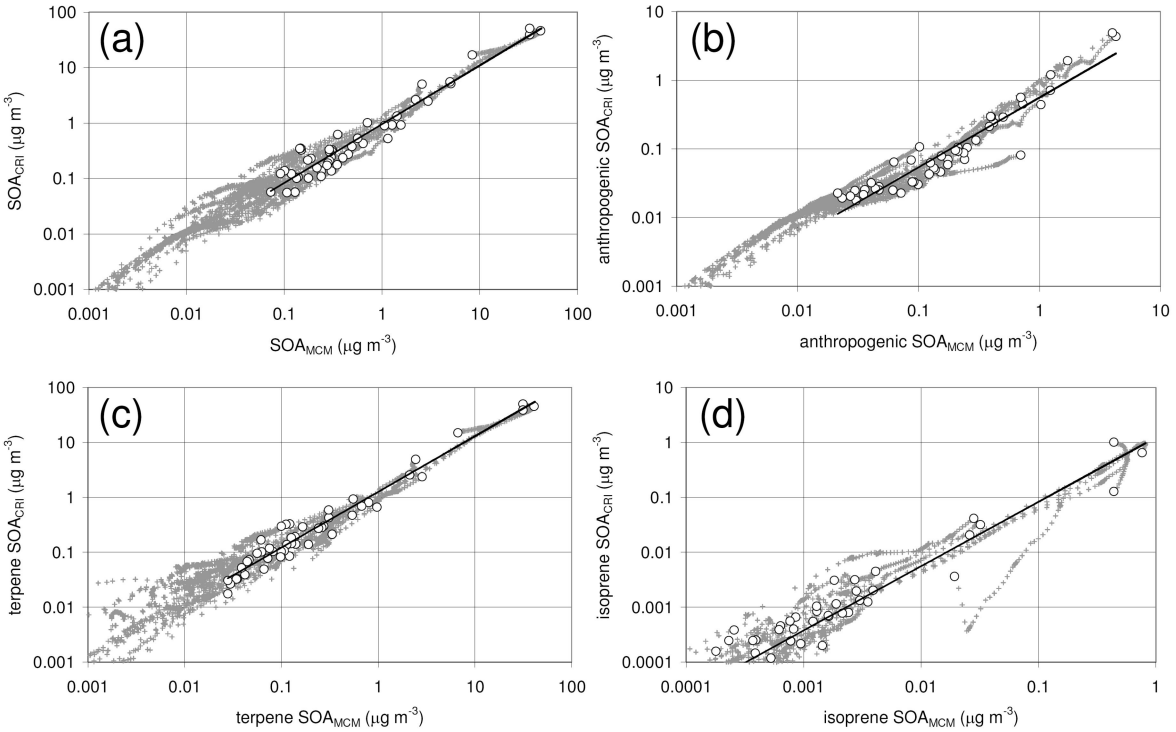

Figure 7.22: Comparison of SOA concentrations simulated with PTM-MCM v3.1 and PTM-CRI v2 (panel (a)), and of the concentrations of anthropogenic SOA (panel (b)), terpene-derived SOA (panel (c)) and isoprene-derived SOA (panel (d)). Data are shown for the end-point concentrations in each of the 50 case studies (large open points), and for hourly intervals along each of the 96-hour back-trajectories (small crosses). Lines are best fits to end-point concentrations. (a) $y = 0.96\ x^{1.06}$, $R^2 = 0.93$; (b) $y = 0.56\ x^{1.02}$, $R^2 = 0.90$ (c) $y = 1.26\ x^{1.01}$, $R^2 = 0.96$; (d) $y = 1.22\ x^{1.17}$, $R^2 = 0.87$.

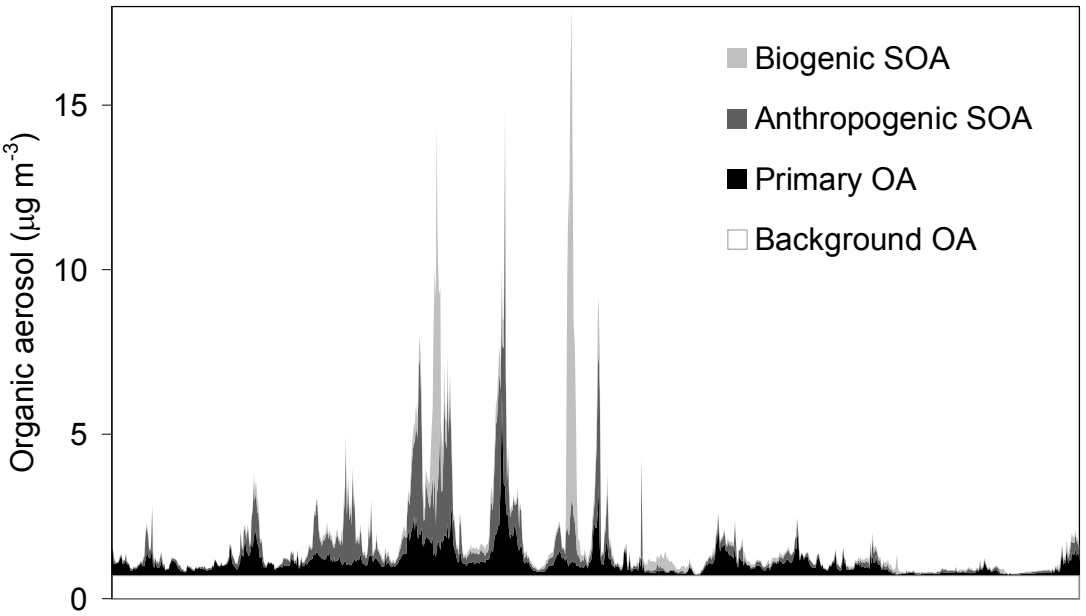

Figure 7.23: Hourly mean organic aerosol mass concentrations simulated with PTM-CRI v2 for the entire TORCH campaign, broken down into component contributions.

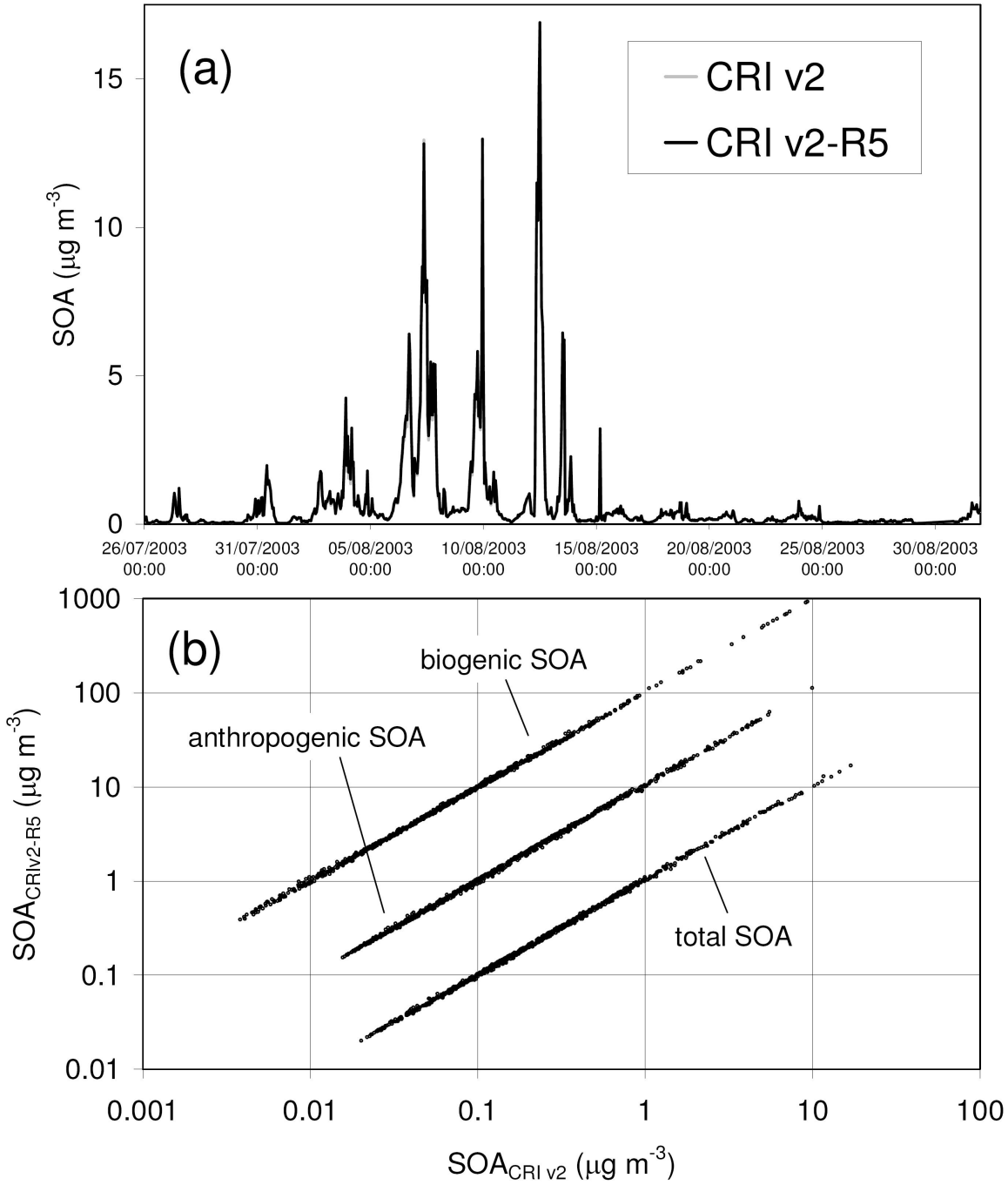

Figure 7.24: (a) Comparison of total SOA mass concentrations simulated for the TORCH campaign with PTM-CRI v2 and PTM-CRI v2-R5. (b) Correlation of the ca. 800 hourly data points for each of total SOA, anthropogenic SOA and biogenic SOA (the latter two cases have been offset by factors of 10 and 100, respectively, to facilitate clear presentation of the data).

7.5 Calculation of Secondary Organic Aerosol Potentials (SOAPs)

Laboratory studies are beginning to unravel the complex story of secondary organic aerosol SOA formation, as indicated in the mechanism development work described in Section 7.4. It is commonly understood that the atmospheric oxidation of organic compounds leads to the formation of low vapour pressure oxidation products which preferentially become adsorbed into the particulate phase on the pre-existing aerosol. Policy actions aimed at SOA therefore need to address the emissions of those organic substances that contribute most to SOA formation. This is exactly analogous to the situation for photochemical ozone formation where control policies ideally should focus on the emissions of those organic species that exhibit the highest reactivity.

The two most common atmospheric chemical reaction mechanisms employed in policy studies in the USA, Carbon Bond Mechanism CBM v4 and Statewide Air Pollution Research Center SAPRC 99, do not have an explicit representation of peroxy radical species but have a counter mechanism that works well for photochemical ozone formation. Unfortunately, this counter mechanism cannot be extended to treat the peroxy radical species that give rise to SOA formation. At present, the MCM is the only widely used chemical mechanism that has the potential ability to represent accurately both photochemical ozone formation and SOA formation.

Work has been undertaken to investigate whether the concepts of reactivity scales that have been so influential in policy making for ozone, have some potential for policy development with SOA formation. The concept of the secondary organic aerosol potential, SOAP, has been developed to reflect the propensity of each organic compound to form SOA on an equal mass emitted basis relative to toluene. SOAPs are calculated by running the UK PTM model for an appropriate base case and then running sensitivity cases for a wide range of VOC species by adding a small additional mass emission of each VOC species and determining the additional SOA mass formed relative to the base case. SOAPs are calculated using:

$$SOAP_i = \frac{\text{Increment in SOA concentration with species, i}}{\text{Increment in SOA with toluene}} \times 100$$

The SOAP represents the propensity for an organic compound to form secondary organic aerosol when an additional mass emission of that compound is added to the ambient atmosphere expressed relative to that secondary organic aerosol formed when the same mass of toluene is added. SOAPs are expressed as an index relative to toluene = 100. Toluene was chosen as the base compound for the SOAP scale because its emissions and atmospheric chemistry are well characterised.

The SOAPs calculated for a range of organic compounds using the back-track trajectory for 7th August 2003 are tabulated in Table 7.7 alongside those reported by Jenkin (2008) for 6th August 2003, during the same TORCH campaign.

In the next phase of the study, attention has been switched from the TORCH campaign to the standard trajectory case that has been used extensively in previous work with the UK PTM characterising POCPs. This standard trajectory case follows photochemical ozone and SOA formation in an air parcel as it travels along a five day trajectory path from Austria to the United Kingdom. The first set of SOAPs were calculated using a base case which employed 1999 emissions of SO_2, NO_x, VOCs, CO and NH_3 emissions from EMEP and the NAEI. Subsequent sets of SOAPs were calculated assuming 50% and 90% across-the-board reductions in NO_x emissions. These SOAPs are tabulated in Table 7.8 below.

The results show a dramatic dependence of SOAP on the availability of NO_x. For some VOCs, the SOAPs decrease steadily with NO_x reduction from the base case to the 90% NO_x reduction case and these include: benzene, styrene and benzaldehyde. Some other VOCs show a dramatic enhancement to their SOAPs with increasing NO_x reduction and these include: o-xylene, m-ethyltoluene and the trimethylbenzenes. There is also a class of VOCs whose SOAPs are largely independent of the availability of NO_x and these include: p-xylene, o-ethyltoluene and p-ethyltoluene.

Table 7.7: SOAPs calculated for two separate days during the TORCH campaign.

Organic compound	SOAP, 7th August	SOAP, 6th August
benzene	117.17	132.1
toluene	100.0	100.0
ethylbenzene	109.09	100.1
o-xylene	93.60	86.8
m-xylene	90.23	89.0
p-xylene	88.22	55.9
n-propylbenzene	105.05	108.2
i-propylbenzene	98.99	102.9
1,2,3-trimethylbenzene	43.10	53.7
1,2,4-trimethylbenzene	19.52	24.0
1,3,5-trimethylbenzene	12.79	17.7
o-ethyltoluene	92.93	82.9
m-ethyltoluene	110.10	85.0
p-ethyltoluene	65.66	61.5
3,5-dimethylethylbenzene	12.12	14.0
3,5-diethyltoluene	8.08	12.9
benzaldehyde	360.94	442.7
styrene	356.23	443.2
α-pinene	17.85	14.9
β-pinene	18.18	15.13

Table 7.8: SOAPs for a range of VOCs calculated using the standard trajectory case with 1999 emissions and subsequently with 50% and 90% across-the-board reductions in NO_x emissions.

Organic compound	SOAP, Standard trajectory case	SOAP, 50% NO_x reduction	SOAP, 90% NO_x reduction
benzene	92.9	56.0	17.5
toluene	100	100	100
o-xylene	95.5	100.6	147.6
m-xylene	84.5	91.4	188.1
p-xylene	67.1	69.7	91.3
ethylbenzene	111.6	109.7	118.3
n-propylbenzene	109.7	97.7	63.5
i-propylbenzene	95.5	87.4	65.9
1,2,3-trimethylbenzene	43.9	59.4	203.2
1,2,4-trimethylbenzene	20.6	27.4	96.8
1,3,5-trimethylbenzene	13.5	21.7	123.8
o-ethyltoluene	94.8	96.6	119.0
m-ethyltoluene	100.6	101.7	166.7
p-ethyltoluene	69.7	66.9	65.9
benzaldehyde	216.1	98.3	12.7
styrene	212.3	94.3	7.9
α-pinene	17.4	30.3	199.2
β-pinene	18.1	27.4	127.0

Results from this work were key to the assessment of the impacts of solvent substitution on SOA formation undertaken for the trichloroethylene case study described in Section 9 (Objective 7). This assessment was based on the use of SOAP values estimated for trichloroethylene and its potential replacement.

7.6 Maintenance of the MCM Website

The MCM website (http://mcm.leeds.ac.uk/MCM) has continued to be maintained and developed primarily through joint work carried out as part of the NERC Knowledge Transfer (KT) funded "Integration and Co-Development of the MCM and IUPAC databases/websites" project. The website and its supporting staff at the University of Leeds have played a key role in the developments of the MCM, the CRIv2 and its reduced schemes and the new chemical schemes, including those for SOAs described above.

The main objective of the maintenance project is to create a common interactive toolkit for atmospheric chemistry through the integration of the IUPAC (http://www.iupac-kinetic.ch.cam.ac.uk/) and MCM databases/websites and the development of tools that will facilitate their usage and sustainability. The following briefly summarises work carried out over the past year:

- Both the MCM database and IUPAC summary table have been converted into more comprehensive searchable and flexible databases by making use of emerging standardised formats and nomenclature from the chemo-informatics communities as well as developing our own libraries and schemas. The use of such technology is vital for the sustainability of both databases.
- Using standard nomenclature for chemical species is crucial to the interoperability of the databases and ease-of-use by third parties. Each individual species is tagged using its IUPAC International Chemical Identifier (InChi: http://www.iupac.org/inchi). Therefore, each species can now be linked to other online databases such as the NIST chemistry web book (http://webbook.nist.gov/chemistry/) and PubChem (http://pubchem.ncbi.nlm.nih.gov/) and can be exposed to popular webcrawler search engines (e.g. Google™). Such databases provide invaluable additional thermodynamic and spectroscopic information.
- The ease of maintenance of the MCM and its accuracy has been enhanced by linking of IUPAC datasheets to the appropriate reactions in the MCM database with links displayed on each webpage.
- Common web-based tools have been developed for clear, simultaneous searching of both databases and easy extraction of data. The new advanced search facility will enable the user to search across both databases using various formats including IUPAC name, SMILES, InChi and different synonyms. The search facility also includes a Java Applet which enables the user to draw a structure or a series of functional groups and search both databases for either an individual species or a list of species containing the functionalities specified.

The new development website is currently being tested and will be made live in early 2009. The above Leeds KT activities are only supported through the existing project until June 2009 with the help of some funds acquired for National Centre for Atmospheric Science (NCAS) work. Further funding to help support further development, maintenance and linkage of both websites/databases will be required subsequently.

Ongoing activities as part the EU EUROCHAMP Programme (http://www.eurochamp.org/) involve the development of tools to facilitate the evaluation of the MCM and will promote its wider use, these include:

- An open source modelling toolkit, based on the MCM and using a FORTRAN code, has been developed which is aimed at laboratory, field and chamber scientists. Simple box models containing all or subset extractions of the MCM can be run easily, independently and inexpensively by the user by downloading the model from the MCM website or on a server based in Leeds. A graphical user interface is currently being developed to make the model easier to use.
- A *retro extraction* tool has been developed which can post-process model results in order to gain information on the sources of a certain product at a certain time during the model experiment run. Visualisation tools are also being developed, in collaboration with the Department of Computing, University of Leeds, in order to track the temporal evolution of the product of interest more easily.

8 Maintenance and Improvements to the OSRM and Comparison With Eulerian Models (Objective 4)

The original aim of Objective 4 for this project was to improve the representation of meteorological processes within OSRM in order to improve its ability to predict concentrations of ozone. The exact work plan was subject to the outcome of the independent review of existing ozone modelling tools commissioned by Defra in 2007 following the start of this project. Following the recommendations of this review in November 2007 (referred to as the Monks' Review), and following discussions with Defra, the scope of Objective 4 was revised with two principal aims:

- To maintain the OSRM for Defra ozone policy applications with only modest improvements, involving treatment of emissions and chemistry in the model, and

- To compare the performance of the OSRM and PTM with Eulerian models that use a different approach for dealing with the transport of a chemically reacting air mass. The purpose of this is to enable a more informed decision to be made on the merits of investing in making improvements to the representation of meteorological processes in the OSRM given the availability of other widely used models utilising a Eulerian instead of Lagrangian modelling approach

The OSRM is recognised as a vital ozone policy tool, but with the Monks Review making strong recommendations towards moving Defra's ozone modelling activity to an Eulerian basis, a comparison of the OSRM and PTM with Eulerian models was deemed essential. An additional requirement of this project was to undertake an initial assessment of specific recommendations of the Monks' Review in terms of how far the OSRM goes in meeting these recommendations.

During the last year of this project, the initial assessment of the OSRM has been carried out and work is in progress maintaining and making limited improvements to the OSRM. A summary of this assessment is given in this report. Progress has been made on setting up and running the Eulerian-based CMAQ model and initial results are also reported.

8.1 Performance of the OSRM Against Recommendations of the Defra Review on Tools for Modelling Tropospheric Ozone

Defra requested an assessment of three specific recommendations of the Monks' Review in the context of the performance of the OSRM and how far it goes in meeting these recommendations. Taken from the Review's report (Monks et al, 2007), these recommendations were:

1) Use of emission estimates:
R3.1 Defra should ensure that its chosen models have transparent sources of emission estimates.

R3.2 Defra should ensure that its chosen models have recognised and realistic schemes for the spatial and temporal disaggregation of emission estimates. Some assessment is also required of how these might change in the future.

R3.3 Defra should ensure its models are able to use the information in the NAEI.

R3.4 Defra should investigate the policy need for its chosen models to include improved biogenic emission estimates, or land use data in conjunction with biogenic emission factors.

2) Model evaluation and comparison
R4.1 Defra should ensure:

- any contracts let for ozone modelling include a review of the performance of its chosen models with observations, to ensure their continued performance levels;
and
- regular comparisons between UK ozone models choosing, perhaps, periods of peak and background ozone, to ensure that the performance of the Defra chosen models is satisfactory.

R4.2 Defra should ensure that UK ozone policy models have a strong peer-reviewed evidence base.

3) Quality control of models and outputs
R5.1 Defra should require the principal investigators for its chosen models to consider the recommendations of the Royal Meteorological Society (1995) on the use of models and, where appropriate, to follow them.

An assessment was made then on:

1) The use of emission estimates in the OSRM;

2) The evaluation of the performance of the OSRM and the PTM by comparison with ambient measurements of ozone concentrations;

3) Quality control and outputs and how the OSRM follows the modelling guidelines of the Royal Meteorological Society.

The performance assessment was presented in detail in a separate report submitted to Defra (Murrells et al, 2008). Only the main conclusions of the report are presented here.

8.1.1 Use of emissions information in the OSRM

In the area of emissions information, it was concluded that the OSRM does treat emissions from UK and other European sources using the best available emissions inventory information and in a manner as well as any other ozone model is currently capable of, but there is room for improvement:

- The OSRM uses the best available emissions inventory information for both the UK (the NAEI) and the rest of Europe (EMEP). Some improvements can be made in the transparency of sources and versions of emission projections used in the OSRM for non-UK sources and for shipping.

- The OSRM uses the best speciated VOC inventory currently available from the NAEI, but as this was developed some years ago, this would benefit from a further review of its relevance to current and future emission sources. Its appropriateness to all European countries could also be considered.

- Like most state-of-the-art ozone policy models, the OSRM relies on the assignment of the detailed NAEI speciated VOC inventory to a small number of surrogate VOC species in the OSRM's simplified chemical mechanism. However, the transparency of the assignment process could be improved and checked using the POCP concept to see how the implied POCP-weighted emissions in the OSRM compare with the POCP-weighted emissions from the NAEI.

- Introducing more surrogate species into the OSRM has the potential for improving the accuracy of the ozone predictions. It would also improve the capability of the OSRM to reflect changes in VOC speciation associated with specific policy options such as VOC substitution. Improvements to the chemical scheme used in the OSRM to be carried out might allow this and should at least allow traceability of the assignment process to the latest version of the MCM.

- The OSRM does use a realistic and transparent method to convert annual emission estimates to instantaneous emission rates using pollutant- and soure-dependent temporal profiles based on real activity data. The OSRM would need to be developed to accommodate different

temporal emission profiles in different European countries.

- The OSRM does use the best available technique for estimating biogenic emissions given currently available methodologies, vegetation and meteorological data and emission functions. However, this is a developing area of reseach and it will be important to keep abreast of the literature

8.1.2 Evaluation of the performance of the OSRM and the PTM by comparison with ambient measurements of ozone concentrations

On model evaluation and comparison with monitoring data, the performance of the OSRM has been assessed against observations and some other models in this and previous Defra project reports and more recently in the AQEG report on ozone in the UK (AQEG, 2008), but these have to date lacked a strong external peer-review.

Further assessments made for this study compared the performance of the OSRM against 2005 and 2006 data at two rural and one urban AURN site and comparisons also made with the performance of the UK PTM, a similar Lagrangian trajectory model used for DEFRA policy employing more explicity chemistry.

Based on specified performance criteria, involving comparing modelled and measured monthly averages of the daily maximum hourly ozone concentrations at Harwell, Yarner Wood and London Bloomsbury, the main conclusions from this assessment were that:

- In 2006, a high ozone year, the OSRM performs relatively well for most months of the year at the two rural sites, but tends to underestimate peak ozone. It performs less well at the urban London site where it tends to over-predict average peak ozone in most months during 2006.

- In 2005, a low ozone year, the OSRM performs relatively well for the two rural sites and does better than in 2006. Again, it performs less well at the urban London site where it tends to over-predict average peak ozone in most months during 2005.

- The performance of the UK PTM at Harwell in 2006 was rather better than the OSRM in terms of the performance criteria used.

- The performances of the OSRM, UK PTM and other European ozone models in 2006 will have been affected by biomass burning events occurring in Russia that are likely to have contributed to ozone episodes that year, but which are not included in models.

Purely as an illustration of the type of evaluation carried out, Figures 8.1 and 8.2 show the OSRM and PTM predictions of the monthly average daily maximum concentrations of ozone at the Harwell AURN site in 2006, respectively, taken from the assessment report (Murrells et al, 2008). The report also gave various modelled *vs* observed comparison statistics.

8.1.3 Modelling guidelines of the Royal Meteorological Society

The modelling guidelines of the Royal Meteorological Society refer explicitly to atmospheric dispersion modelling and are not always directly appropriate for the applications of the OSRM to Defra policy support. Nevertheless, the general principles they invoke are applicable to the OSRM. The guidelines refer mainly to atmospheric dispersion modelling related to the design of industrial plant and operating conditions, modelling supporting applications to regulatory bodies and exposure risk assessments. They give guidelines on the justification of choice and use of appropriate model(s), communicating and reporting results and emphasise fitness for purpose.

All ten aspects of the modelling guidelines were considered and on balance the view was that the OSRM is fit-for-purpose and a better than satisfactory tool, but it is difficult to defend this position based on the current absence of peer-reviewed publications and widely accessible and transparent documentation and there are a number of areas where the OSRM falls short.

Figure 8.1. OSRM predicted and observed concentrations – Harwell monthly average of daily maximum hourly mean in 2006

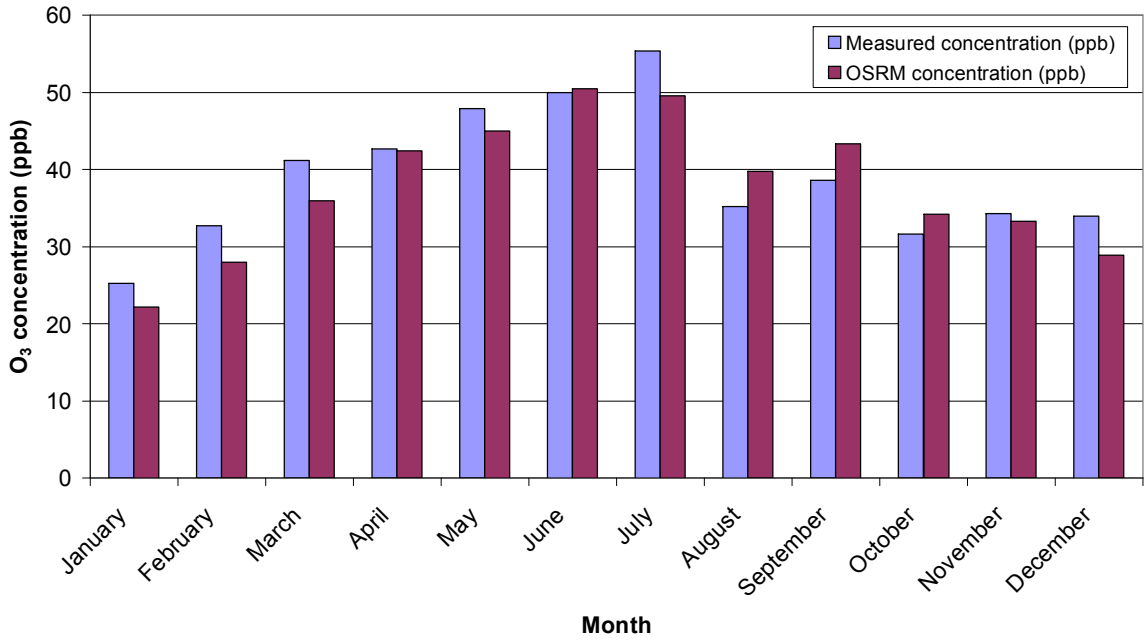

Figure 8.2. UK PTM predicted and observed concentrations – Harwell monthly average of daily maximum hourly mean in 2006

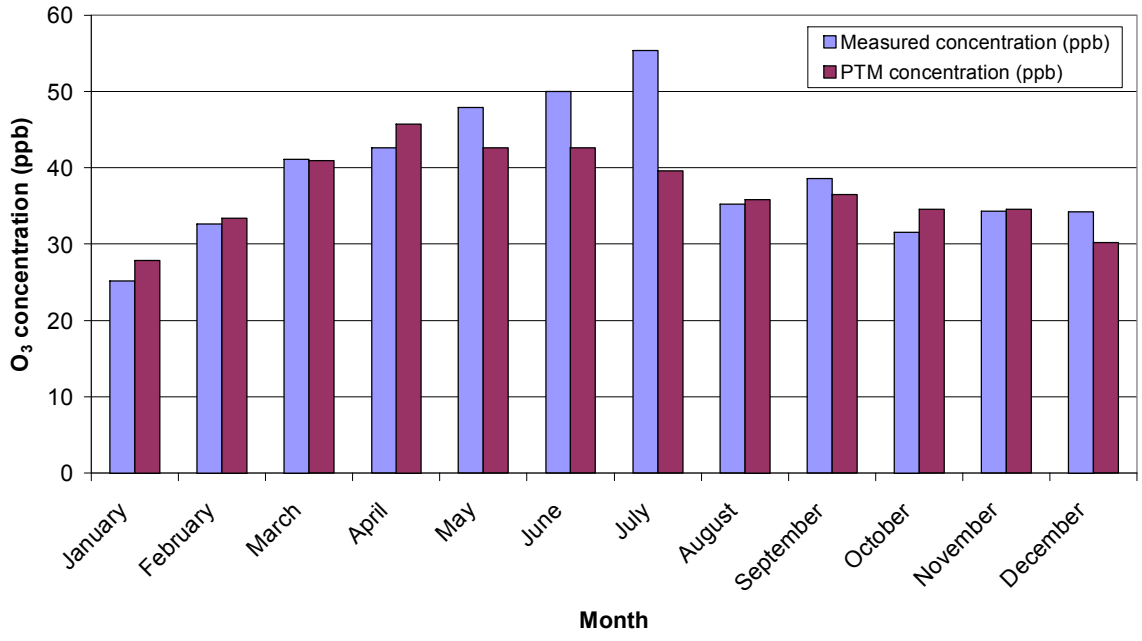

The performance assessment report was sent by Defra for independent peer-review and the reviewers pointed out several areas where the report fell short in the area of model evaluation and comparison with monitoring data and other models. However, the report was only meant as an initial appraisal and further, more rigorous evaluation is being carried out in the project, as reported in the next section.

8.2 Comparison With Eulerian Models

The aim of this task is to evaluate ozone simulations by a selection of Eulerian air quality Chemistry Transport Models (CTM) by comparison with measurements and the current OSRM and PTM models used for Defra policy applications.

8.2.1 Eulerian model overview

The three Eulerian models being considered are the US model, **CMAQ** (Community Multiscalar Air Quality); **Chimere**, and the unified **EMEP** model. Prior to running these Eulerian air quality models, data for meteorology, emissions, and initial/boundary conditions must be acquired and processed into formats suitable for each model. Figure 8.3 shows an outline of the inter-relationships in the CTM model system. The standard data format, netCDF, is common for the selected CTMs. Whilst the model input files are not identical, the common data format facilitates the process of creating them. It should be possible to create the input files from the same meteorology simulations and emissions pre-processing. The same analysis and visualisation tools can be adapted for use with all three models.

Figure 8.3: Eulerian CTM system overview

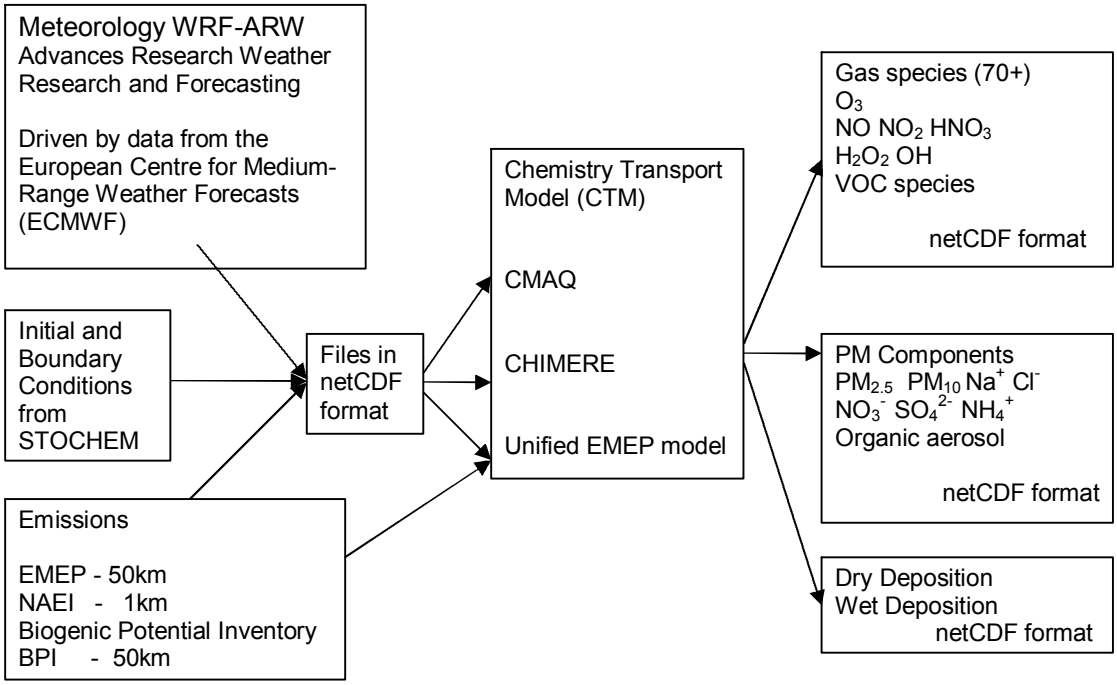

8.2.2 Meteorology Model - WRF-ARW

WRF-ARW (Advanced Research Weather Research and Forecasting) was selected as the numerical weather prediction model (NWP) for this project. It has been used in applications of all three CTMs. WRF simulations are driven using data from ECMWF (European Centre for Medium-range Weather Forecasting) on a 6-hourly basis. The ECMWF data are based on a method in which the model is constantly modified to provide a best fit to observations and it is supported by the European Met. Offices.

WRF-ARW can be utilised as a numerical weather prediction model and it is well suited for Eulerian CTMs. One of the options allows files to be written in a version of netCDF. The WRF-ARW solves compressible non-hydrostatic Euler equations with conservation of scalar variables; prognostic variables include horizontal and vertical wind components; water vapour mixing ratio; hydrometer mixing ratios; perturbation potential temperature; geopotential and surface pressure, Otkin et al. (2008); Xiao et al. (2008).

There are nine microphysical schemes to choose from, all utilising prognostic equations which describe the relationships between water vapour mixing ratio and the five hydrometeor mixing ratio: cloud liquid water, rain, snow and graupel. These schemes vary in complexity from single-moment schemes (predicts mass only) to double-moment schemes (predicts both mass and number).

The WRF-ARW code and documentation is freely available at www.wrf-model.org/index.php.

WRF has procedures allowing it to be initiated by meteorological data from (amongst others) ECMWF and the GFS (Global forecasting system) from NCEP ([USA] National Centre for Environmental Prediction). The availability of meteorology data is different for research and commercial organisations. ECMWF data are available on a commercial basis and include over 40 years of data - the most recent data being approximately 2 weeks old. These data are available for purchase by commercial organisations. Non-profit research organisations pay a reduced fee to cover data extraction.

GFS/NCEP data are available on the internet from two different organisations. The most recent 2-3 months data (updated daily) are available for free download from NCEP. Data up to 18 months old are distributed free through NCAR ([USA] National Centre for Atmospheric Research) but are only available to non-profit organisations. Older data can be made available for a charge.

CMAQ has been used with data archived from the operational MetUM model from the Met. Office. The MetUM archive was not used for this project for two reasons. Firstly it does not use the netCDF file format, and whilst the interface to CMAQ exists it is not known if or how it could be used by CHIMERE or EMEP. Secondly it is only available on the internet for research.

8.2.3 Emissions data

European and UK emissions are available from the internet as annual spatially distributed files. CMAQ and CHIMERE both require input as hourly time resolved files. Temporal profiles are used to create these files. Biogenic emissions are calculated using calculations based on the BPI (Biogenic Potential Inventory), temperature and radiation. The same temporal profiles and BPI calculations are used for the OSRM.

EMEP and NAEI emissions for 2006 are available on the internet for VOCs, NO_x, SO_2, NH_3, CO, PM_{10} and $PM_{2.5}$ by SNAP source sector. Data are available at a higher resolution over the UK from the NAEI, including detailed emissions from individual large point sources. At present the UK emissions data used in the model are the same data that are available from on the NAEI website. However the data are extracted directly from the NAEI as a netCDF file.

Several issues have arisen concerning the European EMEP gridded emissions data. The EMEP data produced a number of spurious results during the processing, which resulted in small negative values. This may be caused by the grid interpolation procedure. To prevent this, rather than extract the activity sectors separately all the sectors were extracted in the same file. This resolved the negative value problem, but following the initial CMAQ simulation the EMEP emissions seem to be high and the values need to be checked.

The NAEI stack emissions have been introduced as a fixed elevated source, which will be modified to use the stack details before the annual run.

8.2.4 Initial/Boundary conditions

Monthly variable initial and boundary conditions for the European grid were extracted from STOCHEM simulations run by Prof. Derwent.

8.2.5 Eulerian Chemistry-Transport Models Considered

Three Eulerian models are being considered for comparison with the existing OSRM and PTM Lagrangian models. Features of these Eulerian models are given below.

CMAQ

- A community model first developed as part of a US EPA project, and supported by CMAS (Community Modelling and Analysis System) and the wider community.
- Grid resolution chosen to suit each project with one-way nesting to a finer resolution
- Carbon Bond 05 (CB05) and [California] Statewide Air Pollution Research Centre chemical mechanism (SAPRC99) used.
- Can be modified to accept different chemical schemes.
- Most users are in the USA, but it is used around the world including several European countries eg Spain, Germany, France, Bulgaria, Italy
- Many of the associated tools are USA-based but can be adapted for Europe.
- CMAQ model code and documentation are available at www.cmaq-model.org.

CHIMERE

- A model developed in France by INERIS.
- The MELCHIOR chemistry scheme was developed for Chimere, based on the EMEP scheme.
- Grid resolution chosen to suit each project with one-way nesting to a finer resolution
- The code is open source but it is mostly run within a few research institutes
- CHIMERE model code and documentation are available at http://euler.lmd.polytechnique.fr/chimere.

Unified EMEP model

- The open source model is only available on the 0.5° EMEP grid (approx 50km). A 4km version is operational for the UK (EMEP4UK) but this is not open source.
- EMEP model code and documentation are available at www.emep.int/OpenSource/

The focus of the comparison exercise has been initially on CMAQ. The work has started with the development of the meteorology and emissions for CMAQ to run a single month simulation, for the month of June 2006. Once the processes are established and satisfactory results obtained, then a year-long simulation for 2006 will be done.

8.2.6 CMAQ simulations for UK ozone in June 2006

An initial simulation for June 2006 has been completed for the meteorology using WRF-ARW and subsequently for ozone using CMAQ. This exploratory run has highlighted a number of required refinements to WRF, the emissions processing and CMAQ.

The simulation uses 2 nested grids - the European grid at 48km resolution and a UK grid at 12km resolution, both using 27 vertical layers, with 8 layers below 100m. Figure 8.4 shows the ground level ozone and the vertical layers across the south of England simulated at 13:00 on 29th June 2006. Initial and boundary conditions for the European grid are from STOCHEM, the European grid providing boundary conditions for the 12km nest.

On a first visual evaluation of daytime ozone in the European and UK simulations, the ozone was higher than expected in the European grid. On further investigation the NO_2 and VOC emissions are higher than expected. This results in higher values for the boundary conditions of the UK grid. Figure 8.5 shows the spatial distribution of ozone and oxidant OX (O_3 + NO_2) in the UK on a high and low ozone day in June 2006. The distribution of ozone shows a plume of lower ozone radiating away from areas of high local NO_x emissions, which correspond to the areas with high NO_2.

Figure 8.4: Ozone concentrations in June 2006 at ground level and a vertical cross-section on the 12x12km UK grid

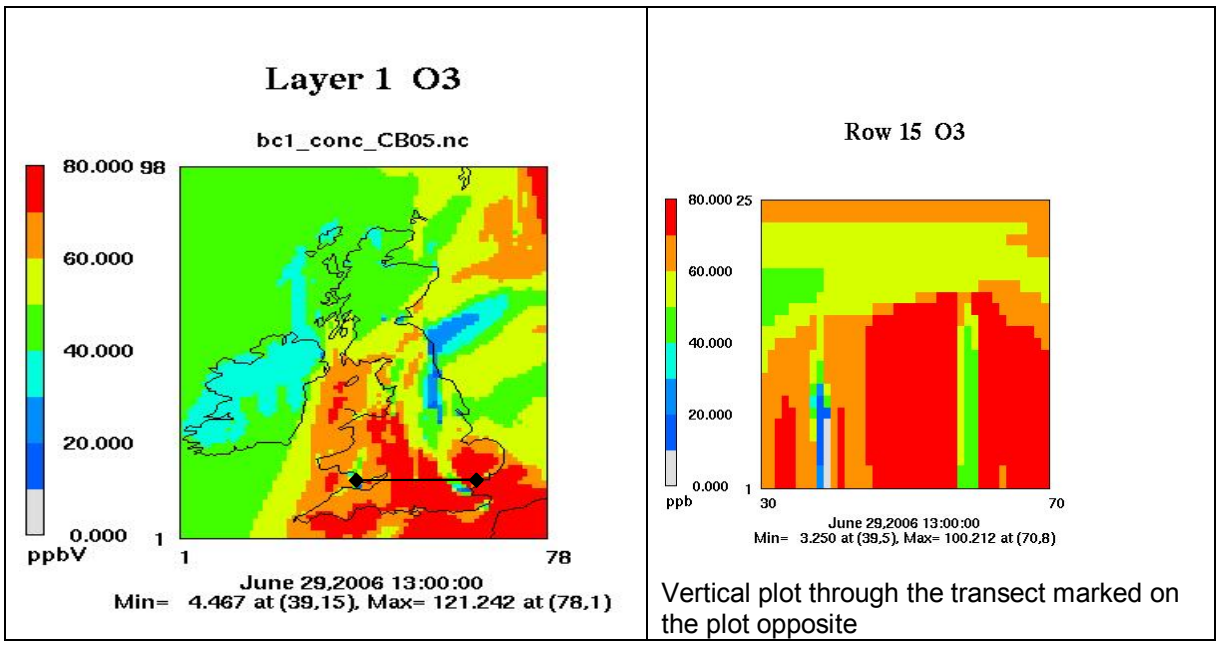

Figure 8.5: Examples of the distribution of O_3, OX and NO_2 in the UK for a high and low ozone day.

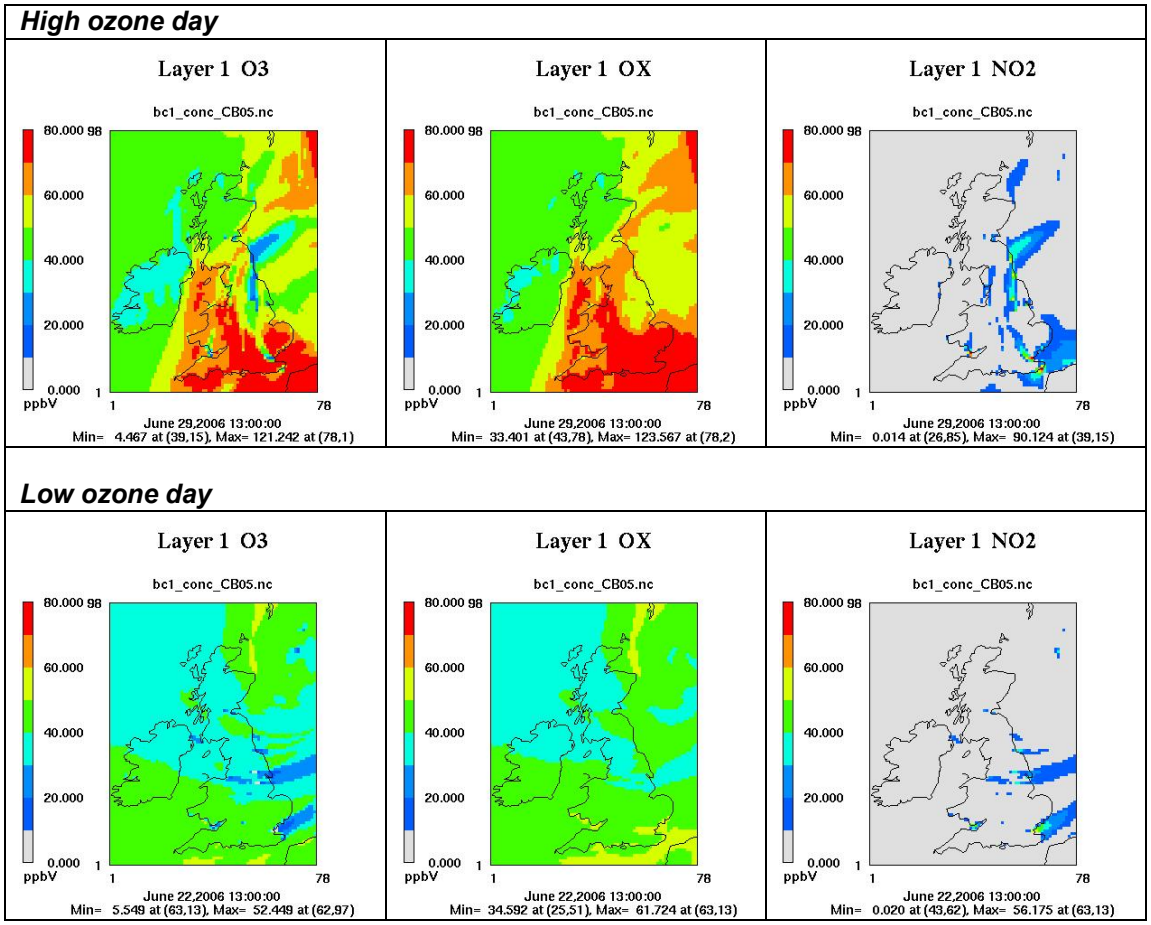

For an initial evaluation the simulated results were compared to measurements of O_3, NO, and NO_2 at a number of AURN rural monitoring stations listed in Table 8.1. The statistics in Table 8.2 indicate that bias and error values fall within the acceptable limit of ±15% and 35% respectively, as suggested in the US EPA (2005) guidelines. The later US EPA (2007) guidelines place less emphasis on the fixed statistical limit and more on the overall performance of the model, including diagnostic evaluation.

Table 8.1: AURN sites used in the model evaluation

ID	Site	Species
AH	Aston Hill	O_3, limited NO, NO_2
GDF	Great Dun Fell	O_3
HAR	Harwell	O_3, NO, NO_2
HM	High Muffles	O_3, limited NO, NO_2
LB	Ladybower	O_3
LH	Lullington Heath	O_3, NO, NO_2
PEMB	Narberth	O_3, NO, NO_2
SIB	Sibton	O_3
SOM	Somerton	O_3, NO, NO_2
WFEN	Wicken Fen	O_3, NO, NO_2
YW	Yarner Wood	O_3, NO, NO_2

Table 8.2: Statistical evaluation of ozone and OX at a selection of rural monitoring sites using CMAQ (June 2006 predictions)

	O_3	OX
No.Sites	11	6
No. Observations	6693	3587
Mean Observation (ppb)	37.21	42.04
Mean Model (ppb)	38.42	48.13
Max Observed (ppb)	105.00	108.98
Max Model (ppb)	101.10	118.09
Difference		
FAC2 (within a factor of 2)	86%	93%
MB (mean bias) –ppb	1.2	6.1
MAGE (mean absolute gross error) – ppb	11.5	11.6
Relative difference		
MNB (mean normalized bias)	13%	26%
MNAE (mean normalized gross error)	38%	35%
NMB (normalized mean bias)	3%	14%
NMAE (normalized mean error)	31%	28%

Figure 8.6 includes plots showing a range of different evaluations including the mixing ratios of ozone (modelled and observed), the NMB and MNAE averaged across all 11 sites. These are followed by box plots showing the variation between measurement and model results across different sites, days and diurnal variation. For the last of these, measurement and modelled results follow the same profile, giving confidence that the O_3 is responding as it should.

Figure 8.6: Evaluation of CMAQ simulations of ozone at rural monitoring sites in June 2006. Modelled and measured data are shown either as averages over 11 monitoring sites of for individual sites

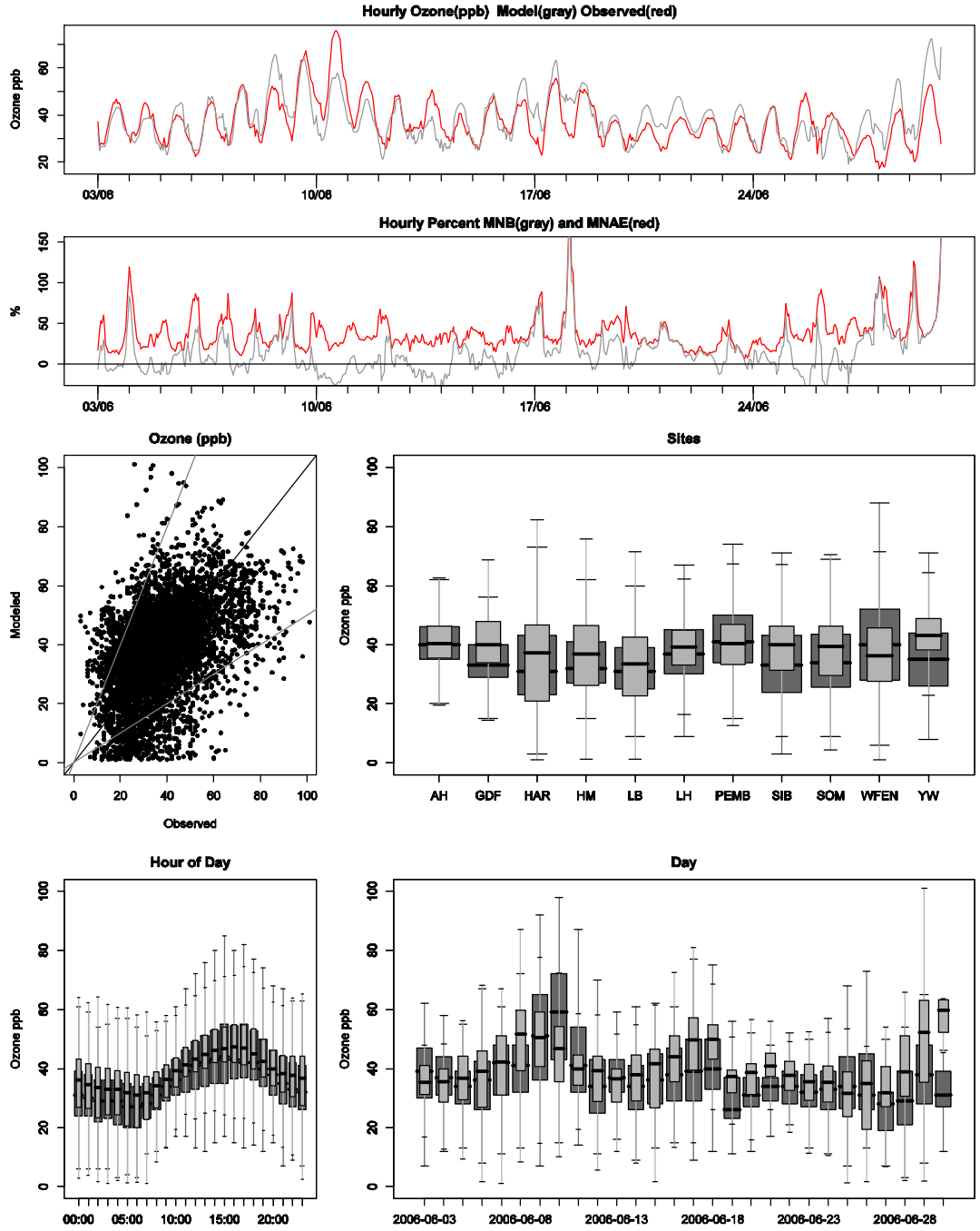

Box and Whisker plots Dark – Monitoring data
Light – Model

Centre line – 50th percentile
Box - 25th – 75th percentile
Whiskers - 5th – 95th percentile

Looking at the details for Harwell (Figure 8.7), one of the poorer performing sites for OX and NO_2, it is evident that the main discrepancy is in the overnight NO_2 mixing ratios. This is not seen at all the rural sites and is most likely a function of the emissions from Didcot power station, which is close to Harwell to the North East. The high night time NO_2 peaks are not seen when the wind direction is predominantly from the west. This raises the possibility that the emissions of NO_x are too high during the night time and that the wrong temporal profile has been used in the emission processing.

Figure 8.7: Evaluation of CMAQ simulations for O_3, OX, and NO_2 at the Harwell monitoring site in June 2006

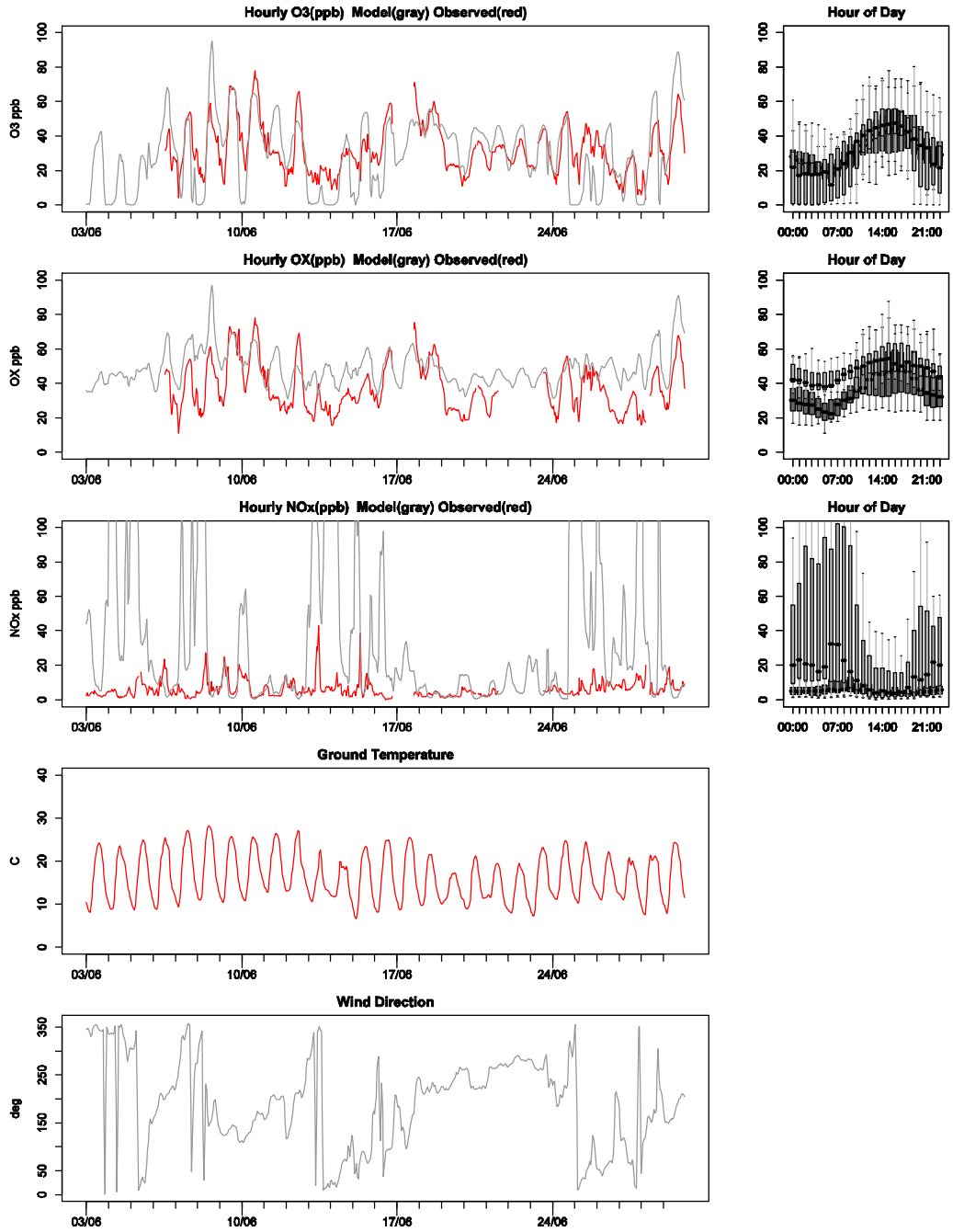

Box and Whisker plots Dark – Monitoring data
Light – Model

Centre line – 50th percentile
Box - 25th – 75th percentile
Whiskers - 5th – 95th percentile

Figures 8.6 and 8.7 are a first evaluation of CMAQ for one month in 2006. Ideally a standardised set of analyses should be done for each simulation. This will document the relative strength and weakness of each version of the model, and should incorporate the recommendations that will be developed as part of the protocol for model evaluation.

CMAQ is a 'one atmosphere' model and in addition to ozone and related gases, concentrations of the PM components are also produced. To date this simulation has concentrated on the simulation of ozone - additional work would be required to represent the PM component emissions more accurately. The distribution of $PM_{2.5}$ and PM sulphate are shown Figure 8.8 - the location of the large power stations can be identified by the sulphate plume. Wet and dry depositions are also generated in the standard simulation. There are many options to generate additional diagnostic data, including reaction rate flux; process flux and distribution of particle numbers.

Figure 8.8: Distribution of $PM_{2.5}$ and PM sulphate (ASO4) for the UK

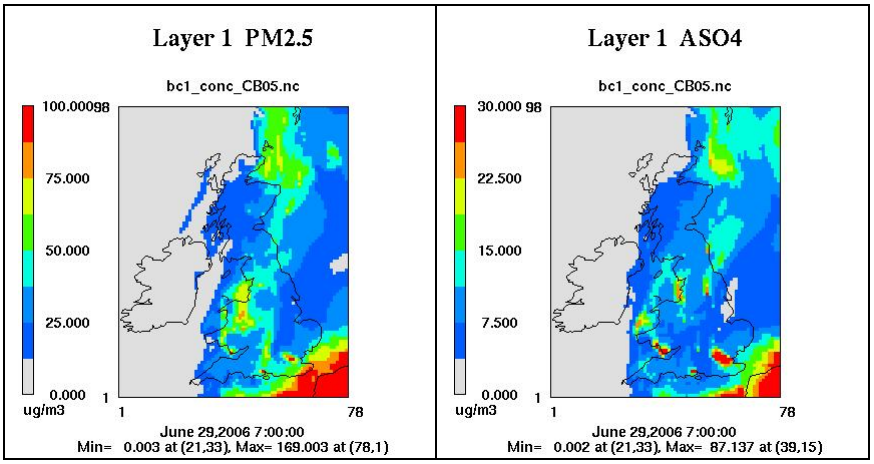

8.2.7 Current observations on CMAQ Modelling

From our experiences so far in getting CMAQ running to simulate UK ozone and other pollutants, a few observations have been made:

a) Chemistry mechanism used in CMAQ

At present, CMAQ uses a photochemical reaction scheme involving 72 species and 156 chemical reactions - in the past, chemical mechanisms with over 300 species have been tested. Tools exist within CMAQ to facilitate the addition of new or modified mechanisms. In the past the main difficulties involved have been processing time, preparation of emissions and establishing the rates required for the mechanism. The CRIv5 is now of a size that could reasonably be tested in CMAQ and most of the problems above have been resolved as part of its development.

The release version of CMAQ limits the number of species that can be used, but the US EPA have development versions which can handle more species. Given sufficient interest in incorporating a CRI mechanism into CMAQ, Deborah Luecken at the US EPA has expressed a willingness to help.

b) Emissions data

The EMEP European emissions data can be processed ready for CMAQ but there are some issues with the data source which we believe required further checking.

The NAEI UK emissions data can be processed but there is some concern about the temporal profile used for point source emissions which require further checking.

CMAQ is operational, but we believe updating to v4.7 will allow more accurate processing of stack emissions. CMAQ v4.7 will also improve PM processing.

c) Meteorology

WRF is operational, but there are some concerns about the options selected and issues relating to turbulence and boundary layer parameterisation require checking.

8.2.8 Planned future work

A promising start has been made on evaluating the potential of CMAQ in modelling ozone in the UK. So far, simulations for only one month have been carried out. Clearly, for policy applications, the ability to model ozone over the whole of the UK over a whole calendar year needs to be demonstrated and comparisons made with the OSRM. Meteorology data for the whole of 2006 has been purchased from ECMWF and is now being processed in WRF to enable a full year CMAQ simulation.

It will be necessary to investigate the issues highlighted above relating to WRF, CMAQ and the emissions data and the WRF and CMAQ grids need to be optimised to ensure they provide the analysis required at the optimal computational efficiency.

Once and annual CMAQ simulation has been run, the results will be evaluated with respect to monitoring data and results from the OSRM for 2006. The protocol for carrying out a model comparison needs to be considered in order to give a fair and meaningful performance assessment. Defra is planning to extend the scope over the remaining 6 months of the project to enable such a protocol to be developed. The objectives of the model intercomprison protocol are more far-reaching covering a wider range of pollutants and air pollution issues than just tropospheric ozone, but the work to be carried out on CMAQ comparisons with the OSRM will be a good first demonstration of the protocol.

It is also planned to install and run the test case for the CHIMERE model and evaluate the meteorology and emissions requirements. If existing WRF files can be used then a 2006 simulation will be run for this model under the same conditions to compare with results from CMAQ and the OSRM.

9 Cost, Benefits and Trade-Offs: Volatile Organic Solvents (Objective 7)

Use of solvents is one of the main sources of VOC emissions in the UK, as discussed in Section 5.2. The role of VOCs in forming ground-level ozone is well understood, but policy analysis of VOC control is complicated by the wide range of other impacts that they have, including:

- Direct chemical effects on human health (including cancers), potentially affecting both workers and the general public depending on exposure routes
- Other occupational risks from use of VOCs (e.g. fire hazard)
- Direct chemical effects on ecosystems
- Global warming effects
- Stratospheric ozone layer depletion
- Formation of secondary organic aerosols with associated health impacts
- Life cycle burdens generated by VOC production, use and disposal (e.g. energy use and release of pollutants to air, land and water)

The failure to assess all of the impacts of chemicals in the past has from time to time caused some inconsistency in policy over time. This generates potential inefficiency for industry and additional burdens on society and the environment.

Recognising these problems, research was undertaken with a two-fold objective:

1. To develop a methodology for assessing the costs and benefits of solvent reduction and substitution policies. The methodology would enable full life cycle analysis of alternative approaches to inform and underpin future policy development to meet domestic and international commitments, while also:

2. feeding into the review of the Master Chemical Mechanism (MCM) by illustrating the role of air pollution models based on detailed chemical mechanisms like the MCM in providing inputs to wider policy analysis tools.

In meeting these objectives methods are illustrated with a case study concerning the substitution of trichloroethylene by other VOC solvents (tetrachloroethylene, methylene chloride and limonene) for metal degreasing. This case study is not intended to directly inform policy on the use of solvents for metal degreasing, but simply to illustrate the methods used.

Section 9.1 describes the application of air pollution models using information from the MCM to quantify the effects of substituting trichloroethylene with limonene (a reactive terpene)as a solvent on concentrations of ground-level ozone, secondary organic aerosols (SOAs, contributing to PM) and ambient concentrations of trichloroethylene itself in the UK. Section 9.2 summarises the use of this information and methods used in Cost Benefit Analysis (CBA) of solvent replacement. More details of the CBA approaches are given in Appendix 2 to this report and in a separate report on this work currently being prepared.

9.1 Modelling the Air Quality Impacts of Substituting Trichloroethylene with Limonene as a Solvent

Based on the NAEI VOC speciation, trichloroethylene is responsible for around 9 ktonnes or 2% of total mass emissions of non-methane VOCs in the UK.

The general approach for modelling the impacts on ozone was to apply POCP-weighted across-the-board changes in mass emissions and use the OSRM to model the impacts on health-based and non-health-based ozone concentration metrics across the UK when this amount of trichloroethylene was removed and replaced by the same mass emissions of limonene.

The general approach for modelling the impacts on SOA and PM concentrations was similar, but this time applying SOAP-weighted across-the-board changes in precursor emissions of SOAs and using the Pollution Climate Mapping (PCM) method to map out the impacts on overall population-weighted PM_{10} concentrations.

These procedures take advantage of POCP and SOAP estimates for trichloroethylene and limonene based on UK-PTM trajectory model runs using the full set of explicit chemistry provided by the MCM and being developed in this project. Estimates of POCPs and SOAPs for these two VOCs are shown in Table 9.1 (see also Sections 5.2 and 7.5 in this report).

Table 9.1: Estimates of Photochemical Ozone Creation Potentials (POCPs) and Secondary Organic Aerosol Potentials (SOAPs) based on results from the UK-PTM using the MCM

	POCP	SOAP
Trichloroethylene	29	0
Limonene	70	15

Concentrations of tricholoroethylene in ambient air itself arising from solvent use were mapped using the PCM methods applied to mapping benzene concentrations.

9.1.1 Impacts on ground-gevel ozone concentrations

Because trichloroethylene has a POCP index less than the weighted-average for all anthropogenic VOC sources, the 1.97% of the total mass emissions of VOCs that it accounts for is equivalent to 1.87% of the POCP-weighted emissions. The OSRM was therefore run with a 1.87% across-the-board reduction in mass emissions of VOCs to model the impact of eliminating trichloroethylene emissions from solvent use. The change in ozone concentrations was modelled for 2006 for 4 health-based and 3 non-health-based metrics.

Limonene has a higher POCP than trichloroethylene, so using it as a substitute and leading to the same total mass emissions of limonene will lead to an overall increase in ozone concentrations. This could be modelled by the OSRM using an equivalent 2.64% across-the-board increase in VOC mass emissions.

UK-scale model runs of ozone were made with the OSRM for 2006 and the results are shown in Figure 9.1 as the UK population-weighted means of 4 health-based metrics. The area-weighted means of 3 non-health-based metrics were also calculated. The chart shows that the elimination of trichloroethylene emissions alone leads to an overall decrease in ozone, but the substitution with limonene (a more effect VOC in producing ozone) leads to a net increase in ozone relative to the base case.

Model runs using the UK-PTM also showed that the phasing out trichloroethylene would reduce peak ozone formation by 0.57 ppb.

Figure 9.1: Effect of trichloroethylene emission reduction on UK health-based ozone metrics relative to base in 2006 calculated using the OSRM.
A - Population-Weighted Annual Mean of Daily Maximum Running 8 Hourly Ozone Concentration (µgm-3)
B - Population-Weighted Annual Mean of the Difference (µgm-3) between the Daily Maximum Running 8 Hour Ozone Concentration and 70 µgm-3
C - Population-Weighted Number of Days when the Daily Maximum Running 8 Hourly Ozone Concentration exceeds 100 µgm-3

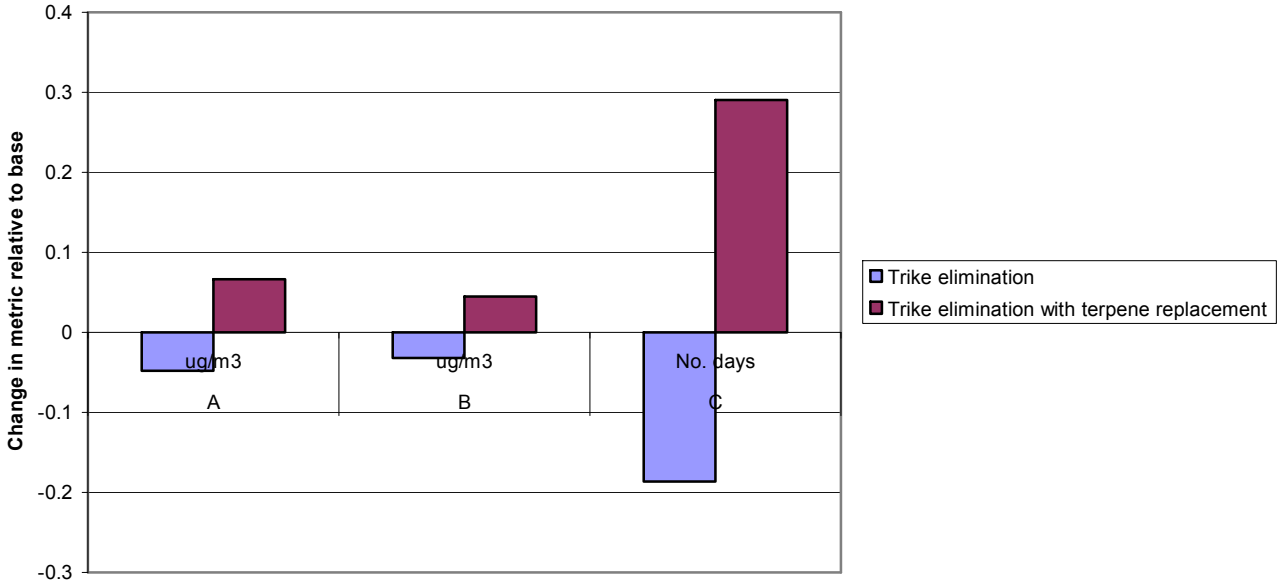

9.1.2 Impacts on PM_{10} concentrations

Table 9.1 indicates that eliminating trichloroethylene emissions will have no overall impact on SOA and hence concentrations of PM_{10}, but substituting with the same emissions of limonene will lead to an overall increase in SOAs an hence PM_{10}.

To estimate how much PM_{10} concentrations would increase, the empirical modelling method of the PCM was used taking into account the contributions of SOAs to overall PM_{10} concentrations in the UK. From the developments of SOA chemistry in the MCM and using the UK-PTM trajectory model combined with the NAEI indicates that the average SOAP value for all anthropogenic sources in the UK is 19.2. From this, the replacement of trichloroethylene emission by limonene with a SOAP value of 15 leads to an equivalent 1.54% across-the-board increase in SOAP-weighted VOC emissions from anthropogenic sources. However, anthropogenic emissions make only a small contribution to concentrations of SOAs in the UK, mainly from aromatic sources which are declining. Based on previous modelling estimates, anthropogenic emissions were responsible for 2.2% of SOAs in UK in 2006, the remainder being from biogenic sources such as α-pinene. Taking this into account, then replacement of trichloroethylene with limonene would lead to a 0.03% overall increase in SOAs in the UK. Using the PCM mapping method and the contribution made by SOAs to total PM_{10}, it is estimated that this change in SOA would lead to an overall increase in the population-weighted annual man PM_{10} concentration of 0.0003 μgm^{-3} in 2006.

9.1.3 Impacts on ambient trichloroethylene concentrations

As trichloroethylene is itself a toxic VOC, then the cost-benefit analysis of any solvent substitution policy should take into account the effect of population exposure to ambient concentrations of the chemical as a result of its release from solvent applications and degreasing.

The NAEI uses a distribution grid based on employment data to map out surface cleaning emissions. This grid was used to map out the trichloroethylene emissions and the same dispersion modelling

techniques used by the PCM to map out concentrations of benzene were used to map out concentrations of trichloroethylene and derive a population-weighted annual mean concentration of trichloroethylene of 0.385 μgm^{-3} in 2006. It is assumed that elimination of trichloroethylene as a solvent would reduce the concentrations to zero.

9.2 Methodology for Assessing the Costs and Benefits of Solvent Reduction and Substitution Policies

9.2.1 Introduction

A methodology for assessing the costs and benefits of solvent reduction and substitution takes analysis from the point of recommending which VOCs should be considered for further control through identification of alternatives and assessment of costs and health, social and environmental impacts. It brings together a number of techniques into a unified methodological framework. These include:

- Stakeholder consultation
- Cost-effectiveness analysis (CEA)
- Life cycle analysis (LCA)
- Risk assessment
- Impact pathway analysis (IPA)
- Cost-benefit analysis (CBA)
- Multi-criteria decision analysis (MCA/MCDA)
- Uncertainty assessment

The methodology developed is briefly discussed here, with a more detailed technical summary given in Appendix 2 while a separate full report on this study is currently being prepared.

Results from the air quality modelling studies described in Section 9.1 would be among the information used in the impacts assessments. In combining the above methods the study describes a general methodological framework. It is not recommended that this be used in full in every case – methods should naturally be kept as simple as possible. The way that the framework is applied will therefore vary from case to case, sometimes used in full, sometimes in part. An understanding of the merits and weaknesses of the different tools that are available will help identify what is appropriate in any case.

In adopting a complex methodological framework it is essential that a number of key questions are borne in mind throughout the analysis:

1. What are the main reasons for concern about use of a specific VOC? This provides a focus for the work which is essential when dealing simultaneously with a number of different impacts.

2. Are there alternatives to using the VOC in question that offer a net benefit when all social, economic and environmental factors are brought together?

3. If there are no alternatives and the VOC in question has impacts of some concern, is the service or product provided by the VOC necessary? [To illustrate, the use of a propellant with a high global warming potential (GWP) in medical inhalers may be considered essential, whilst use of the same propellant in novelty goods (such as ‘silly string’) may be considered non-essential.]

4. Do any options likely to be recommended have impacts of concern? Whilst an option may perform better overall than its competitors, it is possible that it could perform sufficiently badly on a single criterion to call its use into serious question. This sort of information may be made difficult to identify through seeking to aggregate across a large number of impacts.

There were several aspects to the study discussed briefly in the following sections relating to the case study based on trichloroethylene replacement.

9.2.2 Case study on trichloroethylene used for metal degreasing

In a typical case, it would first be necessary to identify which VOC or VOCs should be prioritised for control. From the background of transboundary air pollution VOCs may be prioritised according to their individual contribution to tropospheric ozone formation or their sector's contribution – results for both are available from past MCM model outputs. Under the EU's REACH Regulation for chemicals, a number of chemicals will be prioritised according to their direct health or environmental impacts. Elsewhere, VOCs may be prioritised according to their contribution to climate change or ozone depletion, and so on.

The use of trichloroethylene for metal degreasing was adopted as the case study for this work. It was selected simply for the availability of data both on trichloroethylene and possible substitute solvents (tetrachloroethylene, methylene chloride and limonene) and is not intended to directly inform future policy development on this VOC. It was instead simply selected to provide an illustration of the methods outlined in the main report. A more complete assessment of trichloroethylene would have assessed its use generally, rather than in metal degreasing alone.

Consideration of the alternatives to using a specific VOC can be a complex task. For the case study we considered only one use of trichloroethylene (metal degreasing) and a limited set of options (replacement with other VOC solvents). However, for many policy assessments it may be necessary to consider all uses of the targeted VOC. This can lead to a considerable number of alternatives being identified. Full assessment of all possible options can be a truly daunting task. Prioritisation of alternatives may therefore be necessary.

A preliminary screening of alternatives is recommended in order to understand which are most likely to yield health and environmental benefits, and which could lead to increased damage.

The screening assessment here considered the following criteria:

- Human carcinogenicity
- Non-carcinogenic human health effects
- EALs (environmental assessment levels, recommended by the UK Environment Agency for health protection)
- POCP (photochemical oxidant creation potential – relevant to tropospheric ozone formation)
- ODP (ozone depletion potential – relevant to stratospheric ozone)
- SOAP (secondary organic aerosol potential)
- GWP (global warming potential)
- Wider risks to the environment
- Specific risks of production
- Specific risks of disposal

In some cases the screening process drew on quantitative information (e.g. POCPs used in ozone modelling described above) for all of the chemicals considered. In others the assessment was more qualitative.

Several effects on industry need to be considered in assessing the economic costs of solvent substitution:

- Capital, operating and maintenance costs of the alternatives for solvent producers and users
- Differences in performance (for the case study, the effectiveness of trichloroethylene in metal degreasing *vs*. the effectiveness of the alternative solvents, which could lead to higher processing times, higher reject rates, etc.)
- Other costs (e.g. fire protection, controlling occupational exposure, etc.).

There are also costs through the need for additional regulation (e.g. ensuring that chemicals are not used for specific purposes) and to consumers (e.g. through changes in the price of goods).

Operations like metal degreasing can be very variable in terms of the size of operation, the type of products being treated, the quality of output required, etc. Further complexity was highlighted in the case study through there being a large number of alternatives to the use of trichloroethylene. For the

purposes of this work only the use of alternative volatile organic solvents was considered, but several other options require no use of VOC. It is clear that a major consultation effort would be required to develop a good understanding of the consequences of additional regulation on this or similarly variable sectors.

The health and environmental impact assessment part of the analysis applies a number of tools – life cycle analysis, risk analysis and impact pathway analysis to first characterise the burdens of the options under consideration and then to quantify their likely impacts. The impacts on tropospheric ozone illustrated in Section 9.1 derived from the OSRM modelling using POCPs were quantified and monetised using functions previously used in development of the UK's Air Quality Strategy. The ozone assessment was extended to include damage to crops and rubber. The impacts of trichloroethylene substitution on SOAs and PM_{10} also proceeded through to quantification of impacts and monetised equivalents using functions adopted in development of the UK's Air Quality Strategy.

Overall results were dominated by effects through ozone formation (for which tetrachloroethylene and methylene chloride performed better than trichloroethylene, but limonene performed significantly worse) and global warming (for which tetrachloroethylene and methylene chloride performed worse than trichloroethylene, but limonene performed better). These results highlight the need to undertake a holistic assessment in order to understand how the different types of effect balance against one another. Policy driven solely by concerns about ozone formation would bias against limonene, whilst policy driven solely by concerns over climate change would bias against tetrachloroethylene and methylene chloride.

A first step sums costs and benefits for each option relative to those for continued use of trichloroethylene to identify which option or options yield the greatest net benefit. For our case study the greater cost of tetrachloroethylene made it the least desirable option when all quantified elements of the analysis were combined. The preferred options were methylene chloride and limonene.

CBA and Multi Criteria Analysis (MCA) are useful tools for bringing complex analysis together into a more easily understood form. However, the most robust policy is likely to be developed not from consideration of CBA/MCA results on their own, but also through consideration of the underlying detail, for example, understanding where important trade-offs are present and what risks are revealed through the uncertainty analysis. A good illustration for this was provided in the case study with respect to limonene, one of the two best performing options overall, but the one that fared worst with respect to ozone formation.

In general, the study highlighted that:

1. With many criteria to consider there is a strong potential that no single option would perform best on all counts. This makes it necessary to apply techniques such as CBA or MCA in order to develop a clear rationale for preferring one or some over others.

2. When aggregating across a number of impacts it is possible that some key policy messages could be lost. For example, where significant negative effects of an option are mitigated by a number of smaller positive effects. It is important that results are provided in sufficient detail that the presence of such trade-offs is clear.

3. There is no certainty that the results of CBA and MCA would be in agreement as to which options were preferable. Where they are not, the reasons for disagreement should be considered and further analysis carried out if necessary.

The variety of impacts relevant to this work means that it has implications beyond transboundary air pollution (the direct remit for this work), in particular for wider assessment of chemicals, including under the EU's REACH Regulation. This observation led to considerably more dissemination and consultation being performed during the development of the work than was originally foreseen, for example with the Advisory Committee on Hazardous Substances convened by Defra and members of the Socio-Economic Assessment Committee under REACH, but the feedback and interest received has been extremely useful for the study.

The report on the study will need to be seen against the context in which it has been developed – a short term research project that sought to assess ways in which existing analytical approaches for

informing policy development on controlling the formation of tropospheric ozone could be extended to increase benefits and reduce the risk of significant contradiction in policy.

The report recommends that a database be compiled of the properties, etc. of VOCs, including information on POCPs, GWPs, risk factors and so on. This would be extremely valuable in the screening stage discussed above. It would also improve the consistency of future assessments. Some of the necessary expertise is available among those developing the MCM, though experts in other disciplines, perhaps most notably health risk assessment would also be needed.

The MCM team has provided essential input to this work in a number of ways, most obviously in relation to the quantification of ozone and secondary organic aerosol formation as a result of VOC emissions. Less obvious has been essential guidance provided by the MCM team drawing on the knowledge that they have accumulated in relation to the wider properties of VOCs (e.g. with respect to GWPs) and to knowledge of the emitting sectors.

10 Other Project Activities

Other project activities have been carried out during 2008, the second year of the project, involving the project consortium members.

10.1 Air Quality Expert Group Report on Ozone

Professor Pilling (Chair), Professor Derwent, Dr Jenkin and Dr Murrells (*ex-officio*) are member of Defra's Air Quality Expert Group (AQEG). AQEG has prepared a a report on "*Ozone in the UK*", the initial draft of which was released for consultation during 2008. These members of the project consortium have contributed in various ways to the report building on research carried out in this project and attended several AQEG meeting during 2008. The project was used to support Jenny Young (University of Leeds) in providing the secretariat for completing the consultation draft of the report. Following review of comments made by the consulation and amendments to the report, the final report is about to be published by Defra.

10.2 Review of Transboundary Air Pollution (RoTAP)

Members of the project team have made contributions or assisted other members on text for the Defra Review of Transboundary Air Pollution (RoTAP). This review is including a chapter on ozone modelling. In particular, the OSRM has been used to provide surface ozone flux metrics on a 10x10km grid covering the UK for wheat, potatoes and beech in 2003 and 2020.

10.3 Project Meetings and Reports

The project team met at Defra in January 2008 to discuss the work plan for Objective 7 (*Cost, Benefits and Trade-Offs: Volatile Organic Solvents*). Additional meetings of the project partners have been held during 2008 at Harwell and the University of Leeds.

Andrea Fraser attended a conference on developments of CMAQ at the USEPA, Chapel Hill, North Carolina, USA in October 2008.

Sally Cooke and John Abbott from AEA attended the MESO-NET CREMO Workshop held in June in London. The workshop was organised by the Environment Agency and NERC and the purpose was to explore how potential users can benefit from comprehensive model calculations and to identify realistic case studies to demonstrate the feasibility of CMAQ, which could be integrated into the CREMO/MESO-NET programme. Potential applications of CMAQ were discussed. There was also a presentation on EMEP4UK model by CEH Edinburgh.

Mike Holland (EMRC) gave a presentation "***Modelling solvent dispersion, chemistry and health impacts to inform policy development on VOC control***", (M Holland, T Murrells, D Derwent and M Jenkin) at the Eleventh Annual UK Review Meeting on Outdoor and Indoor Air Pollution Research, 15-16 April at Cranfield University

Three quarterly progress reports were prepared for Defra providing a summary of the progress made on each of the various project objectives and project management related issues.

10.4 Technical Reports and Publications

The following technical reports have been prepared by the project consortium in 2008:

Performance of the Ozone Source Receptor Model Against Recommendations of the DEFRA Review on Tools for Modelling Tropospheric Ozone. T P Murrells, S. Cooke and R.G. Derwent. Report for the Department for Environment, Food and Rural Affairs and the Devolved Administrations. AEA Report AEAT/ENV/R/2653, July 2008

The following papers have been produced by the project consortium in 2008 for publication in the scientific literature:

"Up in the air" Derwent, D., Jenkin, M., Passant, N., Pilling, M. (2008). Chemistry and Industry, 26 May 2008

"Particulate matter at a rural location in southern England during 2006: Model sensitivities to precursor emissions". Derwent, R., Witham, C., Redington, A., Jenkin, M., Stedman, J., Yardley, R., Hayman, G. (2008). Atmospheric Environment doi:10.1016/j.atmosenv.2008.09.077.

"Trends in ozone concentration distributions in the UK since 1990: Local, regional and global influences" Jenkin, M.E. (2008) Atmospheric Environment 42 (2008) 5434–5445

"Modelling the impact of elevated primary NO_2 and HONO emissions on regional scale oxidant formation in the UK", Jenkin, M.E., S.R. Utembe, R.G. Derwent Atmospheric Environment 42 (2008) 323–336

"A Common Representative Intermediates (CRI) mechanism for VOC degradation. Part 1: Gas phase mechanism development" Jenkin M.E., Watson L.A., Utembe S.R. and Shallcross D.E. (2008).. Atmospheric Environment, 42, 7185-7195.

"A Common Representative Intermediates (CRI) mechanism for VOC degradation. Part 2: Gas phase mechanism reduction." Watson L.A., Shallcross D.E., Utembe S.R. and Jenkin M.E. (2008). Atmospheric Environment, 42, 7196-7204.

11 Conclusions and Policy Relevance

The work carried out on the project during 2008 can be broadly characterised as **application** of existing models for policy purposes and further **research and development** of the models and the underpinning science. The main conclusions from the work and the policy relevance are as follows:

11.1 Application of Tropospheric Ozone Models for Policy Support

UK Ozone Climate in 2007

The UK ground-level ozone climate for 2007 has been characterised by the Pollution Climate Mapping (PCM) empirical modelling approach and the Ozone Source Receptor Model (OSRM). Both models indicated 2007 was a relatively low ozone year.

Results from the PCM, that are based on 2007 ozone monitoring data, are summarised for the EU Target Value for ozone concentration metrics for human health and vegetation in 2010 (an average over the past 3 years) and the Long-term Objectives for ozone in Tables 11.1 and 11.2, respectively.

Table 11.1: UK summary results of air quality assessment relative to the Target Values for ozone for 2010

Target Value	*Number of zones exceeding*
Max Daily 8-hour mean Target Value	none
AOT40 Target Value	none

Table 11.2: UK summary results of air quality assessment relative to the Long-term Objectives for ozone

Long-term Objective	*Number of zones exceeding*
Max Daily 8-hour mean Long-term Objective	41 zones (24 measured + 17 modelled)
AOT40 Long-term Objective	3 zones (1 measured + 2 modelled)

The areas with the most number of days exceeding the objective concentration threshold for human health tended to be in the east of England.

The OSRM is a process model calculating the formation of ozone in the UK based on a chemical transport modelling approach using emissions inventory and real meteorological data for 2007. The OSRM shows broadly similar patterns to the empirical maps with higher concentrations in the east of the UK, however there are some specific spatial differences. The majority of the higher ozone concentration areas identified by OSRM in 2007 are in coastal fringe areas. The OSRM in 2007 has generally overestimated Third Daughter Directive ozone metrics compared with measured data, continuing the trend found previously that indicates the OSRM overestimates these ozone metrics in low ozone years (2004, 2005 and 2007) and underestimates them in high ozone years (2003 and 2006) compared with measured data. The PCM empirical model continues to produce results that are closer to the measured concentrations than the OSRM and should continue to be used in its current capacity (contributing modelled data in fulfilment of UK reporting obligations to the European Commission.

Further Modelling and Assessments Relating to Ozone Policy

The UK PTM has been used to study trends in both episodic peak and annual mean of the daily maximum ozone metrics from 1990-2010. The aim has been to determine the contribution to the observed trends in the ozone metrics from:

- NO_x and VOC precursor emission reductions

- intercontinental trans-Atlantic ozone transport
- non-linearities in ozone formation
- the ambition level achieved in international policy negotiations

The conclusion was that the balance between the contributions appear to be significantly different for the episodic peak and annual mean ozone metrics, but all four influences appear to be important to one or other of the ozone metrics.

The UK PTM model has been used to evaluate the contribution to ozone formation from solvents using the detailed emission speciation data from the NAEI and the explicit chemical mechanism described in the MCM. The contributions from usage of solvents and other products such as aerosol sprays are only slightly lower than that of VOC emissions from road transport. The contribution to episodic ozone from all 53 emission sub-sectors that make up the solvent and other product usage sector were examined. There is no one sector that dominates overall. The picture is one of detail and complexity, with many different solvent activities and applications and no dominant activity or process upon which to focus policy

The work on evaluating the potential impacts of solvent control policies has been extended by the development of a methodology for assessing the wider costs and benefits of solvent reduction and substitution policies covering a range of economic, health, social and environmental impacts. The methodology would enable full life cycle analysis of alternative approaches to inform and underpin future policy development to meet domestic and international commitments. It has also illustrated the role of air pollution models based on detailed chemical mechanisms like the Master Chemical Mechanism (MCM) in providing inputs to wider policy analysis tools. This has been illustrated by a case study based on the substitution of trichloroethylene by other VOC solvents including a natural product, limonene, for metal degreasing. The OSRM, UK-PTM and PCM modelling approaches using reactivity information on these species based on the MCM were used to provide quantitative data on the impacts of replacing trichloroethylene with limonene on ground-level ozone, secondary organic aerosols (SOAs, contributing to PM) and ambient concentrations of trichloroethylene in the UK.

Further work was undertaken with the UK-PTM to develop a PM Closure Model. The PTM was used to estimate mass concentrations of $PM_{2.5}$ components at the Harwell site in each day in 2006 and to test the linearity of mechanisms forming secondary PM to reductions in precursor emissions. Emission sensitivity coefficients were developed for the different PM components for 30% across-the-board reductions in precursor emissions of SO_2, NO_x, NH_3, VOCs and CO. These revealed that the chemical environment is ammonia-limited such that policy strategies for secondary PM precursors should focus on the abatement of NH_3.

11.2 Research and Development of Models for Ozone and Secondary Organic Aerosols

Model Development and Validation

As a scenario model for predicting UK ozone concentrations in response to changes in emissions, the OSRM has continued to be maintained and utilised. An initial assessment of specific recommendations of the independent review of existing ozone modelling tools commissioned by Defra in 2007 was carried out on the OSRM in terms of its performance and how far the OSRM goes in meeting these recommendations.

The assessment covered:

- The use of emission estimates in the OSRM;
- The evaluation of the performance of the OSRM and the PTM by comparison with ambient measurements of ozone concentrations;
- Quality control and outputs and how the OSRM follows the modelling guidelines of the Royal Meteorological Society

In the area of emissions information, it was concluded that the OSRM does treat emissions from UK and other European sources using the best available emissions inventory information, but there is room for improvement.

On model evaluation and comparison with monitoring data, further assessments were made for this study comparing the performance of the OSRM against 2005 and 2006 monitoring data at two rural and one urban AURN site and comparisons also made with the performance of the UK PTM. These showed reasonable model performance, but much more rigorous assessment is required against other models and this needs to be backed up by strong external peer-review.

On the modelling guidelines of the Royal Meteorological Society, these refer explicitly to atmospheric dispersion modelling and are not always directly appropriate for the applications of the OSRM to Defra policy support. Nevertheless, the general principles they invoke are applicable to the OSRM. All ten aspects of the modelling guidelines were considered and on balance the view was that the OSRM is fit-for-purpose and a better than satisfactory tool, but it is difficult to defend this position based on the current absence of peer-reviewed publications and widely accessible and transparent documentation and there are a number of areas where the OSRM falls short.

The Defra Review on ozone modelling made a strong case for Eulerian models. Progress has been made in this project on trialling certain Eulerian models for Defra's ozone policy. The USEPA's Eulerian model CMAQ has been set up to run with ECMWF meteorology data processed in WRF and a month's simulation of UK-scale ozone concentrations has been completed for June 2006. Initial results comparing ozone concentrations with AURN monitoring data look promising, but further work is required to optimise the meteorology and emissions inventory data before a year's simulation is carried out. Work will then be extended to the Chimere model. A protocol for carrying out a model comparison is required in order to give a fair and meaningful performance assessment. Defra is planning to extend the scope over the remaining 6 months of the project to enable such a protocol to be developed. The objectives of the model intercomprison protocol are more far-reaching covering a wider range of pollutants and air pollution issues than just tropospheric ozone, but the work to be carried out on CMAQ comparisons with the OSRM will be a good first demonstration of the protocol.

Chemical Mechanisms in Models for Ozone and Secondary Organic Aerosols

Following the comprehensive review of the MCM in 2007, a work programme was agreed with the Department in 2008 aimed at improving and maintaining the status of the MCM and related mechanisms and assessing and guiding the improvement of the representation of organic chemistry in atmospheric models used in policy applications. The four main tasks to be carried out are:

- Development of a hierarchy of traceable reduced mechanisms from the MCM
- Development of new MCM schemes
- A major revision of the MCM protocol
- Development and application of a secondary organic aerosol (SOA) code

Considerable progress has been made in all these areas.

A reduced chemical mechanism describing the formation of ozone traceable to the MCM (Common Representative Intermediates mechanism, CRI v2) previously developed has been thoroughly tested and shown to perform well in comparison with the MCM over a range of conditions. The CRIv2 has been further reduced by progressive and systematic redistribution of emission species and lumping into groups. The most reduced version (CRIv2-R5) now comprises just 22 VOCs, 196 species and 555 reactions and still shows very good performance in comparison with the MCM.

Work is in progress on expanding the MCM with the development of new chemical degradation schemes for new biogenic VOCs covering a wider reactivity range. Four representative monoterpenes have been identified, mechanisms for two of which have already been developed (α– and β–pinene), and the construction of a detailed, MCM-compatible, gas phase mechanism for one of these, limonene, has been completed.

Work has commenced revising the protocol defining a set of rules for the development of the gas-phase degradation mechanisms in the MCM. The protocol ensures different people write consistent and compatible chemistry schemes and as new research information emerges this protocol needs to be periodically updated.

Codes for secondary organic aerosols (SOA) in the MCM have been developed and applied. A code for SOA has been developed, optimized and validated in the UK-PTM against measurements of organic aerosols from the TORCH campaign and shows good performance. A reduced SOA code for the CRIv2 and CRIv2-R5 has also been developed and tested. This represents a major advance in the treatment of secondary organic aerosol formation and hence modeling of PM in chemical transport models. As an application of this, the concept of the secondary organic aerosol potential, SOAP, has been developed to reflect the propensity of each organic compound to form SOA on an equal mass emitted basis relative to toluene. SOAPs for 18 different aromatic compounds plus α– and β–pinene were calculated by running the UK PTM model with the MCM for a range of conditions thus opening the door for efficient policy applications similar to the concept for POCPs.

NO_x-NO_2-O_3 Relationships

A number of analyses of monitoring data has been undertaken to provide more information on local, regional and global contributions to oxidant at UK locations, and to improve the description of the partitioning of oxidant into its component species (i.e., O_3 and NO_2). The focus of the research this year has been on the analysis and interpretation of monitoring data to gain further insight into the geographical dependence of the hemispheric baseline contributions and regional modifications to the background oxidant concentrations in the UK. This has enabled the development of expressions describing the spatial variation in the hemispheric and regional oxidant components and year-specific parameters for use in empirical modelling of annual mean background oxidant concentrations in the UK. The outputs of these analyses are being used to improve and update the representation of the oxidant partitioning method in the Pollution Climate Model (PCM), in relation to assessments of annual mean NO_2 and O_3 levels. Further analysis of oxidant at roadside monitoring sites using the Netcen Primary NO_2 Model, extended to 2007, has yielded further information on regional variations in trends in primary NO_2 emissions to compare directly with trends predicted by the national emissions inventory.

An analysis of hourly-mean O_3 and NO_X data from a series of historical photochemical episodes in the UK has commenced, with the aim of evaluating urban-scale oxidant production in the London conurbation. The analysis will examine whether there is evidence for an apparent increase in the background oxidant level, $[OX]_B$, during east-to-west passage over the London conurbation.

12 Acknowledgements

The consortium partners acknowledge the support provided by the Department for Environment, Food and Rural Affairs (Defra) and the Devolved Administrations (the Welsh Assembly Government, the Scottish Executive and the Department of the Environment for Northern Ireland) under contract AQ0704. We especially acknowledge the help and support of Dr Paola Cassanelli and Dr Soheila Amin-Hanjani of Air Quality and Industrial Pollution (AQIP) Division of Defra in facilitating the direction of the project in 2008.

We are grateful for the help of John Abbott and Trevor Davies at AEA for assistance with the operation of the OSRM and CMAQ, Ioannis Tsagatakis for help with emissions data and John Stedman for directing the work using the PCM.

Lynette Clapp (Imperial College London) is gratefully acknowledged for provision of the $[OX]_H$ and $[OX]_R$ data used in the analyses described in Section 6.1

The work described in Section 7.1 and Section 7.4.4 was carried out in collaboration with Steven Utembe, Laura Watson and Dudley Shallcross (University of Bristol). The work described in Section 7.2 has received additional support from the NERC thematic project APPRIASE, as part of the ACES consortium.

13 References

Abbott, J (2005). "*Primary Nitrogen Dioxide Emissions from Road Traffic: Analysis of Monitoring Data*". Report for The Department for Environment, Food and Rural Affairs, Welsh Assembly Government, the Scottish Executive and the Department of the Environment for Northern Ireland. AEA Report AEAT/ENV/R/1925 (March 2005)

Aitken A., Decarlo P.F., Kroll J.H., Worsnop D.R., Huffmann J.A., Docherty K.S., Ulbrich I.M., Mohr C., Kimmel J.R., Sueper D., Sun Y., Zhang Q., Trimborn A., Northway M., Ziemann P.J., Canagaranta M.R., Onasch T.B., Alfarra M.R., Prevot A.H., Dommen J., Duplissy J., Metzger A., Baltensperger U. and Jimenez J.L. (2008). *O/C and OM/OC ratios of primary, secondary, and ambient organic aerosols with high-resolution time-of-flight aerosol mass spectrometry*. Environmental Science and Technology, **42**, 4478–4485.

Alfarra M.R. (2004). *Insights into atmospheric organic aerosols using an aerosol mass spectrometer.* Ph.D. Thesis, University of Manchester.

Allan J.D., Alfarra M.R., Bower K.N., Williams P.I., Gallagher M.W., Jimenez J.L., McDonald, A.G., Nemitz E., Canagaratna M.R., Jayne J.T., Coe H. and Worsnop D.R. (2003). *Quantitative Sampling Using an Aerodyne Aerosol Mass Spectrometer – 2. Measurements of Fine Particulate Chemical Composition in Two U.K. Cities*. Journal of Geophysical Research, 108(D3), 4091, doi:10.1029/2002JD002359.

AQEG (2004). *Nitrogen dioxide in the United Kingdom*. Report of the UK Air Quality Expert Group, AQEG. Prepared for the Department for Environment Food and Rural Affairs, the Scottish Executive, the Welsh Assembly and the Department of the Environment in Northern Ireland. Defra publications, London.

AQEG (2005). *Particulate matter in the United Kingdom*. Report of the Air Quality Expert Group, Prepared for the Department for Environment Food and Rural Affairs, the Scottish Executive, the Welsh Assembly and the Department of the Environment in Northern Ireland. Defra publications, London

AQEG (2007). *Trends in primary nitrogen dioxide in the UK*. Report of the UK Air Quality Expert Group, AQEG. Prepared for the Department for Environment Food and Rural Affairs, the Scottish Executive, the Welsh Assembly and the Department of the Environment in Northern Ireland. Defra publications, London, 2007. ISBN 978-0-85521-179-0.

AQEG (2008). *Ozone in the UK*. Draft Report of the UK Air Quality Expert Group, AQEG. Prepared for the Department for Environment Food and Rural Affairs, the Scottish Executive, the Welsh Assembly and the Department of the Environment in Northern Ireland. Defra publications, October 2008.

Aumont B., Szopa1 S. and Madronich S. (2005). *Modelling the evolution of organic carbon during its gas-phase tropospheric oxidation: development of an explicit model based on a self generating approach*. Atmospheric Chemistry and Physics, **5**, 2497–2517.

Baker J., Arey J. and Atkinson R. (2005). *Formation and reaction of hydroxycarbonyls from the reaction of OH radicals with 1,3-butadiene and isoprene*. Environmental Science and Technology, **39**, 4091-4099.

Baum E.J. (1998). *Chemical property estimation: theory and application*, CRC Press, Florida, ISBN 0-87371-938-7.

Boissard, C., Cao, X.-L., Juan, C.-Y., Hewitt, C.N. and Gallagher, M. (2001). *Seasonal variations in VOC emission rates from gorse*, Atmospheric Environment, 35, 917–927.

Bush, T and J Targa, (2005). *Ozone Mapping Techniques for the 3rd Daughter Directive; OSRM vs Empirical modelling Comparison Report*. A report to The Department for Environment, Food and Rural

Affairs, Welsh Assembly Government, The Scottish Executive and the Department of the Environment for Northern Ireland. AEA Technology plc, Netcen, Harwell. Report AEAT/ENV/R/2053

Camredon M., Aumont B., Lee-Taylor J. and Madronich S. (2007). *The SOA/VOC/NO_X system: an explicit model of secondary organic aerosol formation*. Atmospheric Chemistry and Physics, **7**, 5599–5610.

Capouet M., Mueller J.F., Ceulemans K., Compernolle S., Vereecken L. and Peeters J. (2008). *Modeling aerosol formation in alpha-pinene photo-oxidation experiments*. Journal of Geophysical Research-Atmospheres, **113** (D2), Article Number: D02308 .

Carter W.P.L. (1994). *Development of ozone reactivity scales for volatile organic compounds*. J.Air & Waste Manage.Assoc., 44, 881-899.

Clapp L.J. and Jenkin M.E. (2001). *Analysis of the relationship between ambient levels of O_3, NO_2 and NO as a function of NOx in the UK*. Atmospheric Environment, **35**, 6391-6405

Coe H., Allan J.D., Alfarra M.R., Bower K.N., Flynn M.J., McFiggans G.B., Topping D.O., Williams P.I., O'Dowd C.D., Dall'Osto M., Beddows D.C.S. and Harrison R.M. (2006). *Chemical and physical characteristics of aerosol particles at a remote coastal location, Mace Head, Ireland, during NAMBLEX*. Atmospheric Chemistry and Physics, **6**, 3289-3301.

Derwent R.G. and Jenkin M.E. (1991). *Hydrocarbons and the long-range transport of ozone and PAN across Europe.* Atmospheric Environment, **25A**, 1661-1678.

Derwent, R.G., Jenkin, M.E., Saunders, S.M., Pilling, M.J., (1998). *Photochemical ozone creation potentials for organic compounds in northwest Europe calculated with a Master Chemical Mechanism*. Atmospheric Environment 32, 2429–2441.

Derwent R.G., Jenkin M.E., Saunders S.M., Pilling M.J. and Passant N.R. (2004). *Multi-day Ozone Formation of Alkenes and Carbonyls investigated with a Master Chemical Mechanism under European conditions*. Atmospheric Environment, 39, 627-635

Derwent, R.G., Simmonds, P.G., Manning, A.J. Spain, T.G., (2007a). *Trends over a 20-year period from 1987 to 2007 in surface ozone at the atmospheric research station, Mace Head, Ireland*. Atmospheric Environment, **39**, 9091-9098.

Derwent RG, ME Jenkin, TP Murrells, MJ Pilling and AR Rickard (2007b). *A Review of the Master Chemical Mechanism*. Report to Defra under contract 'Modelling of Tropospheric Ozone' (CSA 7267/AQ03508). July 2007

Derwent R.G., Jenkin M.E., Passant N.R. and Pilling M.J. (2007c). *Reactivity-based strategies for photochemical ozone control in Europe*. Environmental Science and Policy, **10** (5), 445-453.

Derwent, D., Jenkin, M., Passant, N., Pilling, M (2008a). "*Up in the air*". Chemistry and Industry, 26 May 2008

Derwent, R., Witham, C., Redington, A., Jenkin, M., Stedman, J., Yardley, R., Hayman, G. (2008b). *Particulate matter at a rural location in southern England during 2006: Model sensitivities to precursor emissions*. Atmospheric Environment doi:10.1016/j.atmosenv.2008.09.077.

Dore, C. J., Goodwin, J.W.L., Watterson, J. D., Murrells, T. P, Passant, N. R, Hobson, M. M, Haigh, K. E., Baggott, G., Thistlethwaite, G., Pye, S. T., Coleman, P. J., King, K. R. (2003a). *UK Emissions of Air Pollutants 1970-2001*. National Atmospheric Emissions Inventory Report, AEAT/ENV/R/1593, ISBN 1-85580-033-0.

Dore, C., Hayman, G., Scholefield, P., Hewitt, N., Winiwarter, W., and Kressler, F. (2003b). *Mapping of biogenic VOC emissions in England and Wales*, Environment Agency R&D Technical Report E1-122/TR, ISBN 1-84432-092-8.

Draxler R.R. and Rolph G.D. (2003). HYSPLIT (HYbrid Single-Particle Lagrangian Integrated Trajectory) Model access via NOAA ARL READY Website (http://www.arl.noaa.gov/ready/hysplit4.html). NOAA Air Resources Laboratory, Silver Spring, MD.

Duarte, R. M. (2006), *Mass balance and characterization of organic matter in atmospheric aerosols*, Ph.D. thesis, University of Aveiro, Aveiro, Portugal.

Fu T.M., Jacob D.J., Palmer P.I., Chance K., Wang Y.X.X., Barletta B., Blake D.R., Stanton J.C. and Pilling M.J. (2007). *Space-based formaldehyde measurements as constraints on volatile organic compound emissions in east and south Asia and implications for ozone*. Journal of Geophysical Research - Atmospheres, **112**(D6), article number D06312.

Gelencsér A., May B., Simpson D., Sánchez-Ochoa A., Kasper-Giebl A., Puxbaum H., Caseiro A., Pio C. and Legrand M. (2007). *Source apportionment of $PM_{2.5}$ organic aerosol over Europe: Primary/secondary, natural/anthropogenic, and fossil/biogenic origin*. Journal of Geophysical Research, **112**, D23S04, doi:10.1029/2006JD008094.

Grosjean, D. and Seinfeld, J.H. (1989). *Parameterisation of the formation potential of secondary organic aerosols*. Atmospheric Environment, **23** (8), 1733-1747.

Harrison R.M. and Yin J. (2008). *Sources and processes affecting carbonaceous aerosol in central England*. Atmospheric Environment, **42**, 1413–1423.

Hayman, G.D., Jenkin, M.E., Pilling, M.J. and Derwent, R.G. (2002) *Modelling of Tropospheric Ozone Formation*. A Final Project Report produced for the Department for Environment, Food and Rural Affairs and Devolved Administrations on Contract EPG 1/3/143.

Hayman, G. D., Abbott, J., Thomson, C., Bush, T., Kent, A., Derwent, R. G., Jenkin, M. E., Pilling, M. J., Rickard, A., and Whitehead, L. (2005) *Modelling of Tropospheric Ozone*. Second Annual Report produced for the Department for Environment, Food and Rural Affairs and the Devolved Administrations on Contract EPG 1/3/200.

Hayman, G.D., J. Abbott, C. Thomson, T. Bush, A. Kent, RG Derwent, ME Jenkin, MJ Pilling, A. Rickard and L. Whitehead, (2006a) "*Modelling of Tropospheric Ozone*". Final Report (AEAT/ENV/R/2100 Issue 1) produced for the Department for Environment, Food and Rural Affairs and the Devolved Administrations on Contract EPG 1/3/200.

Hayman, G.D., Y Xu, J. Abbott, T. Bush, (2006b) "*Modelling of Tropospheric Ozone"*. Report on the Contract Extension produced for the Department for Environment, Food and Rural Affairs and the Devolved Administrations on Contract EPG 1/3/200, AEA Report AEAT/ENV/R/2321 Issue 1, October 2006.

Jenkin M.E., Saunders S.M. and Pilling M.J. (1997). *The tropospheric degradation of volatile organic compounds: a protocol for mechanism development*. Atmospheric Environment, **31**, 81-104.

Jenkin M.E. and Hayman G.D. (1999). *Photochemical ozone creation potentials for oxygenated volatile organic compounds: sensitivity to variations in kinetic and mechanistic parameters*. Atmospheric Environment, 33, 1275-1293.

Jenkin M.E., Murrells T.P., Passant N.R. (2000a) *The Temporal Dependence of Ozone Precursor Emissions: Estimation and Application*. AEA Technology report AEAT/R/ENV/0355 Issue 1. Prepared for Department of the Environment, Transport and the Regions

Jenkin M.E., Shallcross D.E. and Harvey J.N. (2000b). *Development and application of a possible mechanism for the formation of cis-pinic acid from the ozonolysis of α-and β-pinene*. Atmospheric Environment, **34**, 2837-2850.

Jenkin M.E., Saunders S.M., Wagner V. and Pilling M.J (2003). *Protocol for the development of the Master Chemical Mechanism, MCM v3 (Part B): tropospheric degradation of aromatic volatile organic compounds*. Atmospheric Chemistry and Physics, **3**, 181-193.

Jenkin, M.E. (2004a). *Analysis of sources and partitioning of oxidant in the UK-Part 1: the NOx-dependence of annual mean concentrations of nitrogen dioxide and ozone*. Atmospheric Environment 38 5117–5129.

Jenkin M.E. (2004b). *Modelling the formation and composition of secondary organic aerosol from α- and β-pinene ozonlysis using MCM v3.* Atmospheric Chemistry and Physics, **4**, 1741–1757.

Jenkin, M.E. (2008). *"Trends in ozone concentration distributions in the UK since 1990: Local, regional and global influences***"** Atmospheric Environment 42 (2008) 5434–5445

Jenkin M.E., Watson L.A., Utembe S.R. and Shallcross D.E. (2008). *A Common Representative Intermediates (CRI) mechanism for VOC degradation. Part 1: Gas phase mechanism development*. Atmospheric Environment, **42**, 7185-7195.

Johnson D., Jenkin M.E., Wirtz K. and Martin-Reviejo M. (2004). *Simulating the formation of secondary organic aerosol from the photooxidation of toluene*. Environmental Chemistry, **1**, 150–165.

Johnson D., Jenkin M.E., Wirtz K. and Martin-Reviejo M. (2005). *Simulating the formation of secondary organic aerosol from the photooxidation of aromatic hydrocarbons*. Environmental Chemistry, **2**, 35-48.

Johnson D., Utembe S.R., Jenkin M.E., Derwent R.G., Hayman G.D, Alfarra M.R., Coe H. and McFiggans G. (2006). *Simulating regional scale secondary organic aerosol formation during the TORCH 2003 campaign in the southern UK*. Atmospheric Chemistry and Physics, **6**, 403-418.

Jönsson M. and Anderson P. (2007). *Emission of oilseed rape volatiles after pollen beetle infestation; behavioural and electrophysiological responses in the parasitoid Phradis morionellus.* Chemoecology, 17, 201-207.

Kanakidou, M., Seinfeld, J. H., Pandis, S. N., Barnes, I., Dentener, F. J., Facchini, M. C., Van Dingenen, R., Ervens, B., Nenes, A., Nielsen, C. J., Swietlicki, E., Putaud, J. P., Balkanski, Y., Fuzzi, S., Hjorth, J., Moortgat, G. K., Winterhalter, R., Myhre, C. E. L., Tsigaridis, K., Vignati, E., Stephanou, E. G. and Wilson, J. (2005). *Organic aerosol and global climate modelling: a review*, Atmospheric Chemistry and Physics, **5**, 1053–1123.

Kent, A. J. and Stedman, J. R. (2008a). *UK and Gibraltar air quality modelling for annual reporting 2007 on ambient air quality assessment under Council Directives 96/62/EC and 2002/3/EC relating to ozone in ambient air*. AEA Technology Energy & Environment. Report AEAT/ENV/R/2681, September 2008

Kent, A. J. and Stedman, J. R. (2008b) *UK air quality modelling for annual reporting 2006 on ambient air quality assessment under Council Directives 96/62/EC and 2002/3/EC relating to ozone in ambient air.* AEA Technology Energy & Environment. Report AEAT/ENV/R/2499

Kiss G., Varga B., Galambos I. and Ganszky I. (2002). *Characterization of water-soluble organic matter isolated from atmospheric fine aerosol*. Journal of Geophysical Research, 107 (D21), 8339, doi:10.1029/2001JD000603.

Krivácsy Z., Gelencsér A., Kiss G., Mészáros E., Molnár Á., Hoffer A., Mészáros T., Sárvári Z., Temesi D., Varga B., Baltensperger U., Nyeki S. and Weingartner E. (2001). *Study on the chemical character of water soluble organic compounds in fine atmospheric aerosol at the Jungfraujoch*. Journal of Atmospheric Chemistry, **39**, 235–259.

Kroll J.H. and Seinfeld J.H. (2008). *Chemistry of secondary organic aerosol: Formation and evolution of low-volatility organics in the atmosphere*. Atmospheric Environment, 42 (39), 3593-3624.

McFiggans G., Alfarra M.R., Allan J., Bower K., Coe H., Cubison M., Topping D., Williams P., Descari S., Facchini C. and Fuzzi S. (2005). *Simplification of the representation of the organic component of atmospheric particulates*. Faraday Discussions, **130**, 341–362.

Metcalfe, S.E, Whyatt, J.D, Derwent, R.G and O'Donoghue (2002) *The Regional Distribution of Ozone Across the British Isles and its Response to Control Strategies*. Atmospheric Environment, 36, 4045-4055.

Monks P., R.S. Blake and P Borrell. *Review of tools for modelling tropospheric ozone formation and assessing impacts on human health & ecosystems*. Report to Defra, November 2007

Murrells, T.P., Cooke, S., Kent, A., Grice, S., Derwent, R.G., Jenkin, M., Pilling, M.J., Rickard, A. and Redington, A (2008). "*Modelling of Tropospheric Ozone. First Annual Report"* produced for The Department for Environment, Food and Rural Affairs, Welsh Assembly Government, the Scottish Executive and the Department of the Environment for Northern Ireland under Contract AQ03508, AEA Report AEAT/ENV/R/2567, January 2008.

Ng N.L., Chhabra P.S., Chan A.W.H., Surratt J.D., Kroll J.H., Kwan A.J., McCabe D.C., Wennberg P.O., Sorooshian A. , Murphy S.M., Dalleska N.F., Flagan R.C. and Seinfeld J.H. (2007). *Effect of NO_X level on secondary organic aerosol (SOA) formation from the photooxidation of terpenes*. Atmospheric Chemistry and Physics, **7**, 5159–5174.

Olivier J.G.J., Bouwman A.F., Van der Maas C.W.M., Berdowski J.J.M., Veldt C., Bloos J.P.J., Visschedijk A.J.H., Zandveld P.Y.J. and Haverlag J.L. (1996). *Description of EDGAR Version 2.0: A set of global emission inventories of greenhouse gases and ozone-depleting substances for all anthropogenic and most natural sources on a per country basis and on $1^\circ \times 1^\circ$ grid*. National Institute of Public Health and the Environment (RIVM), Bilthoven. Report no. 771060 002/TNO-MEP report no. R96/119.

Otkin, J,A and Greenwald, T.J. (2008) *Comparison of WRF Model-Simulated and MODIS-Derived Cloud Data*. *Mon. Wea. Rev.,* 136**,** 1957–1970

Owen S.M., Boissard C. and Hewitt C.N. (2001). *Volatile organic compounds (VOCs) emitted from 40 Mediterranean plant species: VOC speciation and extrapolation to habitat scale*. Atmospheric Environment, **35**, 5393-5409.

Palmer P.I., Barkley M.P., Kurosu T.P., Lewis A.C., Saxton J.E., Chance K. and Gatti L.V. (2007). *Interpreting satellite column observations of formaldehyde over tropical South America*. Philosophical Transactions of the Royal Society A - Mathematical Physical and Engineering Sciences, **365**, 1741-1751.

Pankow J.F. (2004). *An absorption model of gas/particle partitioning involved in the formation of secondary organic aerosol*. Atmospheric Environment, **28**, 189–193.

Pio C.A., Legrand M., Oliveira T., Afonso J., Santos C., Caseiro A., Fialho P., Barata F., Puxbaum H., Sanchez-Ochoa A., Kasper-Gieb A., Gelencsér A., Preunkert S. and Schock M. (2007). *Climatology of aerosol composition (organic versus inorganic) at nonurban sites on a west-east transect across Europe*. Journal of Geophysical Research, **112** D23S02, doi:10.1029/2006JD008038.

PORG (1997). *Ozone in the United Kingdom*. Fourth report of the UK Photochemical Oxidants Review Group, Department of the Environment, Transport and the Regions, London. Published by Institute of Terrestrial Ecology, Bush Estate, Penicuik, Midlothian, EH26 0QB, UK. ISBN: 0-870393-30-9, and available at www.aeat.co.uk/netcen/airqual/reports/home.html.

Presto A.A., Hartz K.E.H. and Donahue N.M. (2005). *Secondary organic aerosol production from terpene ozonolysis. 2. Effect of NO_X concentration*. Environmental Science and Technology, **39** (18), 7046-7054.

Salma A., Ocskay R. Chi X. and Maenhaut W. (2007). *Sampling artefacts, concentration and chemical composition of fine water-soluble organic carbon and humic-like substances in a continental urban atmospheric environment*. Atmospheric Environment, **41**, 4106–4118.

Saunders S.M., Jenkin M.E., Derwent R.G. and Pilling M.J (2003). *Protocol for the development of the Master Chemical Mechanism, MCM v3 (Part A): tropospheric degradation of non-aromatic volatile organic compounds*. Atmospheric Chemistry and Physics, **3**, 161-180.

Simpson, D., Guenther, A., Hewitt, C.N., Steinbrecher, R. (1995) *Biogenic Emissions in Europe 1. Estimates and Uncertainties*. Journal of Geophysical Research, 100, 22875-22890.

Stedman, J.R., Andrew, A.J., Grice, S., Bush, T.J., Derwent, R.G. (2007). "*A consistent method for modelling PM_{10} and $PM_{2.5}$ concentrations across the United Kingdom in 2004 for air quality assessment*". Atmospheric Environment 41, 161-172.

Stein S.E. and Brown R.L. (1994). *Estimation of normal boiling points from group contributions*. J. Chem. Info. Comp. Sci., **34**, 581–587.

USEPA, 2005: *Guidance on the use of models and other analyses in the attainment demonstration for the 8-hour ozone NAAQS*. US EPA report NO. EPA-454/R-05-002

USEPA, 2007: *Guidance on the use of models and other analyses for demonstrating attainment of air quality goals for ozone. $PM_{2.5}$* US EPA report NO. EPA-454/B-07-002

Utembe S.R., Jenkin M.E., Derwent R.G., Lewis A.C., Hopkins J.R. and Hamilton J.F. (2005). *Modelling the ambient distribution of organic compounds during the August 2003 ozone episode in the southern UK*. Faraday Discussions, **130**, 311-326.

Xia A.G., Michelangeli D.V. and Makar P.A. (2008). *Box model studies of the secondary organic aerosol formation under different HC/NO_X conditions using the subset of the Master Chemical Mechanism for α-pinene oxidation*. Journal of Geophysical Research, **113**, D10301, doi:10.1029/2007JD008726.

Xiao Q., Kuo Y.-H., MA Z., Huang W., Huang X.Y., Zhang X., Barker D.M., Michalakes J., and Dudhia, J. (2008) *Application of an Adiabatic WRF Adjoint to the Investigation of the May 2004, McMurdo, Antarctica, Severe Wind Event . Mon. Wea. Rev.,* 136, 3696-3713.

Appendices

CONTENTS

Appendix 1

Listing of the atmospheric degradation mechanism for limonene in FACSIMILE format

Limonene degradation scheme

Reaction listing (936 reactions)

```
% 4.28D-11*EXP(401/TEMP)*0.408 : LIMONENE + OH = LIMAO2             ;
% 4.28D-11*EXP(401/TEMP)*0.222 : LIMONENE + OH = LIMBO2             ;
% 4.28D-11*EXP(401/TEMP)*0.370 : LIMONENE + OH = LIMCO2             ;
% KRO2NO*0.772                : LIMAO2 + NO = LIMAO + NO2          ;
% KRO2NO*0.228                : LIMAO2 + NO = LIMANO3              ;
% KRO2NO3                     : LIMAO2 + NO3 = LIMAO + NO2         ;
% KRO2HO2*0.914               : LIMAO2 + HO2 = LIMAOOH             ;
% 9.20D-14*RO2*0.7            : LIMAO2 = LIMAO                     ;
% 9.20D-14*RO2*0.3            : LIMAO2 = LIMAOH                    ;
% KDEC                        : LIMAO = LIMAL + HO2                ;
% KRO2NO*0.772                : LIMBO2 + NO = LIMBO + NO2          ;
% KRO2NO*0.228                : LIMBO2 + NO = LIMBNO3              ;
% KRO2NO3                     : LIMBO2 + NO3 = LIMBO + NO2         ;
% KRO2HO2*0.914               : LIMBO2 + HO2 = LIMBOOH             ;
% 8.80D-13*RO2*0.6            : LIMBO2 = LIMBO                     ;
% 8.80D-13*RO2*0.2            : LIMBO2 = LIMAOH                    ;
% 8.80D-13*RO2*0.2            : LIMBO2 = LIMBCO                    ;
% KDEC                        : LIMBO = LIMAL + HO2                ;
% KRO2NO*0.772                : LIMCO2 + NO = LIMCO + NO2          ;
% KRO2NO*0.228                : LIMCO2 + NO = LIMCNO3              ;
% KRO2NO3                     : LIMCO2 + NO3 = LIMCO + NO2         ;
% KRO2HO2*0.914               : LIMCO2 + HO2 = LIMCOOH             ;
% 9.20D-14*RO2*0.7            : LIMCO2 = LIMCO                     ;
% 9.20D-14*RO2*0.3            : LIMCO2 = LIMCOH                    ;
% KDEC                        : LIMCO = LIMKET + HCHO + HO2        ;
% 6.20D-11                    : LIMANO3 + OH = LIMAL + NO2         ;
% 7.36D-11                    : LIMAOOH + OH = LIMAO2              ;
% J<41>                       : LIMAOOH = LIMAO + OH               ;
% 7.02D-11                    : LIMAOH + OH = LIMBCO + HO2         ;
% 5.91D-11                    : LIMBNO3 + OH = LIMBCO + NO2        ;
% 1.04D-10                    : LIMBOOH + OH = LIMBCO + OH         ;
% J<41>                       : LIMBOOH = LIMBO + OH               ;
% 6.70D-11                    : LIMBCO + OH = C923CO3              ;
% 9.31D-11                    : LIMCNO3 + OH = LIMKET + HCHO + NO2 ;
% 1.03D-10                    : LIMCOOH + OH = LIMCO2              ;
% J<41>                       : LIMCOOH = LIMCO + OH               ;
% 9.94D-11                    : LIMCOH + OH = LIMKET + HCHO + HO2  ;
% J<15>                       : LIMAL = C923O2 + CO + HO2          ;
% 1.10D-10*0.712              : LIMAL + OH = LIMALO2               ;
% 1.10D-10*0.288              : LIMAL + OH = C923CO3               ;
% KRO2NO*0.941                : LIMALO2 + NO = LIMALO + NO2        ;
% KRO2NO*0.059                : LIMALO2 + NO = LIMALNO3            ;
% KRO2NO3                     : LIMALO2 + NO3 = LIMALO + NO2       ;
% KRO2HO2*0.914               : LIMALO2 + HO2 = LIMALOOH           ;
% 9.20D-14*RO2*0.7            : LIMALO2 = LIMALO                   ;
% 9.20D-14*RO2*0.3            : LIMALO2 = LIMALOH                  ;
% KDEC                        : LIMALO = LMLKET + HCHO + HO2       ;
% 3.01D-11                    : LIMALNO3 + OH = LMLKET + HCHO + NO2 ;
% 4.65D-11                    : LIMALOOH + OH = LIMALO2            ;
% J<41>                       : LIMALOOH = LIMALO + OH             ;
% 4.31D-11                    : LIMALOH + OH = LMLKET + HCHO + HO2 ;
% KAPNO                       : C923CO3 + NO = C923O2 + NO2        ;
% KRO2NO3*1.6                 : C923CO3 + NO3 = C923O2 + NO2       ;
% KFPAN                       : C923CO3 + NO2 = C923PAN            ;
% KBPAN                       : C923PAN = C923CO3 + NO2            ;
% KAPHO2*0.71                 : C923CO3 + HO2 = C923CO3H           ;
% KAPHO2*0.29                 : C923CO3 + HO2 = LIMONONIC + O3     ;
% 1.00D-11*RO2*0.7            : C923CO3 = C923O2                   ;
% 1.00D-11*RO2*0.3            : C923CO3 = LIMONONIC                ;
% KRO2NO*0.843                : C923O2 + NO = C923O + NO2          ;
% KRO2NO*0.157                : C923O2 + NO = C923NO3              ;
% KRO2NO3                     : C923O2 + NO3 = C923O + NO2         ;
% KRO2HO2*0.890               : C923O2 + HO2 = C923OOH             ;
% 1.32D-12*RO2*0.6            : C923O2 = C923O                     ;
% 1.32D-12*RO2*0.2            : C923O2 = C923OH                    ;
% 1.32D-12*RO2*0.2            : C923O2 = NORLIMAL                  ;
% KDEC                        : C923O = C924O2                     ;
% KRO2NO                      : C924O2 + NO = C924O + NO2          ;
% KRO2NO3                     : C924O2 + NO3 = C924O + NO2         ;
% KRO2HO2*0.890               : C924O2 + HO2 = C924OOH             ;
% 8.80D-13*RO2*0.6            : C924O2 = C924O                     ;
% 8.80D-13*RO2*0.2            : C924O2 = C924OH                    ;
% 8.80D-13*RO2*0.2            : C924O2 = C924CO                    ;
% KDEC                        : C924O = CH3CO3 + C622CHO           ;
```

```
% 6.93D-11                    : C923PAN + OH = NORLIMAL + CO + NO2  ;
% 7.29D-11                    : C923CO3H + OH = C923CO3             ;
% J<41>                       : C923CO3H = C923O2 + OH              ;
% 6.98D-11                    : LIMONONIC + OH = C923O2             ;
% 5.82D-11                    : C923NO3 + OH = NORLIMAL + NO2       ;
% J<53>                       : C923NO3 = C923O + NO2               ;
% 7.39D-11                    : C923OOH + OH = NORLIMAL + OH        ;
% J<41>                       : C923OOH = C923O + OH                ;
% 6.91D-11                    : C923OH + OH = NORLIMAL + HO2        ;
% 8.69D-11                    : C924OOH + OH = C924CO + OH          ;
% J<41>                       : C924OOH = C924O + OH                ;
% 7.47D-11                    : C924OH + OH = C924CO + HO2          ;
% J<15>                       : NORLIMAL = C816O2 + CO + HO2        ;
% 8.00D-11*0.712              : NORLIMAL + OH = NORLIMO2            ;
% 8.00D-11*0.288              : NORLIMAL + OH = C816CO3             ;
% KRO2NO                      : NORLIMO2 + NO = NORLIMO + NO2       ;
% KRO2NO3                     : NORLIMO2 + NO3 = NORLIMO + NO2      ;
% KRO2HO2*0.890               : NORLIMO2 + HO2 = NORLIMOOH          ;
% 9.20D-14*RO2                : NORLIMO2 = NORLIMO                  ;
% KDEC                        : NORLIMO = C817CO + HCHO + HO2       ;
% 3.64D-11                    : NORLIMOOH + OH = NORLIMO2           ;
% J<41>                       : NORLIMOOH = NORLIMO + OH            ;
% KAPNO                       : C816CO3 + NO = C816O2 + NO2         ;
% KFPAN                       : C816CO3 + NO2 = C816PAN             ;
% KBPAN                       : C816PAN = C816CO3 + NO2             ;
% KRO2NO3*1.6                 : C816CO3 + NO3 = C816O2 + NO2        ;
% KAPHO2                      : C816CO3 + HO2 = C816CO3H            ;
% 1.00D-11*RO2                : C816CO3 = C816O2                    ;
% KRO2NO                      : C816O2 + NO = C816O + NO2           ;
% KRO2NO3                     : C816O2 + NO3 = C816O + NO2          ;
% KRO2HO2*0.859               : C816O2 + HO2 = C816OOH              ;
% 2.50D-13*RO2                : C816O2 = C816O                      ;
% 2.00D+14*EXP(-6824/TEMP)    : C816O = MACR + MEKAO2               ;
% KROSEC*O2                   : C816O =  C816CO + HO2               ;
% 5.92D-11                    : C816PAN + OH = C816CO + CO + NO2    ;
% 6.28D-11                    : C816CO3H + OH = C816CO3             ;
% J<41>                       : C816CO3H = C816O2 + OH              ;
% 8.06D-11                    : C816OOH + OH = C816CO + OH          ;
% J<41>                       : C816OOH = C816O + OH                ;
% J<22>                       : C816OOH = C816O + OH                ;
% J<35>                       : C924CO = C622CO3 + CH3CO3           ;
% 6.67D-11                    : C924CO + OH = C925O2                ;
% KRO2NO                      : C925O2 + NO = C925O + NO2           ;
% KRO2NO3                     : C925O2 + NO3 = C925O + NO2          ;
% KRO2HO2*0.890               : C925O2 + HO2 = C925OOH              ;
% 9.20D-14*RO2                : C925O2 = C925O                      ;
% KDEC                        : C925O = C818CO + HCHO + HO2         ;
% 2.45D-11                    : C925OOH + OH = C925O2               ;
% J<41>                       : C925OOH = C925O + OH                ;
% J<15>                       : LMLKET = C817O2 + CO + HO2          ;
% 3.60D-11*0.748              : LMLKET + OH = C817CO3               ;
% 3.60D-11*0.252              : LMLKET + OH = C926O2                ;
% KAPNO                       : C817CO3 + NO = C817O2 + NO2         ;
% KFPAN                       : C817CO3 + NO2 = C817PAN             ;
% KBPAN                       : C817PAN = C817CO3 + NO2             ;
% KRO2NO3*1.6                 : C817CO3 + NO3 = C817O2 + NO2        ;
% KAPHO2*0.71                 : C817CO3 + HO2 = C817CO3H            ;
% KAPHO2*0.29                 : C817CO3 + HO2 = KLIMONONIC + O3     ;
% 1.00D-11*RO2*0.7            : C817CO3 = C817O2                    ;
% 1.00D-11*RO2*0.3            : C817CO3 = KLIMONONIC                ;
% KRO2NO*0.862                : C817O2 + NO = C817O + NO2           ;
% KRO2NO*0.138                : C817O2 + NO = C817NO3               ;
% KRO2NO3                     : C817O2 + NO3 = C817O + NO2          ;
% KRO2HO2*0.859               : C817O2 + HO2 = C817OOH              ;
% 1.30D-12*0.6                : C817O2 = C817O                      ;
% 1.30D-12*0.2                : C817O2 = C817OH                     ;
% 1.30D-12*0.2                : C817O2 = C817CO                     ;
% KDEC                        : C817O = C818O2                      ;
% KRO2NO                      : C818O2 + NO = C818O + NO2           ;
% KRO2NO3                     : C818O2 + NO3 = C818O + NO2          ;
% KRO2HO2*0.859               : C818O2 + HO2 = C818OOH              ;
% 1.30D-12*0.6                : C818O2 = C818O                      ;
% 1.30D-12*0.2                : C818O2 = C818OH                     ;
% 1.30D-12*0.2                : C818O2 = C818CO                     ;
% KDEC                        : C818O = C517CHO + CH3CO3            ;
% 1.92D-11                    : C817PAN + OH = C817CO + CO + NO2    ;
% 2.28D-11                    : C817CO3H + OH = C817CO3             ;
% J<41>                       : C817CO3H = C817O2 + OH              ;
```

```
% J<22>*2                    : C817CO3H = C817O2 + OH             ;
% 1.97D-11                   : KLIMONONIC + OH = C817CO2          ;
% J<22>*2                    : KLIMONONIC = C817O2 + HO2          ;
% 1.62D-11                   : C817NO3 + OH = C817CO + NO2        ;
% J<53>                      : C817NO3 = C817O + NO2              ;
% J<22>*2                    : C817NO3 = C817O + NO2              ;
% 3.21D-11                   : C817OOH + OH = C817CO + OH         ;
% J<41>                      : C817OOH = C817O + OH               ;
% J<22>*2                    : C817OOH = C817O + OH               ;
% 2.31D-11                   : C817OH + OH = C817CO + HO2         ;
% J<22>*2                    : C817OH = C818O2 + HO2              ;
% 3.94D-11                   : C818OOH + OH = C818CO + OH         ;
% J<41>                      : C818OOH = C818O + OH               ;
% J<22>*2                    : C818OOH = C517CHO + CH3CO3 + OH    ;
% 2.72D-11                   : C818OH + OH = C818CO + HO2         ;
% J<22>*2                    : C818OH = C517CHO + CH3CO3 + HO2    ;
% J<18>                      : C816CO = MACO3 + MEKAO2            ;
% J<19>                      : C816CO = MACO3 + MEKAO2            ;
% 5.20D-11                   : C816CO + OH = C819O2               ;
% KRO2NO                     : C819O2 + NO = C819O + NO2          ;
% KRO2NO3                    : C819O2 + NO3 = C819O + NO2         ;
% KRO2HO2                    : C819O2 + HO2 = C819OOH             ;
% 9.20D-14*RO2               : C819O2 = C819O                     ;
% KDEC                       : C819O = ACETOL + CO2C4CO3          ;
% 2.72D-11                   : C817CO + OH = C727CO3              ;
% KAPNO                      : C727CO3 + NO = C727O2 + NO2        ;
% KFPAN                      : C727CO3 + NO2 = C727PAN            ;
% KBPAN                      : C727PAN = C727CO3 + NO2            ;
% KRO2NO3*1.6                : C727CO3 + NO3 = C727O2 + NO2       ;
% KAPHO2                     : C727CO3 + HO2 = C727CO3H           ;
% 1.00D-11*RO2               : C727CO3 = C727O2                   ;
% KRO2NO                     : C727O2 + NO = C727O + NO2          ;
% KRO2NO3                    : C727O2 + NO3 = C727O + NO2         ;
% KRO2HO2*0.820              : C727O2 + HO2 = C727OOH             ;
% 8.80D-13*RO2               : C727O2 = C727O                     ;
% KDEC                       : C727O = CH3CO3 + CO2C4CHO          ;
% 1.41D-11                   : C818CO + OH = C820O2               ;
% KRO2NO                     : C820O2 + NO = C820O + NO2          ;
% KRO2NO3                    : C820O2 + NO3 = C820O + NO2         ;
% KRO2HO2*0.859              : C820O2 + HO2 = C820OOH             ;
% 9.20D-14*RO2               : C820O2 = C820O                     ;
% KDEC                       : C820O = CH3CO3 + C614CO            ;
% 1.35D-11                   : C819OOH + OH = C819O2              ;
% J<41>                      : C819OOH = C819O + OH               ;
% J<22>*2                    : C819OOH = C819O + OH               ;
% 6.89D-12                   : C727PAN + OH = C727CO + CO + NO2   ;
% 1.05D-11                   : C727CO3H + OH = C727CO3            ;
% J<41>                      : C727CO3H = C727O2 + OH             ;
% J<22>*2                    : C727CO3H = C727O2 + OH             ;
% J<41>                      : C727OOH = C727O + OH               ;
% 2.42D-11                   : C727OOH + OH = C727CO + OH         ;
% 1.76D-11                   : C820OOH + OH = C820O2              ;
% J<41>                      : C820OOH = C820O + OH               ;
% J<35>                      : C820OOH = C820O + OH               ;
% J<22>                      : C820OOH = C820O + OH               ;
% J<15>                      : C622CHO = C622O2 + CO + HO2        ;
% 8.67D-11*0.288             : C622CHO + OH = C622CO3             ;
% 8.67D-11*0.712             : C622CHO + OH = C728O2              ;
% KAPNO                      : C622CO3 + NO = C622O2 + NO2        ;
% KFPAN                      : C622CO3 + NO2 = C622PAN            ;
% KBPAN                      : C622PAN = C622CO3 + NO2            ;
% KRO2NO3*1.6                : C622CO3 + NO3 = C622O2 + NO2       ;
% KAPHO2*0.71                : C622CO3 + HO2 = C622CO3H           ;
% KAPHO2*0.29                : C622CO3 + HO2 = C622CO2H + O3      ;
% 1.00D-11*RO2*0.7           : C622CO3 = C622O2                   ;
% 1.00D-11*RO2*0.3           : C622CO3 = C622CO2H                 ;
% KRO2NO*0.922               : C622O2 + NO = C622O + NO2          ;
% KRO2NO*0.078               : C622O2 + NO = C622NO3              ;
% KRO2NO3                    : C622O2 + NO3 = C622O + NO2         ;
% KRO2HO2*0.770              : C622O2 + HO2 = C622OOH             ;
% 1.30D-12*RO2*0.6           : C622O2 = C622O                     ;
% 1.30D-12*RO2*0.2           : C622O2 = C622OH                    ;
% 1.30D-12*RO2*0.2           : C622O2 = C518CHO                   ;
% KRO2PRIM*O2                : C622O = C518CHO + HO2              ;
% KRO2NO*0.969               : C728O2 + NO = C728O + NO2          ;
% KRO2NO*0.031               : C728O2 + NO = C728NO3              ;
% KRO2NO3                    : C728O2 + NO3 = C728O + NO2         ;
% KRO2HO2*0.770              : C728O2 + HO2 = C728OOH             ;
```

```
% 9.20D-14*RO2*0.7          : C728O2 = C728O                      ;
% 9.20D-14*RO2*0.3          : C728O2 = C728OH                     ;
% KDEC                      : C728O = C517CHO + HCHO + HO2        ;
% 5.95D-11                  : C622PAN + OH = C518CHO + CO + NO2   ;
% 6.31D-11                  : C622CO3H + OH = C622CO3             ;
% J<41>                     : C622CO3H = C622O2 + OH              ;
% 6.00D-11                  : C622CO2H + OH = C622O2              ;
% 5.64D-11                  : C622NO3 + OH = C518CHO + NO2        ;
% J<53>                     : C622NO3 = C622O + NO2               ;
% 7.17D-11                  : C622OOH + OH = C518CHO + OH         ;
% J<41>                     : C622OOH = C622O + OH                ;
% 6.29D-11                  : C622OH + OH = C518CHO + HO2         ;
% 3.28D-11                  : C728NO3 + OH = C517CHO + HCHO + NO2 ;
% 4.52D-11                  : C728OOH + OH = C728O2               ;
% J<41>                     : C728OOH = C728O + OH                ;
% 4.18D-11                  : C728OH + OH = C517CHO + HCHO + HO2  ;
% J<15>                     : C517CHO = C517O2 + CO + HO2         ;
% 4.35D-11                  : C517CHO + OH = C517CO3              ;
% KAPNO                     : C517CO3 + NO = C517O2 + NO2         ;
% KFPAN                     : C517CO3 + NO2 = C517PAN             ;
% KBPAN                     : C517PAN = C517CO3 + NO2             ;
% KRO2NO3*1.6               : C517CO3 + NO3 = C517O2 + NO2        ;
% KAPHO2*0.71               : C517CO3 + HO2 = C517CO3H            ;
% KAPHO2*0.29               : C517CO3 + HO2 = C517CO2H + O3       ;
% 1.00D-11*RO2*0.7          : C517CO3 = C517O2                    ;
% 1.00D-11*RO2*0.3          : C517CO3 = C517CO2H                  ;
% KRO2NO*0.948              : C517O2 + NO = C517O + NO2           ;
% KRO2NO*0.052              : C517O2 + NO = C517NO3               ;
% KRO2NO3                   : C517O2 + NO3 = C517O + NO2          ;
% KRO2HO2*0.706             : C517O2 + HO2 = C517OOH              ;
% 1.30D-12*RO2*0.6          : C517O2 = C517O                      ;
% 1.30D-12*RO2*0.2          : C517O2 = C517OH                     ;
% 1.30D-12*RO2*0.2          : C517O2 = HMVKBCHO                   ;
% KROPRIM*O2                : C517O = HMVKBCHO + HO2              ;
% 1.79D-11                  : C517PAN + OH = HMVKBCHO + CO + NO2  ;
% J<41>                     : C517CO3H = C517O2 + OH              ;
% 2.15D-11                  : C517CO3H + OH = C517CO3             ;
% 1.84D-11                  : C517CO2H + OH = C517O2              ;
% J<53>                     : C517NO3 = C517O + NO2               ;
% 1.38D-11                  : C517NO3 + OH = HMVKBCHO + NO2       ;
% J<41>                     : C517OOH = C517O + OH                ;
% 4.93D-11                  : C517OOH + OH = HMVKBCHO + OH        ;
% 2.81D-11                  : C517OH + OH = HMVKBCHO + HO2        ;
% J<15>                     : C518CHO = ISOPDO2 + CO + HO2        ;
% 8.70D-11*0.288            : C518CHO + OH = C518CO3              ;
% 8.70D-11*0.712            : C518CHO + OH = C623O2               ;
% KAPNO                     : C518CO3 + NO = ISOPDO2 + NO2        ;
% KFPAN                     : C518CO3 + NO2 = C518PAN             ;
% KBPAN                     : C518PAN = C518CO3 + NO2             ;
% KRO2NO3*1.6               : C518CO3 + NO3 = ISOPDO2 + NO2       ;
% KAPHO2*0.71               : C518CO3 + HO2 = C518CO3H            ;
% KAPHO2*0.29               : C518CO3 + HO2 = C518CO2H + O3       ;
% 1.00D-11*RO2*0.7          : C518CO3 = ISOPDO2                   ;
% 1.00D-11*RO2*0.3          : C518CO3 = C518CO2H                  ;
% KRO2NO*0.970              : C623O2 + NO = C623O + NO2           ;
% KRO2NO*0.030              : C623O2 + NO = C623NO3               ;
% KRO2NO3                   : C623O2 + NO3 = C623O + NO2          ;
% KRO2HO2*0.770             : C623O2 + HO2 = C623OOH              ;
% 8.00D-13*RO2*0.7          : C623O2 = C623O                      ;
% 8.00D-13*RO2*0.3          : C623O2 = C623OH                     ;
% KDEC                      : C623O = HMVKBCHO + HCHO + HO2       ;
% 5.75D-11                  : C518PAN + OH = HCOC5 + CO + NO2     ;
% J<41>                     : C518CO3H = ISOPDO2 + OH             ;
% 6.11D-11                  : C518CO3H + OH = C518CO3             ;
% 5.80D-11                  : C518CO2H + OH = ISOPDO2             ;
% 3.51D-11                  : C623NO3 + OH = HMVKBCHO + HCHO + NO2 ;
% J<41>                     : C623OOH = C623O + OH                ;
% 5.26D-11                  : C623OOH + OH = C623O2               ;
% 4.91D-11                  : C623OH + OH = HMVKBCHO + HCHO + HO2 ;
% J<15>                     : HMVKBCHO = HMVKBO2 + CO + HO2       ;
% 3.51D-11                  : HMVKBCHO + OH = HMVKBCO3            ;
% KAPNO                     : HMVKBCO3 + NO = HMVKBO2 + NO2       ;
% KFPAN                     : HMVKBCO3 + NO2 = HMVKBPAN           ;
% KBPAN                     : HMVKBPAN = HMVKBCO3 + NO2           ;
% KRO2NO3*1.6               : HMVKBCO3 + NO3 = HMVKBO2 + NO2      ;
% KAPHO2*0.71               : HMVKBCO3 + HO2 = HMVKBCO3H          ;
% KAPHO2*0.29               : HMVKBCO3 + HO2 = HMVKBCO2H + O3     ;
% 1.00D-11*RO2*0.7          : HMVKBCO3 = HMVKBO2                  ;
```

```
% 1.00D-11*RO2*0.3            : HMVKBCO3 = HMVKBCO2H                ;
% 1.43D-11                    : HMVKBPAN + OH = BIACETOH + CO + NO2 ;
% J<41>                       : HMVKBCO3H = HMVKBO2 + OH            ;
% 1.79D-11                    : HMVKBCO3H + OH = HMVKBCO3           ;
% 1.48D-11                    : HMVKBCO2H + OH = HMVKBO2            ;
% J<35>                       : C727CO = CH3CO3 + CO2C4CO3          ;
% 5.67D-12                    : C727CO + OH = C821O2                ;
% KRO2NO                      : C821O2 + NO = C821O + NO2           ;
% KRO2NO3                     : C821O2 + NO3 = C821O + NO2          ;
% KRO2HO2*0.859               : C821O2 + HO2 = C821OOH              ;
% 8.80D-13*RO2                : C821O2 = C821O                      ;
% KDEC                        : C821O = CH3CO3 + CO + CO2C3CHO      ;
% J<41>                       : C821OOH = C821O + OH                ;
% J<35>                       : C821OOH = C821O + OH                ;
% 5.42D-11                    : C821OOH + OH = C821O2               ;
% 9.97D-11*0.647              : LIMKET + OH = LMKAO2                ;
% 9.97D-11*0.353              : LIMKET + OH = LMKBO2                ;
% KRO2NO*0.760                : LMKAO2 + NO = LMKAO + NO2           ;
% KRO2NO*0.240                : LMKAO2 + NO = LMKANO3               ;
% KRO2NO3                     : LMKAO2 + NO3 = LMKAO + NO2          ;
% KRO2HO2*0.914               : LMKAO2 + HO2 = LMKAOOH              ;
% 9.20D-14*RO2*0.7            : LMKAO2 = LMKAO                      ;
% 9.20D-14*RO2*0.3            : LMKAO2 = LMKAOH                     ;
% KDEC                        : LMKAO = LMLKET + HO2                ;
% KRO2NO*0.760                : LMKBO2 + NO = LMKBO + NO2           ;
% KRO2NO*0.240                : LMKBO2 + NO = LMKBNO3               ;
% KRO2NO3                     : LMKBO2 + NO3 = LMKBO + NO2          ;
% KRO2HO2*0.914               : LMKBO2 + HO2 = LMKBOOH              ;
% 8.80D-13*RO2*0.6            : LMKBO2 = LMKBO                      ;
% 8.80D-13*RO2*0.2            : LMKBO2 = LMKAOH                     ;
% 8.80D-13*RO2*0.2            : LMKBO2 = LMKBCO                     ;
% KDEC                        : LMKBO = LMLKET + HO2                ;
% 9.20D-12                    : LMKANO3 + OH = LMLKET + NO2         ;
% 2.08D-11                    : LMKAOOH + OH = LMKAO2               ;
% J<41>                       : LMKAOOH = LMKAO + OH                ;
% 1.74D-11                    : LMKAOH + OH = LMKBCO + HO2          ;
% 6.30D-12                    : LMKBNO3 + OH = LMKBCO + NO2         ;
% 4.76D-11                    : LMKBOOH + OH = LMKBCO + OH          ;
% J<41>                       : LMKBOOH = LMKBO + OH                ;
% 2.95D-15*EXP(-783/TEMP)*0.730 : LIMONENE + O3 = LIMOOA            ;
% 2.95D-15*EXP(-783/TEMP)*0.270 : LIMONENE + O3 = LIMOOB            ;
% KDEC*0.5                    : LIMOOA = LIMALAO2 + OH              ;
% KDEC*0.5                    : LIMOOA = LIMALBO2 + OH              ;
% KDEC*0.5                    : LIMOOB = LIMBOO                     ;
% KDEC*0.5                    : LIMOOB = C923O2 + CO + OH           ;
% 1.20D-15                    : LIMBOO + CO = LIMAL                 ;
% 1.00D-14                    : LIMBOO + NO = LIMAL + NO2           ;
% 1.00D-15                    : LIMBOO + NO2 = LIMAL + NO3          ;
% 7.00D-14                    : LIMBOO + SO2 = LIMAL + SO3          ;
% 2.00D-18*H2O                : LIMBOO = LIMONONIC                  ;
% 1.40D-17*H2O                : LIMBOO = LIMAL + H2O2               ;
% KRO2NO                      : LIMALAO2 + NO = LIMALAO + NO2       ;
% KRO2NO3                     : LIMALAO2 + NO3 = LIMALAO + NO2      ;
% KRO2HO2*0.914               : LIMALAO2 + HO2 = LIMALAOOH          ;
% 8.80D-13*RO2*0.6            : LIMALAO2 = LIMALAO2                 ;
% 8.80D-13*RO2*0.2            : LIMALAO2 = LIMALAOH                 ;
% 8.80D-13*RO2*0.2            : LIMALAO2 = LIMALACO                 ;
% KDEC                        : LIMALAO = C729CHO + CH3CO3          ;
% J<41>                       : LIMALAOOH = LIMALAO + OH            ;
% J<22>                       : LIMALAOOH = C729CHO + OH + CH3CO3   ;
% 1.06D-10                    : LIMALAOOH + OH = LIMALACO + OH      ;
% J<22>                       : LIMALAOH = C729CHO + HO2 + CH3CO3   ;
% 9.34D-11                    : LIMALAOH + OH = LIMALACO + HO2      ;
% J<35>                       : LIMALACO = C729CO3 + CH3CO3         ;
% 8.34D-11                    : LIMALACO + OH = C729CHO + CH3CO3    ;
% KRO2NO                      : LIMALBO2 + NO = LIMALBO + NO2       ;
% KRO2NO3                     : LIMALBO2 + NO3 = LIMALBO + NO2      ;
% KRO2HO2*0.914               : LIMALBO2 + HO2 = LIMALBOOH          ;
% 8.80D-13*RO2*0.9            : LIMALBO2 = LIMALBO2                 ;
% 8.80D-13*RO2*0.05           : LIMALBO2 = LIMALBOH                 ;
% 8.80D-13*RO2*0.05           : LIMALBO2 = LIMALBCO                 ;
% KDEC                        : LIMALBO = C822CO3 + HCHO            ;
% J<41>                       : LIMALBOOH = LIMALBO + OH            ;
% J<22>                       : LIMALBOOH = C822CO3 + HCHO + OH     ;
% 9.73D-11                    : LIMALBOOH + OH = LIMALBCO + OH      ;
% J<22>                       : LIMALBOH = C822CO3 + HCHO + HO2     ;
% 9.04D-11                    : LIMALBOH + OH = LIMALBCO + HO2      ;
% J<34>                       : LIMALBCO = C822CO3 + CO + HO2       ;
```

```
% 1.01D-10                  : LIMALBCO + OH = C822CO3 + CO        ;
% KAPNO                     : C822CO3 + NO = C822CO2 + NO2        ;
% KFPAN                     : C822CO3 + NO2 = C822PAN             ;
% KBPAN                     : C822PAN = C822CO3 + NO2             ;
% KRO2NO3*1.6               : C822CO3 + NO3 = C822CO2 + NO2       ;
% KAPHO2*0.71               : C822CO3 + HO2 = C822CO3H            ;
% KAPHO2*0.29               : C822CO3 + HO2 = C822CO2H + O3       ;
% 1.00D-11*RO2*0.7          : C822CO3 = C822CO2                   ;
% 1.00D-11*RO2*0.3          : C822CO3 = C822CO2H                  ;
% KDEC*0.8                  : C822CO2 = C823CO3                   ;
% KDEC*0.2                  : C822CO2 = C822O2                    ;
% 8.46D-11                  : C822PAN + OH = C729CHO + CO + NO2   ;
% J<41>                     : C822CO3H = C822CO2 + OH             ;
% 8.82D-11                  : C822CO3H + OH = C822CO3             ;
% 8.47D-11                  : C822CO2H + OH = C822CO2             ;
% KAPNO                     : C823CO3 + NO = C823O2 + NO2         ;
% KFPAN                     : C823CO3 + NO2 = C823PAN             ;
% KBPAN                     : C823PAN = C823CO3 + NO2             ;
% KRO2NO3*1.6               : C823CO3 + NO3 = C823O2 + NO2        ;
% KAPHO2*0.71               : C823CO3 + HO2 = C823CO3H            ;
% KAPHO2*0.29               : C823CO3 + HO2 = LIMONIC + O3        ;
% 1.00D-11*RO2*0.7          : C823CO3 = C823O2                    ;
% 1.00D-11*RO2*0.3          : C823CO3 = LIMONIC                   ;
% 5.82D-11                  : C823PAN + OH = C823CO + CO + NO2    ;
% J<41>                     : C823CO3H = C823O2 + OH              ;
% 6.18D-11                  : C823CO3H + OH = C823CO3             ;
% 5.89D-11                  : LIMONIC + OH = C823O2               ;
% KRO2NO*0.862              : C823O2 + NO = C823O + NO2           ;
% KRO2NO*0.138              : C823O2 + NO = C823NO3               ;
% KRO2NO3                   : C823O2 + NO3 = C823O + NO2          ;
% KRO2HO2*0.859             : C823O2 + HO2 = C823OOH              ;
% 1.30D-12*RO2*0.6          : C823O2 = C823O                      ;
% 1.30D-12*RO2*0.2          : C823O2 = C823OH                     ;
% 1.30D-12*RO2*0.2          : C823O2 = C823CO                     ;
% KDEC                      : C823O = C825O2                      ;
% KRO2NO                    : C825O2 + NO = C825O + NO2           ;
% KRO2NO3                   : C825O2 + NO3 = C825O + NO2          ;
% KRO2HO2*0.859             : C825O2 + HO2 = C825OOH              ;
% 8.80D-12*RO2*0.6          : C825O2 = C825O                      ;
% 8.80D-12*RO2*0.2          : C825O2 = C825OH                     ;
% 8.80D-12*RO2*0.2          : C825O2 = C825CO                     ;
% KDEC                      : C825O = C622CHO + HO2               ;
% J<53>                     : C823NO3 = C823O + NO2               ;
% 5.53D-11                  : C823NO3 + OH = C823CO + NO2         ;
% J<41>                     : C823OOH = C823O + OH                ;
% 7.06D-11                  : C823OOH + OH = C823CO + OH          ;
% 6.16D-11                  : C823OH + OH = C823CO + HO2          ;
% J<15>                     : C823CO = C825O2 + HO2               ;
% 7.70D-11                  : C823CO + OH = C825O2                ;
% J<41>                     : C825OOH = C825O + OH                ;
% 7.90D-11                  : C825OOH + OH = C825CO + OH          ;
% 6.69D-11                  : C825OH + OH = C825CO + HO2          ;
% J<22>                     : C825CO = C622CO3 + HO2              ;
% 6.64D-11                  : C825CO + OH = C622CO3               ;
% KRO2NO*0.862              : C822O2 + NO = C822O + NO2           ;
% KRO2NO*0.138              : C822O2 + NO = C822NO3               ;
% KRO2NO3                   : C822O2 + NO3 = C822O + NO2          ;
% KRO2HO2*0.859             : C822O2 + HO2 = C822OOH              ;
% 1.30D-12*RO2*0.6          : C822O2 = C822O                      ;
% 1.30D-12*RO2*0.2          : C822O2 = C822OH                     ;
% 1.30D-12*RO2*0.2          : C822O2 = C729CHO                    ;
% KDEC                      : C822O = C824O2                      ;
% KRO2NO                    : C824O2 + NO = C824O + NO2           ;
% KRO2NO3                   : C824O2 + NO3 = C824O + NO2          ;
% KRO2HO2*0.859             : C824O2 + HO2 = C824OOH              ;
% 8.80D-12*RO2*0.6          : C824O2 = C824O                      ;
% 8.80D-12*RO2*0.2          : C824O2 = C824OH                     ;
% 8.80D-12*RO2*0.2          : C824O2 = C824CO                     ;
% KDEC                      : C824O = C624CHO + CO + HO2          ;
% J<53>                     : C822NO3 = C822O + NO2               ;
% 8.31D-11                  : C822NO3 + OH = C729CHO + NO2        ;
% J<41>                     : C822OOH = C822O + OH                ;
% 9.71D-11                  : C822OOH + OH = C729CHO + OH         ;
% 8.80D-11                  : C822OH + OH = C729CHO + HO2         ;
% J<41>                     : C824OOH = C824O + OH                ;
% 1.02D-10                  : C824OOH + OH = C824CO + OH          ;
% 9.34D-11                  : C824OH + OH = C824CO + HO2          ;
% J<34>                     : C824CO = C624CO3 + CO + HO2         ;
```

```
% 7.46D-11                    : C824CO + OH = C624CO3 + CO          ;
% 1.06D-10*0.447              : C729CHO + OH = C729CO3              ;
% 1.06D-10*0.553              : C729CHO + OH = C8262O2              ;
% J<15>*2                     : C729CHO = C729O2 + CO + HO2         ;
% KAPNO                       : C729CO3 + NO = C729O2 + NO2         ;
% KFPAN                       : C729CO3 + NO2 = C729PAN             ;
% KBPAN                       : C729PAN = C729CO3 + NO2             ;
% KRO2NO3*1.6                 : C729CO3 + NO3 = C729O2 + NO2        ;
% KAPHO2*0.71                 : C729CO3 + HO2 = C729CO3H            ;
% KAPHO2*0.29                 : C729CO3 + HO2 = C729CO2H + O3       ;
% 1.00D-11*0.7                : C729CO3 = C729O2                    ;
% 1.00D-11*0.3                : C729CO3 = C729CO2H                  ;
% KRO2NO*0.889                : C729O2 + NO = C729O + NO2           ;
% KRO2NO*0.111                : C729O2 + NO = C729NO3               ;
% KRO2NO3                     : C729O2 + NO3 = C729O + NO2          ;
% KRO2HO2*0.820               : C729O2 + HO2 = C729OOH              ;
% 1.30D-12*0.6                : C729O2 = C729O                      ;
% 1.30D-12*0.2                : C729O2 = C622CHO                    ;
% 1.30D-12*0.2                : C729O2 = C622CHO                    ;
% KDEC                        : C729O = C622CO3                     ;
% 8.33D-11                    : C729PAN + OH = C622CHO + CO + NO2   ;
% 8.69D-11                    : C729CO3H + OH = C729CO3             ;
% J<41>                       : C729CO3H = C729O2 + OH              ;
% J<15>                       : C729CO3H = C729O2 + OH              ;
% 8.38D-11                    : C729CO2H + OH = C729O2              ;
% J<15>                       : C729CO2H = C729O2 + HO2             ;
% 7.51D-11                    : C729NO3 + OH = C622CHO + NO2        ;
% J<53>                       : C729NO3 = C729O + NO2               ;
% 9.57D-11                    : C729OOH + OH = C622CHO + OH         ;
% J<41>                       : C729OOH = C729O + OH                ;
% J<15>                       : C729OOH = C729O + OH                ;
% KRO2NO*0.931                : C826O2 + NO = C826O + NO2           ;
% KRO2NO*0.069                : C826O2 + NO = C826NO3               ;
% KRO2NO3                     : C826O2 + NO3 = C826O + NO2          ;
% KRO2HO2*0.859               : C826O2 + HO2 = C826OOH              ;
% 9.20D-14*RO2*0.7            : C826O2 = C826O                      ;
% 9.20D-14*RO2*0.3            : C826O2 = C826OH                     ;
% KDEC                        : C826O = C626CHO + HCHO + HO2        ;
% 4.59D-11                    : C826NO3 + OH = C626CHO + HCHO + NO2 ;
% 6.05D-11                    : C826OOH + OH = C826O2               ;
% J<41>                       : C826OOH = C826O + OH                ;
% J<15>*2                     : C826OOH = C826O + OH                ;
% 5.70D-11                    : C826OH + OH = C826O                 ;
% J<15>*2                     : C826OH = C826O + HO2                ;
% 8.26D-11*0.288              : C624CHO + OH = C624CO3              ;
% 8.26D-11*0.712              : C624CHO + OH = C730O2               ;
% KAPNO                       : C624CO3 + NO = C624O2 + NO2         ;
% KFPAN                       : C624CO3 + NO2 = C624PAN             ;
% KBPAN                       : C624PAN = C624CO3 + NO2             ;
% KRO2NO3*1.6                 : C624CO3 + NO3 = C624O2 + NO2        ;
% KAPHO2*0.71                 : C624CO3 + HO2 = C624CO3H            ;
% KAPHO2*0.29                 : C624CO3 + HO2 = C624CO2H + O3       ;
% 1.00D-11*RO2*0.7            : C624CO3 = C624O2                    ;
% 1.00D-11*RO2*0.3            : C624CO3 = C624CO2H                  ;
% KRO2NO*0.791                : C624O2 + NO = C624O + NO2           ;
% KRO2NO*0.209                : C624O2 + NO = C624NO3               ;
% KRO2NO3                     : C624O2 + NO3 = C624O + NO2          ;
% KRO2HO2*0.770               : C624O2 + HO2 = C624OOH              ;
% 2.50D-13*RO2*0.6            : C624O2 = C624O                      ;
% 2.50D-13*RO2*0.2            : C624O2 = C624OH                     ;
% 2.50D-13*RO2*0.2            : C624O2 = C624CO                     ;
% KROSEC*O2                   : C624O = C624CO + HO2                ;
% 4.00D+14*EXP(-6990/TEMP)    : C624O = MACR + HOCH2CH2O2           ;
% 5.89D-11                    : C624PAN + OH = C624CO + CO + NO2    ;
% 6.25D-11                    : C624CO3H + OH = C624CO3             ;
% J<41>                       : C624CO3H = C624O2 + OH              ;
% 5.94D-11                    : C624CO2H + OH = C624O2              ;
% 2.92D-11                    : C624NO3 + OH = C624CO + NO2         ;
% J<54>                       : C624NO3 = C624O + NO2               ;
% 1.10D-10                    : C624OOH + OH = C624CO + OH          ;
% J<41>                       : C624OOH = C624O + OH                ;
% 9.53D-11                    : C624OH + OH = C624CO + HO2          ;
% 6.04D-11                    : C624CO + OH = C625O2                ;
% J<22>                       : C624CO = MACO3 + HOCH2CH2O2         ;
% KRO2NO                      : C625O2 + NO = C625O + NO2           ;
% KRO2NO3                     : C625O2 + NO3 = C625O + NO2          ;
% KRO2HO2*0.770               : C625O2 + HO2 = C625OOH              ;
% 9.20D-14*RO2*0.7            : C625O2 = C625O                      ;
```

```
% 9.20D-14*RO2*0.3          : C625O2 = C625OH                      ;
% KDEC                      : C625O = ACETOL + HOC2H4CO3           ;
% 3.04D-11                  : C625OOH + OH = C625O2                ;
% J<41>                     : C625OOH = C625O + OH                 ;
% J<22>                     : C625OOH = HOC2H4CO3 + ACETOL + OH    ;
% 2.70D-11                  : C625OH + OH = HOC2H4CO3 + ACETOL     ;
% J<22>                     : C625OH = HOC2H4CO3 + ACETOL + HO2    ;
% KRO2NO*0.944              : C730O2 + NO = C730O + NO2            ;
% KRO2NO*0.056              : C730O2 + NO = C730NO3                ;
% KRO2NO3                   : C730O2 + NO3 = C730O + NO2           ;
% KRO2HO2*0.820             : C730O2 + HO2 = C730OOH               ;
% 9.20D-14*RO2*0.7          : C730O2 = C730O                       ;
% 9.20D-14*RO2*0.3          : C730O2 = C730OH                      ;
% KDEC                      : C730O = C519CHO + HCHO + HO2         ;
% 3.09D-11                  : C730NO3 + OH = C519CHO + HCHO + NO2  ;
% 4.00D-11                  : C730OOH + OH = C730O2                ;
% J<41>                     : C730OOH = C730O + OH                 ;
% 3.66D-11                  : C730OH + OH = C519CHO + HCHO + HO2   ;
% 5.41D-11                  : C626CHO + OH = C626CO3               ;
% J<15>*2                   : C626CHO = C626O2 + CO + HO2          ;
% KAPNO                     : C626CO3 + NO = C626O2 + NO2          ;
% KFPAN                     : C626CO3 + NO2 = C626PAN              ;
% KBPAN                     : C626PAN = C626CO3 + NO2              ;
% KRO2NO3*1.6               : C626CO3 + NO3 = C626O2 + NO2         ;
% KAPHO2*0.71               : C626CO3 + HO2 = C626CO3H             ;
% KAPHO2*0.29               : C626CO3 + HO2 = C626CO2H + O3        ;
% 1.00D-11*0.7              : C626CO3 = C626O2                     ;
% 1.00D-11*0.3              : C626CO3 = C626CO2H                   ;
% KRO2NO*0.922              : C626O2 + NO = C626O + NO2            ;
% KRO2NO*0.078              : C626O2 + NO = C626NO3                ;
% KRO2NO3                   : C626O2 + NO3 = C626O + NO2           ;
% KRO2HO2*0.770             : C626O2 + HO2 = C626OOH               ;
% 1.30D-12*0.6              : C626O2 = C626O                       ;
% 1.30D-12*0.2              : C626O2 = C517CHO                     ;
% 1.30D-12*0.2              : C626O2 = C511CHO                     ;
% KDEC                      : C626O = C622CO3                      ;
% 3.14D-11                  : C626PAN + OH = C517CHO + CO + NO2    ;
% 3.50D-11                  : C626CO3H + OH = C626CO3              ;
% J<41>                     : C626CO3H = C626O2 + OH               ;
% J<15>                     : C626CO3H = C626O2 + OH               ;
% 3.19D-11                  : C626CO2H + OH = C626O2               ;
% J<15>                     : C626CO2H = C626O2 + HO2              ;
% 2.84D-11                  : C626NO3 + OH = C517CHO + NO2         ;
% J<53>                     : C626NO3 = C626O + NO2                ;
% 4.38D-11                  : C626OOH + OH = C517CHO + OH          ;
% J<41>                     : C626OOH = C626O + OH                 ;
% J<15>                     : C626OOH = C626O + OH                 ;
% 3.50D-11                  : C519CHO + OH = C519CO3               ;
% KAPNO                     : C519CO3 + NO = C519O2 + NO2          ;
% KFPAN                     : C519CO3 + NO2 = C519PAN              ;
% KBPAN                     : C519PAN = C519CO3 + NO2              ;
% KRO2NO3*1.6               : C519CO3 + NO3 = C519O2 + NO2         ;
% KAPHO2*0.71               : C519CO3 + HO2 = C519CO3H             ;
% KAPHO2*0.29               : C519CO3 + HO2 = C519CO2H + O3        ;
% 1.00D-11*RO2*0.7          : C519CO3 = C519O2                     ;
% 1.00D-11*RO2*0.3          : C519CO3 = C519CO2H                   ;
% KRO2NO                    : C519O2 + NO = C519O + NO2            ;
% KRO2NO3                   : C519O2 + NO3 = C519O + NO2           ;
% KRO2HO2*0.706             : C519O2 + HO2 = C519OOH               ;
% 8.80D-13*RO2*0.6          : C519O2 = C519O                       ;
% 8.80D-13*RO2*0.2          : C519O2 = C519OH                      ;
% 8.80D-13*RO2*0.2          : C519O2 = C519CO                      ;
% KDEC                      : C519O = CH3CO3 + HOC2H4CHO           ;
% 1.01D-11                  : C519PAN + OH = C519CO + CO + NO2     ;
% 1.37D-11                  : C519CO3H + OH = C519CO3              ;
% J<41>                     : C519CO3H = C519O2 + OH               ;
% J<22>                     : C519CO3H = C519O2 + OH               ;
% 1.06D-11                  : C519CO2H + OH = C519O2               ;
% 2.74D-11                  : C519OOH + OH = C519CO + OH           ;
% J<41>                     : C519OOH = C519O + OH                 ;
% J<22>                     : C519OOH = CH3CO3 + HOC2H4CHO + OH    ;
% 1.52D-11                  : C519OH + OH = C519CO + HO2           ;
% J<22>                     : C519OH = CH3CO3 + HOC2H4CHO + HO2    ;
% J<35>                     : C519CO = CH3CO3 + HOC2H4CO3          ;
% 1.39D-11                  : C519CO + OH = CO23C4CHO + HO2        ;
% 5.13D-11                  : C511CHO + OH = C511CO3               ;
% KAPNO                     : C511CO3 + NO = C511O2 + NO2          ;
% KFPAN                     : C511CO3 + NO2 = C511PAN              ;
```

```
% KBPAN                      : C511PAN = C511CO3 + NO2             ;
% KRO2NO3*1.6                : C511CO3 + NO3 = C511O2 + NO2        ;
% KAPHO2                     : C511CO3 + HO2 = C511CO3H            ;
% 1.00D-11*RO2               : C511CO3 = C511O2                    ;
% 2.78D-11                   : C511PAN + OH = CO23C4CHO + CO + NO2 ;
% 3.14D-11                   : C511CO3H + OH = C511CO3             ;
% J<41>                      : C511CO3H = C511O2 + OH              ;
% J<15>                      : C511CO3H = C511O2 + OH              ;
% 8.30D-18*0.670             : LIMAL + O3 = LIMALOOA + HCHO        ;
% 8.30D-18*0.330             : LIMAL + O3 = LMLKET + CH2OOF        ;
% KDEC                       : LIMALOOA = C926O2 + OH              ;
% KRO2NO                     : C926O2 + NO = C926O + NO2           ;
% KRO2NO3                    : C926O2 + NO3 = C926O + NO2          ;
% KRO2HO2*0.890              : C926O2 + HO2 = C926OOH              ;
% 9.20D-14*RO2*0.7           : C926O2 = C926O                      ;
% 9.20D-14*RO2*0.3           : C926O2 = C926OH                     ;
% KDEC                       : C926O = CH3CO3 + CO25C6CHO          ;
% J<41>                      : C926OOH = C926O + OH                ;
% J<15>*2                    : C926OOH = C926O + OH                ;
% 3.08D-11                   : C926OOH + OH = C926O2               ;
% J<15>*2                    : C926OH = C926O + HO2                ;
% 2.73D-11                   : C926OH + OH = CH3CO3 + CO25C6CHO    ;
% J<15>                      : CO25C6CHO = C627O2 + CO + HO2       ;
% 2.69D-11                   : CO25C6CHO + OH = CO25C6CO3          ;
% KAPNO                      : CO25C6CO3 + NO = C627O2 + NO2       ;
% KFPAN                      : CO25C6CO3 + NO2 = C627PAN           ;
% KBPAN                      : C627PAN = CO25C6CO3 + NO2           ;
% KRO2NO3*1.6                : CO25C6CO3 + NO3 = C627O2 + NO2      ;
% KAPHO2*0.71                : CO25C6CO3 + HO2 = CO25C6CO3H        ;
% KAPHO2*0.29                : CO25C6CO3 + HO2 = CO25C6CO2H + O3   ;
% 1.00D-11*RO2*0.7           : CO25C6CO3 = C627O2                  ;
% KRO2NO                     : C627O2 + NO = C627O + NO2           ;
% KRO2NO3                    : C627O2 + NO3 = C627O + NO2          ;
% KRO2HO2*0.770              : C627O2 + HO2 = C627OOH              ;
% 2.50D-12*RO2*0.6           : C627O2 = C627O                      ;
% 2.50D-12*RO2*0.2           : C627O2 = C627OH                     ;
% 2.50D-12*RO2*0.2           : C627O2 = CO2C4GLYOX                 ;
% KDEC                       : C627O = CO2C4CO3 + HCHO             ;
% 6.15D-12                   : C627PAN + OH = CO2C4GLYOX + CO + NO2 ;
% J<41>                      : CO25C6CO3H = C627O2 + OH            ;
% J<22>*2                    : CO25C6CO3H = C627O2 + OH            ;
% 9.75D-11                   : CO25C6CO3H + OH = CO25C6CO3         ;
% J<22>*2                    : CO25C6CO2H = C627O2 + HO2           ;
% 6.67D-12                   : CO25C6CO2H + OH = C627O2            ;
% J<41>                      : C627OOH = C627O + OH                ;
% J<22>*2                    : C627OOH = CO2C4CO3 + HCHO + OH      ;
% 1.51D-11                   : C627OOH + OH = CO2C4GLYOX + OH      ;
% J<22>*2                    : C627OH = CO2C4CO3 + HCHO + HO2      ;
% 8.25D-12                   : C627OH + OH = CO2C4GLYOX + HO2      ;
% J<34>                      :  CO2C4GLYOX = CO2C4CO3 + CO + HO2   ;
% 1.83D-11                   :  CO2C4GLYOX + OH = CO2C4CO3 + CO    ;
% 1.50D-16*0.730             : LIMKET + O3 = LMKOOA                ;
% 1.50D-16*0.270             : LIMKET + O3 = LMKOOB                ;
% KDEC*0.5                   : LMKOOA = LMLKAO2 + OH               ;
% KDEC*0.5                   : LMKOOA = LMLKBO2 + OH               ;
% KDEC*0.5                   : LMKOOB = LMKBOO                     ;
% KDEC*0.5                   : LMKOOB = C817O2 + CO + OH           ;
% 1.20D-15                   : LMKBOO + CO = LMLKET                ;
% 1.00D-14                   : LMKBOO + NO = LMLKET + NO2          ;
% 1.00D-15                   : LMKBOO + NO2 = LMLKET + NO3         ;
% 7.00D-14                   : LMKBOO + SO2 = LMLKET + SO3         ;
% 2.00D-18*H2O               : LMKBOO = KLIMONONIC                 ;
% 1.40D-17*H2O               : LMKBOO = LMLKET + H2O2              ;
% KRO2NO                     : LMLKAO2 + NO = LMLKAO + NO2         ;
% KRO2NO3                    : LMLKAO2 + NO3 = LMLKAO + NO2        ;
% KRO2HO2*0.914              : LMLKAO2 + HO2 = LMLKAOOH            ;
% 8.80D-13*RO2*0.6           : LMLKAO2 = LMLKAO2                   ;
% 8.80D-13*RO2*0.2           : LMLKAO2 = LMLKAOH                   ;
% 8.80D-13*RO2*0.2           : LMLKAO2 = LIMALACO                  ;
% KDEC                       : LMLKAO = C626CHO + CH3CO3           ;
% J<41>                      : LMLKAOOH = LMLKAO + OH              ;
% J<22>                      : LMLKAOOH = C626CHO + OH + CH3CO3    ;
% 5.79D-11                   : LMLKAOOH + OH = LIMALACO + OH       ;
% J<22>                      : LMLKAOH = C626CHO + HO2 + CH3CO3    ;
% 4.57D-11                   : LMLKAOH + OH = LIMALACO + HO2       ;
% J<35>                      : LMLKACO = C626CO3 + CH3CO3          ;
% 3.58D-11                   : LMLKACO + OH = C626CHO + CH3CO3     ;
% KRO2NO                     : LMLKBO2 + NO = LMLKBO + NO2         ;
```

```
% KRO2NO3                  : LMLKBO2 + NO3 = LMLKBO + NO2        ;
% KRO2HO2*0.914            : LMLKBO2 + HO2 = LMLKBOOH            ;
% 8.80D-13*RO2*0.9         : LMLKBO2 = LMLKBO2                   ;
% 8.80D-13*RO2*0.05        : LMLKBO2 = LMLKBOH                   ;
% 8.80D-13*RO2*0.05        : LMLKBO2 = LMLKBCO                   ;
% KDEC                     : LMLKBO = C731CO3 + HCHO             ;
% J<41>                    : LMLKBOOH = LMLKBO + OH              ;
% J<22>                    : LMLKBOOH = C731CO3 + HCHO + OH      ;
% 4.77D-11                 : LMLKBOOH + OH = LMLKBCO + OH        ;
% J<22>                    : LMLKBOH = C731CO3 + HCHO + HO2      ;
% 4.09D-11                 : LMLKBOH + OH = LMLKBCO + HO2        ;
% J<34>                    : LMLKBCO = C731CO3 + CO + HO2        ;
% 5.09D-11                 : LMLKBCO + OH = C731CO3 + CO         ;
% KAPNO                    : C731CO3 + NO = C731CO2 + NO2        ;
% KFPAN                    : C731CO3 + NO2 = C731PAN             ;
% KBPAN                    : C731PAN = C731CO3 + NO2             ;
% KRO2NO3*1.6              : C731CO3 + NO3 = C731CO2 + NO2       ;
% KAPHO2*0.71              : C731CO3 + HO2 = C731CO3H            ;
% KAPHO2*0.29              : C731CO3 + HO2 = C731CO2H + O3       ;
% 1.00D-11*RO2*0.7         : C731CO3 = C731CO2                   ;
% 1.00D-11*RO2*0.3         : C731CO3 = C731CO2H                  ;
% KDEC*0.8                 : C731CO2 = C732CO3                   ;
% KDEC*0.2                 : C731CO2 = C731O2                    ;
% 3.82D-11                 : C731PAN + OH = C626CHO + CO + NO2   ;
% J<41>                    : C731CO3H = C731CO2 + OH             ;
% 4.18D-11                 : C731CO3H + OH = C731CO3             ;
% 3.88D-11                 : C731CO2H + OH = C731CO2             ;
% KAPNO                    : C732CO3 + NO = C732O2 + NO2         ;
% KFPAN                    : C732CO3 + NO2 = C732PAN             ;
% KBPAN                    : C732PAN = C732CO3 + NO2             ;
% KRO2NO3*1.6              : C732CO3 + NO3 = C732O2 + NO2        ;
% KAPHO2*0.71              : C732CO3 + HO2 = C732CO3H            ;
% KAPHO2*0.29              : C732CO3 + HO2 = KLIMONIC + O3       ;
% 1.00D-11*RO2*0.7         : C732CO3 = C732O2                    ;
% 1.00D-11*RO2*0.3         : C732CO3 = KLIMONIC                  ;
% 1.80D-11                 : C732PAN + OH = C732CO + CO + NO2    ;
% J<41>                    : C732CO3H = C732O2 + OH              ;
% 2.16D-11                 : C732CO3H + OH = C732CO3             ;
% 1.85D-11                 : KLIMONIC + OH = C732O2              ;
% KRO2NO*0.862             : C732O2 + NO = C732O + NO2           ;
% KRO2NO*0.138             : C732O2 + NO = C732NO3               ;
% KRO2NO3                  : C732O2 + NO3 = C732O + NO2          ;
% KRO2HO2*0.859            : C732O2 + HO2 = C732OOH              ;
% 1.30D-12*RO2*0.6         : C732O2 = C732O                      ;
% 1.30D-12*RO2*0.2         : C732O2 = C732OH                     ;
% 1.30D-12*RO2*0.2         : C732O2 = C732CO                     ;
% KDEC                     : C732O = C734O2                      ;
% KRO2NO                   : C734O2 + NO = C734O + NO2           ;
% KRO2NO3                  : C734O2 + NO3 = C734O + NO2          ;
% KRO2HO2*0.859            : C734O2 + HO2 = C734OOH              ;
% 8.80D-12*RO2*0.6         : C734O2 = C734O                      ;
% 8.80D-12*RO2*0.2         : C734O2 = C734OH                     ;
% 8.80D-12*RO2*0.2         : C734O2 = C734CO                     ;
% KDEC                     : C734O = C517CHO + HO2               ;
% J<53>                    : C732NO3 = C732O + NO2               ;
% 7.97D-12                 : C732NO3 + OH = C732CO + NO2         ;
% J<41>                    : C732OOH = C732O + OH                ;
% 4.95D-11                 : C732OOH + OH = C732CO + OH          ;
% 2.82D-11                 : C732OH + OH = C732CO + HO2          ;
% J<15>                    : C732CO = C734O2 + HO2               ;
% 2.81D-11                 : C732CO + OH = C734O2                ;
% J<41>                    : C734OOH = C734O + OH                ;
% 4.16D-11                 : C734OOH + OH = C734CO + OH          ;
% 2.95D-11                 : C734OH + OH = C734CO + HO2          ;
% J<22>                    : C734CO = C517CO3 + HO2              ;
% 2.43D-11                 : C734CO + OH = C517CO3               ;
% KRO2NO*0.862             : C731O2 + NO = C731O + NO2           ;
% KRO2NO*0.138             : C731O2 + NO = C731NO3               ;
% KRO2NO3                  : C731O2 + NO3 = C731O + NO2          ;
% KRO2HO2*0.859            : C731O2 + HO2 = C731OOH              ;
% 1.30D-12*RO2*0.6         : C731O2 = C731O                      ;
% 1.30D-12*RO2*0.2         : C731O2 = C731OH                     ;
% 1.30D-12*RO2*0.2         : C731O2 = C626CHO                    ;
% KDEC                     : C731O = C733O2                      ;
% KRO2NO                   : C733O2 + NO = C733O + NO2           ;
% KRO2NO3                  : C733O2 + NO3 = C733O + NO2          ;
% KRO2HO2*0.859            : C733O2 + HO2 = C733OOH              ;
% 8.80D-12*RO2*0.6         : C733O2 = C733O                      ;
```

```
% 8.80D-12*RO2*0.2          : C733O2 = C733OH                    ;
% 8.80D-12*RO2*0.2          : C733O2 = C733CO                    ;
% KDEC                      : C733O = C519CHO + CO + HO2         ;
% J<53>                     : C731NO3 = C731O + NO2              ;
% 3.17D-11                  : C731NO3 + OH = C626CHO + NO2       ;
% J<41>                     : C731OOH = C731O + OH               ;
% 4.83D-11                  : C731OOH + OH = C626CHO + OH        ;
% 3.92D-11                  : C731OH + OH = C626CHO + HO2        ;
% J<41>                     : C733OOH = C733O + OH               ;
% 5.51D-11                  : C733OOH + OH = C733CO + OH         ;
% 4.30D-11                  : C733OH + OH = C733CO + HO2         ;
% J<34>                     : C733CO = C519CO3 + CO + HO2        ;
% 2.28D-11                  : C733CO + OH = C519CO3 + CO         ;
% 1.30D-17*0.670            : C622CHO + O3 = C628OOA + HCHO      ;
% 1.30D-17*0.330            : C622CHO + O3 = C517CHO + CH2OOF    ;
% KDEC                      : C628OOA = C628O2 + OH              ;
% KRO2NO                    : C628O2 + NO = C628O + NO2          ;
% KRO2NO3                   : C628O2 + NO3 = C628O + NO2         ;
% KRO2HO2*0.770             : C628O2 + HO2 = C628OOH             ;
% 9.20D-14*RO2*0.7          : C628O2 = C628O                     ;
% 9.20D-14*RO2*0.3          : C628O2 = C628OH                    ;
% KDEC                      : C628O = CO13C4OH + CH3CO3          ;
% J<41>                     : C628OOH = C628O + OH               ;
% J<22>                     : C628OOH = CO13C4OH + CH3CO3 + OH   ;
% J<15>                     : C628OOH = CO13C4OH + CH3CO3 + OH   ;
% 3.14D-11                  : C628OOH + OH = C628O2              ;
% J<22>                     : C628OH = CO13C4OH + CH3CO3 + HO2   ;
% J<15>                     : C628OH = CO13C4OH + CH3CO3 + HO2   ;
% 2.80D-11                  : C628OH + OH = C628O                ;
% 1.30D-17*0.670            : C624CHO + O3 = C629OOA + HCHO      ;
% 1.30D-17*0.330            : C624CHO + O3 = C519CHO + CH2OOF    ;
% KDEC                      : C629OOA = C629O2 + OH              ;
% KRO2NO                    : C629O2 + NO = C629O + NO2          ;
% KRO2NO3                   : C629O2 + NO3 = C629O + NO2         ;
% KRO2HO2*0.770             : C629O2 + HO2 = C629OOH             ;
% 9.20D-14*RO2*0.7          : C629O2 = C629O                     ;
% 9.20D-14*RO2*0.3          : C629O2 = C629OH                    ;
% KDEC*0.5                  : C629O = HO1CO3CHO + CH3CO3         ;
% KDEC*0.5                  : C629O = HO1CO34C5 + CO + HO2       ;
% J<41>                     : C629OOH = C629O + OH               ;
% J<22>                     : C629OOH = HO1CO3CHO + CH3CO3 + OH  ;
% J<15>                     : C629OOH = HO1CO34C5 + CO + HO2 + OH ;
% 3.31D-11                  : C629OOH + OH = C629O2              ;
% J<22>                     : C629OH = HO1CO3CHO + CH3CO3 + HO2  ;
% J<15>                     : C629OH = HO1CO34C5 + CO + HO2 + HO2 ;
% 2.97D-11                  : C629OH + OH = C629O                ;
% 1.30D-17*0.670            : C518CHO + O3 = C520OOA + HCHO      ;
% 1.30D-17*0.330            : C518CHO + O3 = HMVKBCHO + CH2OOF   ;
% KDEC                      : C520OOA = C520O2 + OH              ;
% KRO2NO                    : C520O2 + NO = C520O + NO2          ;
% KRO2NO3                   : C520O2 + NO3 = C520O + NO2         ;
% KRO2HO2*0.706             : C520O2 + HO2 = C520OOH             ;
% 9.20D-14*RO2*0.7          : C520O2 = C520O                     ;
% 9.20D-14*RO2*0.3          : C520O2 = C520OH                    ;
% KDEC*0.5                  : C520O = HOCH2COCHO + CH3CO3        ;
% KDEC*0.5                  : C520O = BIACETOH + CO + HO2        ;
% J<41>                     : C520OOH = C520O + OH               ;
% J<22>                     : C520OOH = HOCH2COCHO + CH3CO3 + OH ;
% J<15>                     : C520OOH = BIACETOH + CO + HO2 + OH ;
% 3.74D-11                  : C520OOH + OH = C520O2              ;
% J<22>                     : C520OH = HOCH2COCHO + CH3CO3 + HO2 ;
% J<15>                     : C520OH = BIACETOH + CO + HO2 + HO2 ;
% 3.40D-11                  : C520OH + OH = C520O                ;
% 1.30D-17*0.670            : C729CHO + O3 = C735OOA + HCHO      ;
% 1.30D-17*0.330            : C729CHO + O3 = C626CHO + CH2OOF    ;
% KDEC                      : C735OOA = C735O2 + OH              ;
% KRO2NO                    : C735O2 + NO = C735O + NO2          ;
% KRO2NO3                   : C735O2 + NO3 = C735O + NO2         ;
% KRO2HO2*0.820             : C735O2 + HO2 = C735OOH             ;
% 9.20D-14*RO2*0.7          : C735O2 = C735O                     ;
% 9.20D-14*RO2*0.3          : C735O2 = C735OH                    ;
% KDEC                      : C735O = CO13C4CHO + CH3CO3         ;
% J<41>                     : C735OOH = C735O + OH               ;
% J<22>                     : C735OOH = CO13C4CHO + CH3CO3 + OH  ;
% J<15>*2                   : C735OOH = CO13C4CHO + CH3CO3 + OH  ;
% 5.07D-11                  : C735OOH + OH = C735O2              ;
% J<22>                     : C735OH = CO13C4CHO + CH3CO3 + HO2  ;
% J<15>*2                   : C735OH = CO13C4CHO + CH3CO3 + HO2  ;
```

```
% 4.73D-11                  : C735OH + OH = C735O                ;
% 1.22D-11                  : LIMONENE + NO3 = NLIMO2            ;
% KRO2NO                    : NLIMO2 + NO = NLIMO + NO2          ;
% KRO2NO3                   : NLIMO2 + NO3 = NLIMO + NO2         ;
% KRO2HO2*0.914             : NLIMO2 + HO2 = NLIMOOH             ;
% 9.20D-14*RO2*0.7          : NLIMO2 = NLIMO                     ;
% 9.20D-14*RO2*0.3          : NLIMO2 = LIMBNO3                   ;
% KDEC                      : NLIMO = LIMAL + NO2                ;
% 4.28D-11                  : NLIMOOH + OH = NLIMO2              ;
% J<41>                     : NLIMOOH = NLIMO + OH               ;
% 2.60D-13*0.988            : LIMAL + NO3 = NLIMALO2             ;
% 2.60D-13*0.092            : LIMAL + NO3 = C923CO3 + HNO3       ;
% KRO2NO                    : NLIMALO2 + NO = NLIMALO + NO2      ;
% KRO2NO3                   : NLIMALO2 + NO3 = NLIMALO + NO2     ;
% KRO2HO2*0.914             : NLIMALO2 + HO2 = NLIMALOOH         ;
% 9.20D-14*RO2*0.7          : NLIMALO2 = NLIMALO                 ;
% 9.20D-14*RO2*0.3          : NLIMALO2 = NLIMALOH                ;
% KDEC                      : NLIMALO = LMLKET + HCHO + NO2      ;
% 4.28D-11                  : NLIMALOOH + OH = NLIMALO2          ;
% J<41>                     : NLIMALOOH = NLIMALO + OH           ;
% 3.93D-11                  : NLIMALOH + OH = LMLKET + HCHO + NO2 ;
% 9.40D-12                  : LIMKET + NO3 = NLMKAO2             ;
% KRO2NO*0.760              : NLMKAO2 + NO = NLMKAO + NO2        ;
% KRO2NO3                   : NLMKAO2 + NO3 = NLMKAO + NO2       ;
% KRO2HO2*0.914             : NLMKAO2 + HO2 = NLMKAOOH           ;
% 9.20D-14*RO2*0.7          : NLMKAO2 = NLMKAO                   ;
% 9.20D-14*RO2*0.3          : NLMKAO2 = LMKBNO3                  ;
% KDEC                      : NLMKAO = LMLKET + NO2              ;
% 1.01D-11                  : NLMKAOOH + OH = NLMKAO2            ;
% J<41>                     : NLMKAOOH = NLMKAO + OH             ;
% KNO3AL*8.5                : C622CHO + NO3 = C622CO3 + HNO3     ;
% 3.30D-13                  : C622CHO + NO3 = NC728O2            ;
% KRO2NO                    : NC728O2 + NO = NC728O + NO2        ;
% KRO2NO3                   : NC728O2 + NO3 = NC728O + NO2       ;
% KRO2HO2*0.770             : NC728O2 + HO2 = NC728OOH           ;
% 9.20D-14*RO2*0.7          : NC728O2 = NC728O                   ;
% 9.20D-14*RO2*0.3          : NC728O2 = NC728OH                  ;
% KDEC                      : NC728O = C517CHO + HCHO + NO2      ;
% 3.94D-11                  : NC728OOH + OH = NC728O2            ;
% J<41>                     : NC728OOH = NC728O + OH             ;
% 3.59D-11                  : NC728OH + OH = C517CHO + HCHO + NO2 ;
% KNO3AL*8.5                : C518CHO + NO3 = C518CO3 + HNO3     ;
% 3.30D-13                  : C518CHO + NO3 = NC623O2            ;
% KRO2NO                    : NC623O2 + NO = NC623O + NO2        ;
% KRO2NO3                   : NC623O2 + NO3 = NC623O + NO2       ;
% KRO2HO2*0.770             : NC623O2 + HO2 = NC623OOH           ;
% 8.00D-13*RO2*0.7          : NC623O2 = NC623O                   ;
% 8.00D-13*RO2*0.3          : NC623O2 = NC623OH                  ;
% KDEC                      : NC623O = HMVKBCHO + HCHO + NO2     ;
% J<41>                     : NC623OOH = NC623O + OH             ;
% 3.96D-11                  : NC623OOH + OH = NC623O2            ;
% 3.62D-11                  : NC623OH + OH = HMVKBCHO + HCHO + NO2 ;
% KNO3AL*17.0               : C729CHO + NO3 = C729CO3 + HNO3     ;
% 3.30D-13                  : C729CHO + NO3 = NC826O2            ;
% KRO2NO                    : NC826O2 + NO = NC826O + NO2        ;
% KRO2NO3                   : NC826O2 + NO3 = NC826O + NO2       ;
% KRO2HO2*0.859             : NC826O2 + HO2 = NC826OOH           ;
% 9.20D-14*RO2*0.7          : NC826O2 = NC826O                   ;
% 9.20D-14*RO2*0.3          : NC826O2 = NC826OH                  ;
% KDEC                      : NC826O = C626CHO + HCHO + NO2      ;
% 5.89D-11                  : NC826OOH + OH = NC826O2            ;
% J<41>                     : NC826OOH = NC826O + OH             ;
% J<15>*2                   : NC826OOH = NC826O + OH             ;
% 5.54D-11                  : NC826OH + OH = NC826O              ;
% J<15>*2                   : NC826OH = NC826O + HO2             ;
% KNO3AL*8.5                : C624CHO + NO3 = C624CO3 + HNO3     ;
% 3.30D-13                  : C624CHO + NO3 = NC730O2            ;
% KRO2NO                    : NC730O2 + NO = NC730O + NO2        ;
% KRO2NO3                   : NC730O2 + NO3 = NC730O + NO2       ;
% KRO2HO2*0.820             : NC730O2 + HO2 = NC730OOH           ;
% 9.20D-14*RO2*0.7          : NC730O2 = NC730O                   ;
% 9.20D-14*RO2*0.3          : NC730O2 = NC730OH                  ;
% KDEC                      : NC730O = C519CHO + HCHO + NO2      ;
% 3.58D-11                  : NC730OOH + OH = NC730O2            ;
% J<41>                     : NC730OOH = NC730O + OH             ;
% 3.34D-11                  : NC730OH + OH = C519CHO + HCHO + NO2 ;
% KNO3AL*8.5                : C517CHO + NO3 = C517CO3 + HNO3     ;
% KNO3AL*8.5                : HMVKBCHO + NO3 = HMVKBCO3 + HNO3   ;
```

```
% KNO3AL*8.5                  : C626CHO + NO3 = C626CO3 + HNO3      ;
% KNO3AL*8.5                  : C519CHO + NO3 = C519CO3 + HNO3      ;
% KNO3AL*5.5                  : CO25C6CHO + NO3 = CO25C6CO3 + HNO3  ;
% KNO3AL*8.5                  : LMLKET + NO3 = C817CO3 + HNO3       ;
```

Species listing (337 species)

```
LIMONENE    C817CO3H    C623O       C822O       C519CO2H    C734CO
LIMAO2      KLIMONONIC  C623NO3     C822NO3     C519O       C731O2
LIMBO2      C817O       C623OOH     C822OOH     C519OOH     C731O
LIMCO2      C817NO3     C623OH      C822OH      C519OH      C731NO3
LIMAO       C817OOH     HMVKBCO3    C824O2      C519CO      C731OOH
LIMANO3     C817OH      HMVKBPAN    C824O       C511CHO     C731OH
LIMAOOH     C817CO      HMVKBCO3H   C824OOH     C511CO3     C733O2
LIMAOH      C818O2      HMVKBCO2H   C824OH      C511PAN     C733O
LIMAL       C818O       C821O2      C824CO      C511CO3H    C733OOH
LIMBO       C818OOH     C821O       C624CHO     LIMALOOA    C733OH
LIMBNO3     C818OH      C821OOH     C729CO3     C926O2      C733CO
LIMBOOH     C819O2      LMKAO2      C826O2      C926O       C628OOA
LIMBCO      C819O       LMKBO2      C729O2      C926OOH     C628O2
LIMCO       C819OOH     LMKAO       C729PAN     C926OH      C628O
LIMCNO3     C727CO3     LMKANO3     C729CO3H    CO25C6CHO   C628OOH
LIMCOOH     C727O2      LMKAOOH     C729CO2H    C627O2      C628OH
LIMCOH      C727PAN     LMKAOH      C729O       CO25C6CO3   C629OOA
LIMKET      C727CO3H    LMKBO       C729NO3     C627PAN     C629O2
LIMALO2     C727O       LMKBNO3     C729OOH     CO25C6CO3H  C629O
LIMALO      C727OOH     LMKBOOH     C826O       CO25C6CO2H  C629OOH
LIMALNO3    C820O2      LMKBCO      C826NO3     C627O       C629OH
LIMALOOH    C820O       LIMOOA      C826OOH     C627OOH     C520OOA
LIMALOH     C820OOH     LIMOOB      C826OH      CO2C4GLYOX  C520O2
LMLKET      C727CO      LIMALAO2    C626CHO     C627OH      C520O
C923CO3     C622CHO     LIMALBO2    C624CO3     LMKOOA      C520OOH
C923O2      C622O2      LIMBOO      C730O2      LMKOOB      C520OH
C923PAN     C622CO3     LIMALAO     C624O2      LMLKAO2     C735OOA
C923CO3H    C728O2      LIMALAOOH   C624PAN     LMLKBO2     C735O2
LIMONONIC   C622PAN     LIMALAOH    C624CO3H    LMKBOO      C735O
C923O       C622CO3H    LIMALACO    C624CO2H    LMLKAO      C735OOH
C923NO3     C622CO2H    C729CHO     C624O       LMLKAOOH    C735OH
C923OOH     C622NO3     LIMALBO     C624NO3     LMLKAOH     NLIMO2
C923OH      C622OOH     LIMALBOOH   C624OOH     LIMALACO    NLIMO
NORLIMAL    C622OH      LIMALBOH    C624OH      LMLKBO      NLIMOOH
C924O2      C518CHO     LIMALBCO    C624CO      LMLKBOOH    NLIMALO2
C924O       C622O       C822CO3     C625O2      LMLKBOH     NLIMALO
C924OOH     C728O       C822CO2     C625O       LMLKBCO     NLIMALOOH
C924OH      C728NO3     C822PAN     C625OOH     C731CO3     NLIMALOH
C924CO      C728OOH     C822CO3H    C625OH      C731CO2     NLMKAO2
NORLIMO2    C728OH      C822CO2H    C730O       C731PAN     NLMKAO
C816CO3     C517CHO     C823CO3     C730NO3     C731CO3H    NLMKAOOH
C816O2      C517O2      C823O2      C730OOH     C731CO2H    NC728O2
NORLIMO     C517CO3     C823PAN     C730OH      C732CO3     NC728O
NORLIMOOH   C517PAN     C823CO3H    C519CHO     C732O2      NC728OOH
C816PAN     C517CO3H    LIMONIC     C626CO3     C732PAN     NC728OH
C816CO3H    C517CO2H    C823O       C626O2      C732CO3H    NC623O2
C816O       C517O       C823NO3     C626PAN     KLIMONIC    NC623O
C816OOH     C517NO3     C823OOH     C626CO3H    C732O       NC623OOH
C816CO      C517OOH     C823OH      C626CO2H    C732NO3     NC623OH
C925O2      C517OH      C823CO      C626O       C732OOH     NC826O2
C925O       HMVKBCHO    C825O2      C626NO3     C732OH      NC826O
C925OOH     C518CO3     C825O       C626OOH     C732CO      NC826OOH
C818CO      C623O2      C825OOH     C519CO3     C734O2      NC826OH
C817CO3     C518PAN     C825OH      C519O2      C734O       NC730O2
C817O2      C518CO3H    C825CO      C519PAN     C734OOH     NC730O
C817PAN     C518CO2H    C822O2      C519CO3H    C734OH      NC730OOH
NC730OH ;
```

Appendix 2

Technical Summary: Costs, Benefits and Trade-Offs: Volatile Organic Solvents

Objectives

In recent years, there has been greater emphasis on evidence based policy making and greater use of science and economics in developing policies both domestically and at international level. It is recognised that full cost-benefit analysis of policy options is often not possible due to lack of detailed information on potential impacts both in and outside the primary policy area (which for the Division of Defra that sponsored this work concerns international policy on air quality). As a result, unintended negative trade offs can, and do, occur as a consequence of a lack of or inability to fully analyse impacts of policy decisions on a wide range of social and environmental parameters and evaluate the best overall policy direction. A further problem arises when assessment is restricted to what can be quantified well, and areas where quantification would involve greater uncertainty are given very little attention.

To address these concerns the objectives of this research were:

- To develop a methodology for assessing the costs and benefits of solvent reduction and substitution policies. The methodology would enable full life cycle analysis of alternative approaches to inform and underpin future policy development to meet domestic and international commitments.
- To feed into review of the Master Chemical Mechanism (MCM) describing the atmospheric chemistry of VOCs, particularly with respect to ozone formation.

In meeting these objectives methods are illustrated with a case study concerning the substitution of trichloroethylene by other VOC solvents for metal degreasing. This case study was selected simply because there was a reasonable amount of data available on trichloroethylene and possible alternatives. It is not intended to directly inform policy on the use of solvents for metal degreasing.

Impacts and policies relevant to this research

The original focus for the research was the development of methods for comprehensive assessment of the effects of specific VOCs to better inform the development of UK and international policy on VOC emissions in relation to tropospheric ozone formation. From the outset it was recognised that such emissions have a variety impacts in addition to their effects on health, the environment and some materials (principally rubber) resulting from ozone formation and that these effects vary from VOC to VOC. They include:

- Direct chemical effects on human health (including cancers), potentially affecting both workers and the general public depending on exposure routes
- Other occupational risks from use of VOCs (e.g. fire hazard)
- Direct chemical effects on ecosystems
- Global warming effects
- Ozone layer depletion
- Formation of secondary organic aerosols with associated health impacts
- Life cycle effects linked to VOC production, use and disposal

The final issue in the list, life cycle effects, is not considered in policy analysis of other major transboundary air pollutants (SO_2, NOx, NH_3, $PM_{2.5}$, heavy metals) as those pollutants are released as unwanted by-products of processes such as agriculture and power generation. In contrast, most VOCs are deliberately manufactured for a specific purpose such as use as a solvent. It is therefore logical when assessing alternatives to the use of a specific VOC to factor in the broader impacts associated with VOC production, use and disposal.

The failure to assess all of the impacts of pollutants in the past has from time to time caused some inconsistency in policy over time. This generates potential inefficiency for industry and additional burdens on society and the environment. This problem is clearly linked to the diversity of impacts that any VOC may have and associated gaps in knowledge.

The variety of impacts relevant to this work mean that it has implications beyond transboundary air pollution (the direct remit of the sponsoring department for this work), in particular for wider

assessment of chemicals, including under the EU's REACH Regulation. This observation led to considerably more consultation being performed during the development of the work than was originally foreseen, for example with the Advisory Committee on Hazardous Substances convened by Defra and members of the Socio-Economic Assessment Committee under REACH.

Key questions

In adopting a complex methodological framework it is essential that a number of key questions are borne in mind throughout the analysis:

- What are the main reasons for concern about use of a specific VOC? This provides a focus for the work which is essential when dealing simultaneously with a number of different impacts.

- Are there alternatives to using the VOC in question that offer a net benefit when all social, economic and environmental factors are brought together?

- If there are no alternatives and the VOC in question has impacts of some concern, is the service or product provided by the VOC necessary? [To illustrate, the use of a propellant with a high global warming potential (GWP) in medical inhalers may be considered essential, whilst use of the same propellant in novelty goods (such as 'silly string') may be considered non-essential.]

- Do any options likely to be recommended have impacts of concern? Whilst an option may perform better overall than its competitors, it is possible that it could perform sufficiently badly on a single criterion to call its use into serious question. This sort of information may be made difficult to identify through seeking to aggregate across a large number of impacts.

Methods considered and applied

A variety of methods have been investigated during the work to characterise the costs and benefits of VOC actions:

- Cost-effectiveness analysis, to characterise the most efficient means of reaching a policy objective.
- Life cycle analysis, to describe energy use, pollutant emissions, waste generation, etc.
- Risk assessment, to assess whether the VOCs in question are likely to cause damage to health and the environment.
- Impact pathway analysis, to apply best available knowledge for quantifying impacts to health, society and the environment, similar to risk assessment but going further with quantification.
- Cost-benefit analysis, to bring together diverse impacts into a unified framework where the costs and benefits of actions can be directly compared.
- Multi-criteria decision analysis, like CBA a comparative tool, though one that is less dependent on economic analysis.
- Uncertainty assessment (Monte Carlo analysis, sensitivity analysis, assessment of residual biases) to see if conclusions drawn are robust.

There is a tendency for some of these approaches to be considered mutually-exclusive. However, this analysis has considered how they can be used together. Applied in this way, we conclude that the strengths of the different methods can complement each other and improve understanding. Some weaknesses inevitably remain, but they are reduced in importance when a combined analysis is performed well.

In combining these methods the study describes a general methodological framework. It is not recommended that this be used in full in every case – methods should naturally be kept as simple as possible. The way that the framework is applied will therefore vary from case to case, sometimes used in full, sometimes in part. An understanding of the merits and weaknesses of the different tools that are available will help identify what is appropriate in any case.

Case study on trichloroethylene used for metal degreasing

The use of trichloroethylene for metal degreasing was adopted as the case study for this work. It was selected simply for the availability of data both on trichloroethylene and possible substitute solvents (tetrachloroethylene, methylene chloride and limonene) and is not intended to directly inform future policy development on this VOC. It was instead simply selected to provide illustration of the methods outlined in the report. A more complete assessment of trichloroethylene would have assessed its use generally, rather than in metal degreasing alone. It would also have assessed a much more complete range of alternatives (mechanical degreasing methods, etc.) than those considered here. However, extension of the analysis to account for such issues goes beyond the objectives defined above, which relate to development of methods, rather than policy.

Throughout the analysis any uncertainties should be identified and quantified to the extent possible. They can be brought together at the end of the analysis to test the robustness of initial conclusions on which options are to be preferred.

Identifying VOCs and sectors for control

In a typical case, it would first be necessary to identify which VOC or VOCs should be prioritised for control. From the background of transboundary air pollution VOCs may be prioritised according to their individual contribution to tropospheric ozone formation or their sector's contribution – results for both are available from past MCM outputs. Under REACH, a number of chemicals will be prioritised according to their direct health or environmental impacts. Elsewhere, VOCs may be prioritised according to their contribution to climate change or ozone depletion, and so on.

Such an approach is clearly one-dimensional, focussing on a specific type of impact and ignoring others. It is therefore recommended that an early screening is applied to highlight other concerns relating to the prioritised VOC and is alternatives. This is considered below.

Identifying alternatives

Consideration of the alternatives to using a specific VOC can be a complex task. For the case study we consider only one use of trichloroethylene (metal degreasing[1]) and a limited set of options (replacement with other VOC solvents). However, for many policy assessments it may be necessary to consider all uses of the targeted VOC. This can lead to a considerable number of alternatives being identified. Full assessment of all possible options can be a truly daunting task. Prioritisation of alternatives may therefore be necessary.

A further complication concerning the identification and prioritisation of alternatives is that the actual response of industry to a change in policy may not be the same as originally thought. This explains a significant amount of the difference in costs estimated in ex-ante and ex-post assessments of environmental policy.

It is recommended that consultation with affected parties (industries and non-industry groups) commences at this point. Early involvement is likely to bring benefits to all parties.

During consultation it may become apparent that there are variations on the principal alternatives identified. For the trichloroethylene case study one such variation concerned the application of chemical leasing, where solvents would be leased, used, and returned to the supplier for purification and re-use. Such a system introduces an incentive to users to reduce leakage and has potential for significant benefits.

[1] Referring to metal degreasing as a single use is itself a simplification, given the diversity of metal degreasing operations.

Screening alternatives

A preliminary screening of alternatives is recommended in order to understand which are most likely to yield health and environmental benefits, and which could lead to increased damage. Anything that very obviously falls into the latter category could be eliminated from analysis early on, unless it appeared possible that associated risks could be cost-effectively controlled. In cases where an option is eliminated from further analysis it is recommended that this be mentioned in the summary and conclusions to the work, providing stakeholders with the opportunity to comment should they feel the conclusion to be wrong.

The screening assessment here considered the following criteria:

- Human carcinogenicity
- Non-carcinogenic human health effects
- EALs (environmental assessment levels, recommended by the UK Environment Agency for health protection)
- POCP (photochemical oxidant creation potential – relevant to tropospheric ozone formation)
- ODP (ozone depletion potential – relevant to stratospheric ozone)
- SOAP (secondary organic aerosol potential)
- GWP (global warming potential)
- Wider risks to the environment
- Specific risks of production
- Specific risks of disposal

In some cases the screening process drew on quantitative information (e.g. POCPs) for all of the chemicals considered. In others the assessment was more qualitative, for example, noting that limonene was flammable whilst the other options are not. Where possible, the worst performing option for each criterion was identified. This demonstrated that each of the four options considered performed worst in one or more criteria. Accordingly none stood out as clearly better or worse than the others and all were carried through to the more detailed analysis.

Assessing the economic costs of solvent substitution

Several effects on industry need to be considered:

- Capital, operating and maintenance costs of the alternatives for solvent producers and users
- Differences in performance (for the case study, the effectiveness of trichloroethylene in metal degreasing vs. the effectiveness of the alternative solvents, which could lead to higher processing times, higher reject rates, etc.)
- Other costs (e.g. fire protection, controlling occupational exposure, etc.).

There are also costs through the need for additional regulation (e.g. ensuring that chemicals are not used for specific purposes) and to consumers (e.g. through changes in the price of goods).

Guidance on costing methods is available from several sources. The most notable of these from a UK perspective are the Treasury's Green Book and guidance from the IGCB (Inter-departmental Group on Costs and Benefits).

A critical part of the assessment of alternative solvents (where such alternatives are a valid substitute for the targeted VOC, as in the case study) concerns the amount of chemical required. It is recommended that this be considered in two ways, first from consideration of the chemical and physical properties of the options, and second by contacting affected industries (including not just those that use the chemicals in question, but also, ideally, those that supply them or use or supply alternative options). The first is necessary to gain some understanding of why different quantities of chemical are required and how large these differences are likely to be. It is particularly important when dealing with novel alternatives for which industry's experience may be limited.

Previous consultation with industry has examined the potential for substituting trichloroethylene with various alternatives. An important conclusion from that work was that preference for alternatives to trichloroethylene varied between users, depending on the precise nature of the products being treated.

A further conclusion was that some operators found that the alternative that they had switched to was preferable to trichloroethylene in terms of cost or performance.

For the purposes of the case study the analysis of costs was limited to the costs of buying the different solvents. A true policy assessment should collect more data, though this would have required in-depth consultation with affected industries that was beyond the scope of this study. A significant amount of variation was found in available estimates of the cost of some of the solvents considered. This reflects variation in factors such as purity and the volume purchased. Such issues clearly need to be considered when seeking to make a like-for-like comparison.

Health and environmental impact assessment

This part of the analysis applies a number of tools – life cycle analysis, risk analysis and impact pathway analysis to first characterise the burdens of the options under consideration and then to quantify their likely impacts.

Life cycle analysis
A number of tools are available for life cycle assessment, in theory taking the assessment from extraction of raw materials through production of the solvents in question, to use and finally disposal. The case study used the Simapro 7.1 software linked to the EcoInvent 2.0 database. Simapro was, however, only applied as far as the production phase. No data were available from EcoInvent 2.0 for limonene, though (for the purposes of this case study) it was considered that associated burdens were likely to be small compared to the other solvents given that limonene is produced as a by-product of orange juice manufacture. A consequence of this is that the carbon contained within limonene is part of the natural carbon cycle, and hence can be discounted from quantification of greenhouse gas burdens (though any direct greenhouse effect of limonene, as opposed to its degradation products, should be accounted for). A more detailed assessment of life cycle burdens may be desirable in the event that the use of limonene in preference to trichloroethylene were to be recommended by government or one of its agencies or programmes.

The use and disposal phases were excluded from direct assessment using the LCA tools. These stages can be included by the LCA software but here it was considered appropriate to deal with them externally, partly because of a desire for an explicit sensitivity analysis, partly because of the lack of information within the LCA databases on the GWPs of the solvents considered and partly because the quantification of burdens at the use and disposal phases was considered relatively straightforward. This issue concerning GWPs highlights the need to understand what is and is not included in LCA databases.

Results from LCA are typically summarised for a number of impact categories (global warming potential, ozone formation/depletion potential, acidification, human toxicity, etc.). Within each category the mass quantities of burdens (individual greenhouse gases, etc.) are brought together using equivalence factors. In some areas these factors are known with a reasonable level of confidence, GWPs being an example. In others, particularly concerning human or ecological toxicity, they are far more approximate. ISO-approved LCA methods do not extend to aggregation of effects across the impact categories (e.g. combining climate change with human toxicity, etc.) for good reason – to do so requires judgement as to the relative importance of the different impact categories, which will vary from case to case depending on the magnitude of the differences between best- and worst-performing options in each category. This can be performed using techniques that quantify impacts not in terms of pollutant burden but also through to impacts on health (deaths, increased incidence of ill health, etc.) and then to monetary values as has also been demonstrated in the study. This highlights the advantages of using LCA techniques in combination with other methods.

Inspection of the results of the LCA showed surprisingly large differences between trichloroethylene and tetrachloroethylene. It seems questionable whether these differences are real given that the two solvents can be produced using the same process. For a real policy assessment it may be necessary to look into this question in more detail. For the purposes of the present study, however, it was considered acceptable to leave results as they are, in part to highlight the need for checking LCA output.

Risk assessment

A risk analysis was performed in four parts:

1. **Consideration of workplace hazards.** Representative data for exposures in the workplace were not identified. However, recommendations were made for addressing this issue in future analysis to support policy development.
2. **Assessment of non-cancer effects for the general public.** The dispersion of emissions of trichloroethylene and alternatives was modelled across the UK. Estimated concentrations were well below those identified as minimal risk levels (MRLs) for non-cancer effects and so it was considered unlikely that any such impacts would be significant.
3. **Assessment of cancer impacts on the general public.** This part of the analysis used the dispersion results from [2], but took the conventional assumption for assessment of carcinogenic effects that there was no threshold for impact (in other words, that there is no safe level). The incidence of cancers from exposure to the different solvents was calculated applying risk functions derived by USEPA. Trichloroethylene performed worst of the four options, though in all cases estimated additional incidence of cancer was small (affecting on average less than1 person per year across the UK).
4. **Assessment of the potential for impacts on ecosystems.** This drew on past analysis considering PEC/PNEC (predicted-environmental-concentration/predicted-no-effect-concentration) for ecological receptors in the vicinity of sites producing, formulating and using trichloroethylene.

Impact pathway analysis

Further quantification was performed for releases of other prominent air pollutants from the life cycle of the options considered. This focused on regional air pollutants (SO_2, NO_x, $PM_{2.5}$), greenhouse gases, and reaction products of emitted solvents (ozone and secondary organic aerosols).

The analysis of the regional pollutants, emissions of which were estimated by the LCA, used estimates of damage per tonne of pollutant derived in previous Defra-sponsored research by applying the impact pathway framework.[2]

Analysis of ozone formation used MCM-estimates of the POCP of each of the four solvents. These were combined with modelling using the OSRM (Ozone Source-Receptor Model) to describe the change in ozone concentrations and population exposure linked to estimated emissions. Impacts were quantified and monetised using functions previously used in development of the UK's Air Quality Strategy. The ozone assessment was extended to include damage to crops and rubber.

A similar approach was applied to assessment of the effects of the alternative solvents on secondary organic aerosol (SOA) formation. However, of the four solvents, only limonene is considered likely to generate SOAs. Again, analysis proceeded through to quantification of impacts and monetised equivalents using functions adopted in development of the UK's Air Quality Strategy.

Climate change effects were quantified in monetary terms only, applying estimates of £/tonne of pollutant agreed in previous work for Defra.

Overall results were dominated by effects through ozone formation (for which tetrachloroethylene and methylene chloride performed better than trichloroethylene, but limonene performed significantly worse) and global warming (for which tetrachloroethylene and methylene chloride performed worse than trichloroethylene, but limonene performed better). These results highlight the need to undertake a holistic assessment in order to understand how the different types of effect balance against one another. Policy driven solely by concerns about ozone formation would bias against limonene, whilst policy driven solely by concerns over climate change would bias against tetrachloroethylene and methylene chloride.

Comparing costs and benefits

A first step sums costs and benefits for each option relative to those for continued use of trichloroethylene to identify which option or options yield the greatest net benefit. For our case study the greater cost of tetrachloroethylene made it the least desirable option when all quantified elements

[2] Alternative damage/tonne pollutant estimates are available from the European Commission, reflecting alternative views on input parameters such as concentration-response and valuation functions. They are, however, broadly consistent with the UK data.

of the analysis were combined. The preferred options were methylene chloride and limonene. A second stage of the comparison factors in the uncertainties associated with all stages of the analysis. The key question for the uncertainty analysis is how likely it is that any of the alternatives to trichloroethylene would generate a net benefit.

Analysis to this point of course omits effects that cannot be quantified because of a lack of data. It is possible to extend the analysis to factor in such effects using multi-criteria analysis. Recommendations are made in the report for applying MCA in such work. It is possible that MCA could derive a different conclusion to CBA. Should this occur a round of review would be required to better understand the results prior to making recommendations.

Drawing policy-relevant conclusions from the analysis

CBA and MCA are useful tools for bringing complex analysis together into a more easily understood form. However, the most robust policy is likely to be developed not from consideration of CBA/MCA results on their own, but also through consideration of the underlying detail, for example, understanding where important trade-offs are present and what risks are revealed through the uncertainty analysis. A good illustration for this was provided in the case study with respect to limonene, one of the two best performing options overall, but the one that fared worst with respect to ozone formation.

Presentationally, the value of intermediate results (e.g. cases of specific health impacts, cancers, hospital admissions, etc.) cannot be stressed too much as they provide a clear indication of the depth of the underlying analysis and a link between a change in emissions and some aggregated estimate of total impact.

Dissemination of the project

Considerable effort went into dissemination of the work in order to gain feedback from as wide a range of experts as possible. This includes:

- Presentation of the study to two meetings of Defra's Advisory Committee on Hazardous Substances (ACHS)
- Presentation of a paper entitled 'Modelling solvent dispersion, chemistry and health impacts to inform policy development on VOC control' to the Eleventh Annual UK Review Meeting on Outdoor and Indoor Air Pollution Research
- Presentation of a paper to the European Association of Environment and Resource Economists (EAERE) in Gothenburg
- Information sharing at meetings organised by the European Chemicals Agency (ECHA) concerning development of methods for Socio-Economic Assessment for application under the REACH Regulation

The extent of this dissemination work represents a considerable extension of the original ambition of the project. The feedback received, particularly from ACHS, has been extremely useful in developing a report that should be of wide interest for those dealing not just with control of VOCs in general, but also for those dealing with chemicals regulation more widely.

Final comments and ideas for further work

It is first stressed that the case study is deliberately simplified for the purposes of demonstrating the applied methods, rather than providing analysis intended to support policy development on trichloroethylene.

The report will need to be seen against the context in which it has been developed – a short term research project that sought to assess ways in which existing analytical approaches for informing policy development on controlling the formation of tropospheric ozone could be extended to increase benefits and reduce the risk of significant contradiction in policy. Development of guidance typically involves a much larger number of experts and far wider consultation. It is therefore recommended that the methodology described here be updated when greater experience has been gained in its

application and in related work. Particularly relevant will be socio-economic analysis conducted under the REACH Regulation.

It is also recommended that a database be compiled of the properties, etc. of VOCs, including information on POCPs, GWPs, risk factors and so on. This would be extremely valuable in the screening stage discussed above. It would also improve the consistency of future assessments. Some of the necessary expertise is available within the MCM team, though experts in other disciplines, perhaps most notably health risk assessment would also be needed.

The MCM team has provided essential input to this work in a number of ways, most obviously in relation to the quantification of ozone and secondary organic aerosol formation as a result of VOC emissions. Less obvious has been essential guidance provided by the MCM team drawing on the knowledge that they have accumulated in relation to the wider properties of VOCs (e.g. with respect to GWPs) and to knowledge of the emitting sectors.

AEA Energy & Environment
From the AEA group
The Gemini Building
Fermi Avenue
Harwell International Business Centre
Didcot
Oxfordshire
OX11 0QR

Tel: 0845 345 3302
Fax: 0870 190 6318

E-mail: info@aeat.co,uk

www.aea-energy-and-environment.co.uk